A METHOD TO PREDICT ACCURACY OF FIRST ORDER APPROXIMATION OF MODEL OUTPUT VARIANCE

By

ELLEN WEBER STEVENS

Master of Civil Engineering

Mississippi State University

Mississippi State, Mississippi

1989

/

Submitted to the Faculty of the
Graduate College of the
Oklahoma State University
in partial fulfillment of
the requirements for
the Degree of
DOCTOR OF PHILOSOPHY
December, 1993

OKLAHOMA STATE UNIVERSITY

A METHOD TO PREDICT ACCURACY OF FIRST

ORDER APPROXIMATION OF

MODEL OUTPUT VARIANCE

Thesis Approved:

Thesis Adviser

B. K. Moser

Thomas C. Collins

Dean of the Graduate College

PREFACE

This study provides guidance to conditions under which a first order approximate (FOA) variance of a model output is acceptable. If any of the input parameters for a mathematical model are uncertain, i.e. are random variables, the model output will also be a random variable. Ideally, this random variable should be represented by a probability density function, but in practice it is typically represented by its mean and variance.

The FOA variance is found by approximating the nonlinear model response with a linear surface and finding the variance of the linear approximation. How well the FOA variance performs is a function of how well the linear surface fits the model response and of the uncertainty in the input parameters. The specific objective was to find measures of nonlinearity and parameter uncertainty which could be used to predict the error in the FOA variance. Models with one and two uncertain parameters were evaluated.

Methods to predict the error in the FOA variance of the output of one parameters were developed. For two parameter models, it was only possible to formulate an error predicting procedure when the model response was polynomial in form.

I sincerely thank my doctoral committee - Drs. Charles T. Haan, Barry K. Moser, Daniel E. Storm, and Avdhesh K. Tyagi - for guidance and support in completion of this research.

ACKNOWLEDGMENTS

I wish to express my sincere appreciation to my major advisor, Regents Professor and Sarkey's Distinguished Professor Dr. C.T. Haan for his guidance, assistance, and encouragement throughout the completion of this work. This appreciation also extends to my other committee members, Drs. Barry K. Moser, Daniel E. Storm, and Avdhesh K. Tyagi for their advice and cooperation.

I would also like to express my sincere gratitude to Oklahoma State University Center for Water Research, the Biosystems and Agricultural Engineering Department, and Robert Glenn Rapp Foundation for their generous financial support.

I am very grateful for the friends and family members who came down this path with me, especially my father, who I knew was always there if I needed him and my friend Steven Williams, who gave me moral support through the occasionally difficult process of preparing this thesis.

Finally, I would like to dedicate this to the memory of my mother, Margaret Weber, who made her daughters be good at mathematics and my uncle, Maxwell Davidson, whose final gift to me made it a lot easier for me to leave regular employment and start down a new road.

TABLE OF CONTENTS

LIST OF TABLES

LIST OF FIGURES

CHAPTER ONE

INTRODUCTION

STATEMENT OF PROBLEM

A realistic assessment of the performance of any water resources project requires an assessment of the validity of any predicted loads (hydrologic predictions such as discharge) and capacities (ability to perform under a given load). Typically the loads are assessed using various hydrologic models, generally having a number of parameters which can be determined with varying degrees of accuracy. These parameters are, therefore, better represented as random variables. Consequently, the model response, being a function of random variables, is also a random variable.

A frequent practice in hydrologic assessment is to find the "best" parameters, by whatever means is available, and accept a model output based on these parameters as the result to be used for planning purposes. Since the model output is actually a random variable, it is much better described by a mean, variance, and higher order moments if possible. If the variance is large in relation to the mean, it may not be prudent to base design or policy decisions on this model output alone. Unfortunately, this aspect of modeling is frequently ignored.

One reason that the model output variance is neglected is the difficulty in estimating it. Two methods are generally used in practice - first order approximate

(FOA) and Monte Carlo simulation (MCS). The FOA variance is typically easy to compute, but may be subject to large errors under high parameter uncertainty or model nonlinearity. A MCS is computationally demanding, requiring numerous runs of the model to assure accurate results. An additional complication is the problem of determining how many model runs are required, which is a function of the parameter uncertainty and degree of correlation between the uncertain parameters. It is quite possible that the number of runs required could be in the thousands, which would present a problem if the model was expensive or time consuming to run.

To date, the only widely used criterion for determining if a FOA variance is valid is to restrict parameter coefficient of variation (C_v) to less than 0.2 (Benjamin and Cornell, 1970). This is a very restrictive assumption in hydrologic modeling, where there is often great uncertainty in the parameters. The FOA variance has been shown to perform well when the parameter uncertainty is higher than 0.2. The circumstances under which this occurs has only been developed for specific models, however. Figure 1-1 illustrates that the relative error in FOA variance is not strictly a function of C_v. It is also a function of properties of the model. The models used to generate the data in the figure were explicit functions, i.e., $y = f(x)$ where x was a random variable with a given distribution. Thus, an exact variance could be found by numerical integration and compared with the FOA variance.

As a result, there are two variance estimating procedures - one which may be computationally prohibitive, and one whose applicability is severely limited due to a lack of a procedure for predicating its accuracy. Consequently, neither method is commonly used and model results which may actually contain a great deal of uncertainty are accepted as valid point estimates.

OBJECTIVES

The objective of this work was to develop a methodology for predicting the accuracy of a model output variance estimated by first order (FO) methods. To be useful, this predictor needs to be derived from information readily available to the modeler, such as parameter characteristics and a relatively small number of parameter - model response combinations. The key factors include the uncertainty in the parameters, the nonlinearity of the model or deviation of the model response from a linear surface, and whether the response more closely approximates an exponential or polynomial surface.

These factors are relatively easily obtained. Parameter uncertainty is characterized by the C_v, which is a function of the mean and standard deviation. The linear surface is defined via a Taylor Series (TS) expansion of the model function about the mean values of the parameters. The form of the model response, i.e. exponential or polynomial, can be determined by evaluating first and second derivatives of the response with respect to the parameter(s) at several points and determining if certain criteria are met. If necessary, the derivatives can be found numerically.

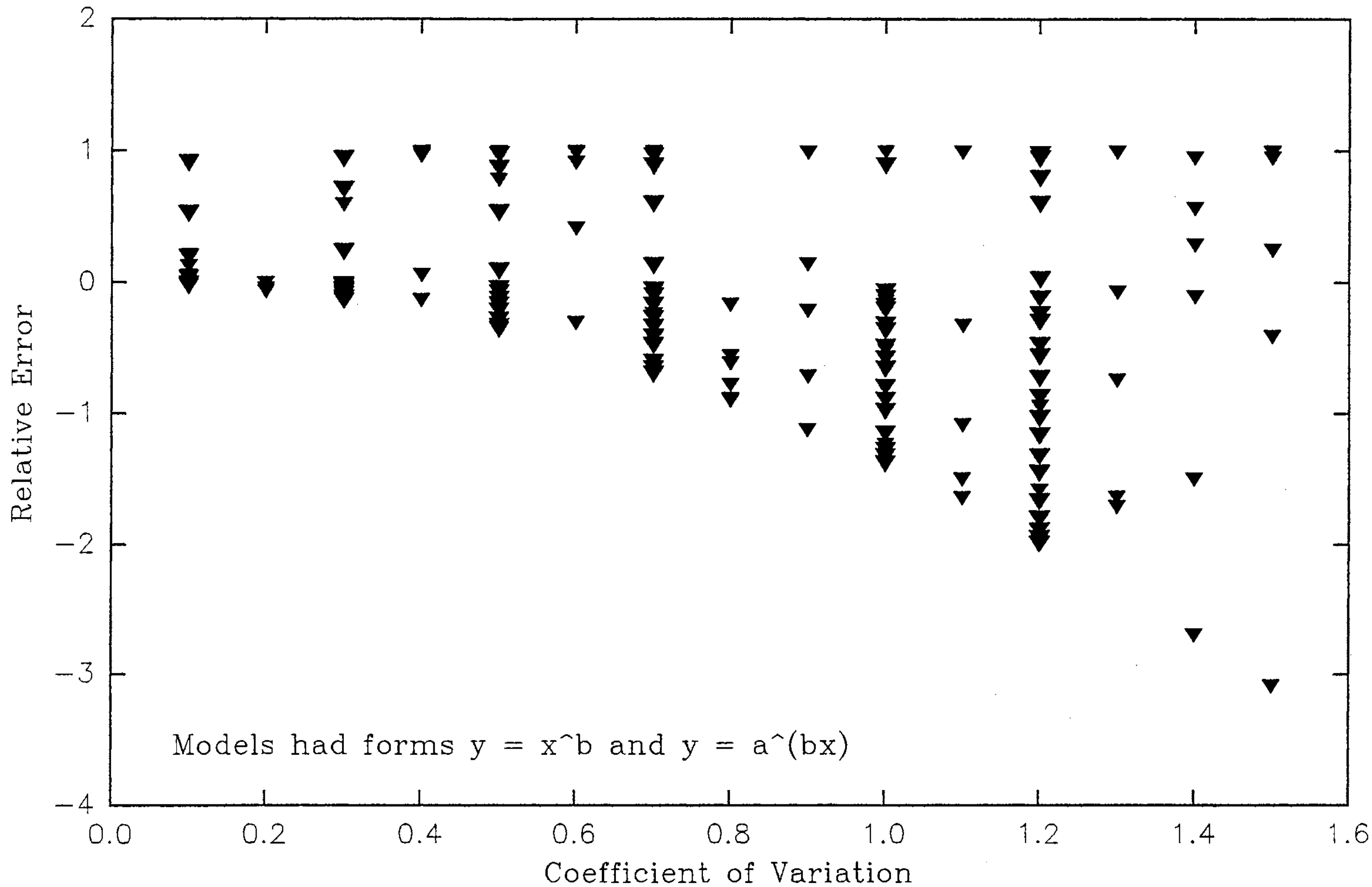

Figure 1−1. Plot of Error in Variance vs Cv

CHAPTER TWO

REVIEW OF LITERATURE

Literature reviewed in support of this study included works which addressed uncertainty and sensitivity analysis techniques in general, papers describing FO approximation procedures, studies comparing FO approximation results with MCS results, literature addressing quantification of model nonlinearity, various supporting statistical literature, and studies describing applications of FO analysis.

Several researchers have compared the accuracy, applicability, and computational demands of various sensitivity and uncertainty analysis techniques. Thomas (1982) discussed the use of Latin Hypercube sampling as a means of obtaining an output probability density function (PDF) and cumulative density function (CDF). An example was cited of a Latin Hypercube procedure requiring 200 model runs agreeing well with a MCS of 1000 model runs. He also describes the adjoint sensitivity analysis procedure, which yields a complete set of sensitivity coefficients for a set of simultaneous linear equations and a response function that is an explicit transformation of the solution of the set of linear equations. A procedure of this sort can be applied to a model utilizing a finite difference approximation that is linear in the parameters.

Doctor (1989) summarized various sensitivity and uncertainty analysis procedures. Sensitivity analysis techniques included using numerical approximations of partial derivatives, linear regression techniques, and the adjoint method. Uncertainty analysis methods appropriate for use with spatially correlated input variables included first and second order approximations, MCS, and "deterministic" uncertainty analysis. The Latin hypercube sampling method was suggested as a means of reducing the computational requirements of a simulation. For parameters which are not normally distributed and do not have a linear dependence, the use of a rank transformation to produce a correlated multivariate sample was described.

A number of works address the formulation of FO analysis procedures and the potential for errors in their use. Dettinger and Wilson (1981) formulated the FO approximation of the covariance matrix and the second order approximation of the mean of a vector of time and space dependent model outputs. They then applied this to transient and steady state piezometric heads found by numerical solution of the partial differential equations. They noted that if the second order mean was substantially different from the FO mean, this could be a sign that the nonlinearity was such that even a second order approximation would be unacceptable. They noted that the first and second order analysis procedure could be applied to nonlinear systems with reasonably small coefficients of variation and cited the 0.2 limit for coefficient of variation proposed in Benjamin and Cornell (1970).

Taylor (1985) looked at two examples of correlated parameters and the resulting error in a FO approximation of the variance of a function of these parameters. The first example was from a typical physics laboratory problem, where two angles are measured, and the errors in their measurements are perfectly negatively correlated. If a FO approximation of the experimental result which depends on these two measurements is computed neglecting the correlation, it will be too small by a factor of square root of 2.

The second example was the correlation between the linear regression coefficients

A and B in $\hat{y} = A + Bx$. These are negatively correlated in that an overestimated A will result in an underestimated B. The variances and covariance of A and B can be computed from the data used in the regression, and the variance of an individual prediction, $\hat{y}$, is a function of the variances and covariance, i.e.

$$\sigma_{\hat{y}}^2=\sigma_A^2+2x\sigma_{AB}+x^2\sigma_B^2 \tag{2-1}$$

where $2x\sigma_{AB}$ is the covariance term. This covariance term can be re-written as

$$\frac{-2\sigma_y^2}{N(\Sigma x_i^2-(\Sigma x_i)^2}x(\Sigma x_i) \tag{2-2}$$

By neglecting this covariance term, the summation of terms of the form xx_i is omitted from the computation of the variance, potentially resulting in significant error.

Asbjornsen (1986) used the function $K = \exp(-u)$, where u is a random variable, to demonstrate that eliminating the second and higher order terms of a TS expansion results in poor estimates of the variance of K. The TS approximation of the variance of K is

$$Var[K]=y^2+\frac{3}{2}y^4+\frac{7}{6}y^6+\frac{247}{576}y^8+... \tag{2-3}$$

where $y = E[u]\sigma_u$. If $y \geq 1$, or equivalently, if the coefficient of variation of u is greater than $1/(E[u]^2)$, then eliminating higher order terms can give a poor approximation of the variance of K.

Kuczera (1988) developed the distribution of model output for a hydrologic model given that the error model was an ARMA model, as opposed to a normal, mean-zero, constant variance model as used in least-squares estimation. The least-squares model is a special case of the ARMA model. An approximate distribution of model output based on the ARMA error model was developed. This approximate distribution used a FO approximation of the model output variance. The use of Beale's nonlinearity measure was suggested as a means of checking if the FOA variance will give satisfactory results. Beale's nonlinearity measure is a function of the difference between the actual model output and the linearized response computed for vectors of parameters sampled on the 90 percent confidence ellipsoid of the parameters, the variance of the residuals, and the number of parameters.

Numerous studies have been completed in which the results of a FO approximation have been compared with the results of a MCS. Song and Brown (1990) used the Streeter-Phelps equation as an example and compared the results of MCS and FO approximation to estimate model output variance when correlations between the model parameters were included or ignored in the analysis. The MCS results including the correlations were considered the "true" results to compare the others against. A multivariate normal distribution was used to generate the inputs. There were nine correlated parameters with C_v's ranging between 0.05 and 0.20. The highest correlation coefficients were 0.8 and 0.6.

They found that neglecting the correlations in the MCS understated the output standard deviation by approximately 13 percent on average. A FO approximation which considered correlations performed considerably better, with an average error of approximately 7 percent. Neglecting the correlations in a FO analysis resulted in a considerably higher error of 20 percent.

The nonlinearity of the Streeter-Phelps model varies and depends on the travel time. The FOA and MCS results agreed well, to within 10 percent, in the vicinity of the dissolved oxygen sag point, where the model is not highly nonlinear. When the travel time approached four times the travel time to the sag point, the MCS and FOA results differed by as much as 25 percent. This was attributed to model nonlinearity. There was no attempt made to quantify this nonlinearity, and it was stated that the significance of model nonlinearity would have to be resolved on a case by case basis.

Garen and Burges (1981) tested the accuracy of a FO approximation of model output variance using the Stanford Watershed Model. This was done considering several combinations of parameters as the uncertain parameters, and selecting C_v's between 0.0 and 0.6. The parameters were treated as uncorrelated, although three parameters were actually interrelated. The MCS was done including and neglecting the correlations with similar results. They concluded that this particular analysis was not sensitive to the correlations and ignored them.

The various test runs were ranked as to whether there was "good", "fair", or "poor" agreement between the variances estimate based on MCS and FO analyses. As the C_v of the parameters was increased, the number of "good" agreements decreased and the number rated as "poor" increased. They concluded that the C_v of parameters to which the model is sensitive should be no more than 0.25, with higher C_v's being acceptable for the less sensitive parameters. They also found that the FO analysis performed better with low intensity storms, which will produce a less nonlinear response. It was mentioned that the model was nonlinear, but no attempt was made to quantify the degree of nonlinearity and relate it to the performance of the FO analysis.

Bates and Townley (1988) studied FO analysis and MCS of prediction uncertainty of a flood event (hydrograph) model. They calibrated the two model parameters k and m by using 8 storm events for each calibration and determined the mean, standard deviation, and C_v for each parameter. The C_v's were small - 0.093 to 0.13. They used the intrinsic and parameter effects measures of nonlinearity of Bates and Watts (1980) to determine the nonlinearity of the model/data set. The parameter effects measures were in excess of the critical value, indicating a nonlinear model. The critical value adopted for both intrinsic and parameter effects is $1/(2\sqrt{F_{p,n-p,\alpha}})$ (Bates, 1988) where p is the number of parameters to be estimated, n is the number of samples used to estimate the parameter, and α is the exceedance probability. They calculated a FO mean and a second order mean and because of their similarity concluded that the degree of nonlinearity was mild.

There was very good agreement between FO, second order, and MCS results for the mean of peak discharge. The FO and MCS results for standard deviation of the peak discharge also agreed well. They concluded that the FO approximation performed satisfactorily when the nonlinearity was "moderate." They were not specific as to whether the Bates and Watts measure or the result of the second order approximation was the basis of their decision.

LaVenue, Andrews, and RamaRao (1989) used a finite difference groundwater flow and transport model. For their particular model, the FOA and MCS means and standard deviations of travel time agreed well. They commented that the simulation approach is preferable when the system is nonlinear or when there is a high degree of uncertainty in the parameters. They did not address the issue of quantifying the nonlinearity or parameter uncertainty.

Mishra and Parker (1989) compared the performance of a FO analysis with a MCS for an unsaturated flow model. Agreement between the two methods for the estimated water content standard deviation tended to be a function of water content. It was noted that the largest discrepancies occurred at the wetting front, where the sharpest gradients occurred. Their uncertain parameters were saturated conductivity and the parameters of the water content vs matric potential model proposed by VanGenuchten, which they incorporated into their model. The VanGenuchten model parameters had C_v's of 0.05 and 0.07. The C_v of K_s was 0.28. Except to cite the presence of the wetting front, an indirect reference to model nonlinearity, Mishra and Parker did not draw any other conclusions about the accuracy of a FO approximation.

Tung and Hathhorn (1988) used the Streeter-Phelps equation and found FO approximations of the mean, variance, skewness, and kurtosis of a critical location X_c (location of minimum dissolved oxygen concentration) in a stream reach. They then constructed normal, lognormal, Weibull, and gamma distributions for X_c, along with a distribution constructed using the Fisher-Cornish expansion. The parametric distributions use only the first two moments, the Fisher-Cornish expansion uses higher order moments. These distributions were compared to a "true" distribution derived by MCS. There appeared to be better agreement for the parametric distributions than for the Fisher-Cornish expansion. The conclusion was that a FO approximation of higher order moments would decrease in accuracy as model nonlinearity increased.

Huang (1986) looked at the uncertainty in the design of an open channel to carry the flow through a sluice gate. He used triangular distributions for the uncertain parameters, such as gate coefficient, Manning's n, gate submergence coefficient, and various geometry parameters, which were assumed to be independent. The FO mean and variance of the load (flow) and resistance (channel capacity) were calculated. The FO approximation of overall reliability (probability of not failing) was computed as 0.987 for load and resistance normally distributed and as .991 for load and resistance lognormally distributed. The result of a MCS was 0.997. The author did not speculate as to the cause of the error. The need to make distributional assumptions was cited as a problem with both procedures.

Protopapas and Bras (1990) used FO and MCS techniques to evaluate model prediction uncertainty for an unsaturated flow and transport model where the soil hydraulic properties were represented as random fields. The model used a linearized (finite difference) approximation. A mean and standard deviation of solute concentration were calculated at each time step and at each depth node. They used two C_v's for K. The FO means and standard deviations agreed much better with the MCS results for the lower C_v. Linearization errors associated with the larger variance were cited as a cause of discrepancy, but no quantification was suggested.

Sagar and Clifton (1983) proposed a groundwater flow and transport model in which inputs such as hydraulic conductivity, specific storage, or boundary conditions are considered random variables. The model uses a numerical approximation of the differential equation governing flow and transport. Outputs are hydraulic head and Darcian velocity fields, which are computed as a second order approximation of the mean of model output. The model also generates a FO approximation of the variance-covariance matrix of these fields. The model was applied to two test cases and the results compared to a MCS. There was good agreement between the hydraulic head fields for both test cases. The FO approximation of the variance-covariance structure resulted in overstated standard deviations of the hydraulic heads at each of the grid nodes. The approximate standard deviations were, on average, 22 percent larger for test case 1 and 18 percent larger for test case 2. The accuracy of the standard deviation prediction was concluded to be a function of the variances and covariances of the uncertain parameters, decreasing as the covariances increased. The paper did not address quantifying the nonlinearity or recommend limits for the covariances.

Sager (1984) reports application of the model to two test cases, using hydraulic conductivity as the only random variable. The cases were identical, except that test case 2 had greater uncertainty in the hydraulic conductivity. Model results were compared to MCS. For both test cases, there was good agreement for the hydraulic head field. The approximate variances and covariances were found to have decreasing accuracy as the uncertainty in the hydraulic conductivity increased. A maximum coefficient of variation of 1.0 was recommended, but it was also noted that the limit would be problem dependent.

Melching and Anmangandla (1992) compared FOA, MCS and advanced FO - second moment methods for constructing the CDF of dissolved oxygen deficit and critical oxygen concentration when the Streeter-Phelps equation is used to compute them. There was good agreement between the FOA and MCS results near the mean values of the uncertain parameters, but the agreement deteriorated as extreme values were approached. The uncertain parameters had C_v's ranging from 0.05 to 0.5. Problems cited with the FOA were failure to account for nonlinearity and inability to make use of the probability distributions of the uncertain parameters.

Smith and Charbeneau (1990) compared use of FOA and MCS with a coupled unsaturated - saturated zone contaminant fate and transport model. Site specific parameters were assumed to be uncertain and contaminant specific parameters were assumed to be known. Trials were done using a variety of contaminants. FOA means and variances tended to agree best with MCS results when the contaminant is strongly sorbed by soil. Model nonlinearity and uncertainty in site parameters were cited as the reasons for large errors, which occurred when the contaminant was easily leached. C_v's of the uncertain parameters ranged from 0.02 to 1.0. It was suggested that nonlinearity could be evaluated by comparing the function gradients at the mean and the mean plus or minus one standard deviation. If they differed by a certain percentage, the model was too nonlinear for FO analysis to be applicable. A range of 5 to 10 percent was proposed, but no specific examples of the test being used successfully were presented.

Three procedures for subjectively or numerically determining the degree of nonlinearity of model response were located in the literature. Kuczera (1990) recommended the use of response surface plots to evaluate model nonlinearity. The response surface is the plot of the squared differences between the actual response and the model response. With more than two parameters, Kuczera recommends taking them two at a time, such that the parameter space $\mathbf{\Theta}^T$ is partitioned as $\mathbf{\Theta}^T = (\mathbf{\Theta}_1^T, \mathbf{\Theta}_2^T)$, where $\mathbf{\Theta}_1$ contains the two parameters of interest and $\mathbf{\Theta}_2$ contains the remainder of the parameters. The variance-covariance matrix, $\mathbf{\Sigma}$, of $\mathbf{\Theta}$ is similarly partitioned

$$\mathbf{\Sigma} = \begin{bmatrix} \Sigma_{11} & \Sigma_{12} \\ \Sigma_{21} & \Sigma_{22} \end{bmatrix} \tag{2-4}$$

then $\mathbf{\Theta}_1 | \mathbf{\Theta}_2 = \hat{\mathbf{\Theta}}_2$ is distributed $N(\hat{\mathbf{\Theta}}_1, \Sigma_{1/2})$ where

$$\Sigma_{1/2} = \Sigma_{11} - \Sigma_{12}\Sigma_{22}^{-1}\Sigma_{21} \tag{2-5}$$

The linearized conditional probability region is the interior of the ellipse

$$(\mathbf{\Theta}_1 - \hat{\mathbf{\Theta}}_1)^T \Sigma_{1/2} (\mathbf{\Theta}_1 - \hat{\mathbf{\Theta}}_1) = 2\chi^2_{(2,\alpha)} \tag{2-6}$$

where $\chi^2_{(2,\alpha)}$ is the chi-squared value for two degrees of freedom and probability $(1-\alpha)$. In the event that this ellipse is extremely elongated in a direction not parallel to a parameter axis (as occurs when there are high correlations), a principal components rotation is recommended.

If the model is not highly nonlinear, there should be a contour in the response surface plot which matches the linearized conditional probability region. The interpretation of the deviation is somewhat subjective. The plot can provide additional information, however. For example, if the largest deviations are at the ends of a principal axes of the ellipse, the model is most highly nonlinear at the extreme high and low values of that parameter.

Beale (1960) proposed a nonlinearity measure for use in determining if model nonlinearity was too high for an approximate linearized confidence interval to be valid. Given a least squares estimate of the p-element parameter vector, $\hat{\boldsymbol{\Theta}}$, and a hyperplane tangent to the response surface at $\hat{\boldsymbol{\Theta}}$, the measure is a function of the squared differences between the response at other points in the parameter space, $\boldsymbol{\Theta}_i$, and the corresponding point on the tangent plane. The $\boldsymbol{\Theta}_i$'s could be obtained by using the intermediate results of the least squares fitting process or obtained through sampling. Using the 2p points at the ends of the principal axes of the 90 percent confidence ellipsoid in parameter space is another possible approach given. The measure is computed as

$$\hat{N}_\theta = ps^2 \frac{\sum_{i=1}^{W} [P(\boldsymbol{\Theta}_i) - T(\boldsymbol{\Theta}_i)]^2}{\sum_{i=1}^{W} [P(\boldsymbol{\Theta}_i) - P(\hat{\boldsymbol{\Theta}})]^4} \tag{2-7}$$

where P(•) is the model response and T(•) is the corresponding point on the tangent hyperplane, p is the number of parameters in $\boldsymbol{\Theta}$, and s^2 is an estimate of the variance of the residuals. The model is sufficiently close to a linear model if

$$\hat{N}_\theta < \frac{0.01}{F_{(\alpha,p,\nu)}} \tag{2-8}$$

where $F_{(\alpha,p,\nu)}$ is the F value corresponding to the α level of the test, with p degrees of freedom in the numerator and ν degrees of freedom in the denominator. ν is equal to n-p, where n is the number of data points used to estimate the parameter vector.

Bates and Watts (1980) proposed measures of intrinsic curvature and parameter effects curvature. Both these measures were functions of the first and second derivatives of the model with respect to the parameters, evaluated at the mean values of the parameters. Given a model $f(x,\mathbf{\Theta})$, n data points $(x_1,x_2,\ldots x_n)$ used to fit the model, and a vector $\mathbf{\Theta} = (\theta_1,\theta_2,\ldots\theta_p)$ of p parameters to be estimated, **V.** is an n x p matrix of the partial derivatives where the pth column is

$$\left(\frac{\partial f(x_1,\mathbf{\Theta})}{\partial\theta_p}\Big|_{\hat{\theta}},\ldots,\frac{\partial f(x_n,\mathbf{\Theta})}{\partial\theta_p}\Big|_{\hat{\theta}}\right)^T \tag{2-9}$$

The matrix **V..** is the n x p x p matrix of partial derivatives such that

$$v_{ijk} = \frac{\partial^2 f(x_i,\mathbf{\theta})}{\partial\theta_j^2\theta_k^2}\Big|_{\hat{\theta}} \tag{2-10}$$

Finding the QR decomposition of **V.** aswhere $\tilde{\mathbf{R}}$ is upper triangular, then the

$$\boldsymbol{V.} = \boldsymbol{QR} = \boldsymbol{Q}\left(\frac{\boldsymbol{R}_{pxp}}{\mathbf{0}_{n-pxp}}\right) \tag{2-11}$$

matrix **L** is the inverse of $\tilde{\mathbf{R}}$ and

$$\boldsymbol{U..} = \boldsymbol{L}^T\boldsymbol{V..L} \tag{2-12}$$

Considering **V..** as an n-high stack of p x p matrices, another n-high stack of p x p matrices is created by pre- and post-multiplying each p x p face of **V..** by the p x p matrices $\mathbf{L}^T$ and **L**.

A final n x p x p array is computed as

$$\boldsymbol{A_{..}}=\boldsymbol{Q}^{T}\boldsymbol{U_{..}} \tag{2-13}$$

The "top" p faces of **A..** form the parameters effects curvature array, $\mathbf{A}_{..}^{PE}$ and the final n-p faces form the intrinsic curvature array, $\mathbf{A}_{..}^{IN}$. Standardized relative curvatures can then be computed as

$$\gamma^{IN}=\|\boldsymbol{d}'\boldsymbol{A}_{..}^{IN}\boldsymbol{d}\| \tag{2-14}$$

$$\gamma^{PE}=\|\boldsymbol{d}'\boldsymbol{A}_{..}^{PE}\boldsymbol{d}\| \tag{2-15}$$

where **d** is a unit vector defining in which direction the curvature is being defined. The selection of **d** such that the relative parameter effects curvature or intrinsic effects curvature is maximized can be found by an iterative procedure described in Bates and Watts (1980).

Bates (1988) compared this measure with Beale's measure as applied to hydrologic modeling, and concluded that Beale's measure may understate nonlinearity, and that the measure of Bates and Watts was potentially more useful since it separated parameter and intrinsic effects. It was noted that the maximum relative curvature, either from intrinsic or parameter effects, was at least as large as the largest element of $\mathbf{A}_{..}^{IN}$ or $\mathbf{A}_{..}^{PE}$.

Works addressing response surface methodology and various other statistical procedures have also provided insight. An alternative method of uncertainty analysis based on experimental design generally referred to Taguchi's Method was evaluated and refined by D'Errico and Zaino (1988). The original Taguchi's method was based on a 3^n factorial design. Given n uncertain parameters for which the mean, μ_i, and standard deviation,σ_i, are known, the response $Y = f(X_1,X_2,\ldots X_n)$ is evaluated for all N possible combinations of $\mu_i \pm \sigma_i(3/2)^{1/2}$, where $N = 3^n$. The first four moments of system response are then computed as

$$m_1=\sum_{i=1}^{N}\frac{Y_i}{N} \tag{2-16}$$

and for k = 2 to 4

$$m_k=\sum_{i=1}^{N}\frac{(Y_i-m_1)^k}{N} \tag{2-17}$$

Taguchis's method was based on replacing the normal distribution of an uncertain parameter with a three point discrete distribution with equal mass at each point. This three point distribution will have the same first, second, and third moments as the $N(\mu, \sigma^2)$ distribution, but the kurtosis coefficient will be 1.5 instead of 3. The use of a three point distribution with a probability of 4/6 at μ and a probability of 1/6 at $\mu \pm \sigma\sqrt{3}$ will reproduce the first four moments of a $N(\mu, \sigma^2)$ distribution. The first moment is then computed as

$$m_1=\sum_{i=1}^{N} w_i Y_i \tag{2-18}$$

where the w_i's are 1/6 when Y_i is a function of $(\mu_i \pm \sigma_i\sqrt{3})$ and 4/6 when Y_i is a function of μ. For multiple parameters, the weights are multiplied, i.e. the weight for Y_i as a function of μ_1 and $\mu_2 + \sigma_2\sqrt{3}$ is the product of the weights, or $1/6 \times 4/6$. The higher moments are computed as

$$m_k=\sum_{i=1}^{N} w_i(Y_i-m_1)^k \tag{2-19}$$

The error in both Taguchi's method and the modification is, for a given function, dependent on the uncertainty in the parameters.

Downing, et al. (1985) compared the results of using a response surface methodology with the results of Latin Hypercube sampling. They concluded that a response surface was appropriate when a range of input values of interest was small, but that Latin Hypercube sampling performed better when the entire range of possible inputs was of interest. They noted that with a five point design of $\mu \pm 2n\sigma$ for $n = 0, 1, 2$ that the ratio of I_2/s was equal to a constant number, and that departures of this ratio from that constant were an indication of nonlinearity. I_2 represented the difference between the responses for minimum and maximum inputs, and s^2 was the sum of the squared deviations $[f(\mu + 2n\sigma) - f(\mu)]^2$. The paper also noted that the partial rank correlation can be used as a measure of the monotonicity in a relationship, with partial rank correlations approaching 1 in absolute value indicating a strongly monotonic relationship.

The FO approximation has been determined to be sufficiently accurate by some researchers to be used as the basis of their conclusions. Burges (1979) evaluated the uncertainty in flood fringe mapping as a function of the uncertainty in the discharge and hydraulic parameters. A FOA standard deviation of floodplain width was computed for various parameter uncertainties expressed as coefficients of variation. These approximations were considered to be sufficiently accurate since the coefficient of variation of any individual parameter was less than 0.2. This analysis showed significant uncertainty in the width of a flood plain, which should be recognized in any planning processes.

Loague and Green used a FO approximation to express the uncertainty of attenuation and retardation factors for pesticide leaching as a function of the uncertainty in soil characteristics and chemical parameters. They found considerable uncertainty (coefficient of variation close to unity) in both the attenuation and retardation factors for all soil orders evaluated. Within the taxonomic categories of a single soil order, the coefficient of variation of the retardation factor was found to decrease as lower categories were evaluated. The accuracy of the FO approximation for this situation was not addressed.

Scott (1993) used FOA to compute the coefficient of variation of the production of pipeline and hopper dredges. Several factors contribute to the uncertainty. Temperature and salinity changes result in uncertainty in water density. Difficulty in site characterization result in uncertainty in the density of the dredged and in-place sediment densities. Errors in measuring flow rates and volumes are another source of uncertainty, with increasing accuracy being associated with time and expense (i.e., more sophisticated equipment and calibration). The procedure presented would enable a user to evaluate which sources of uncertainty contribute most to uncertainty in the production computation and design an optimal instrumentation/site characterization program. FOA accuracy was not addressed in the published paper, but the uncertain parameters had low C_v's (0.1 maximum), so accuracy was not considered a potential problem (personal communication with S. Scott, August 1993).

CHAPTER THREE

THEORY

DERIVATION OF FIRST ORDER APPROXIMATION OF VARIANCE

The FO approximation of mean and variance as described in Benjamin and Cornell (1970) is based on the relationship

$$Var[y] = E[y^2] - (E[y])^2 \tag{3-1}$$

If y is a function of a set of random variables, y = $g(X_1, X_2, \ldots X_p)$, then y can be approximated by a TS expansion about the mean values of the X's as

$$y = g(X) \approx g(\overline{X}) + \sum_{i=1}^{p} \frac{\partial g}{\partial x_i}\Big|_{\overline{X}}(x - \overline{x}_i) + \frac{1}{2}\sum_{j=1}^{p}\sum_{i=1}^{p}\frac{\partial^2 g}{\partial x_j \partial x_i}\Big|_{\overline{X}}(x_i - \overline{x}_i)(x_j - \overline{x}_j) + \ldots \tag{3-2}$$

where the overbar indicates a mean value. The FO approximation of this is

$$y = g(X) \approx g(\overline{X}) + \sum_{i=1}^{p} \frac{\partial g}{\partial x_i}\Big|_{\overline{X}}(x_i - \overline{x}_i) \tag{3-3}$$

Using three properties of expected values, namely E[c] = c, where c is a constant, E[cX] = cE[X], where X is a random variable, and $E[X_1 + X_2] = E[X_1] + E[X_2]$, the FO approximation of the expected value of y is therefore

$$E[y] \approx E[g(\bar{X})] + \sum_{i=1}^{p} \frac{\partial g}{\partial x_i}|_{\bar{x}} E[(x_i - \bar{x}_i)] \qquad (3\text{-}4)$$

Since the expected value of (x_i - $\bar{x}_i$) is zero, this reduces to E[y] $\approx$ g($\bar{\mathbf{X}}$).

Similarly, the expected value of y^2 is

$$E[y^2] \approx E[g(\bar{X})^2] + \sum_{i=1}^{p}\sum_{j=1}^{p} \frac{\partial g}{\partial x_i}\frac{\partial g}{\partial x_j}|_{\bar{X}} E[(x_i - \bar{x}_i)(x_j - \bar{x}_j)] \qquad (3\text{-}5)$$

From equation 3-1, the FO approximation of the variance of y is

$$Var[y] \approx \sum_{i=1}^{p}\sum_{j=1}^{p} \frac{\partial g}{\partial x_i}\frac{\partial g}{\partial x_j}|_{\bar{X}} E[(x_i - \bar{x}_i)(x_j - \bar{x}_j)] \qquad (3\text{-}6)$$

Since E[(x_i - $\bar{x}_i$)(x_j - $\bar{x}_j$)] is equal to Cov[x_i,x_j] for i $\neq$ j and equal to Var[x_i] for i = j, this expression is typically written

$$Var[y] \approx \sum_{i=1}^{p} (\frac{\partial g}{\partial x_i}|_{\bar{x}_i})^2 Var[x_i] + 2\sum_{\substack{i=1 \\ i \neq j}}^{p}\sum_{j=1}^{p} \frac{\partial g}{\partial x_i}|_{\bar{x}_i}\frac{\partial g}{\partial x_j}|_{\bar{x}_j} Cov[x_i,x_j] \qquad (3\text{-}7)$$

ERROR IN FIRST ORDER APPROXIMATION OF VARIANCE

Given a function, y = g(**X**), where **X** is a vector of random variables with PDF f_X(**X**), the exact mean of y is

$$E[y] = \int_{x_1} \ldots \int_{x_p} g(x_1,\ldots,x_p) f_X(x_1,\ldots,x_p) dx_1 \ldots dx_p \qquad (3\text{-}8)$$

The FO approximation of the mean, g($\bar{\mathbf{X}}$), is not equal to this, but it may be a good approximation under some conditions. The second order approximation of y includes the terms of the TS expansion shown in equation 3-2. A second order approximation of the mean of y is

$$E[y] \approx g(\bar{x}) + \frac{1}{2}\sum_{i=1}^{p}\sum_{j=1}^{p} \frac{\partial g^2}{\partial x_i \partial x_j}|_{\bar{X}} Cov[x_i,x_j] \tag{3-9}$$

If the model is not highly nonlinear, the second and mixed partial derivatives will be small. If the parameters have small C_v's, the variances and covariances will be small compared to the means. Under either of these two conditions, the second term will be small compared to the first term, and a FO approximation will be reasonably accurate.

The exact variance of y is

$$Var[y] = \int_{x_1} \cdots \int_{x_p} [g(x_1,\ldots,x_p)]^2 f_X(x_1,\ldots,x_p)dx_1\ldots dx_p - (E[y])^2 \tag{3-10}$$

Geometrically, this amounts to the area under the surface defined by $[g(\mathbf{X})]^2 f_X(\mathbf{X})$ minus the square of the area under the surface defined by $g(\mathbf{X})f_X(\mathbf{X})$. The FO approximation will agree to the extent that the area under the tangent plane surface agrees with the area under the actual surface. This is best illustrated using a one parameter case as an example. The notation $x \sim LN(\mu, \sigma^2)$ indicates that x is lognormally distributed with distribution parameters μ and σ^2. The lognormal PDF is

$$f_X(x) = \frac{1}{\sqrt{2\pi\sigma^2}x}\exp(-\frac{1}{2\sigma^2}[\ln(x)-\mu]^2) \tag{3-11}$$

with $E[x] = \exp(\mu + \sigma^2/2)$ and $Var[x] = \mu^2(\exp(\sigma^2) - 1)$.

Let the parameter be a random variable X with a C_v of 1 and distributed lognormally $x \sim LN(0.347, 0.693)$. The expected value of X is 2.0, and the variance of X is 4.0. If the model is $y = x^2$, then the TS approximation of a linear surface is y $\approx$

4 + 4(x-2). The actual and linear surfaces are shown in Figure 3-1. The range of x values was selected as the range covering approximately 90 percent of the area under the PDF of x. There does not appear to be particularly good agreement between the two surfaces. Using the same X, but changing the model to $y = x^{1.1}$, results in better agreement, as shown in Figure 3-2.

The error in the variance is more precisely represented by the difference between the area under the $[g(\mathbf{X})]^2 f_X(\mathbf{X})$ curve and the area under the $[l(\mathbf{X})]^2 f_X(\mathbf{X})$ curve minus the difference between the squared areas under the $g(\mathbf{X}) f_X(\mathbf{X})$ and $l(\mathbf{X}) f_X(\mathbf{X})$ curves. Here $l(\bullet)$ represents the linear surface. The differences in the $[g(\mathbf{X})]^2 f_X(\mathbf{X})$ and $[l(\mathbf{X})]^2 f_X(\mathbf{X})$ curves for $y = x^2$ and $y = x^{1.1}$ are shown in Figures 3-3 and 3-4. Figures 3-5 and 3-6 illustrate the discrepancies between the $g(\mathbf{X}) f_X(\mathbf{X})$ and $l(\mathbf{X}) f_X(\mathbf{X})$ curves for the same two functions.

These figures show a larger discrepancy between areas for the more highly nonlinear model $y = x^2$, given the same uncertainty in X. The difference in the areas under the curves in Figures 3-5 and 3-6 also represents the differences between the exact means of the y's and the FO approximations of the means. For each model, this difference is smaller than the difference in areas under the curves for squared model and linear surfaces. It appears, therefore, that if the linear surface is satisfactory for approximating model response variance, it will also be satisfactory for approximating the mean of model output.

For these particular examples, the analytical and approximate means and variances compared as follows:

Model	Variance		Mean	
	Analytical	Approximate	Analytical	Approximate
$y = x^2$	956.111	64.000	8.000	4.000
$y = x^{1.1}$	6.513	5.560	2.227	2.144

This exercise demonstrates that a FO approximation can perform satisfactorily with a high parameter C_v if the model is not highly nonlinear, i.e. if the model response does not disagree "too much" with the linear fit. Any prediction of FOA variance accuracy will therefore have to address model nonlinearity.

This is further complicated by the fact that a nonlinear model is more or less nonlinear, depending on the range of the parameter space under consideration. The model in Figure 3-7 is $y = \exp(-x)$. If $X \sim LN(0.347, 0.693)$ with a C_v of 1.0, 99 percent of the area under the PDF of x is between 0.20 and 9.81. For a C_v of 0.25, with $X \sim LN(0.632, 0.061)$, 99 percent of the area under the PDF is between 1.05 to 3.34. The model is less nonlinear in the smaller range. The figure shows the much smaller discrepancy between the model and a linear surface when the smaller range is considered. Figure 3-8 shows the difference between the $[g(\mathbf{X})]^2 f_{\mathbf{X}}(\mathbf{X})$ and $[l(\mathbf{X})]^2 f_{\mathbf{X}}(\mathbf{X})$ curves when the two ranges are considered.

The same principles can be applied to multiple parameter models, although it is not really possible to illustrate this graphically. It is therefore apparent that a method to predict the accuracy of a FO approximation of model response variance must take into account parameter uncertainty, as reflected by C_v, model nonlinearity, represented by deviation from a linear fit or by some measure of curvature, or some combination of both these effects.

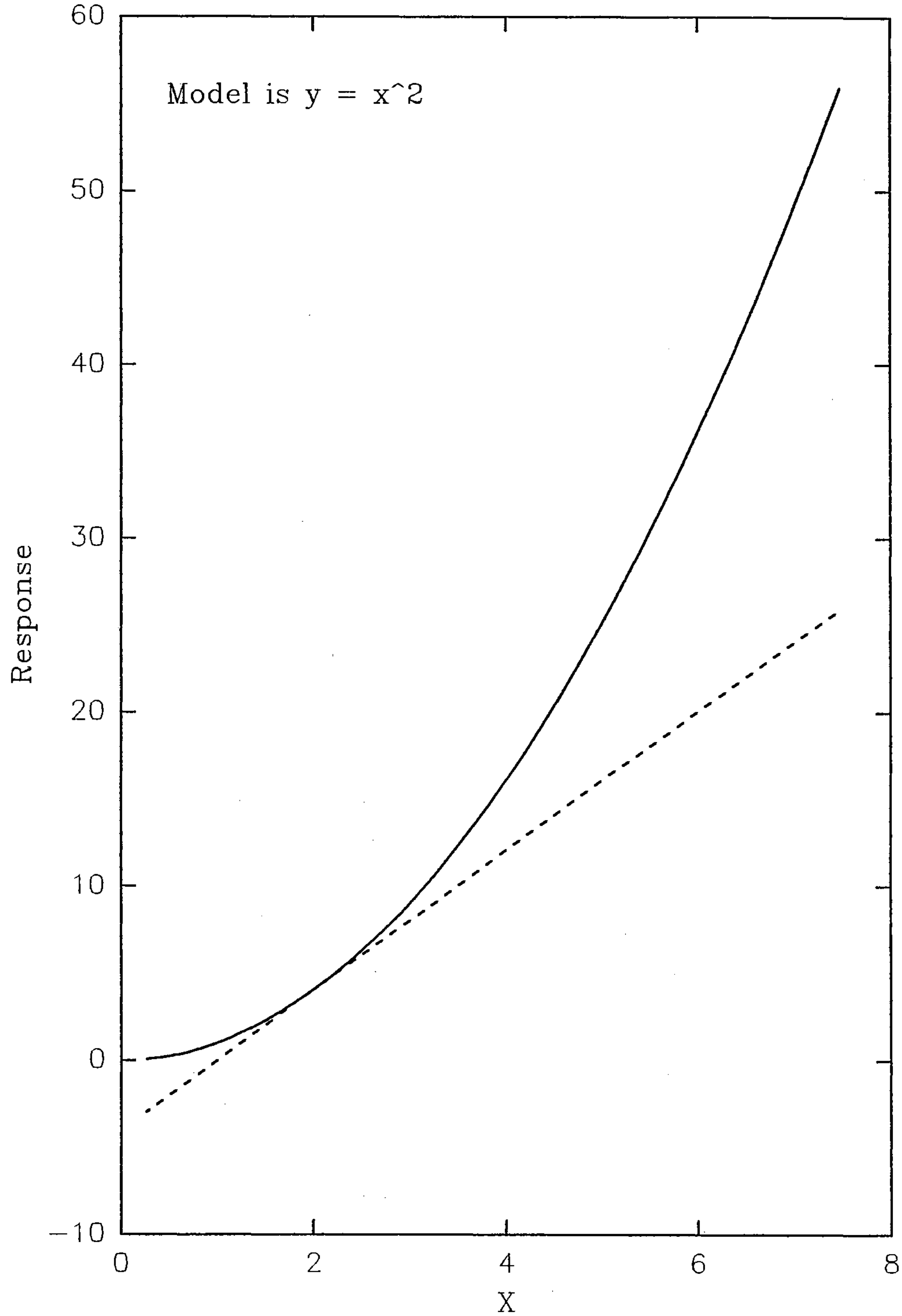

Figure 3−1. Comparison of Model and Linear Fit

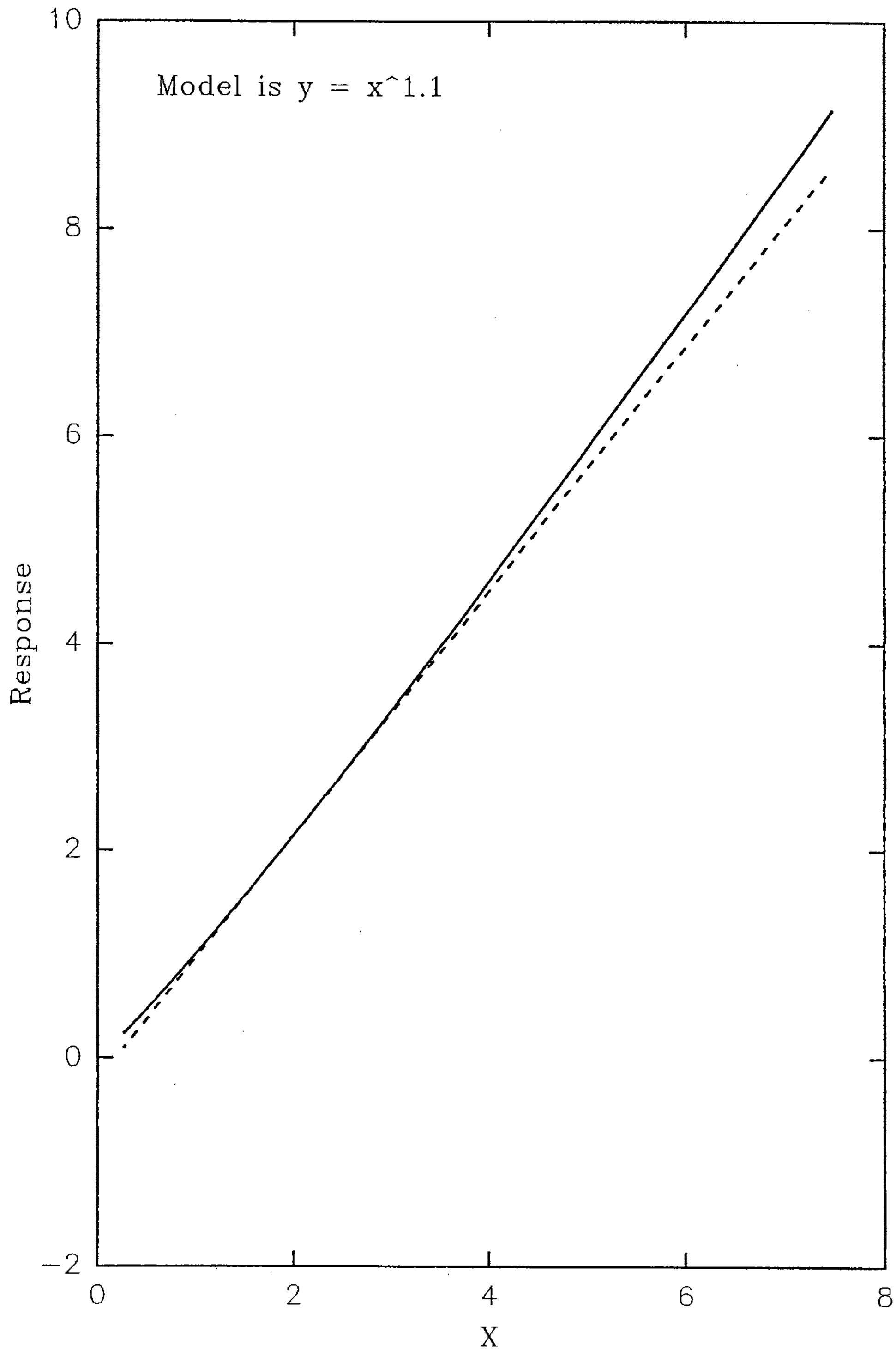

Figure 3–2. Comparison of Model and Linear Fit

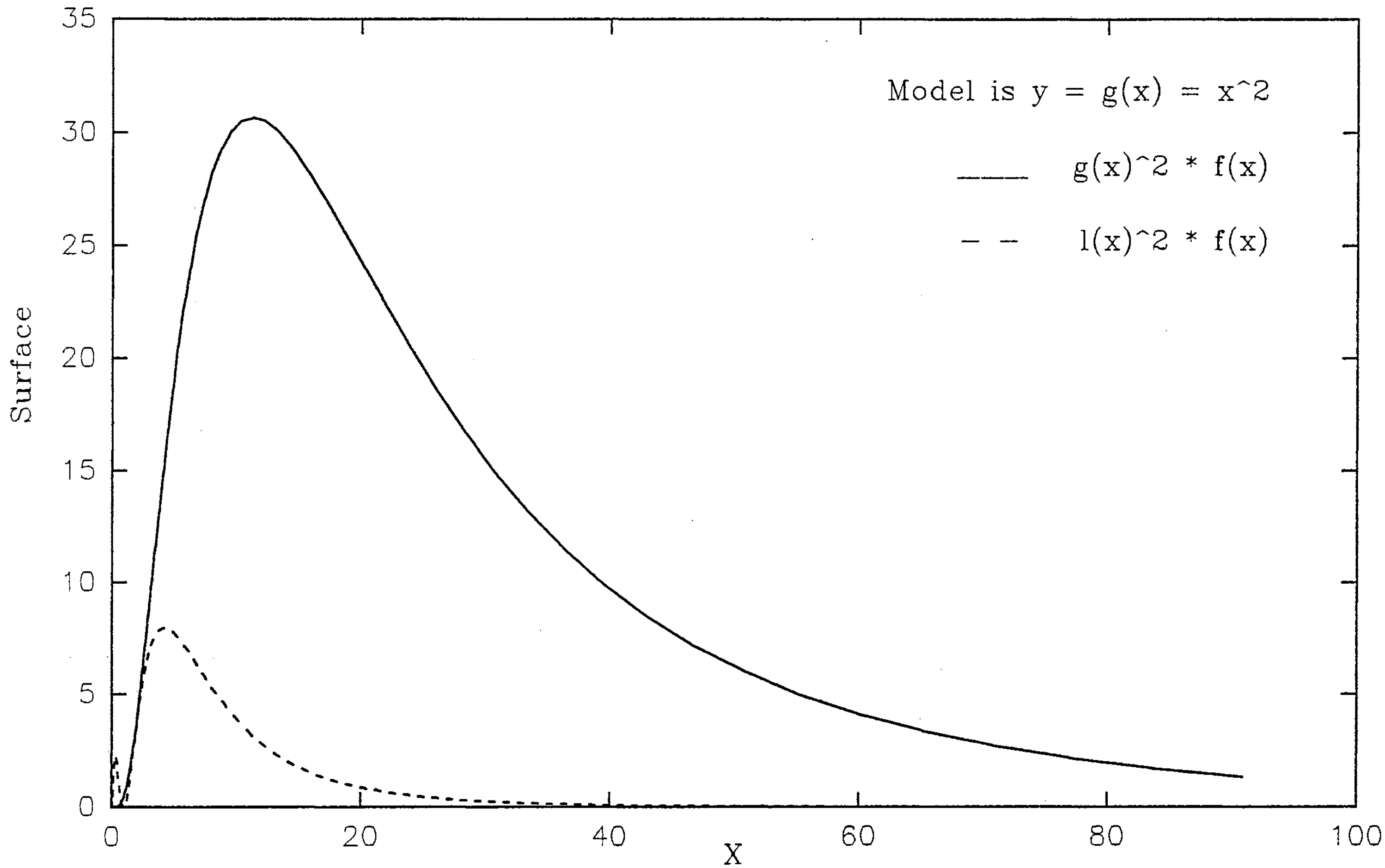

Figure 3-3. Comparison of Surfaces Defined by Model, Linear Fit, and PDF

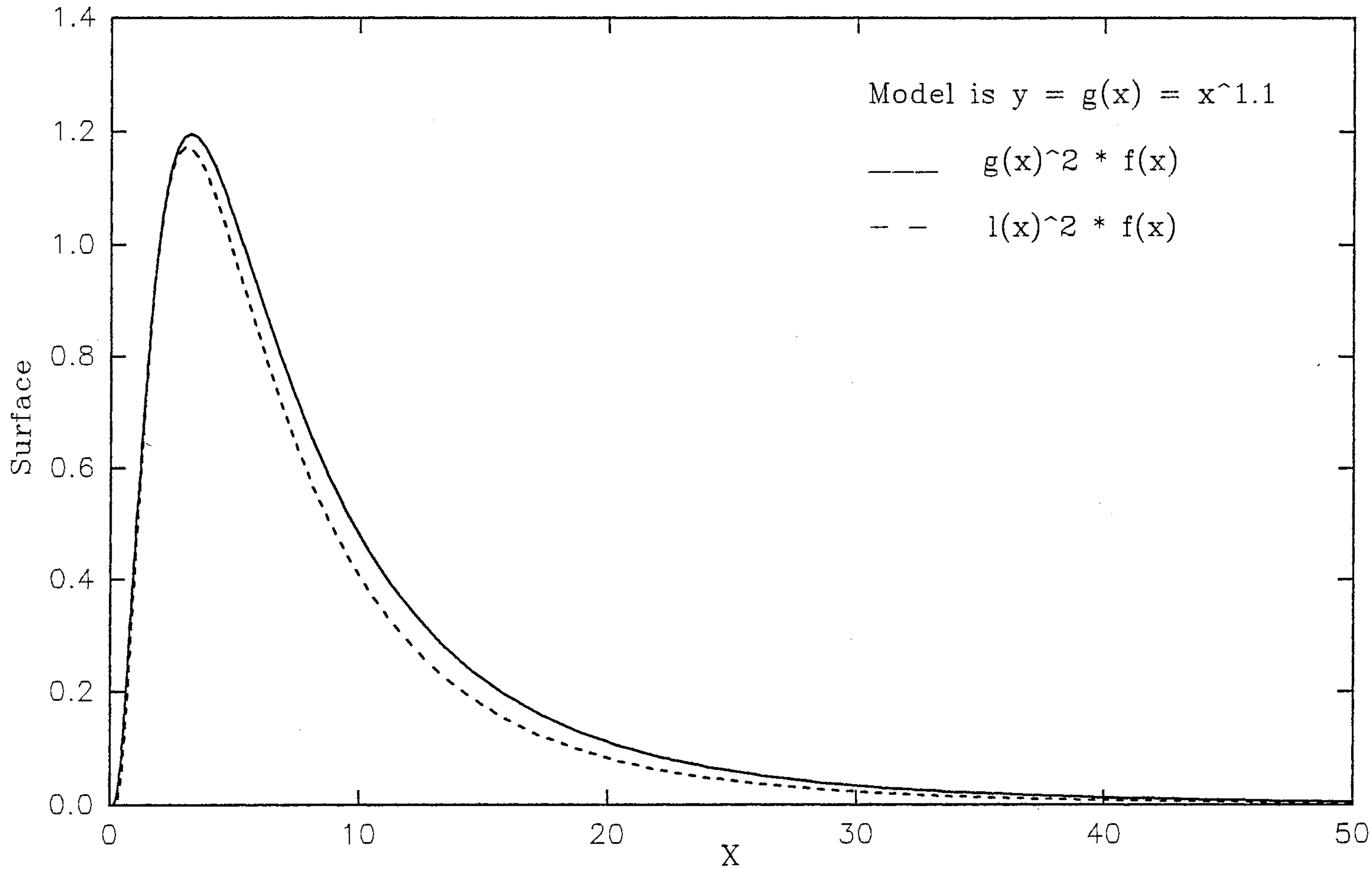

Figure 3-4. Comparison of Surfaces Defined by Model, Linear Fit, and PDF

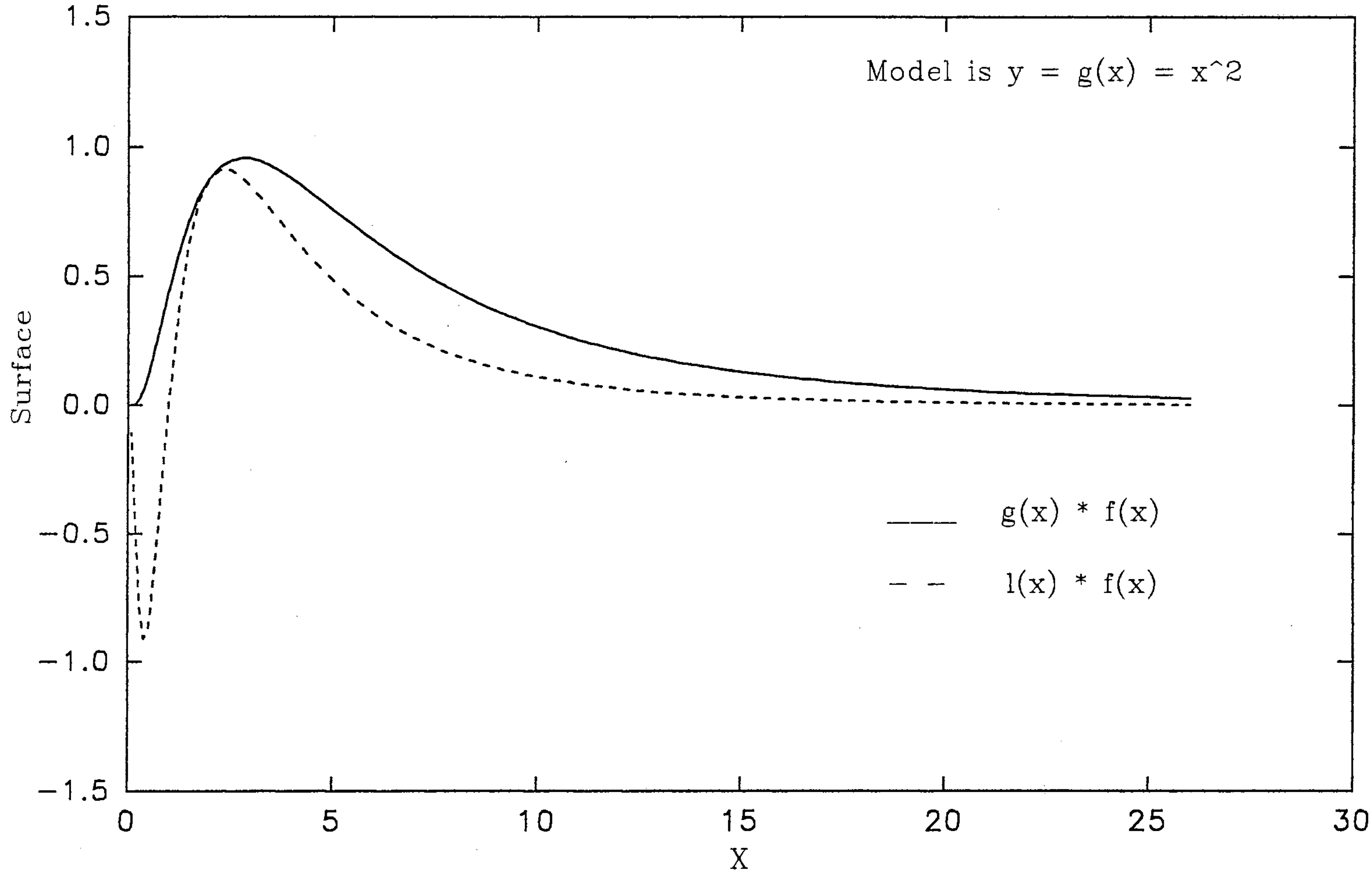

Figure 3-5. Comparison of Surfaces Defined by Model, Linear Fit, and PDF

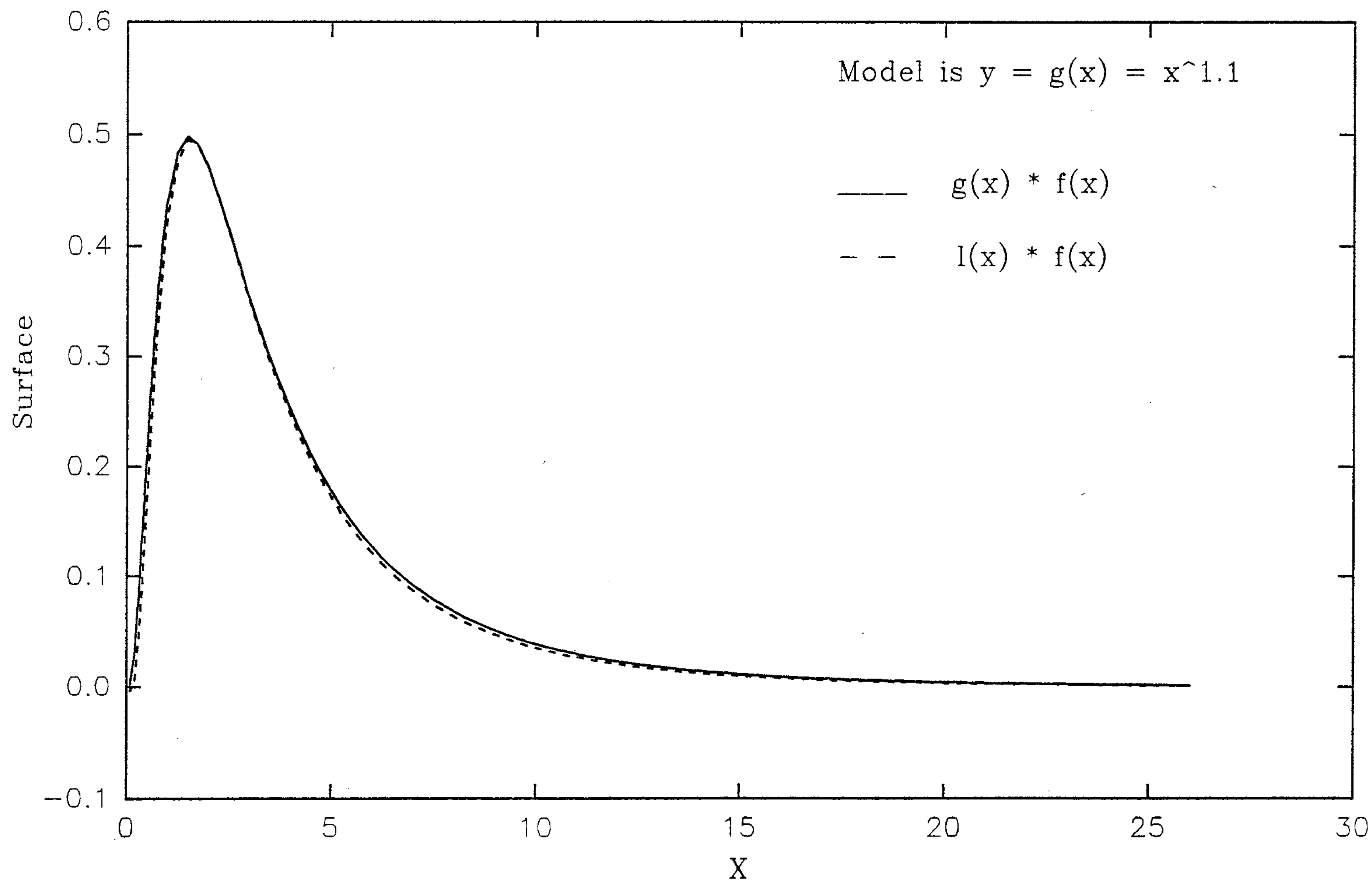

Figure 3−6. Comparison of Surfaces Defined by Model, Linear Fit, and PDF

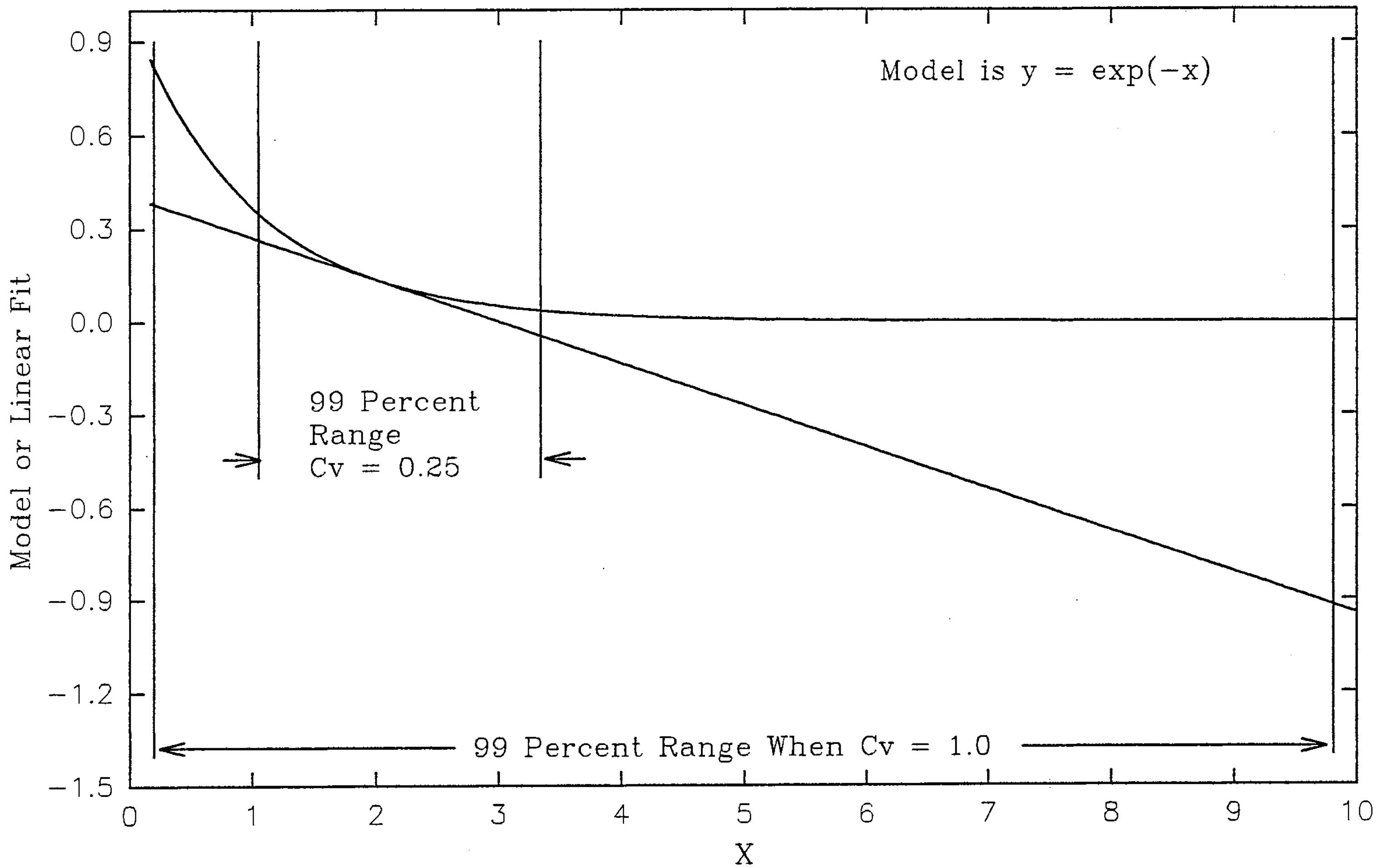

Figure 3–7. 99 Percent Probability Range for Cv = 1.0 and Cv = 0.25

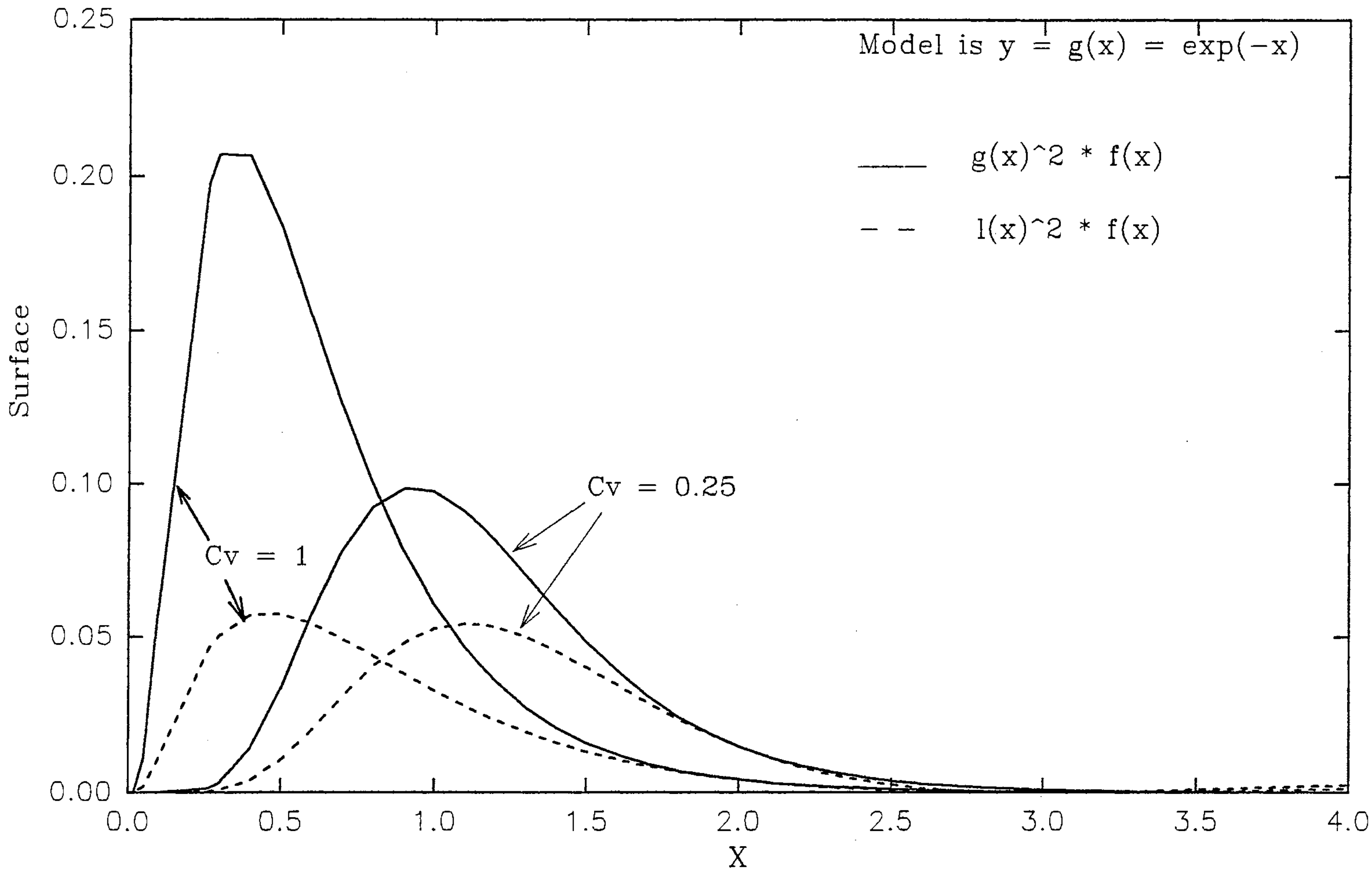

Figure 3–8. Comparison of Surfaces for Different Cv's of X

CHAPTER FOUR

ANALYSIS OF MODELS WITH ONE UNCERTAIN PARAMETER

APPROACH FOR FIRST ORDER ACCURACY PREDICTOR

Comparison of Analytical and Approximate Solution

The prediction technique was developed using FOA variances and analytical variances. Models with one and two uncertain parameters were evaluated in detail. Even though most hydrologic models have several uncertain parameters, the results presented here should still be useful. Sensitivity analysis makes it possible to identify a combination of parameters which are most uncertain and to which the model is most sensitive. An additional reason to restrict the analysis is that the processes of computing derivatives increases as the number of parameters increases. A point may be reached where this effort may equal that of a MCS. This work will not attempt to address how many parameters might represent that point.

Models which are explicit functions of the parameters and for which "analytical" variances could be derived were used to generate the data. Since, in general, closed form solutions to the integrals are not available, the term "analytical" solution will be used to refer to a numerical integration over the parameter space of the product of the model response (or model response squared) and the PDF of the parameters. The FOA variance was computed using the TS expansion as the linear surface.

The data were generated observing three constraints. First, the models were continuous and monotonic in all their parameters. This is not an unreasonable constraint since most models of natural systems respond monotonically to their parameters in the range of allowable parameter values. Exponential models of the form $y = a^{bx}$ and polynomial models of the form $y = x^b$ where x is the uncertain parameter were used.

The second constraint was that parameter C_v ranged between 0.1 and 1.5. Preliminary results indicated that if the parameter C_v was greater than 1.5, the FOA variance had significant errors, even with only mildly nonlinear models. Also, this represented a useful range for water resources modeling.

The final constraint was that numerical results either so large or so small that a significant loss of precision could be suspected were not used. Turbo C^{++} software was used to program an IBM compatible personal computer to perform the numerical integrations. The numerical quantities were assigned the type "double", allowing for 15 digit precision (Borland, 1991).

The models were selected to represent as wide a variety as possible of functional forms and degrees of nonlinearity, given the experimental constraints. For computing the analytical solutions, lognormally distributed parameters were used. This commonly used distribution allows for correlations and suitably represents parameter distributions in many hydrologic modeling applications.

Analysis of normally distributed parameters was also considered, but given the constraints, the choice of models is somewhat limited. Since the parameters can take on negative values, any functions with even powers will not be monotonic. Another result of the inclusion of negative values is that fractional powers cannot be accommodated. Functions which include division by the parameter (or a function of the parameter) will not be continuous. The normally distributed one parameter models are therefore restricted to forms such as exp(x), a constant raised to the power x, or odd-powered polynomials. This is a significant restriction, however, since many hydrologic models include expressions containing parameters raised to negative or fractional powers.

Using a lognormally distributed parameter allows the use of a more interesting and varied set of models, since there are no negative numbers to deal with. The lognormal analysis can include fractional and negative powers, and thus a wide range of model nonlinearity, from nearly linear as in $x^{1.05}$ to very nonlinear as in x^{-2}. The primary problem with the lognormal functions is with increasing functions. The upper tail of the lognormal distribution approaches zero much more slowly than the upper tail of the normal distribution. Thus, to cover the entire range of significant probability of the parameter it is quite possible to be dealing with very high values of the parameter. This can result in overflow errors and loss of precision in the numerical integrations for some power and exponential functions.

Analytical and Approximate Variance Data Generation

For each one parameter model, a set of parameter distributions covering the range of C_v's up to 1.5 was used. As broad a range of means was used as possible, but again the overflow and precision considerations dictated what mean and variance combinations could be used with each model.

The analytical mean and variance of the model response was found by numerical integration of equation 3-10, which requires numerical integration of equation 3-8. For functions of lognormally distributed parameters, the lower limit was initially taken as 0.01 and the upper limit was

$$UL = \exp(\mu + 4.5\sqrt{\sigma^2}) \tag{4-1}$$

where μ and σ are the lognormal distribution parameters. The trapezoidal rule was used. A step size of 0.01 was found to be extremely time consuming, so a step size of 0.05 was tried. The results agreed with the results for the smaller step size to six decimal places, so 0.05 was initially considered an acceptable step size.

Error data for certain decreasing function models did not behave as expected, however. For a given C_v, the computed error in FOA variance for some exponential models was larger with more nearly linear models than it was for some highly nonlinear models. The lower limit of integration was changed to 0.00001. Step size and upper limit of integration were adjusted until results for smaller and larger step sizes agreed to at least 12 decimal places. The error in FOA variance then responded as expected to C_v and model nonlinearity. The procedure adopted for decreasing function models with one lognormally distributed parameter was to set the upper limit as

$$UL = \exp(\mu + 6\sqrt{\sigma^2}) \tag{4-2}$$

and to make the step size equal to UL/500,000.

With rapidly increasing functions, such as $y = ax^b$ where b was greater than 2, as x increases the model response is increasing and the PDF is decreasing. The critical need here is to have the upper limit of integration sufficiently large that the incremental area computed from doing another step is insignificant. Preliminary calculations indicated that for b equal to 5 an upper limit of

$$UL = \exp(\mu + 16\sqrt{\sigma^2}) \tag{4-3}$$

was sufficiently large. A lower limit of

$$LL = \exp(\mu - 4\sqrt{\sigma^2}) \tag{4-4}$$

was also found to be satisfactory. Figure 4-1 shows a PDF times the square of $y = x^2$. This figure shows that the function is not highly nonlinear in the tail of the PDF. Thus, an accurate numerical integration can be carried out with larger step sizes. This is desirable since increasing the range would require increasing the number of steps from 500,000 to perhaps 1 or 1.5 million and would be exceptionally time consuming. However, in the region of the curve where the function is highly nonlinear, the smaller step size is still needed. One way to generate a variable step size is to base the step size on z and compute x as

$$x = \exp(\mu + z\sqrt{\sigma^2}) \tag{4-5}$$

where z ranges between -4 and 20. This was tried using a z step size of 0.005. The results were compared to the previous method using for an upper limit

$$UL = \exp(\mu + 20\sqrt{\sigma^2}) \tag{4-6}$$

and 1.5 million steps. The variances and errors agreed well with the relative errors (defined later) agreeing to three to four decimal places. The ability to use this procedure represented a substantial savings in computation time, with only 4,800 steps required for each numerical integration.

VARIANCE ERROR RESULTS FOR ONE PARAMETER MODELS

The variables of interest for use in formulating a predictor included the C_v of the parameter, the FOA variance from a TS expansion, the first derivatives computed to construct the TS approximation, and a set of parameter - response combinations.From this data, other data such as the area between the model response surface and the linear approximation were derived. The objective was to find something which could be readily computed from the available data and which correlated well with the error in the FOA variance. The various nonlinearity measures proposed in the literature were considered and several attempts were made to develop an original measure. The error in the FOA variance was computed as a relative error

$$error = \frac{analytical\ variance\ -\ FO\ variance}{analytical\ variance} \tag{4-7}$$

Predictors Found to be Unsuitable

The method in Kuzcera (1990) was rejected since it is subjective and the response surface contour plots will be time consuming to construct if the data has to be generated. Similarly, Beale's measure (Beale, 1960) was intended for use with a model that was fitted to experimental data, and required an estimate of the variance of the residuals, which may not be available with a physically based model. A variant of Beale's measure was tried using equation 2-7 but not multiplying by ps^2. For the models and parameter distributions tried, this did not correlate well with the error in a FOA approximation of the variance. Figure 4-2 displays the error vs Beale's measure. Exponential models of the form $y = a^{bx}$, where x is the uncertain parameter, were used. For this example, the x's were lognormally distributed and their C_v was 0.5. The scatter in the data shows that Beale's measure is not a useful predictor.

The intrinsic curvature portion of the Bates and Watts curvature measure (Bates and Watts, 1980, Bates, 1988) was also applied to the data. This did not correlate well with the error in a FOA approximation of variance. It had the additional disadvantage that the matrix of second derivatives was required.

Several other predictors were considered. Some of them required model responses at discrete points and some did not. Since it appeared that the area between the model response and the linear fit squared might be a good predictor, a nonlinearity measure that does not require evaluation of the model at discrete points was formulated as

$$L=\frac{\left[\int_{x1}^{x2}(g(x)-A-Bx)^2dx\right]^{\frac{1}{2}}}{\int_{x1}^{x2}g(x)dx} \tag{4-8}$$

where x is the uncertain parameter, x_1 and x_2 define the range of interest or the range of significant probability, and A and B are linear fit parameters which are found as

$$B=\frac{\int_{x1}^{x2}\frac{d}{dt}g(x)dx}{x2-x1} \tag{4-9}$$

and

$$A=\frac{\int_{x1}^{x2}(g(x)-Bx)dx}{x2-x1} \tag{4-10}$$

This measure appeared to correlate well with what is intuitively more or less linear (Figure 4-3). It did not, however, correlate well with the error in FOA variance, as the scatter in Figure 4-4 shows. The same models and parameter distributions shown in Figure 4-2 were used here. An additional disadvantage is that an integrable surface would have to be fit to the model response if the model was not an explicit function of the parameters.

Another approach which worked fairly well for normally distributed parameters used the slope between the model responses at the points $\mu \pm z_i\sigma$ where $\mathbf{z} = \{\pm 2.5, \pm 0.67, 0.0\}$. The difference between the slopes of the individual segments and of the overall slope along with squared and cross product terms and the error in the FOA variance were input to a step-wise regression program. A good fit, as indicated by correlation coefficient R^2 of 0.982, was obtained. Figure 4-5 shows the predicted vs true errors. The predictor model was then tried with a data set which had not been used in the regression with fair results as also shown in the figure. This approach was even less successful with lognormally distributed variables, however.

Another procedure was suggested in Downing, et al. (1985). Given a linear model, g(x), and a five point design of $x = \mu \pm n\sigma$ where n = (0,1,2), it was found that the ratio I_2/s was always equal to $4/\sqrt{10}$ or 1.2649. Here, I_2 is the range of the model, or $g(\mu+2\sigma)$ minus $g(\mu-2\sigma)$ and s^2 is computed as

$$s^2 = \sum_{n=-2}^{2} [g(\mu+n\sigma)-g(\mu)]^2 \tag{4-11}$$

Some preliminary work indicated that the departure of the ratio I_2/s from 1.2649 matched what intuitively was more or less nonlinear. Figure 4-6 shows these results. This departure did not correlate well with the error, as Figure 4-7 shows. The departure in the figure was computed as a relative departure - $(1.2649 - I_2/S)/1.2649$. The same models and parameter distributions were used as in Figure 4-2.

Since the error in variance is a function of the difference between the areas under the $[g(x)]^2 f_X(x)$ and $[l(x)]^2 f_X(x)$ curves, an attempt was made to approximate the $[g(x)]^2 f_X(x)$ surface by finding the model response and PDF evaluation at the five points in the 5-point design given earlier. This turned out to be a very poor approximation of the actual surface (Figure 4-8), and the difference between the area under the discretized surface and under the linear surface did not correlate at all with the error in the FOA variance.

A final idea came from Bates and Townley (1988). They proposed that a significant difference between the first and second order approximation (SOA) of the mean of a model response was an indication of a nonlinear model. The SOA will agree with the FO approximation if C_v's are small, i.e., a relatively small range of the function is of interest and the function will be more nearly linear the smaller the range under consideration. The other reason for agreement between the first and second order approximations is small second derivatives, which is an indication of a more nearly linear model. A relative difference, (FOA mean - SOA mean)/FOA mean, was computed using the same models and parameter distributions as used earlier. While it produced an interesting plot (Figure 4-9), it would not be a particularly useful predictor.

PREDICTION FACTORS FOR ONE PARAMETER MODELS

A preliminary data set was generated using a lognormally distributed uncertain parameter, denoted x. Exponential models of the form $y = a^{bx}$ and polynomial models of the form $y = x^b$ were used. The initial results showed that the errors behaved differently for different configurations of response. The configurations were classified as increasing concave-up, decreasing concave-up, increasing concave-down, and decreasing concave-down. What form the models take depends on the values of a and

b. Figure 4-10 shows the various forms and the restrictions on a and b required for the models to take those forms.

It was also obvious from the initial data that the polynomial forms behaved differently from the exponential forms. The reason for this may be in how the functions are bounded. Since the parameter, x, was lognormally distributed, x does not take on values less than or equal to zero. However, there are some differences in the way the polynomials and exponentials behave as x decreases and passes through zero. Considering the one term models $y = a^{bx}$ and $y = x^b$, there are both polynomial and exponential forms which are decreasing and concave-up (curve A in Figure 4-10). Both forms asymptotically approach zero as $x \to +\infty$. However, as $x \to 0^+$, the polynomial form goes to $+\infty$, as $x \to 0^-$, the polynomial form goes to $-\infty$, and the function is discontinuous at $x = 0$. The exponential form crosses the y-axis at $y = 1$ and then goes to $+\infty$ as $x \to -\infty$. Similarly, for increasing concave-down forms (curve B in Figure 4-10), both approach zero asymptotically as x increases, but the polynomial forms go to $-\infty$ as $x \to 0^+$ and the exponential forms cross the y-axis at $y = -1$.

The increasing concave-up forms (curve C in Figure 4-10) behave somewhat differently. Both are unbounded as $x \to +\infty$. The exponential forms cross the y-axis at $y = 1$ and go to 0 as $x \to -\infty$. For the polynomials, how the function is bounded as $x \to 0$ is a function of the power. If the power is not an integer, the function is a complex number for $x < 0$. With an even integer power, the function has a minimum at $x = 0$. With an odd integer power, the function approaches $-\infty$ as $x \to -\infty$. The same phenomenon occurs with the decreasing concave-down models (curve D in Figure 4-10), except that the sign of the function value is changed.

Thus, it was necessary to analyze them separately and also find a means of determining which form a response that was not an explicit function of the parameter (or a response that was a combination of exponential and polynomial terms) would take.

Model Classification

The ratio of the second to the first derivative behaves differently, depending on whether the form is exponential or polynomial. For exponential forms, $y = a^{bx}$, the ratio is equal to bln(a), regardless of which value of the parameter (x) is used to evaluate the derivatives. If the model output has a polynomial form, the ratio is not constant. However, the ratio divided by the value of x used to evaluate the derivatives will be constant for all values of x. For a one term polynomial of the form $y = ax^b$, the ratio divided by the value of x is equal to b - 1. These results only work to classify a response if it is strictly exponential or polynomial.

For responses which take on a "mixed" form such as $y = ax^b e^{-x}$ or $y = ax^b + ec^{dx}$, neither the ratio nor the ratio divided by x is constant across the values of x. However, for some models one form may be dominant.

If it is not obvious which form a model takes, one approach is to compute a set of parameter-response pairs and estimate models of the form $y = \text{constant} + ax^b$ and $y = \text{constant} + kc^{dx}$. A recommended set of parameter-response pairs is made up of $x_i = \exp(\mu + \sigma^2/2 + z_i\sigma)$, where $\mathbf{z} = \{\pm 2, \pm 0.64, 0\}$ and the corresponding y_i's. The response then is closest in form to the estimated model with an R^2 closest to unity. Most statistical packages, such as SYSTAT (Wilkinson, 1990), will estimate nonlinear models and provide the R^2. A visual inspection of plots of the response and estimated polynomial and exponential models can also provide insight as to whether or not the model can be classified. Another technique is to construct a semi-log plot with y on a logarithmic scale. If this plot is linear, the model is exponential.

Some models are truly "mixed", in which case neither the polynomial or exponential error estimating procedures work particularly well. If one fitted curve does not match a lot better than the other one, the model is probably "mixed". In this case, a conservative estimate of the error in the FOA variance can be obtained by assuming both forms and accepting the larger error. These model classification procedures will be evaluated in more detail in a later section covering the verification runs.

Results for Exponential Models

Exponential models with forms decreasing concave-up, increasing concave-up, increasing concave-down, and decreasing concave-down (A, B, C, and D respectively in Figure 4-10) were investigated. The models used to generate the predictors for the concave-up models were of the form $y = a^{bx}$. A constant multiplier is irrelevant since is does not change the magnitude of the relative error. Given a constant, k, and a model $y = ka^{bx}$

$$Var[ka^{bx}] = E[k^2a^{2bx}] - (E[ka^{bx}])^2$$

$$= k^2E[a^{2bx}] - (kE[a^{bx}])^2$$

$$= k^2\{E[a^{2bx}] - (E[a^{bx}])^2\}$$

$$= k^2(Var[a^{bx}]) \tag{4-12}$$

The FOA variance is

$$FO\ Var[ka^{bx}] = k^2[\ln(a)]^2 b^2 a^{2bx} Var[x]$$

$$= k^2\{FO\ Var[a^{bx}]\} \tag{4-13}$$

The relative error is

$$error = \frac{k^2\{Var[a^{bx}]\} - k^2\{FO\ Var[a^{bx}]\}}{k^2\{Var[a^{bx}]\}} \tag{4-14}$$

The k^2's cancel, so this relative error is equal to the relative error in the FOA variance of $y = a^{bx}$. This is also the case for the polynomial models.

Decreasing Concave-Up Models and Increasing Concave-Down Models

The models evaluated here are the exponential forms ($y = a^{bx}$) of curves A and B of Figure 4-10. For these models, the x's were lognormally distributed with means ranging between 0.25 and 50 and the x's had C_v's between 0.1 and 1.5. Table 4-1 is a summary of C_v's, means, and variances of x, and the corresponding lognormal parameters. A grid of a - b combinations was constructed, containing 15 models for which a was between 0 and 1 and b was greater than 0 and 15 models for which a was greater than 1 and b was less than zero. Additional a - b combinations were added later to smooth some curved plots.

The error can be computed either as a relative error (equation 4-7), which may be more useful in practice or as a simple difference between the analytical and FOA variances. The term "error" will be used to denote the relative error and "difference" will be used to denote the simple difference.

Both the relative error and the difference are functions of C_v of x (C_{vx}) and E[x], which determine the extent and location of the range of significant probability. They are also functions of a and b, which determine the degree of nonlinearity of the model. The sample correlation coefficient between two random variables is a measure of the strength of the linear relationship between the variables. Since model nonlinearity is important, it was considered worthwhile to select 5 x's, compute the corresponding y's, and compute the sample correlation coefficient ($r_{x,y}$) between the x's and y's. This is calculated as

$$r_{x,y}=\frac{s_{x,y}}{s_x s_y} \tag{4-15}$$

where s_x us the sample standard deviation of x, s_y is the sample standard deviation of y and $s_{x,y}$, the sample covariance between x and y is computed as

$$s_{x,y}=\frac{(\Sigma x_i y_i-\Sigma x_i \Sigma y_i/n)}{n-1} \tag{4-16}$$

The quantity n is the number of (x,y) pairs.

The five x's were selected as

$$x_i=\exp(\mu+\sigma^2/2+z_i\sigma) \tag{4-17}$$

where μ and σ were the lognormal distribution parameters and $\mathbf{z} = \{\pm 2, \pm 0.64, 0\}$. These are the same points recommended for the model classification procedure.

This sample correlation coefficient had to be computed to at least 6 decimal places to be useful. This is because a small difference in the correlation can indicate a large difference in the error. For example, if C_{vx} is 0.5 and the model is $y = a^{-x}$, for a = 1.1, the correlation is -0.99997 and the error in the FOA variance is -0.019. If a = 2.0, the correlation is -0.9984 and the error is -0.127. Thus, a -0.15 percent change in the correlation results in a 568 percent change in the error. For a given C_{vx}, $r_{x,y}$ was plotted against the error. The data plotted as a smooth curve with no scatter, indicating that $r_{x,y}$ in combination with C_v was a successful predictor. To make the plot easier to read and use, $r_{x,y}$ was transformed to a "correlation factor" as

$$factor = \ln(1 - abs(r_{x,y})) \tag{4-18}$$

Due to the way the points are picked, the factor is a function of C_v, E[x], a, and b. This is a further indication that it may be a suitable predictor. Figure 4-11 is a composite plot of error vs factor for all the C_v's. This shows that the maximum errors tend to become larger in absolute value as C_v increases, which is the expected result. There are also some unexpected patterns in these curves which will be analyzed in the remainder of this section. The composite curve requires too small a scale to be useful for predicting errors. Figures 4-12 through 4-18 give the curves for each value of C_v. Error predictions for other C_v's between 0.1 and 1.5 can be found by interpolation between curves.

Consider the exponential model $y = a^{bx}$. For a given a, as b increases the nonlinearity increases. The expected result is, therefore, that given a combination of C_v, E[x], and a, the error in the FOA variance will increase as b increases. This actually turned out not to be the case.

To further investigate the behavior of the difference as a function of C_v, E[x], a, and b, an analytical solution for the difference was formulated. To find values of a and b which gave maximum and minimum errors, the partial derivatives of the difference with respect to a and b were set equal to zero.

First noting that

$$E[y]=\int_0^\infty a^{bx}f_X(x)dx \quad and \quad E[y^2]=\int_0^\infty a^{2bx}f_X(x)dx \tag{4-19}$$

and

$$FO\ Variance=(\frac{dy}{dx})^2 Var(x)=[\ln(a)\,b\,a^{bE[x]}]^2\,Var(x) \tag{4-20}$$

then

$$diff=\int_0^\infty a^{2bx}f_X(x)dx-[\int_0^\infty a^{bx}f_X(x)dx]^2-[\ln(a)ba^{bE[x]}]^2 Var(x) \tag{4-21}$$

Using Leibniz' Rule to evaluate derivatives of an integral

$$\frac{\partial diff}{\partial a}=\frac{2b}{a}\int_0^\infty xa^{2bx}f_X(x)dx-\frac{2b}{a}\int_0^\infty a^{bx}f_X(x)dx\int_0^\infty xa^{bx}f_X(x)dx$$

$$-2\ln(a)b^2a^{(2bE[x]-1)}Var(x)\{1+\ln(a)bE[x]\} \tag{4-22}$$

and

$$\frac{\partial diff}{\partial b}=2\ln(a)\int_0^\infty xa^{2bx}f_X(x)dx-2\ln(a)\int_0^\infty a^{bx}f_Xdx\int_0^\infty xa^{bx}f_X(x)dx$$

$$-2[\ln(a)]^2ba^{2bE[x]}Var(x)\{1+\ln(a)bE[x]\} \tag{4-23}$$

Once these two equations are set equal to zero and some canceling and rearranging is done, they become identical

$$\frac{\partial diff}{\partial(a\,or\,b)} = \int_0^\infty x a^{2bx} f_X(x)dx - \int_0^\infty a^{bx} f_X(x)dx \int_0^\infty x a^{bx} f_X(x)dx$$

$$-\ln(a) b a^{2bE[x]} Var(x)\{1 + \ln(a) b E[x]\} \qquad (4\text{-}24)$$

It is theoretically possible to do this analysis using the relative error rather than the difference, but the resulting expressions would be so lengthy that it would be difficult to derive any useful information from them. While the difference behaves differently from the error with respect to the factor, it will change from positive to negative at the same point.

For b equal to zero, both the partial derivative and the error are equal to zero. For all a's and distributions of x, the evaluation of equation 24 (as a function of b) exhibited the pattern shown in Figure 4-19. The figure also shows that the b's for which equation 24 is equal to zero correspond to the minimum and maximum differences. The locations of these zeros, and the point at which the difference curve crosses the zero axis change as a function of a and the distribution of x. Given a C_v and E[x], the distribution of x is defined. As a increases the b's for minimum difference, maximum difference, and zero difference increase. For a given C_v and value of a, as E[x] increases the b's for minimum, maximum and zero differences all decrease. Given E[x] and a, the point of minimum difference is nearly the same for all values of C_v. The b's for zero and maximum difference increase as C_v increases. Figures 4-20 through 4-22 demonstrate these phenomena.

For all combinations of a and distributions of x, the (relative) error as a function of b exhibits the general pattern shown in Figure 4-23. For a given a and distribution of x, the error curve crosses the zero axis at the same location (value of b) as the difference curve. The b at which the minimum difference occurs is the same as the b for the minimum relative error. In Figure 4-23 the difference was so small with respect to the relative error that it was multiplied by 100 so the curve could be seen. Figures 4-24 through 4-26 illustrate the behavior of the relative error as a, E[x], and C_v change.

The pattern exhibited by the error and difference occurs as a result of the way the FOA variance is computed. Another way of expressing the FOA variance is

$$FO\ Variance = (slope\ of\ tangent)^2 \times Var(x) \tag{4-25}$$

with the slope evaluated at E[x]. Thus, how well the slope evaluated at E[x] represents the "overall" slope of the response determines how well the FOA variance performs.

For any exponential, decreasing concave-up model, the larger the exponent, the faster the response gets close to zero. Thus the slope of the response becomes nearly zero even at relatively small values of x, as shown in Figure 4-27. Given a large E[x], the slope of the tangent computed at that point will be quite small, and given a large b, the slope of the response throughout most of the range of significant probability may also be quite small. This is also illustrated in Figure 4-27, where E[x] is 5.0 and the range covering 99 percent of the area under the PDF is between 1.5 and 13.7. Thus, for large E[x], the slope of the tangent at E[x] becomes more representative of the overall slope as the exponent increases. In addition, for larger E[x], the slope of the tangent is smaller in absolute value than the overall slope, and both the difference and the error are positive.

For relatively small E[x], the slope of the tangent for the curve with the smaller exponent better represents the overall slope. This is shown in Figure 4-28, where E[x] is 0.5 and 99 percent of the area under the PDF is between 0.114 and 1.76. The figure also illustrates that the slope of the tangent is larger than the overall slope, so the difference and error are therefore both negative. As the exponent increases, the absolute value of the error increases.

If the mean falls right in the region of maximum curvature, an increase or decrease in the error will not correspond to an increase or decrease in the exponent. See, for example, Figure 4-29, where E[x] is 2.0 and the 99 percent range is 0.45 to 7.94. Here, it is not at all obvious which tangent would better represent the overall slope.

Since the correlation coefficient, $r_{x,y}$, is a measure of the strength of the linear relationship between x and y, it is expected that the error, or the absolute value of a negative error, would continue to increase as $r_{x,y}$ decreases (or as the factor increases). Figure 4-11 shows that this is not the case. Instead, as the factor increases, the error, which is originally negative, increases in absolute value, reaches a minimum, begins to increase, passes through zero, and has a maximum value of 1. Due to the way the error is computed (equation 4-7), 1 is the maximum possible positive error. The E[x] - a - b combinations closest to the point where the error changed from negative to positive were examined. It was found that the linear fit did not match the response well at all. Also, the $g(x)f_X(x)$ and $l(x)f_X(x)$ curves and the $[g(x)]^2f_X(x)$ and $[l(x)]^2f_X(x)$ curves did not match either. The variance, however, is computed as the difference between the area under $[g(x)]^2f_X(x)$ and the square of the area under $g(x)f_X(x)$. For each C_v - a - b combination, there will be a point such that if the tangent is computed at that point that difference will be equal even though the linear surface does not match the response. Theoretically, then, it is possible to identify points on the factor axis where the error is small, even though the model may be highly nonlinear. It should be noted, however, that the increasing portion of the error vs factor curve (Figure 4-11) is relatively steep, particularly for larger C_v's. When the factor falls in the increasing portion of the curve, predicted errors may not be particularly accurate since a very small change in the factor may result in a large change in the error prediction. It is recommended that the curve only be used to predict errors when the factor is less than the factor corresponding to the minimum point on the curve.

Increasing Concave-Up Models and Decreasing Concave-Down Models

A similar analysis was performed for increasing concave-up models and decreasing concave-down. The models considered were the exponential forms of types C and D in Figure 4-10. The same C_v's were used as in the previous analysis. The highest E[x] was 10, since higher values resulted in computer overflow errors and loss of precision for many of the models.

These models behaved differently from the type A and B models. In all cases, the difference and error was positive, i.e. the exact variance was always greater than the FOA variance. Also, the error always increased as the correlation decreased (or the factor increased). Figure 4-30 shows the curves for all the C_v's. The expected result of increased error with increased C_v is also demonstrated here.

The behavior of the difference and the error with respect to b was as expected. As b increased, the difference increased, as shown in Figure 4-31. Equation 4-24 was evaluated for four example models. For the values of b for which it was possible to get a solution (without overflow errors), the partial derivative was a strictly increasing function, which is also shown in the figure. As b increased, the relative error increased and asymptotically approached its maximum value of 1.0 (Figure 4-32).

For a given b, C_v, and E[x], as a increased, the relative error increased, approaching 1 asymptotically. For a given b, C_v, and a, as E[x] increased, the relative error exhibited the same behavior. Similarly, when given a, b, and E[x], as C_v increased, relative error increased and approached 1 asymptotically. This is demonstrated in Figure 4-33.

These results are due to the form of the response, the way the FOA variance is computed, and the extent of the range of significant probability for a lognormally distributed random variable. In taking a FOA variance, the assumption is that the slope of the tangent at E[x] is representative of the overall slope of the response. With a lognormally distributed random variable, the expected value of the random variable is to the left of center of the range of significant probability. For an increasing model of the form $y = a^{bx}$, the slope becomes increasingly steeper as x increases. Thus, the slope taken at E[x] will be flatter than the overall slope in the range of significant probability and a FOA variance will be less than the true variance.

Figure 4-34 shows the response curves for increasing values of a. As a increases, the slope increases more rapidly as x increases. The slope of the tangent at E[x] then becomes less representative of the overall slope as a increases, and the error in the FOA variance becomes larger.

Figure 4-35 illustrates how the range of significant probability changes as E[x] increases. Here, a and C_v are constant. The vertical bars delineate the ranges for 99 percent of the area under the PDF for each of the values of E[x]. There is obviously a larger discrepancy between the slope of the tangent and the overall slope for E[x] equal to 5.0 than there is for E[x] equal to 1.0. Thus, as E[x] increases, the error in the FOA variance also increases.

For a given E[x] and a, as C_v increases, the range of significant probability increases. This is shown in Figure 4-36. In this Figure, E[x] is 2.0 and the vertical bars indicate the range of 99 percent of the area under the PDF for each C_v. With each increase in C_v more of the rapidly increasing portion of the response is included in the range, and the slope of the tangent at E[x] becomes increasingly smaller than the overall slope. The error in the FOA variance will therefore increase as C_v increases.

Results for Polynomial Models

Polynomial models of the form $y = x^b$ were used to generate the error data. As shown previously for the exponential models, multiplication by a constant would not affect the error in the FOA variance. For all the one term polynomial models, the error data generated showed that the relative error was strictly a function of the power, b and C_{vx}. This differs from the behavior of exponential models, where the error is also a function of E[x]. This difference may be due to the way the slope of the response behaves throughout the range of x.

For exponential models ($y = a^{bx}$), the slope is finite (positive or negative, depending on whether the model is increasing or decreasing) at x equal to zero, and then approaches either zero or $\pm\infty$. For polynomial models, the slope is either zero at x equal to zero and then approaching $\pm\infty$ as x increases or the slope is $\pm\infty$ at x equal to zero and approaches zero as x increases. Thus for polynomials, the slope covers the entire range between 0 and either $-\infty$ or $+\infty$, whereas for exponentials it does not. Thus, for a given C_v and b, the divergence between the model and the linear fit (tangent) throughout the range of significant probability may result in the same error in variance regardless of where the tangent is computed.

In addition to being a function of b and C_v, the difference between the analytical and FOA variance was also a function of E[x]. For positive b, as E[x] increased, the difference increased. For negative b, as E[x] increased in absolute value, the difference increased.

The error vs b curve had the same general form for all values of C_v. For b sufficiently large or small, the error went to 1.0. As C_v increased, the error reached 1.0 at lower values of b. As b approached zero from the negative side, the error decreased and the curve crossed the zero axis. The crossing point was between -0.4 and -0.3 for all the C_v's considered. To investigate if the curves were actually matching well or if this was a computational artifact similar to that which occurred with the exponential function, several response and response squared times PDF curves were plotted, along with the corresponding linear fit times PDF curves. The function was $y = x^{-.34}$ and E[x] was 2.0. How well the curves matched up was a function of the C_v, with a good match being obtained for C_v equal to 0.1 and not particularly good matches for C_v's of 0.5 and 1.0. Figure 4-37 shows these curves. Similar curves were also plotted to look at the effect of E[x] (Figure 4-38). The same function was used and C_{vx} was 0.5. How well the curves corresponded did not appear to change as E[x] changed, confirming the previous observation based on computed errors that the error was a function strictly of b and C_v.

As b approached zero from either direction, the curve rose sharply (spiked) and then returned immediately to the path it had been tracing. To determine exactly what was occurring, errors were computed using b's of ± 0.01, ± 0.001, ± 0.0001, and ± 0.00001. Figure 4-39 shows the curves in the region of b equal to zero for selected C_v's. To ensure that the computations were accurate, the step size was halved so that there were 1,000,000 steps in each numerical integration. At b equal to zero, both the exact and FOA variances are equal to zero. However, the relative error is undefined, since it includes division by zero. Another way to express the relative error is

$$error = 1 - \frac{FO\ variance}{exact\ variance} \tag{4-26}$$

If the ratio of the FOA variance to the exact variance is approaching zero as b approaches zero, then the relative error will, in fact, go to 1.0. This ratio was computed for the various b's and is plotted in Figure 4-40. The figure shows that the ratio does approach zero as b approaches zero, so the relative error approaches 1.0 as b gets close to zero. Figure 4-39 also shows that the rise and fall back to the base curve is sharper for larger C_v's.

Once b is positive, the error decreases and reaches a minimum. This minimum was approximately 0.33 for all C_v's considered. The curve then crosses the zero axis at b equal to 1.0 and the error goes to 1.0 once b is sufficiently large. For b equal to zero, the error should be zero since the model is y = ax, which is linear. For this model, the TS linear fit will match the model exactly, so the FOA variance will equal the exact variance.

The procedure for predicting the error in the FOA variance for models classified as polynomial is to generate a grid of 5 parameter (x) and response combinations as $x_i = \exp(\mu + \sigma^2/2 + z_i\sigma)$ where $\mathbf{z} = \{\pm 2, \pm 0.64, 0\}$. A model of the form y = constant + ax^b is then fit to the five points. A number of commercial statistical packages will perform this operation. The b obtained from the curve fitting process is then used to enter the curve for the appropriate C_v and the relative error predicted. Interpolation between curves may be done, if needed. Figures 4-41 through 4-47 are the error vs b curves for selected C_v's.

Results of Verification Runs

Three sets of verification runs were completed. The models used as verification models had the forms

$$y=ax^{b}+cx^{d} \tag{4-27}$$

$$y=ea^{bx}+fc^{dx} \tag{4-28}$$

and

$$y=ax^{b}+ec^{dx} \tag{4-29}$$

Analytical variances were found by numerical integration and relative errors computed. Relative errors were then predicted based on model classification and either b or the factor. Linear interpolation between b's and factors was used to compute the predicted errors. Predicted relative errors were then compared with the actual relative errors.

For the models with the sum of polynomials form (equation 4-27), a test grid of 24 increasing function models was generated. The C_v's of x were 0.1, 0.5 and 1.0. These C_v's correspond to σ^2's of 0.00995, 0.22314, and 0.69315. The b's were estimated using SYSTAT (Wilkinson, 1990). Table 4-2 shows μ, σ^2, the model constants a, b, c, d, and the b power estimated by fitting this curve:

$$y = constant + ax^{b} \tag{4-30}$$

Of the 24 models in the test run, the predicted relative error was correct to within ± 0.01 in 19 cases (79 percent). The predicted error was correct to four decimal places in 10 cases (42 percent). For all but one of the cases for which the predicted error was more than ± 0.01 off, the actual and predicted errors were at least 0.67 and the predicted errors were off by no more than 0.03. In this range, the FOA variances are obviously unacceptable, so it is not quite so critical to predict the error to within ± 0.01. There was one case where the difference between the predicted and actual errors was greater than 0.01 and the error was in a range where it would be desirable to predict the error closely. Here, the actual error was 0.162, and the predicted error was off by 0.013. Table 4-2 also shows the actual and predicted errors.

A test grid of 21 decreasing sum of polynomial models was created. The fitted curve was estimated, and five cases were eliminated because the estimated power was less than -5. Actual and predicted errors were compared. In 10 out of 16 cases (63 percent), the difference between the actual and predicted errors was less than 0.01. In 6 of those 10 cases, the difference was less than 0.001. There were five cases (31 percent) with differences between 0.02 and 0.08, all with errors overpredicted. For two cases, the difference was approximately 0.20. The actual errors were -0.22 and -0.36 and the predicted errors were -0.44 and -0.57, respectively. This is a similar result to the result for increasing function models, where the more erroneous predictions were made in cases where the FOA variance would probably be rejected anyway. Table 4-2 also includes these results. Figure 4-48 is a plot of the actual vs predicted errors for all the sum of polynomial test runs.

A set of 18 decreasing and 14 increasing sum of exponential models (equation 4-28) was created. There were 18 increasing functions to start with, but overflow errors occurred during the numerical integrations, so four were eliminated. Table 4-3 gives μ, σ^2 and the model constants a, b, c, d, e, and f. The factors were computed and the relative errors computed.

Of the 18 decreasing function models, the difference between the actual and predicted error was less than 0.01 for 7 cases (39 percent), and less than 0.05 for 14 cases (78 percent). The largest difference was 0.11. For this case, the actual error was -0.22 and the predicted error was -0.33. The other three predictions which were off by more than 0.05 also involved errors with absolute values greater than 0.25. The error was overpredicted in all cases. As with the polynomials, these represent situations in which the FOA variance would probably be rejected anyway. The actual and predicted errors are also in Table 4-3.

Of the 14 increasing function models, the difference between the actual and predicted errors was less than 0.01 for 10 models (71 percent). For three other models, the difference was less than 0.02, so overall the difference was less than 0.02 for 93 percent of the models. For one model, the actual error was 0.96 and the predicted error was 0.562. The C_{vx} for this model was 1.0, the factor was -7.2, and this factor was in the very steep portion of the error vs factor curve. These results are also in Table 4-3. Figure 4-49 shows predicted vs actual errors for all the sum of exponential models.

There were 23 test cases of decreasing function mixed sums (equation 4-29). Curves of the form $y = \text{constant} + ax^b$ and $y = \text{constant} + ka^{bx}$ were fitted to the five recommended points. The R^2 from the regression was used to classify the models. Errors were predicted using both the polynomial and exponential methods. The model was then classified according to which method performed better. Using R^2, 19 models were correctly classified, two could not be classified, and two were incorrectly classified. The two models could not be classified because the R^2 from the exponential curve fitting was zero and polynomial curve estimation would not converge to a solution. Of the correctly classified models, 10 had prediction errors, i.e. predicted error minus actual error, less than 0.05 in absolute value. Five models had prediction errors between 0.06 and 0.1, and none had prediction errors with absolute values greater than 0.2. If an acceptable range for the error in the FOA variance is ± 0.2, there would only have been one case in which an acceptable FOA variance would have been rejected and none in which an unacceptable FOA variance would have been accepted.

For one incorrectly classified model, the error predicted using the polynomial method was 0.17 too large and the error predicted using the exponential method was 0.19 too small. Classification of this model was questionable since the R^2's were 0.999168 (exponential) and 0.999155 (polynomial). A clear choice between the two types of models was not really indicated. Choosing the larger (polynomial) error prediction of 0.41 would have most likely resulted in rejection of the FOA variance. The actual error was 0.24, which would also have probably been considered unacceptable by most users.

The other incorrectly classified model appeared clearly polynomial, with a polynomial R^2 of 0.999 and an exponential R^2 of 5E-11. The polynomial error prediction was -.084 and the actual error in the FOA variance was -0.253. In this case, a possibly unacceptably erroneous (but at least conservative) estimate of the variance would most likely have been accepted. Table 4-4 gives the actual error, errors predicted by both methods, R^2's from both curve fittings, factor, and estimated b power for all the models.

There were 18 test cases of mixed sums of increasing functions. Twelve models could be classified correctly by comparing the R^2 from the curve fitting. Three could not be classified, since the R^2 from both curve estimations was zero, and three were classified incorrectly. For the 12 classified correctly, the absolute value of the difference between the actual and predicted errors was less then 0.005. Again, assume that a reasonable limit on the error in the FOA variance is ± 0.2. For the three models incorrectly classified, basing an accept or reject decision on the predicted error would not have resulted in making an incorrect decision. Table 4-4 shows the actual error, errors predicted by both methods, R^2's from both curve fittings, factor, and estimated b power for each model. Figure 4-50 shows actual vs predicted error for the mixed models.

The test cases showed that extremely accurate error predictions could be made for models which are strictly polynomial or exponential. With mixed polynomial - exponential models, the R^2 from a curve fitting process was a good indicator of whether the form of the output was more closely exponential or polynomial. The error predictions were quite accurate when the models could be properly classified. If the purpose of predicting the error is to determine if the FOA variance is sufficiently accurate, and if the standard for acceptance is error between -0.2 and +0.2, then there were only two out of 36 test cases in which an erroneous accept/reject decision would have been made with the mixed polynomial - exponential models. Considering all models evaluated, only 2 out 113 erroneous accept/reject decisions would have been made.

SUMMARY OF ERROR PREDICTION PROCEDURE

The first step in the error prediction procedure is to classify the model. The model should be evaluated at the five recommended points, $x_i = \exp(\mu + \sigma^2/2 + z_i\sigma)$ where $\mathbf{z} = \{\pm 2, \pm 0.64, 0\}$. First and second derivatives should be evaluated at those points, either analytically or numerically. If the ratio of the second to first derivative is constant for all x_i, then the model is exponential. If the ratio divided by x_i is constant, then the model is polynomial.

If the derivative ratio is not conclusive, curves of the forms $y = \text{constant} + ax^b$ and $y = \text{constant} + ka^{bx}$ should be estimated. If either the polynomial or exponential curve clearly fits the data better, then that error estimating procedure should be used. If both curves appear to fit well and it is not clear which form the model takes, both procedures can be applied and the larger error accepted. For some models, the curve estimation process may not converge to a solution or the R^2's may both be very close to zero. For these models, it is not possible to predict the error in the FOA variance.

If the model is polynomial, the b power derived in the curve fitting process and C_{vx} are used to find the error in the FOA variance. Curves giving error vs b are provided for selected C_v's. It may be necessary to interpolate between curves. If the b power has an absolute value greater than 5, then the accuracy of the FOA variance is highly questionable. This is also the case for C_v's greater than 1.5.

If the model is exponential, the correlation factor is computed using the x's and y's at the five recommended points. Curves giving factor vs error are provided for selected C_v's. It may be necessary to interpolate between curves. If the factor is in the steeply rising portion of the error vs factor curve, then the error prediction and the accuracy of the FOA variance may be questionable. Again, if C_{vx} is greater than 1.5, the FOA variance will not be accurate.

RESULTS OF EXAMPLE APPLICATIONS

The procedure was tested using two models for which the output is not an explicit function of the parameters. One model computes the sediment washoff from urban streets. The other routes a flood hydrograph through a reach of river using the kinematic wave approximation.

The sediment washoff model uses the Soil Conservation Service (SCS) curve number method (SCS, 1972) to calculate the runoff in 10-minute increments resulting from a 10-year, 1-hour storm. The total rainfall near Stillwater, Oklahoma, for this event is 2.7 inches, with incremental values for six time steps selected as 0.32, 0.79, 0.63, 0.48, 0.32, and 0.16 inches. This rainfall was considered to have no uncertainty.

A hypothetical urban area with 1700 square foot, single family dwellings on 1/4 acre lots was assumed. The 160 acre watershed had 32 acres in woods (SCS curve number 55), 108 acres in lawns (SCS curve number 61), and 40 acres of roadway and roof surface. Thirty acres of the road and roof surfaces were directly connected to the drainage system. SCS Curve number for the directly connected impervious areas was 98. Runoff was generated by computing the runoff from impervious and pervious areas separately and summing to get the total runoff for each time increment.

The washoff equation used in United States Geological Survey model DR3M (Alley and Smith, 1982) was used to model washoff of sediment from the impervious areas. The weight of pollutant (tons) washed off during a time step is

$$W = L_o[1 - \exp(-K_3 R \Delta t)] \tag{4-31}$$

where L_o is the weight of the pollutant of interest on the impervious surfaces at the beginning of the time step, R is the runoff rate (inches/hour) during the time step, and Δt is the length of the time step (hours). K_3 is a rate constant, which is estimated via calibration. Runoff rate is computed for each time step. L_o is known from the previous time step. Washoff is computed, and L_o is adjusted to start the next time step.

Alley and Smith (1982) recommend 4.6 inches^{-1} as an initial starting value for K_3. For the illustration, K_3 was taken as the uncertain parameter, lognormally distributed, with mean 4.6, and C_v's of .1, .25, .5, and 1. The initial weight of sediment on impervious surfaces was taken as 50 tons for convenience. Since the model is linear in that parameter, its actual value does not affect the accuracy of a FOA variance.

Each of the C_v - mean combinations defines a distribution for K_3. A random sample of 10,000 K_3's was drawn from each distribution. This was established to be a sufficient number of samples as part of another study (Stevens and Haan, 1993). The cumulative washoff for the duration of the storm was computed using the 10,000 K_3's in each sample. The variance of the generated output was accepted as the "true" variance of the model response.

The model was run at the five points found as $K_3 = \exp(\mu + \sigma^2/2 + z\sigma)$ where $z = \{0, \pm 0.64, \pm 2\}$ and μ and σ are the lognormal distribution parameters corresponding to the mean and variance of K_3. The model was also run using values of K_3 which were 0.99 and 1.01 times the five K_3's to generate the results needed to compute the first and second derivatives. The ratio of the second derivative to the first derivative was 0.64 at all five points for all four distributions of K_3, indicating an exponential model. For C_v of K_3 equal to 0.1, the estimated exponential model was W = 50.00 - 50.00 × $2.704^{-0.646K3}$. Figure 4-51 is a plot of the five K_3 - model output pairs and a smooth curve plotted using the estimated exponential model. Visual inspection of this plot indicates that the model output has the correct exponential form. The estimated exponential models for the other C_v's of K_3 had nearly the same constants. All estimated models had an R^2 equal to 1.000000.

FOA variances were computed based on the four distributions for K_3 and compared to the variances derived via simulation. The results are shown in Table 4-5. The correlation between five model outputs and K_3's was computed. The correlation factor used to predict the error for exponential functions was computed and the error in the FOA variance predicted. It was necessary to interpolate between the curves for C_v equal to 0.1 and C_v equal to 0.3 to find the predicted error for C_v equal to 0.25. Figure 4-52 illustrates use of the curves to predict the error. The factors and predicted errors are also in Table 4-5. The predicted errors compared very well with the actual errors, with the maximum difference being 0.017.

The second model used the kinematic wave approximation to route an inflow hydrograph through a reach of river. A forward difference scheme was used to find the simultaneous solutions of the continuity equation

$$\frac{\partial Q}{\partial x}+\frac{\partial A}{\partial t}=0 \tag{4-32}$$

and Manning's equation

$$Q=\alpha A^{\beta} \tag{4-33}$$

where β is equal to 5/3 and

$$\alpha=\frac{\sqrt{S_f}}{np^{\frac{2}{3}}} \tag{4-34}$$

S_f is the friction slope, p is the wetted perimeter, and n is Manning's roughness coefficient. Substituting equation 4-33 into the continuity equation and using a forward difference approximation of the partial derivatives gives

$$\frac{(\alpha A_{i+1,j+1})^{\beta}}{\Delta x}+\frac{A_{i+1,j+1}}{\Delta t}-\frac{(\alpha A_{i,j+1})^{\beta}}{\Delta x}+\frac{A_{i+1,j}}{\Delta t}=0 \tag{4-35}$$

Figure 4-52 is a diagram of the grid in the x-t plane. The step size in the x direction was 1 mile (5,280 feet). The step size in the t direction was 6 hours (21,600 seconds).

The unknown in equation 4-35 is $A_{i+1,j+1}$ and the equation is nonlinear in that quantity. An interval bisecting method was used to solve the equation. Once $A_{i+1,j+1}$ is found, $Q_{i+1,j+1}$ can be computed from equation 4-33. The peak flow at the end of the reach of river was selected as the model output of interest for the example.

For convenience, a wide rectangular channel was selected. The channel was one half mile wide (2640 feet) and had a bottom slope of 0.004 feet/foot. The Manning's roughness coefficient (n) was the uncertain parameter. The n-value of 0.025 recommended for clean and straight natural river channels (Henderson, 1966) was used as the mean of n. A lognormal distribution for n was assumed. C_v's of 0.1, and 0.25 were selected to define the distributions of n. The base flow was assumed to be 500,000 cubic feet per second (cfs). The inflow hydrograph was a simple triangular hydrograph, peaking at 2,000,000 cfs in 60 hours (2.5 days) hours and returning to base flow at 120 hours (5 days). The river and storm properties are not intended to represent any real places or events. This is merely an example to illustrate the technique.

The simulation was first run with 2000 samples. To test if 2000 samples were sufficient for the simulation to converge to a true solution the mean and variance were found using the first 1000 generated outputs (simulation 1), the first 1500 generated outputs (simulation 2), and the entire sample of 2000 (simulation 3). If the percent change in the variance between simulation 1 and simulation 2 and between simulation 2 and simulation 3 was less than 1, then the 2000 samples would be considered adequate. The percent changes were 1.2 and 3.4 respectively. Additional groups of 500 samples were generated and added on, and the percent change between the original group and group plus 500 computed. This was continued until the percent change for two successive groups was less than 1. This occurred when the entire sample had 5000 members. The percent change in variance between a sample of 4000 and 4500 members was -0.21. The percent change between the 4500-member and 5000-member samples was 0.07. Thus, 5000 runs was determined to be an adequate number for a valid simulation.

The model was evaluated at the five recommended points and at the recommended points plus and minus one percent to assess the form of the output. Neither the ratio of second to first derivatives or that ratio divided by n was constant. The FOA variance was computed using the numerical first derivative evaluated at the mean. The FOA variance was found to be 7,116,837. The variance by simulation was 234,828,478, and the relative error was 0.97. A visual inspection of the model output vs n curve (Figure 4-54) indicated that the model was not highly nonlinear, and this great of an error might be questionable. It was felt that the step size used for taking the numerical derivatives should be evaluated in more detail. Accordingly, step sizes ranging between 0.0005 and 0.01 were used. Model outputs were generated so the derivative at the mean of n could be evaluated using either a two-point central difference or four-point central difference approximation. The step size for which the two agreed most closely was 0.006. The four-point approximation of the first derivative with respect to n was -6,252,159. Using this gave a FOA variance of 241,240,305 and a relative error of -.027. This was much more reasonable, given that the model was not particularly nonlinear in n.

To further check whether 6,252,159 was a reasonable approximation of the first derivative, a linear model was estimated using the five recommended points. The estimated slope was -6,285,380. Again, given that the model was not highly nonlinear, this is further evidence that the original first derivative of -1,067,096 was not accurate. The R^2 of the estimated linear model was 0.99, confirming that the model is not highly nonlinear in n.

Using the new step size of 0.006, the first and second derivatives were repeated. Again, neither the ratio or ratio divided by n was a constant. Since the derivatives were not useful for classifying the model, the SYSTAT (Wilkinson, 1990) statistical software was used to estimate models of the form

$$\hat{Q} = constant + an^{b} \tag{4-36}$$

and

$$\hat{Q} = constant + ka^{bn} \tag{4-37}$$

For C_v of n equal to 0.1, the R^2 for the polynomial model was 0.97 and the power was -2.098. The statistical software SYSTAT (Wilkinson, 1990) would not estimate the exponential model y = constant + ka^{bx}. An error message indicating that the function was undefined at an estimated parameter value was returned.

With a power of -2.098 and a C_v for the parameter of 0.1, the predicted error for a polynomial model was 0.079. Figure 4-55 shows use of the curve to predict the error. While it was not possible to estimate an exponential model, the correlation factor could still be computed and was found to equal -4.89. Using this and the exponential decreasing function curve for C_v equal to 0.1 gave a predicted error on -0.006. This process is shown in Figure 4-56.

For this example it appeared that the form of the output was more closely polynomial, so the error predicted using the polynomial technique should be most accurate. The predicted error was fairly close to the actual error. In addition, the predicted error was sufficiently small that the FOA variance would probably not have been rejected, although what constitutes an acceptable error is a matter of individual judgment. Given that a FOA variance would be judged acceptable if the predicted error is between -0.2 and 0.2 the result would have been to accept the FOA variance as sufficiently accurate.

For the second run, the mean of n was still 0.025 and the C_v was increased to 0.25. Since the C_v of n would not affect the first derivative at the mean, the same first derivative of 6,252,159 found earlier was used. The FOA variance was 1,526,933,288. Since 5,000 samples had been required for a valid simulation with C_v equal to 0.1, it seemed likely that even more samples would be required with a more uncertain parameter. A total of 8,000 samples were generated to start with. A similar percent change analysis was done, starting with 5,000 samples and adding on in increments of 500. None of the percent changes between 5,000 and 8,000, i.e. between 5000 and 5500, 5500 and 6000, etc., were greater than 1 percent. Also, they were neither consistently positive or negative, so the variance was neither increasing or decreasing as more samples were added. Thus 8,000 samples was considered sufficient. The sample variance was 1,421,857,185 and the relative error in the FOA variance was -0.074.

A polynomial model with the form of equation 4-30 was estimated. The R^2 was 0.98 and the b power was -0.00366. Using the curve for C_v equal to 0.1 gave a predicted error of -0.0008. The curve for C_v equal to 0.3 gave an error of -0.042. Straight line interpolation between the curves yielded an error of -0.032 for C_v of 0.25. This compares very well with the actual error of -0.074. It was not possible to estimate an exponential model, again because of parameter out of range errors. The correlation factor could be computed, and was -5.964. The predicted error for this factor for C_v's of 0.1 and 0.3 were -0.0149 and -0.0803, respectively. By straight line interpolation, the predicted error was -0.064. This is also a very accurate prediction and illustrates that if the form the model takes is uncertain, good results can be obtained by computing errors using both the polynomial and exponential methods and accepting the larger error.

Several conclusions can be drawn from the applications. If the model output has exactly the correct form, as confirmed by derivative ratios, the error predicting method is very accurate. If fact, in these cases, it may be possible to use the predicted error and the FOA variance to make a very precise estimate of the actual variance. Just the one example given here is not sufficient to prove this, but this may be a promising approach to pursue as a subject for future research.

If the derivative ratios do not indicate a strictly polynomial or exponential model, then estimating a model using a statistical package can give an indication of the form of the output. In the flow routing example, the derivative ratios were not constant, but the statistical software was unable to estimate exponential models and polynomial models with R^2's very close to unity were estimated. It therefore appeared that the form was polynomial. Good error predictions were obtained using both methods. However, these results should only be used to make an assessment of whether or not the FOA variance is within an acceptable range. Using the predicted error to estimate a variance by correcting the FOA variance would not be recommended, since the predicted error had the wrong sign in one case.

Another factor concerning FOA variances illustrated by these examples is the affect of the accuracy of numerical derivatives. With the washoff model, the derivative ratio was constant. Given an exponential model $y = \text{constant} + ka^{bx}$, the derivative ratio is equal to bln(a). For all four C_v's of K_3 the estimated bln(a) was equal to -0.6423. Thus, the numerical derivatives could be accepted without much question.

With the hydrograph, the output was a rougher curve and the numerical derivative was unstable, i.e. decreasing the step size would not necessarily result in a more accurate approximation of the derivative. (If the step size is too large truncation errors can occur and if the step size is too small round off errors can occur.) Round off errors are even more likely with an example such as this where the response is a very large number and the step size is much less than 1, and the change is response and step size differ by approximately 7 orders of magnitude. Thus, the optimum step size needed to be identified. The FOA variance computed using the arbitrary step size of plus and minus 1 percent was extremely inaccurate, while the FOA variances computed using the step size identified as optimum were quite accurate.

TABLE 4-1

MEAN, VARIANCE, C_v, AND LOGNORMAL DISTRIBUTION PARAMETERS OF UNCERTAIN PARAMETER, x

E[x]	Var[x]	C_v	μ	σ^2
0.25	0.000625	0.1	-1.391270	0.009950
0.25	0.005625	0.3	-1.429383	0.086178
0.25	0.015625	0.5	-1.497866	0.223144
0.25	0.030625	0.7	-1.585682	0.398776
0.25	0.0625	1.0	-1.732868	0.693147
0.25	0.09	1.2	-1.832293	0.891998
0.25	0.140625	1.5	-1.975622	1.178655
0.5	0.0025	0.1	-0.698122	0.009950
0.5	0.0225	0.3	-0.736236	0.086178
0.5	0.0625	0.5	-0.804719	0.223144
0.5	0.1225	0.7	-0.892535	0.398776
0.5	0.25	1.0	-1.039721	0.693147
0.5	0.36	1.2	-1.139146	0.891998
0.5	0.5625	1.5	-1.282475	1.178655
1	0.01	0.1	-0.004975	0.009950
1	0.09	0.3	-0.043089	0.086178
1	0.25	0.5	-0.111572	0.223144
1	0.49	0.7	-0.199388	0.398776
1	1	1.0	-0.346574	0.693147
1	1.44	1.2	-0.445999	0.891998
1	2.25	1.5	-0.589327	1.178655
2	0.04	0.1	0.688172	0.009950
2	0.36	0.3	0.650058	0.086178
2	1	0.5	0.581575	0.223144
2	1.96	0.7	0.493759	0.398776
2	4	1.0	0.346574	0.693147
2	5.76	1.2	0.247148	0.891998
2	9	1.5	0.103820	1.178655
5	0.25	0.1	1.604463	0.009950
5	2.25	0.3	1.566349	0.086178
5	6.25	0.5	1.497866	0.223144
5	12.25	0.7	1.410050	0.398776
5	25	1.0	1.262864	0.693147
5	36	1.2	1.163439	0.891998
5	56.25	1.5	1.020110	1.178655
10	1	0.1	2.297610	0.009950
10	9	0.3	2.259496	0.086178
10	25	0.5	2.191013	0.223144
10	49	0.7	2.103197	0.398776
10	100	1.0	1.956012	0.693147

TABLE 4-1 (CONTINUED)

MEAN, VARIANCE, C_v, AND LOGNORMAL DISTRIBUTION PARAMETERS OF UNCERTAIN PARAMETER, x

E[x]	Var[x]	C_v	μ	σ^2
10	144	1.2	1.856586	0.891998
10	225	1.5	1.713258	1.178655
15	2.25	0.1	2.703075	0.009950
15	20.25	0.3	2.664961	0.086178
15	56.25	0.5	2.596478	0.223144
15	110.25	0.7	2.508662	0.398776
15	225	1.0	2.361477	0.693147
15	324	1.2	2.262051	0.891998
15	506.25	1.5	2.118723	1.178655
25	6.25	0.1	3.213901	0.009950
25	56.25	0.3	3.175787	0.086178
25	156.25	0.5	3.107304	0.223144
25	306.25	0.7	3.019488	0.398776
25	625	1.0	2.872302	0.693147
25	900	1.2	2.772877	0.891998
25	1406.25	1.5	2.629548	1.178655
35	12.25	0.1	3.550373	0.009950
35	110.25	0.3	3.512259	0.086178
35	306.25	0.5	3.443776	0.223144
35	600.25	0.7	3.355960	0.398776
35	1225	1.0	3.208774	0.693147
35	1764	1.2	3.109349	0.891998
35	2756.25	1.5	2.966021	1.178655
50	25	0.1	3.907048	0.009950
50	225	0.3	3.868934	0.086178
50	625	0.5	3.800451	0.223144
50	1225	0.7	3.712635	0.398776
50	2500	1.0	3.565449	0.693147
50	3600	1.2	3.466024	0.891998
50	5625	1.5	3.322696	1.178655

TABLE 4-2

RESULTS OF POLYNOMIAL TEST RUNS

μ	σ^2	a	b	c	d	est. power	error	pred. error
Decreasing Models								
1.60446	0.00995	-2	0.2	-2.5	0.15	0.173	-0.006	-0.006
0.58158	0.22314	-2	0.2	-2.5	0.15	0.173	-0.152	-0.153
-0.34657	0.69315	-2	0.2	-2.5	0.15	0.172	-0.573	-0.577
0.58158	0.22314	-2	0.8	-2.5	0.15	0.532	-0.147	-0.095
-0.34657	0.69315	-2	0.8	-2.5	0.15	0.496	-0.573	-0.357
0.58158	0.22314	-2	0.2	-2.5	0.9	0.694	-0.113	-0.058
-0.34657	0.69315	-2	0.2	-2.5	0.9	0.661	-0.439	-0.223
0.58158	0.22314	-2	0.8	-2.5	0.9	0.858	-0.059	-0.058
-0.34657	0.69315	-2	0.8	-2.5	0.9	0.858	-0.202	-0.200
1.60446	0.00995	-2	0.5	-1.5	0.5	0.500	-0.006	-0.006
0.58158	0.22314	-2	0.5	-1.5	0.5	0.500	-0.152	-0.152
-0.34657	0.69315	-2	0.5	-1.5	0.5	0.500	-0.571	-0.571
1.60446	0.00995	-2	0.5	-1.5	0.1	0.387	-0.007	-0.006
0.58158	0.22314	-2	0.5	-1.5	0.1	0.360	-0.162	-0.153
-0.34657	0.69315	-2	0.5	-1.5	0.1	0.344	-0.619	-0.576
0.58158	0.22314	-2	0.5	-1.5	0.9	0.710	-0.108	-0.085
Increasing Models								
1.60446	0.00995	2	1.1	1.5	1.05	1.080	0.002	0.002
0.58158	0.22314	2	1.1	1.5	1.05	1.079	0.037	0.038
-0.34657	0.69315	2	1.1	1.5	1.05	1.079	0.116	0.117
1.60446	0.00995	3	2	2.5	1.75	1.911	0.030	0.031
0.58158	0.22314	3	2	2.5	1.75	1.904	0.502	0.509
-0.34657	0.69315	3	2	2.5	1.75	1.902	0.901	0.905
1.60446	0.00995	2	1.1	0.5	1.15	1.111	0.002	0.002
0.58158	0.22314	2	1.1	0.5	1.15	1.110	0.053	0.053
-0.34657	0.69315	2	1.1	0.5	1.15	1.110	0.148	0.162
1.60446	0.00995	3	2	1.5	2.5	2.266	0.048	0.050
0.58158	0.22314	3	2	1.5	2.5	2.239	0.672	0.685
-0.34657	0.69315	3	2	1.5	2.5	2.228	0.961	0.980
1.60446	0.00995	0.75	1.05	0.5	1.15	1.094	0.002	0.002
0.58158	0.22314	0.75	1.05	0.5	1.15	1.095	0.045	0.045
-0.34657	0.69315	0.75	1.05	0.5	1.15	1.092	0.135	0.138
1.60446	0.00995	2	2.5	1.5	2.5	2.500	0.062	0.062
0.58158	0.22314	2	2.5	1.5	2.5	2.500	0.777	0.777
-0.34657	0.69315	2	2.5	1.5	2.5	2.500	0.994	0.994
1.60446	0.00995	0.75	1.05	1.5	1.05	1.050	0.001	0.001
0.58158	0.22314	0.75	1.05	1.5	1.05	1.050	0.023	0.023
-0.34657	0.69315	0.75	1.05	1.5	1.05	1.050	0.073	0.073
1.60446	0.00995	2	2.5	2.5	1.75	2.300	0.050	0.053
0.58158	0.22314	2	2.5	2.5	1.75	2.248	0.676	0.700
-0.34657	0.69315	2	2.5	2.5	1.75	2.224	0.960	0.983

TABLE 4-3
RESULTS OF EXPONENTIAL TEST RUNS

μ	σ^2	a	b	c	d	e	f	factor	pred. error	error
decreasing models										
1.60446	0.00995	1.50	-0.25	2.00	-0.25	100	200	-6.59	-0.014	-0.014
1.60446	0.00995	0.75	0.50	0.50	0.50	100	200	-5.43	-0.013	-0.011
1.60446	0.00995	0.75	0.50	0.50	1.25	100	200	-5.11	-0.010	0.014
1.60446	0.00995	1.50	-0.25	2.00	-1.00	100	200	-4.97	-0.007	0.014
1.60446	0.00995	0.75	1.25	0.50	1.25	100	200	-4.24	0.018	0.030
1.60446	0.00995	1.50	-1.00	2.00	-1.00	100	200	-4.11	0.025	0.030
0.58158	0.22314	1.50	-0.25	2.00	-0.25	100	200	-5.27	-0.207	-0.206
0.58158	0.22314	0.75	0.50	0.50	0.50	100	200	-3.96	-0.318	-0.311
0.58158	0.22314	1.50	-0.25	2.00	-1.00	100	200	-2.77	-0.355	-0.292
0.58158	0.22314	1.50	-1.00	2.00	-1.00	100	200	-2.63	-0.344	-0.324
0.58158	0.22314	0.75	0.50	0.50	1.25	100	200	-2.53	-0.330	-0.221
0.58158	0.22314	0.75	1.25	0.50	1.25	100	200	-2.44	-0.316	-0.256
-0.34657	0.69315	1.50	-0.25	2.00	-0.25	100	200	-5.49	-0.515	-0.513
-0.34657	0.69315	0.75	0.50	0.50	0.50	100	200	-4.11	-0.866	-0.860
-0.34657	0.69315	1.50	-0.25	2.00	-1.00	100	200	-2.78	-1.281	-1.243
-0.34657	0.69315	1.50	-1.00	2.00	-1.00	100	200	-2.70	-1.302	-1.288
-0.34657	0.69315	0.75	0.50	0.50	1.25	100	200	-2.47	-1.356	-1.281
-0.34657	0.69315	0.75	1.25	0.50	1.25	100	200	-2.44	-1.363	-1.316

TABLE 4-3 (CONTINUED)
RESULTS OF EXPONENTIAL TEST RUNS

μ	σ^2	a	b	c	d	e	f	factor	pred. error	error
increasing models										
1.60446	0.00995	0.50	-0.15	0.75	-0.15	0.25	0.75	-8.02	0.013	0.014
1.60446	0.00995	0.50	-0.15	0.75	-0.85	0.25	0.75	-5.75	0.056	0.056
1.60446	0.00995	0.50	-0.15	0.75	-0.85	0.25	0.75	-5.75	0.056	0.056
1.60446	0.00995	1.25	0.50	1.75	0.50	0.25	0.75	-5.47	0.068	0.068
1.60446	0.00995	1.25	1.50	1.75	0.50	0.25	0.75	-5.28	0.077	0.077
1.60446	0.00995	0.50	-0.85	0.75	-0.85	0.25	0.75	-4.19	0.177	0.180
1.60446	0.00995	1.25	1.50	1.75	1.50	0.25	0.75	-3.37	0.330	0.342
0.58158	0.22314	0.50	-0.15	0.75	-0.15	0.25	0.75	-6.89	0.128	0.130
0.58158	0.22314	0.50	-0.15	0.75	-0.85	0.25	0.75	-4.70	0.486	0.495
0.58158	0.22314	0.50	-0.15	0.75	-0.85	0.25	0.75	-4.70	0.486	0.495
0.58158	0.22314	1.25	0.50	1.75	0.50	0.25	0.75	-4.45	0.599	0.613
0.58158	0.22314	1.25	1.50	1.75	0.50	0.25	0.75	-4.27	0.712	0.729
0.58158	0.22314	0.50	-0.85	0.75	-0.85	0.25	0.75	-3.50	1.000	1.000
-0.34657	0.69315	0.50	-0.15	0.75	-0.15	0.25	0.75	-7.22	0.562	0.962

TABLE 4-4
RESULTS OF MIXED POLYNOMIAL-EXPONENTIAL TEST RUNS

error	exp. R^2	factor	exp. pred.	poly. R^2	b	poly. pred.	R^2 class	better pred.
Decreasing Models								
0.237	0.999168	-1.65	0.044	0.999055	-1.09	0.413	exp	poly
-0.075	0.998908	-2.39	-0.306	0.999675	-0.40	0.029	poly	poly
-0.224	0.999932	-2.27	-0.278	0.998014	-0.47	0.062	exp	exp
0.082	0.999656	-1.75	-0.037	0.998288	-0.96	0.335	exp	exp
-0.314	0.999952	-2.87	-0.360	0.998844	-0.10	-0.093	exp	exp
-0.096	0	-4.32	-0.288	0.999917	0.43	-0.158	poly	poly
0.297	0.99806	-1.70	0.003	0.999754	-1.05	0.387	poly	poly
0.123	0.997547	-2.09	-0.218	0.999947	-0.65	0.157	poly	poly
-0.184	0.999671	-2.37	-0.303	0.998918	-0.40	0.029	exp	exp
0.036	0.998898	-1.99	-0.178	0.999378	-0.72	0.199	poly	poly
-0.254	5.48E-11	-2.84	-0.359	0.999327	-0.12	-0.085	poly	exp
-0.089	0	-3.44	-0.353	0.999923	0.14	-0.148	poly	poly
0.335	0.997147	-1.73	-0.021	0.99996	-1.02	0.371	poly	poly
0.261	0.996742	-1.89	-0.124	0.999995	-0.84	0.268	poly	poly
-0.131	8.22E-14	-2.52	-0.328	0.999662	-0.31	-0.010	poly	poly
-0.011	4.93E-13	-2.30	-0.286					
-0.172	4.62E-15	-2.79	-0.356	0.99977	-0.15	-0.074	poly	poly
-0.073	0	-2.99	-0.363					
0.355	0.996438	-1.76	-0.042	1	-0.99	0.355	poly	poly
-0.062	0	-2.70	-0.350	0.999999	-0.21	-0.054	poly	poly
-0.055	0	-2.69	-0.349	0.999503	-0.15	-0.075	poly	poly
-0.065	5.33E-16	-2.72	-0.351	0.999796	-0.15	-0.074	poly	poly
-0.058	0	-2.73	-0.352	0.999786	-0.15	-0.076	poly	poly

TABLE 4-4 (CONTINUED)
RESULTS OF MIXED POLYNOMIAL-EXPONENTIAL TEST RUNS

error	exp. R^2	factor	exp. pred.	poly. R^2	b	poly. pred.	R^2 class	better pred.
Increasing Models								
0.002	0	-10.64	0.003	0	-20.07			
0.002	0	-10.68	0.003	0	-17.53			
0.034	0	-6.10	0.044	0	-18.37			
0.034	2.16E-16	-6.10	0.044	1	2.00	0.035	poly	poly
0.034	0	-6.10	0.044	1	2.00	0.035	poly	poly
0.109	1.14E-16	-4.95	0.099	0.99998	2.81	0.082	poly	exp
0.048	0.999993	-8.03	0.069	1	1.10	0.051	poly	poly
0.048	0.999993	-8.04	0.069	1	1.10	0.051	poly	poly
0.557	0	-3.88	0.953	1	2.01	0.558	poly	poly
0.556	0	-3.88	0.951	1	2.00	0.556	poly	poly
0.556	0	-3.89	0.950	1	2.00	0.556	poly	poly
1.000	0	-3.70	0.991	0.999985	2.14	0.623	poly	exp
0.147	0.999984	-7.74	0.288	1	1.10	0.143	poly	poly
0.147	0.999984	-7.75	0.286	1	1.10	0.142	poly	poly
0.935		-4.03	1.000	1	2.01	0.935	poly	poly
0.933		-4.04	1.000	1	2.00	0.934	poly	poly
0.933		-4.04	1.000	1	2.00	0.933	poly	poly
1.000		-3.96	1.000	0.999998	2.09	0.949	poly	exp

TABLE 4-5
RESULTS OF WASHOFF MODEL APPLICATION

C_v	variance FOA	variance sim.	actual error	factor	pred. error
0.1	0.592	0.606	0.022	-3.92	0.040
0.25	3.70	4.49	0.18	-2.28	0.18
0.5	14.8	22.8	0.35	-1.36	0.36
1	59.3	93.3	0.36	-0.863	0.36

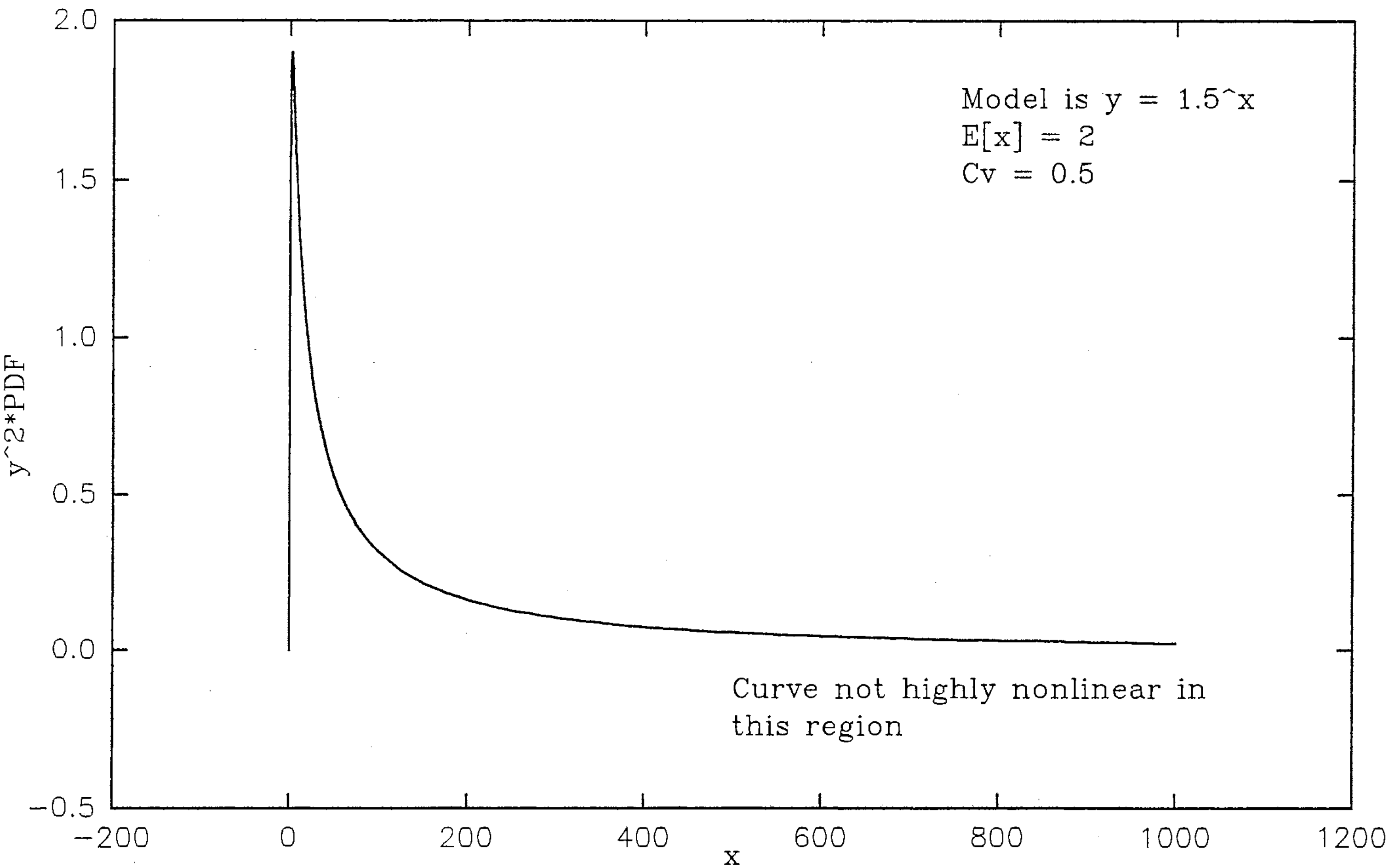

Figure 4−1. Nonlinearity in Tail of PDF Times Model Squared

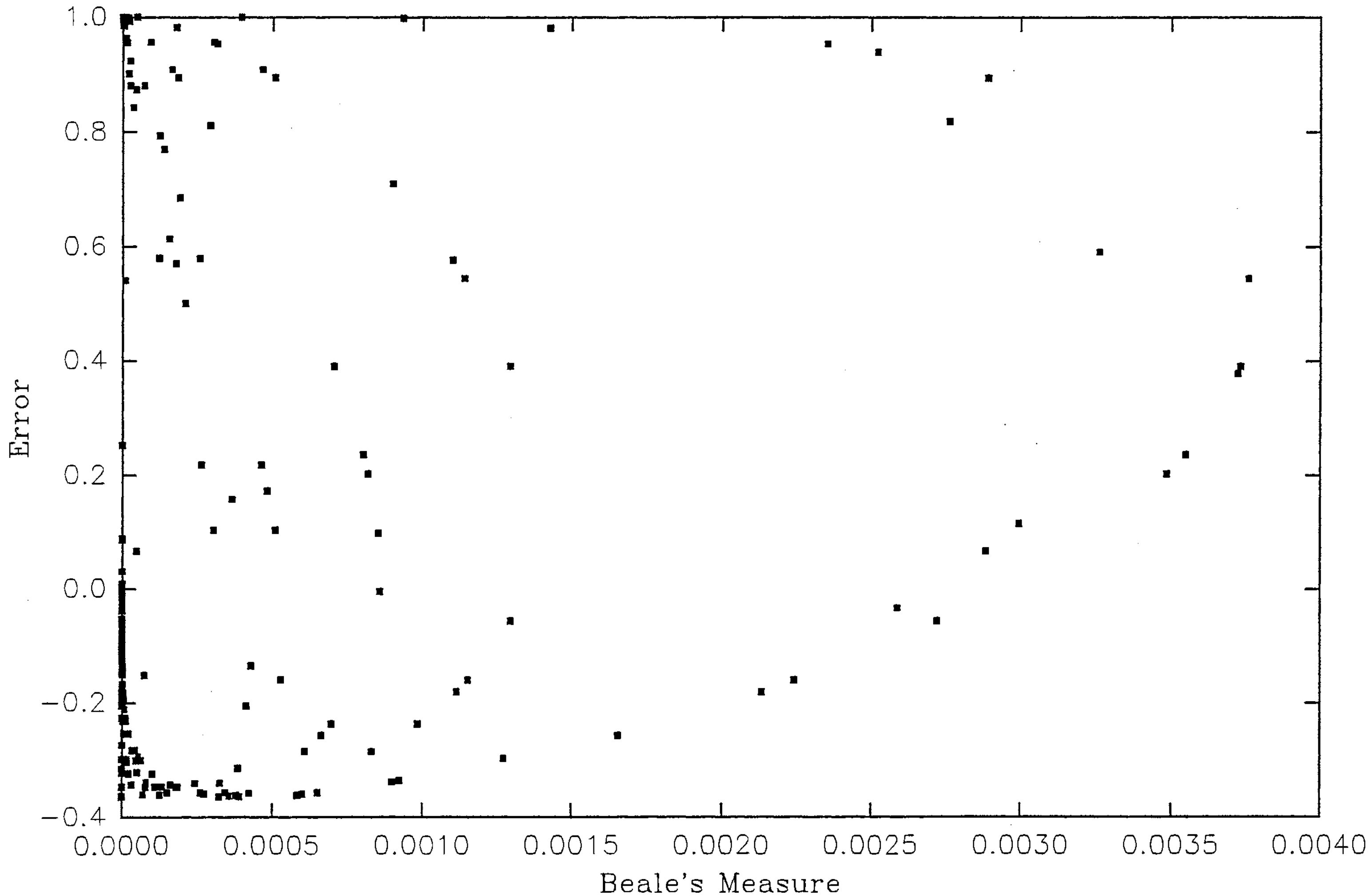

Figure 4–2. Relative Error vs Beale's Measure of Nonlinearity

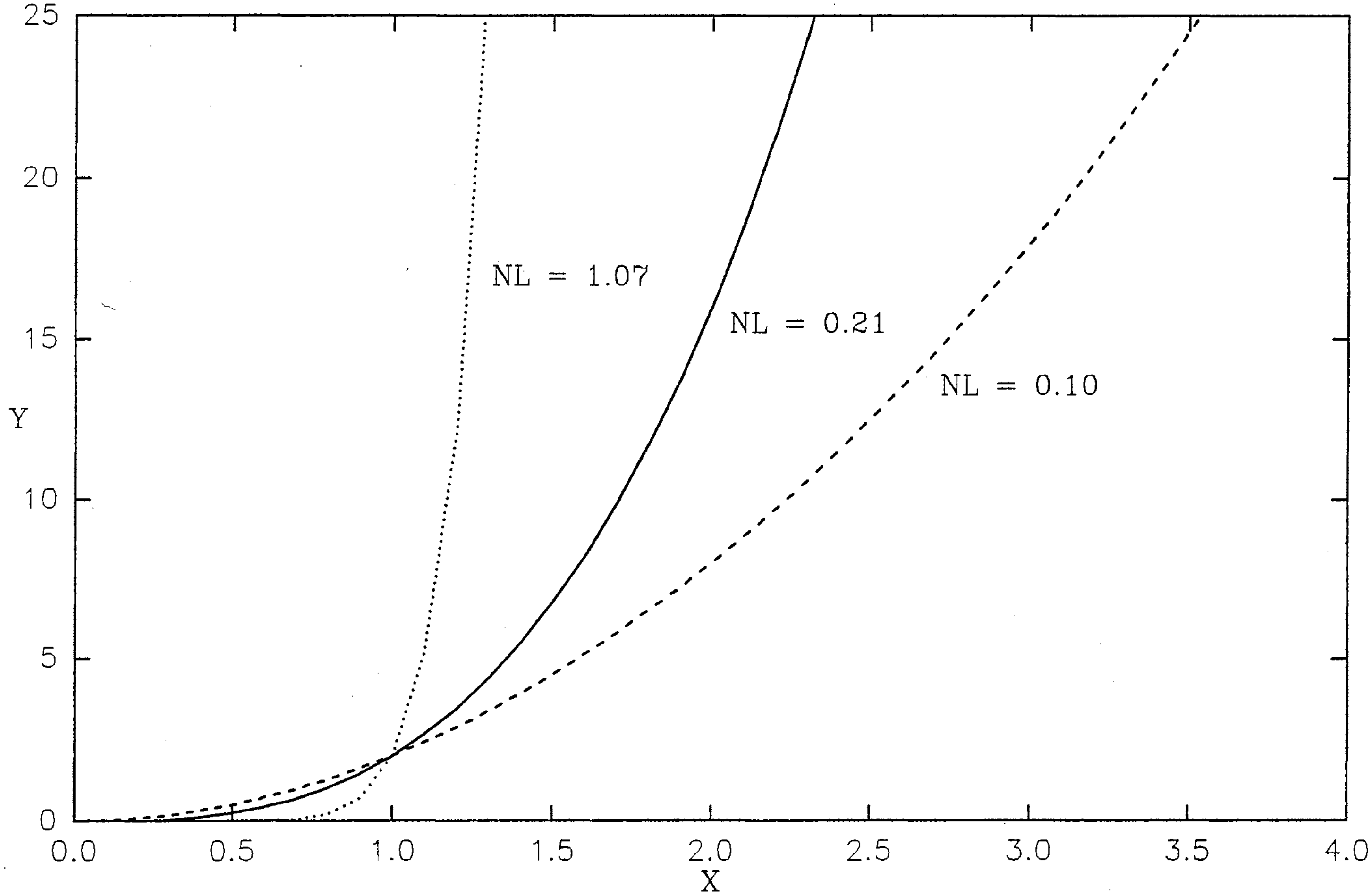

Figure 4-3. Comparison of Three Nonlinear Models and the Nonlinearity Measure

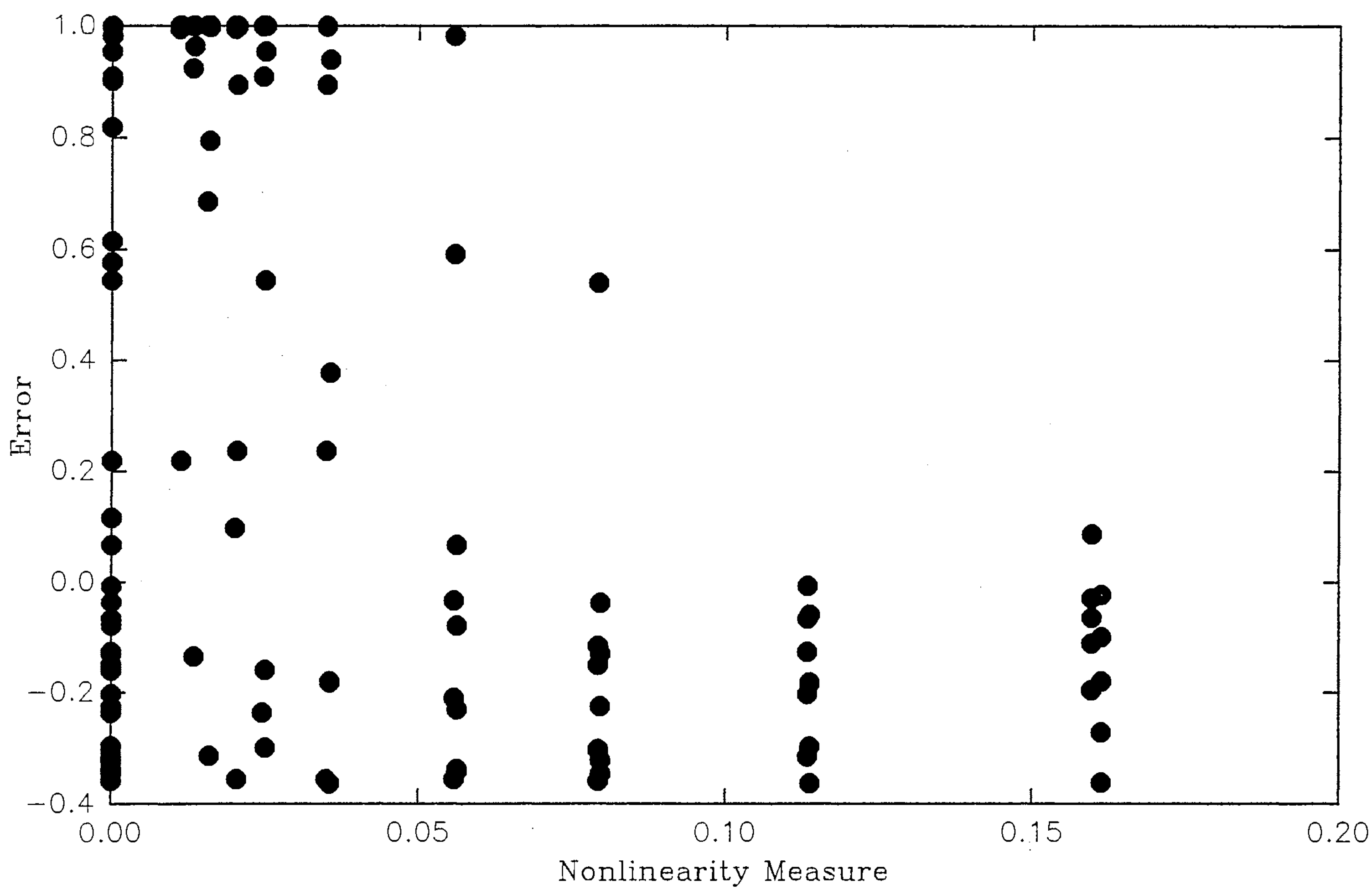

Figure 4−4. Error in FOA Variance vs Nonlinearity Measure

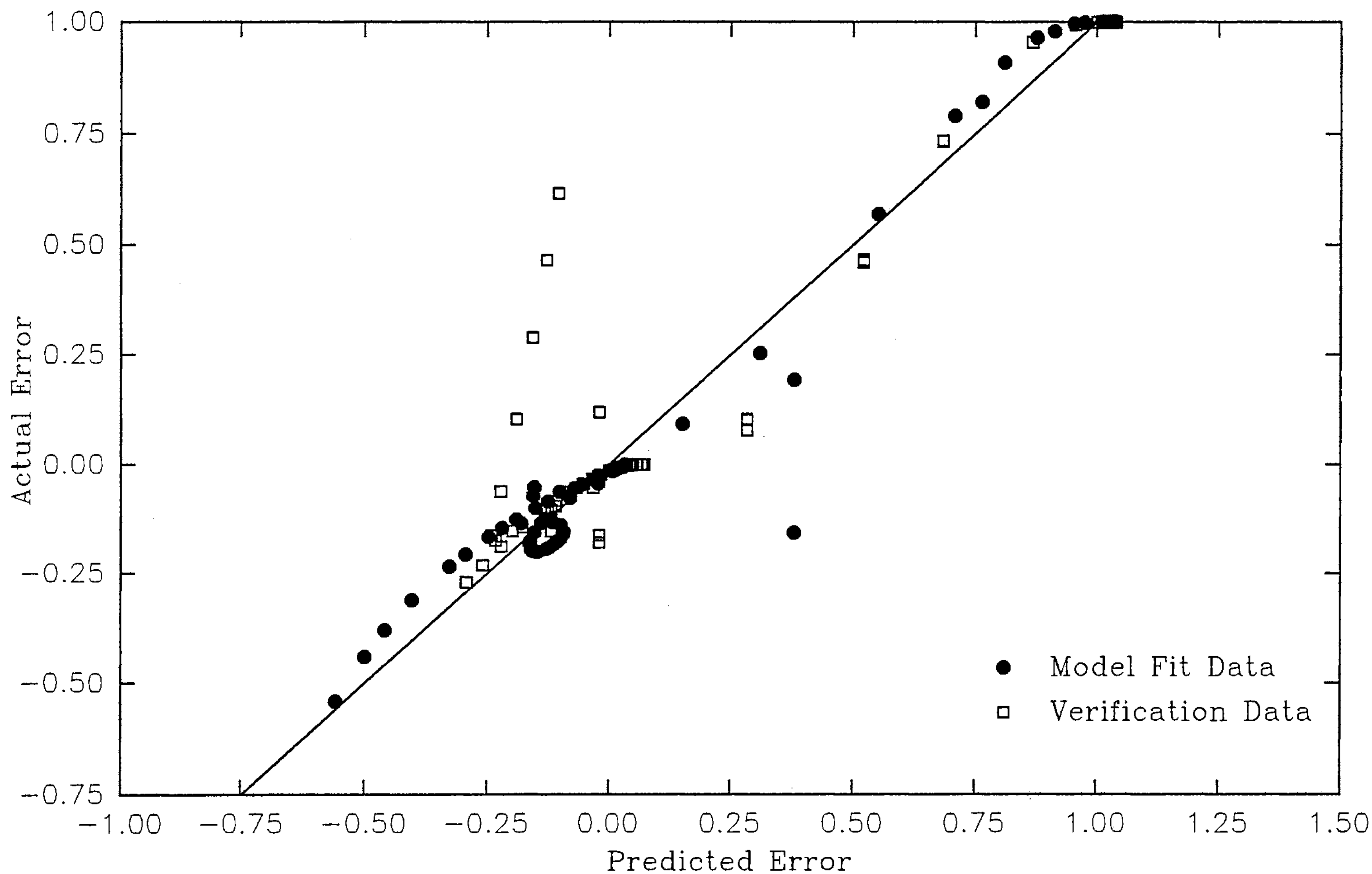

Figure 4-5. Error Data for Slope Factor Method

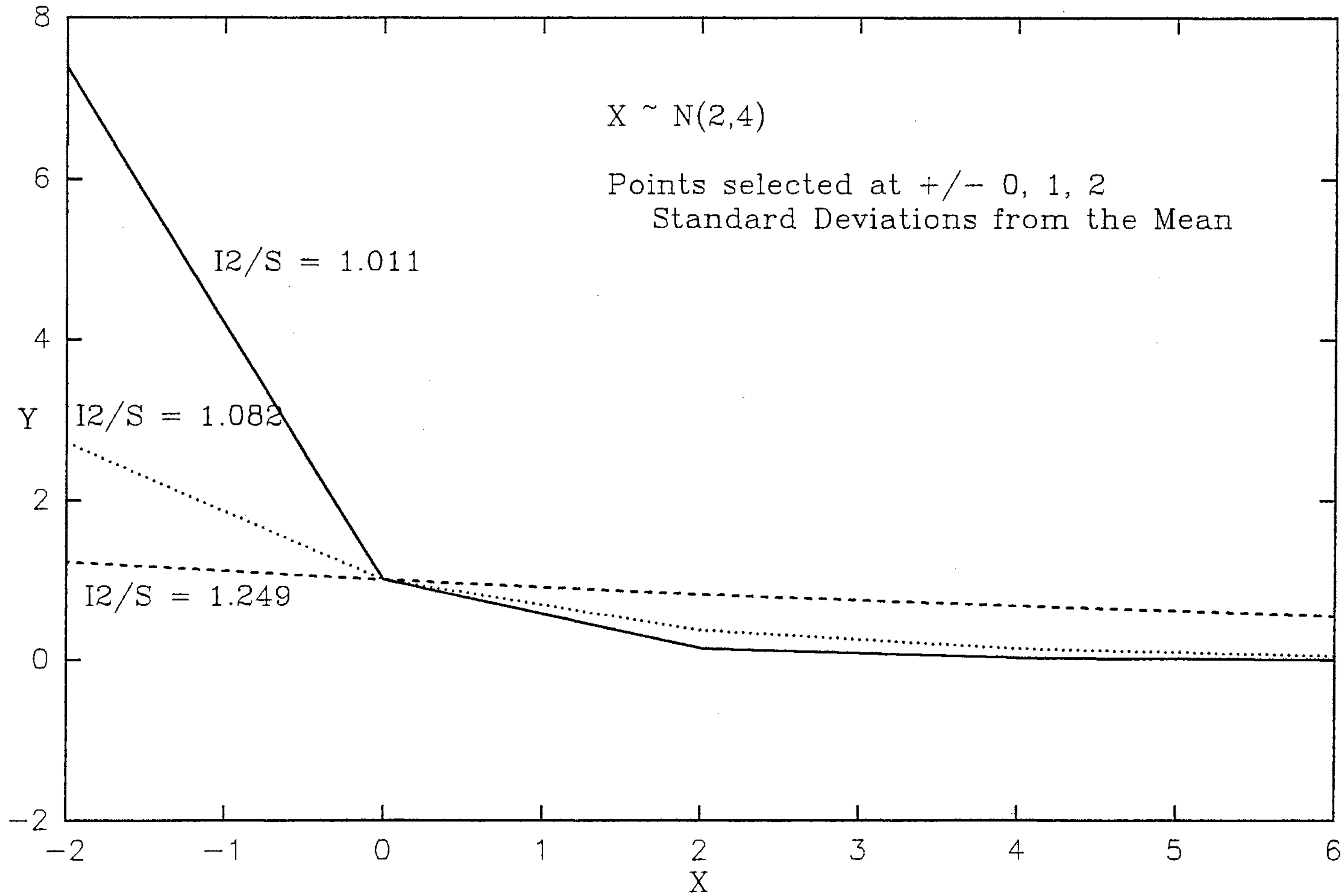

Figure 4-6. Comparison of Nonlinear Models and I2/S Ratios

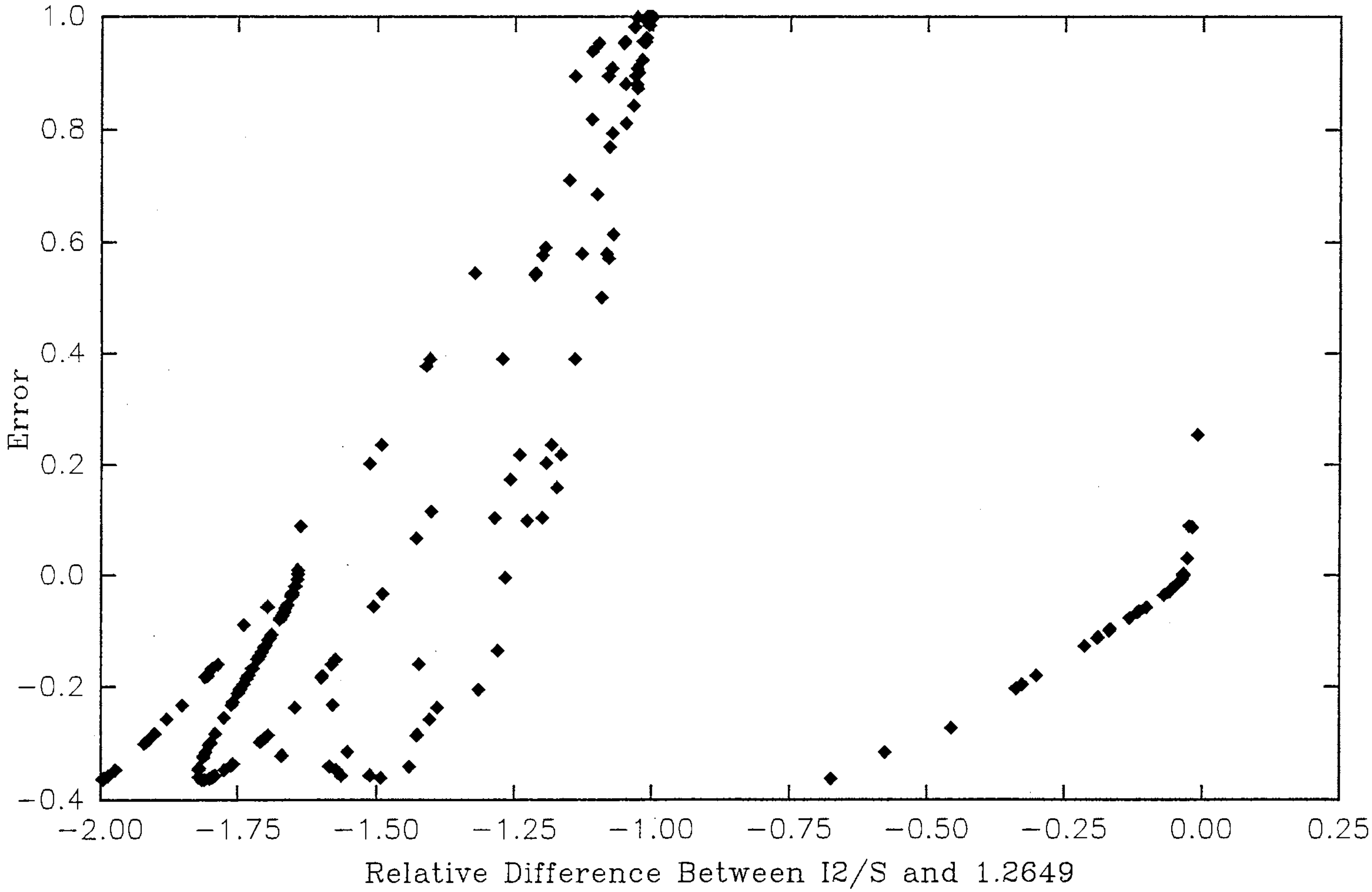

Figure 4-7. Error vs Departure of I2/S Ratio From Linearity

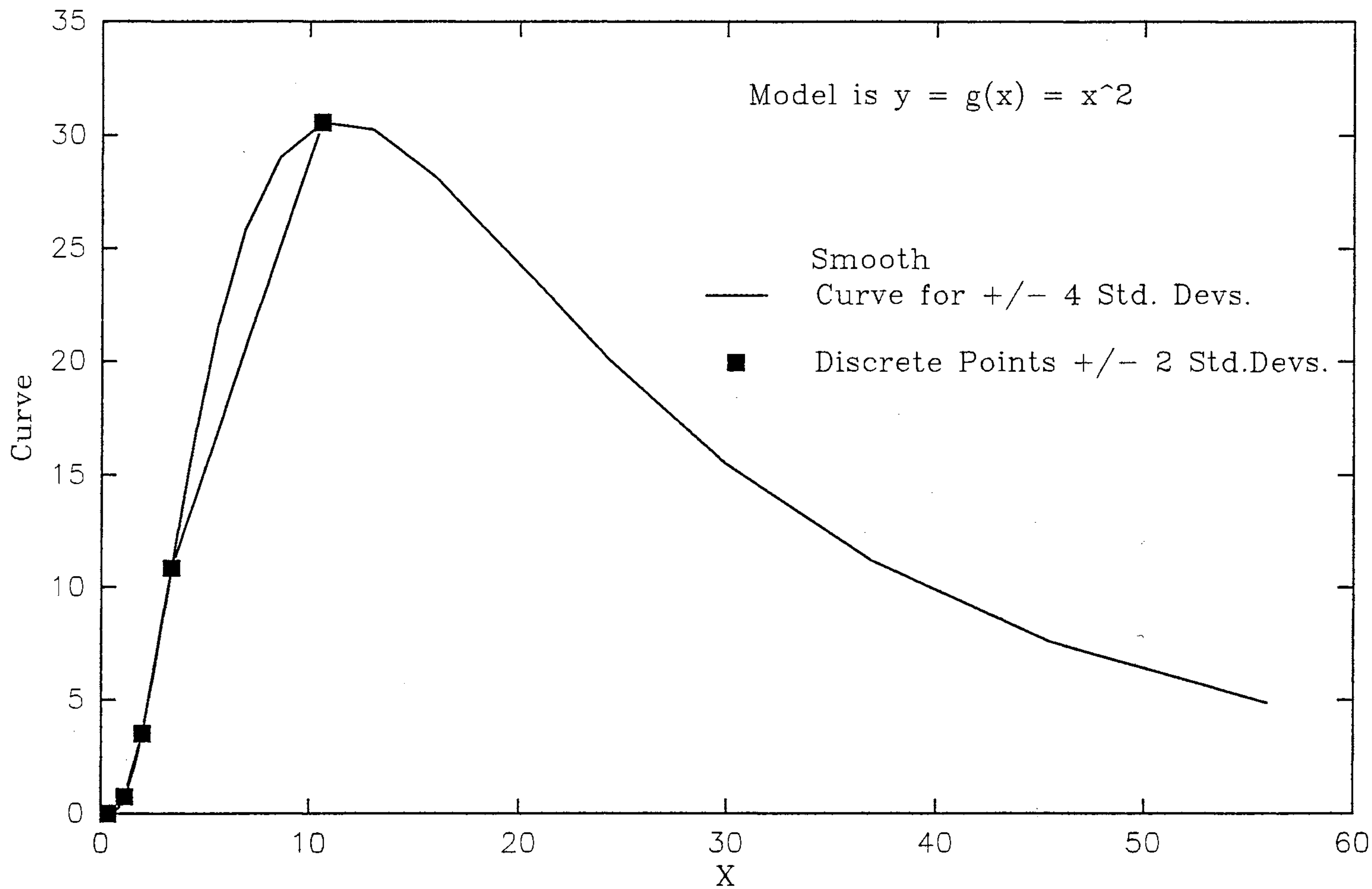

Figure 4-8. Comparison of g(x)^2 * f(x) Curves - Smooth Curve and Discrete Points

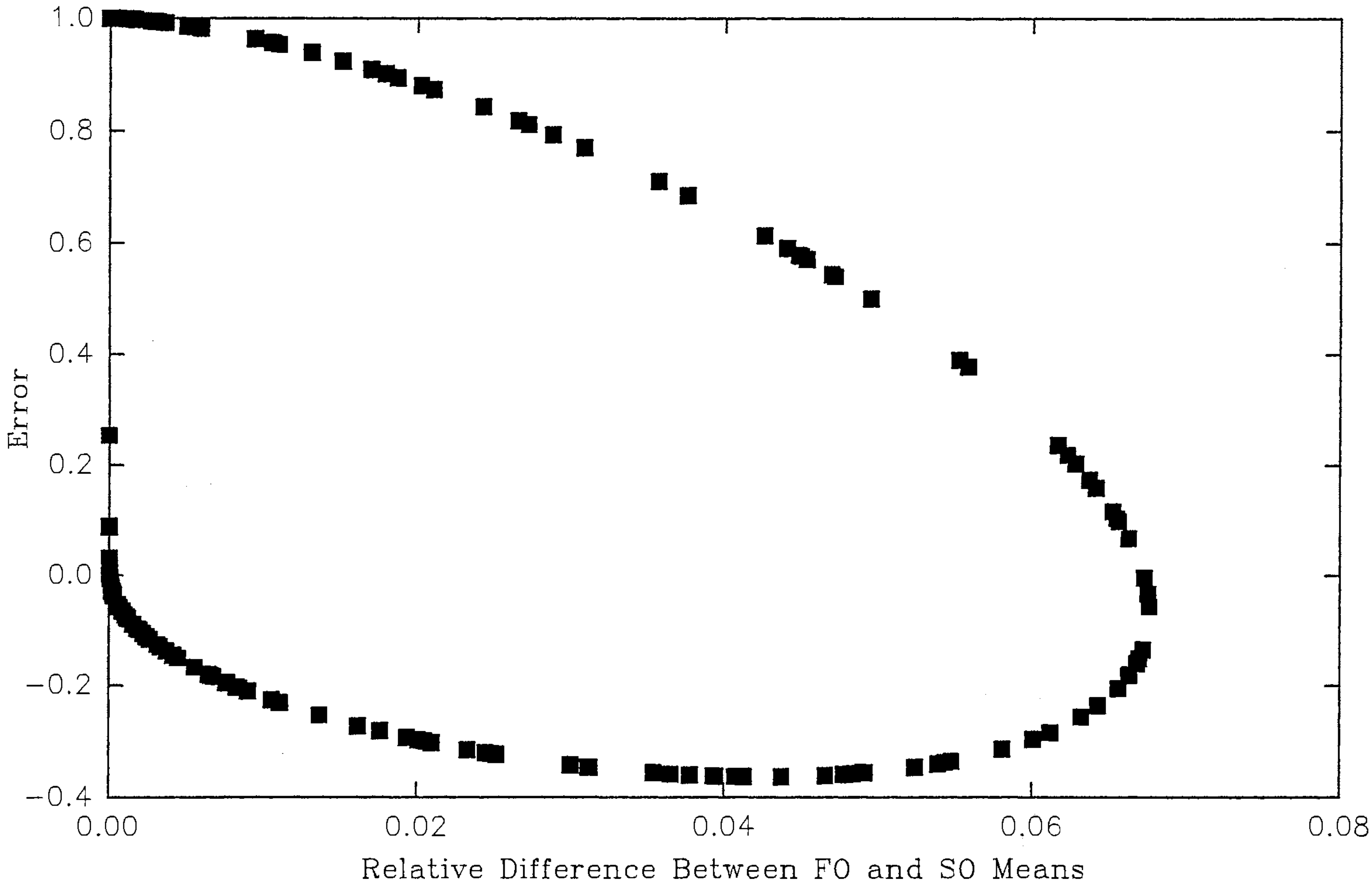

Figure 4−9. Error vs Relative Difference in FO and SO Mean

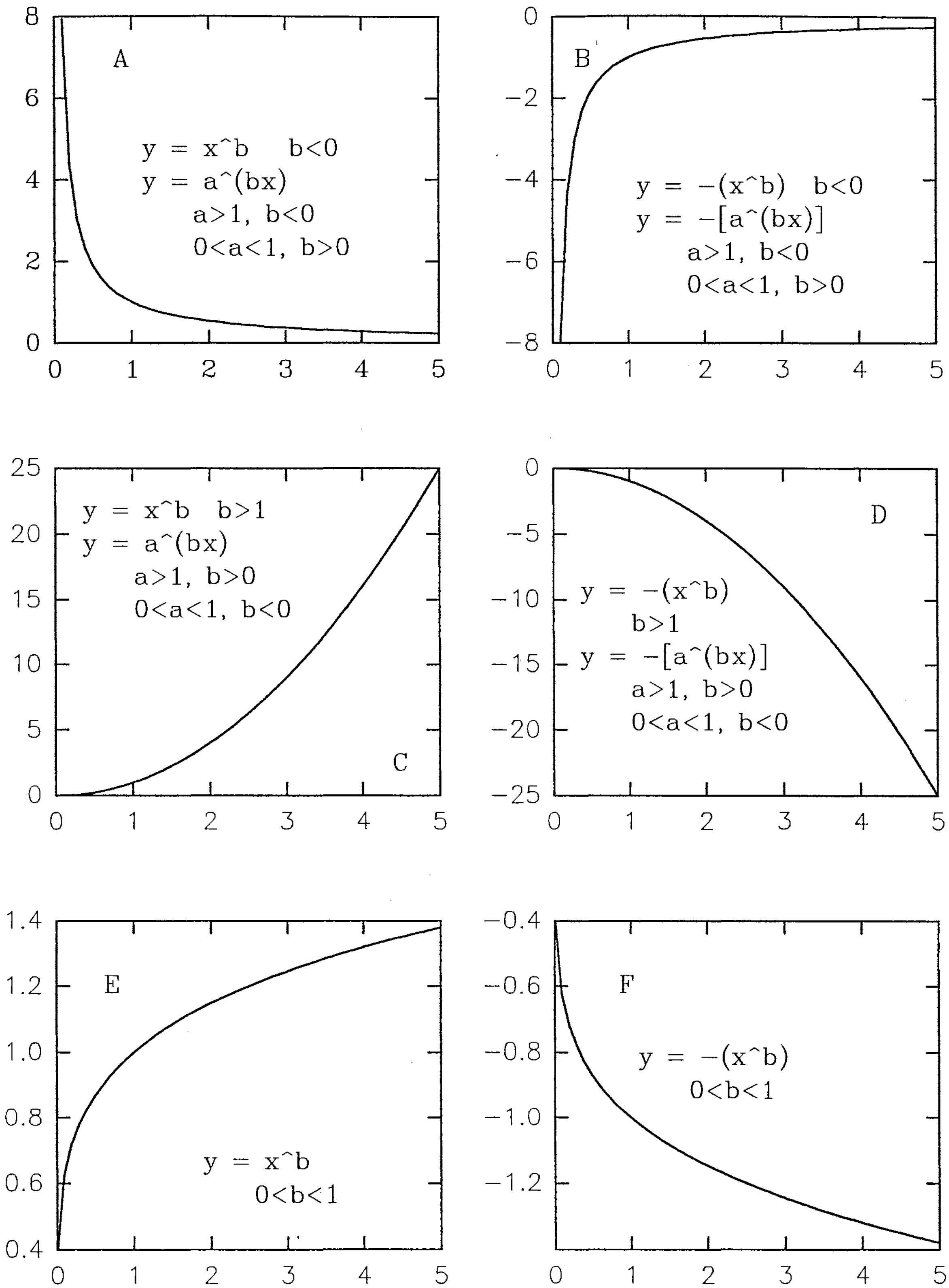

Figure 4–10. Forms of Polynomial and Exponential Models and Restrictions on a and b

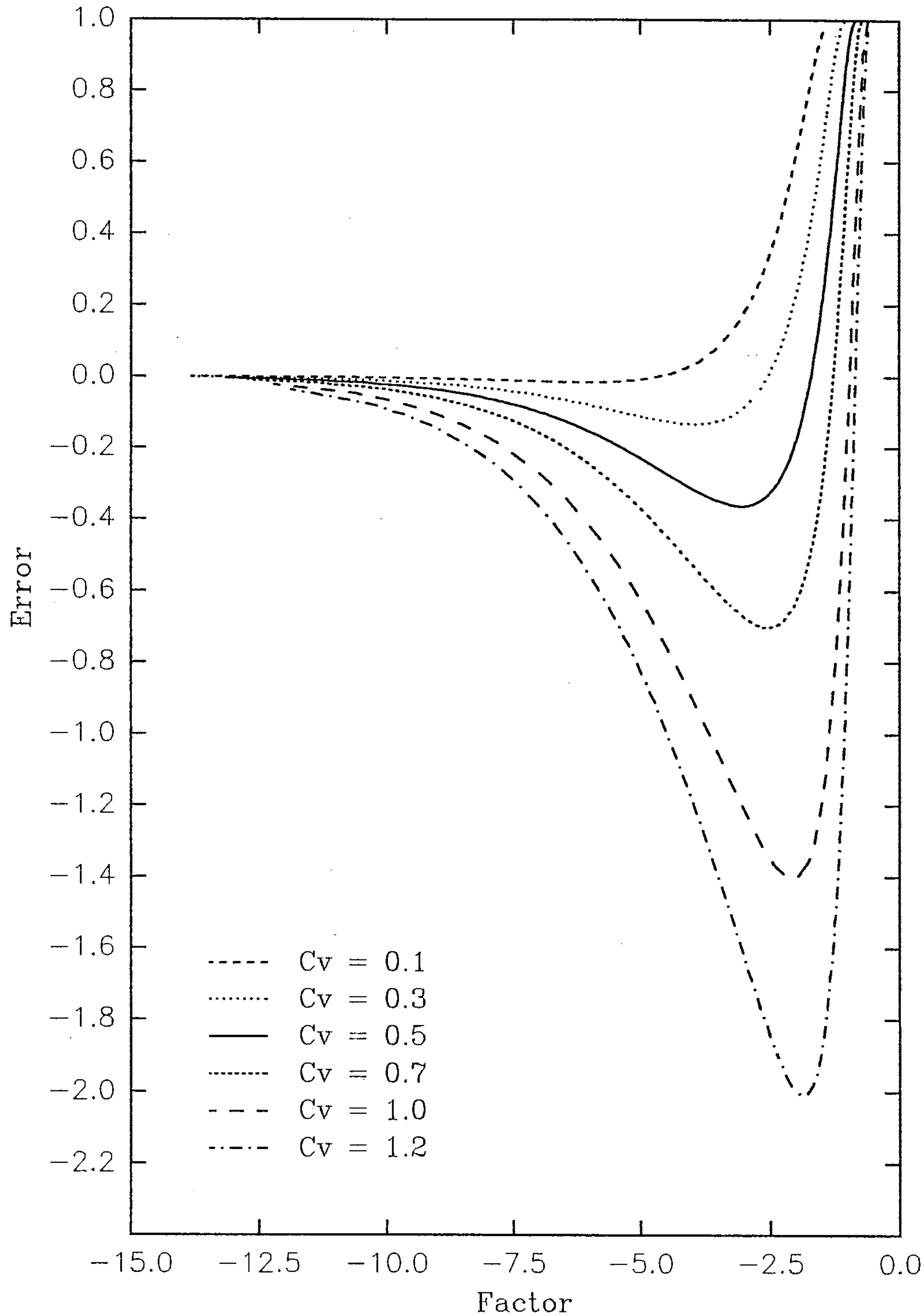

Figure 4−11. Error vs Factor for Type A and B Exponential Models

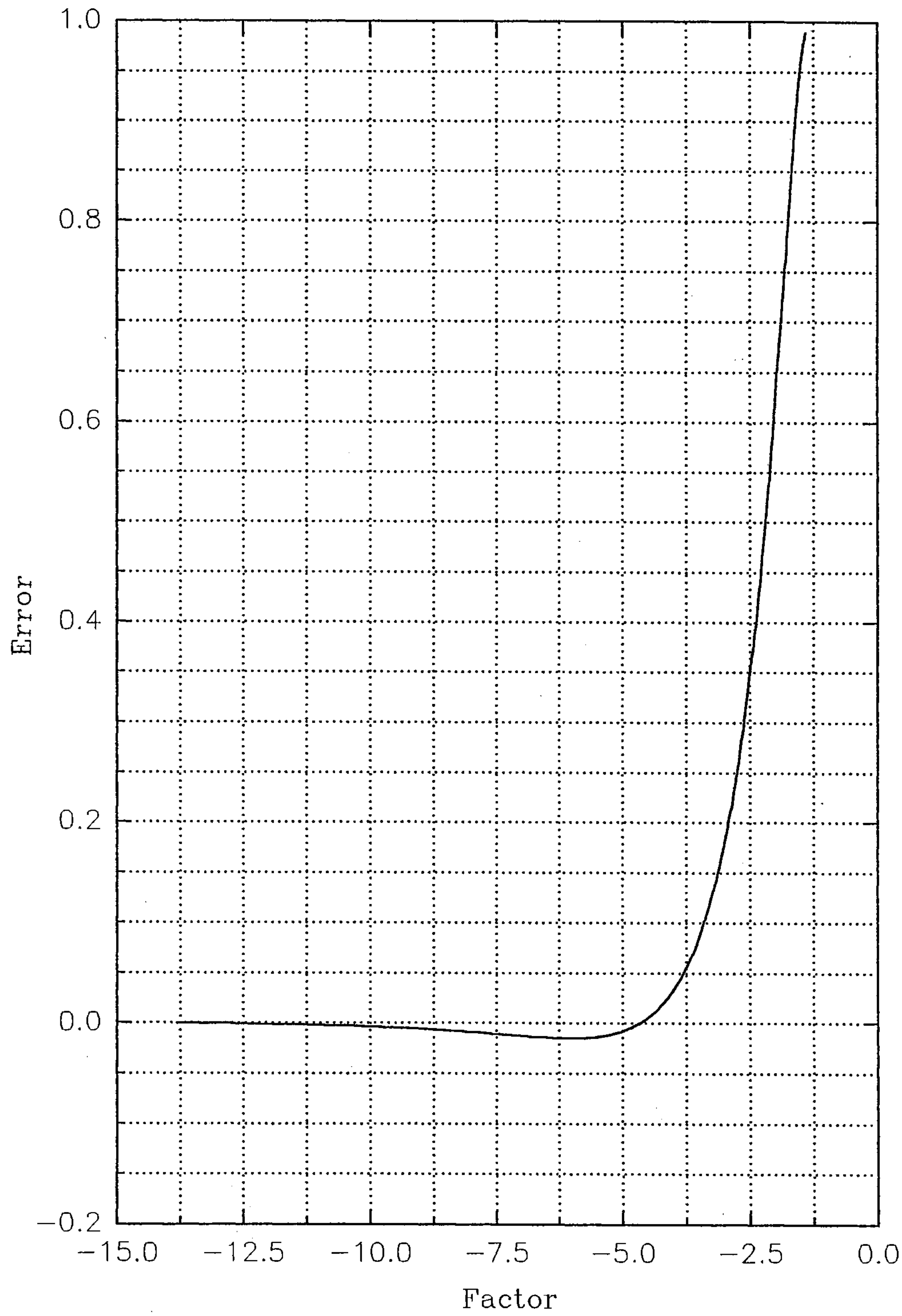

Figure 4−12. Error vs Factor for Cv = 0.1

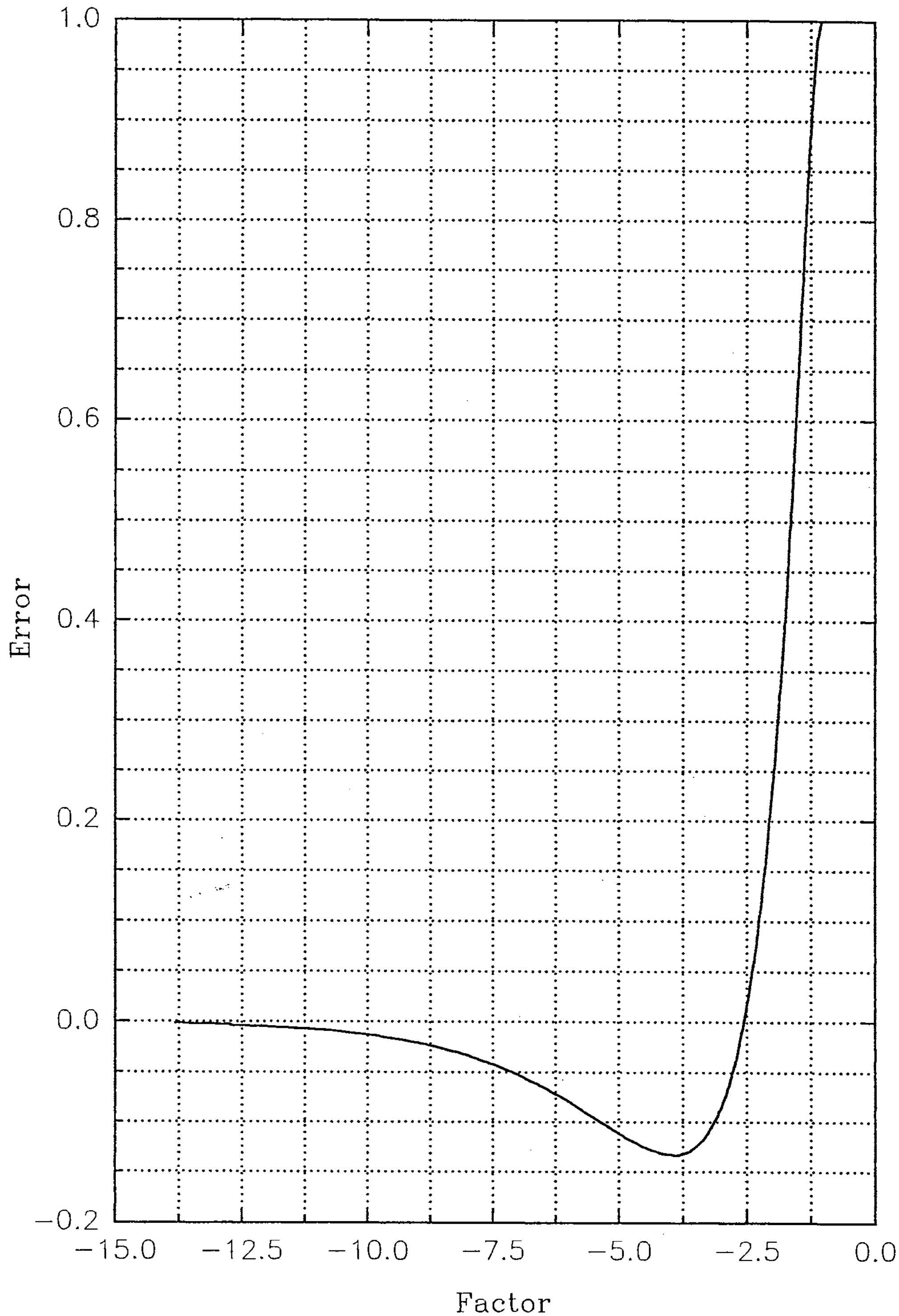

Figure 4−13. Error vs Factor for Cv = 0.3

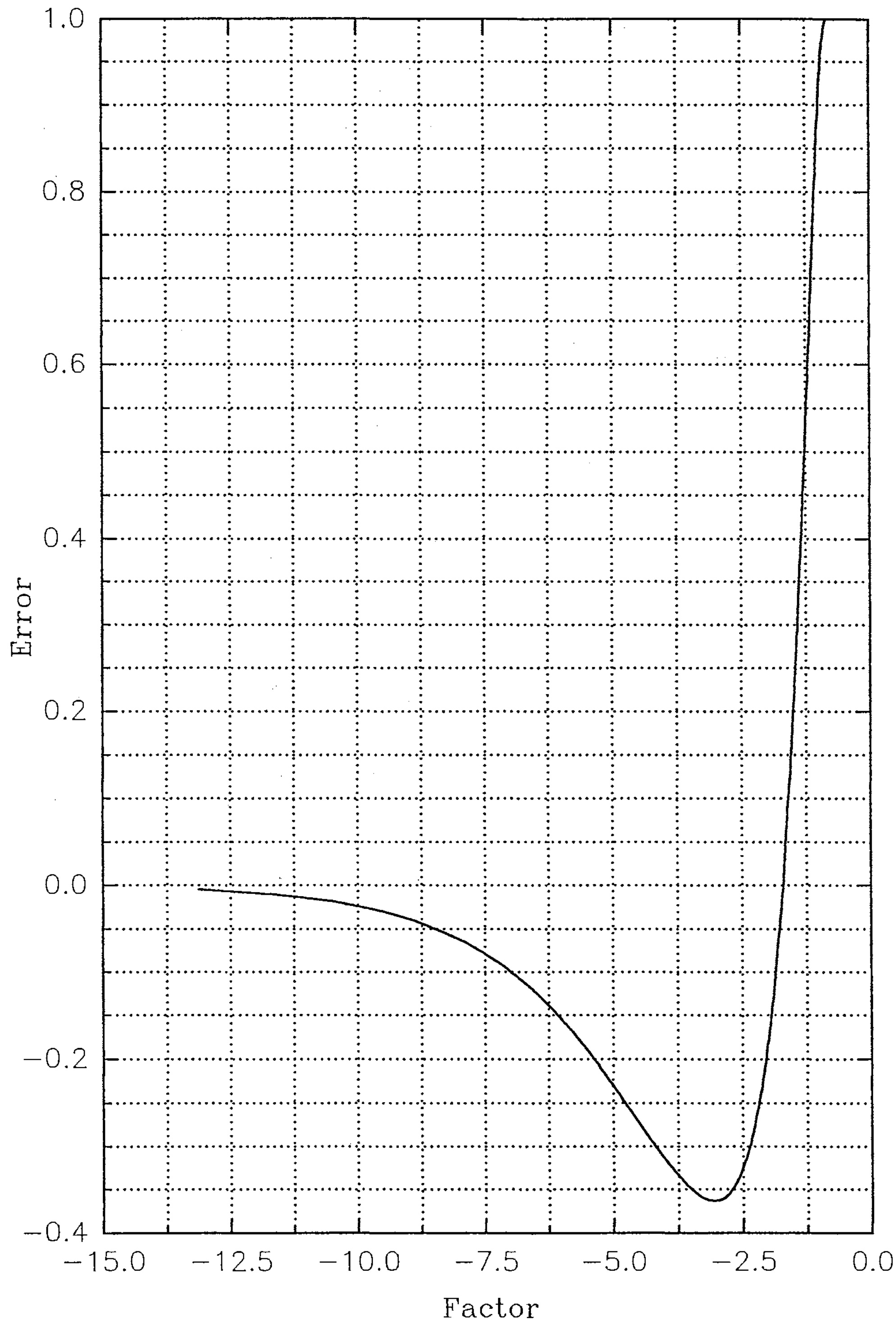

Figure 4−14. Error vs Factor for Cv = 0.5

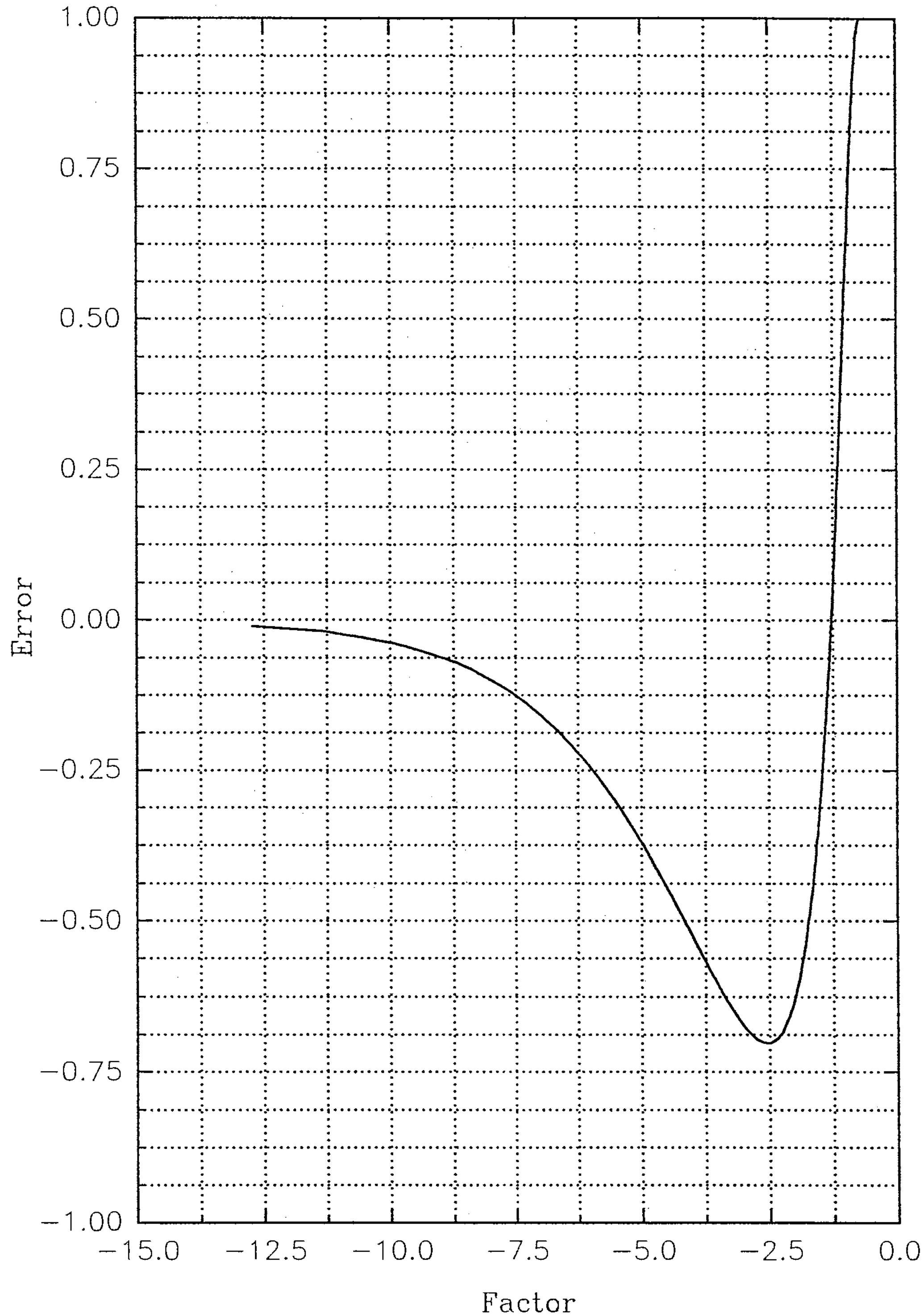

Figure 4−15. Error vs Factor for Cv = 0.7

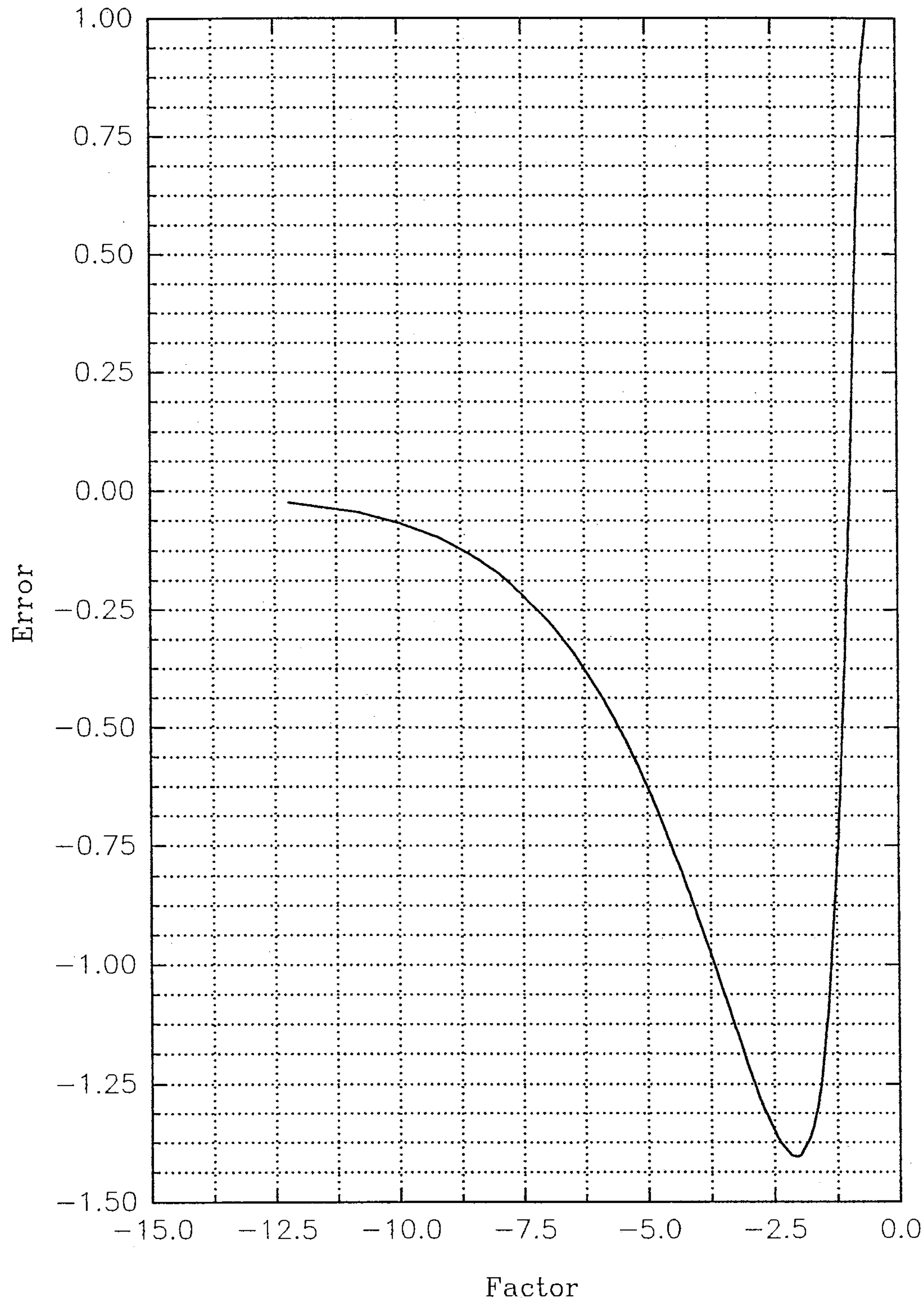

Figure 4−16. Error vs Factor for Cv = 1.0

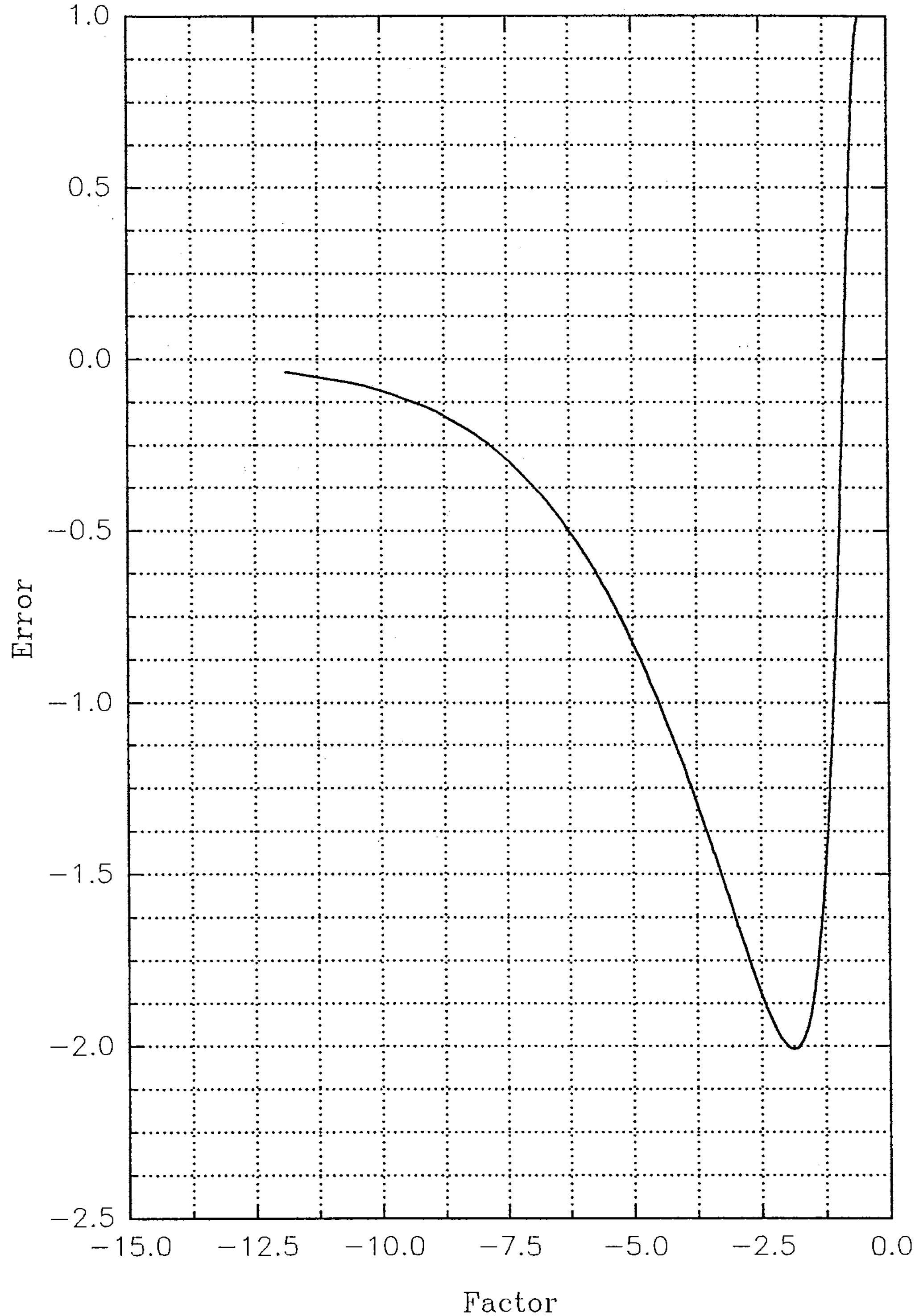

Figure 4−17. Error vs Factor for Cv = 1.2

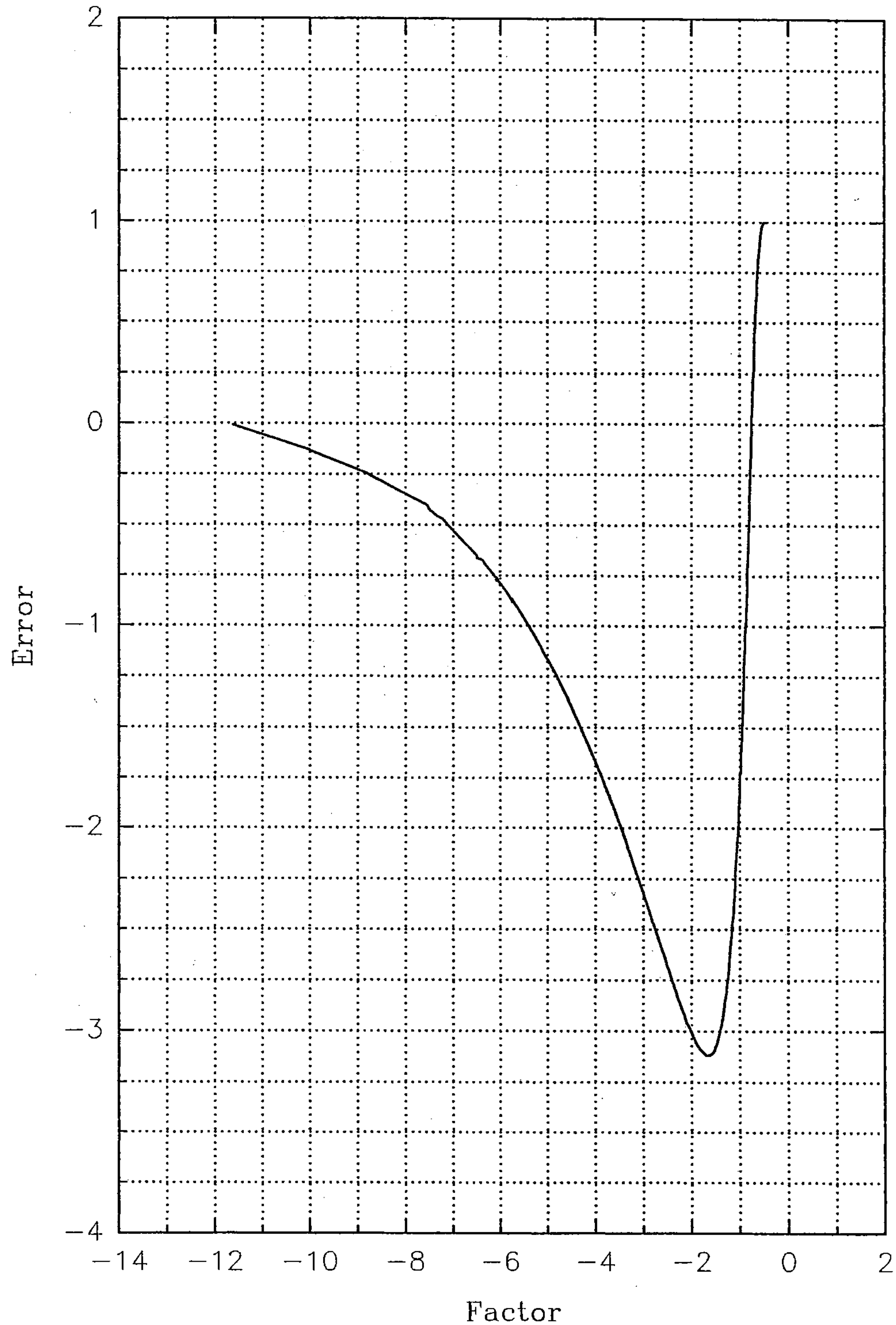

Figure 4−18. Error vs Factor for Cv = 1.5

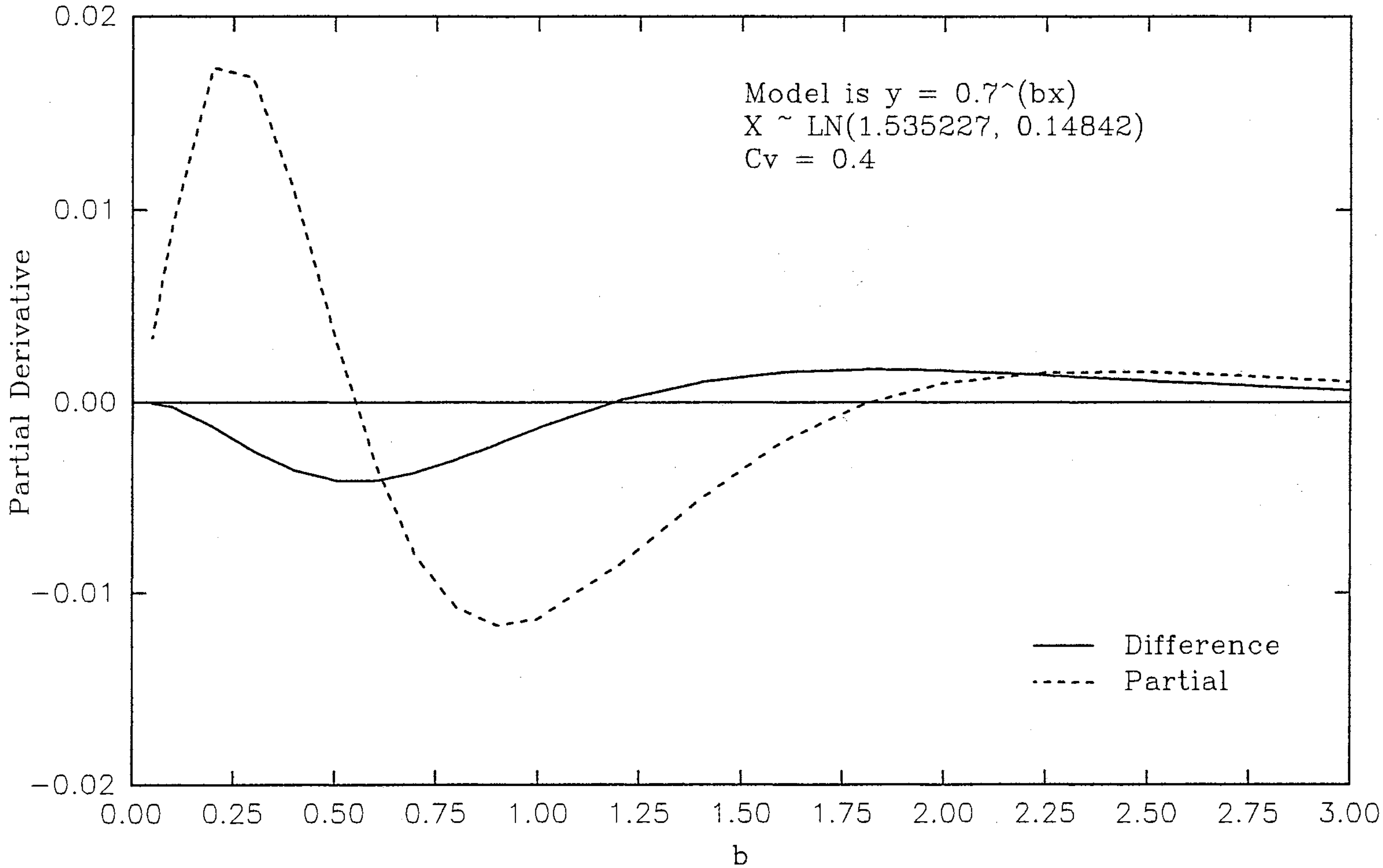

Figure 4−19. Partial Derivative and Difference as a Function of b

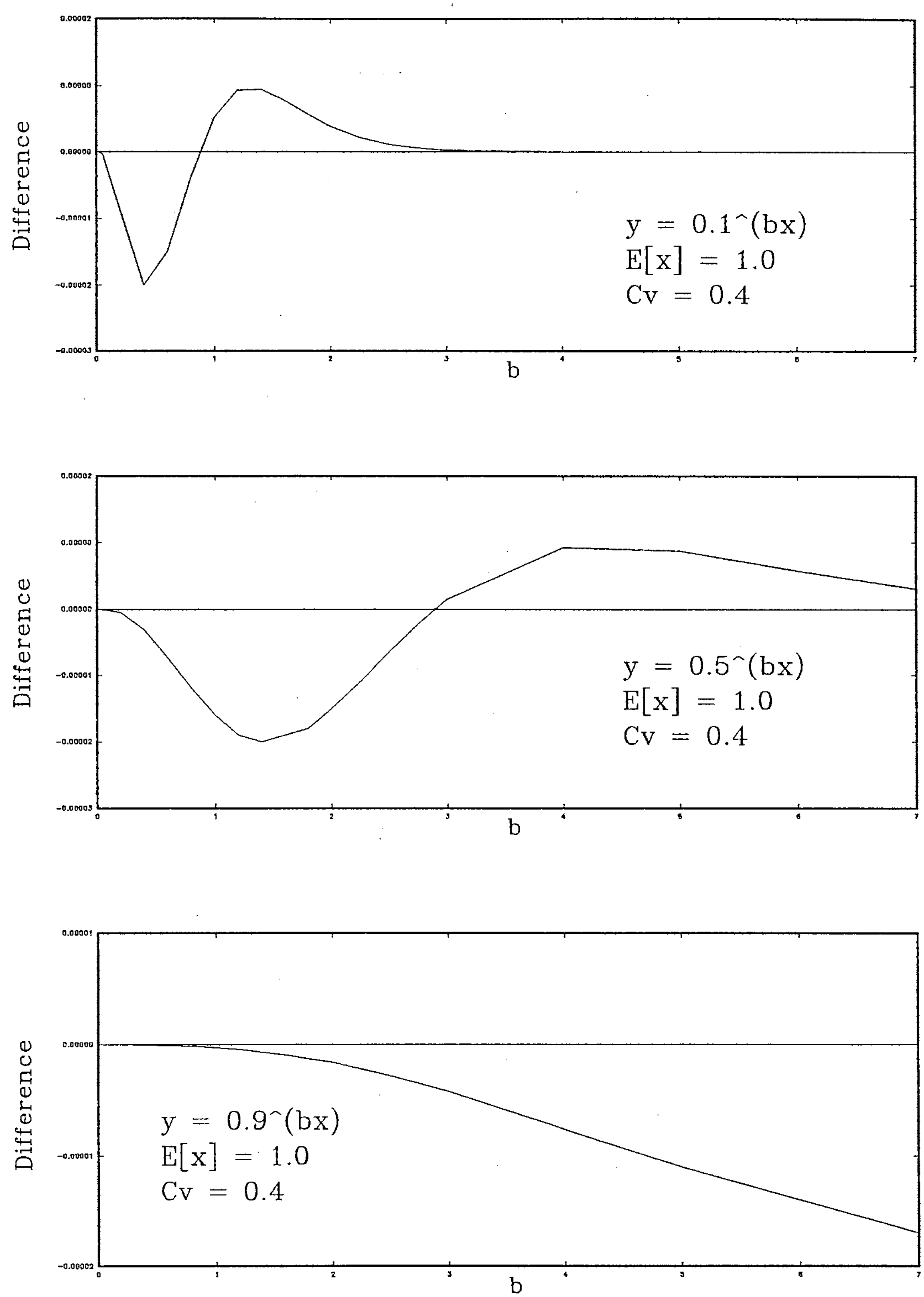

Figure 4–20. Behavior of Difference as a Increases

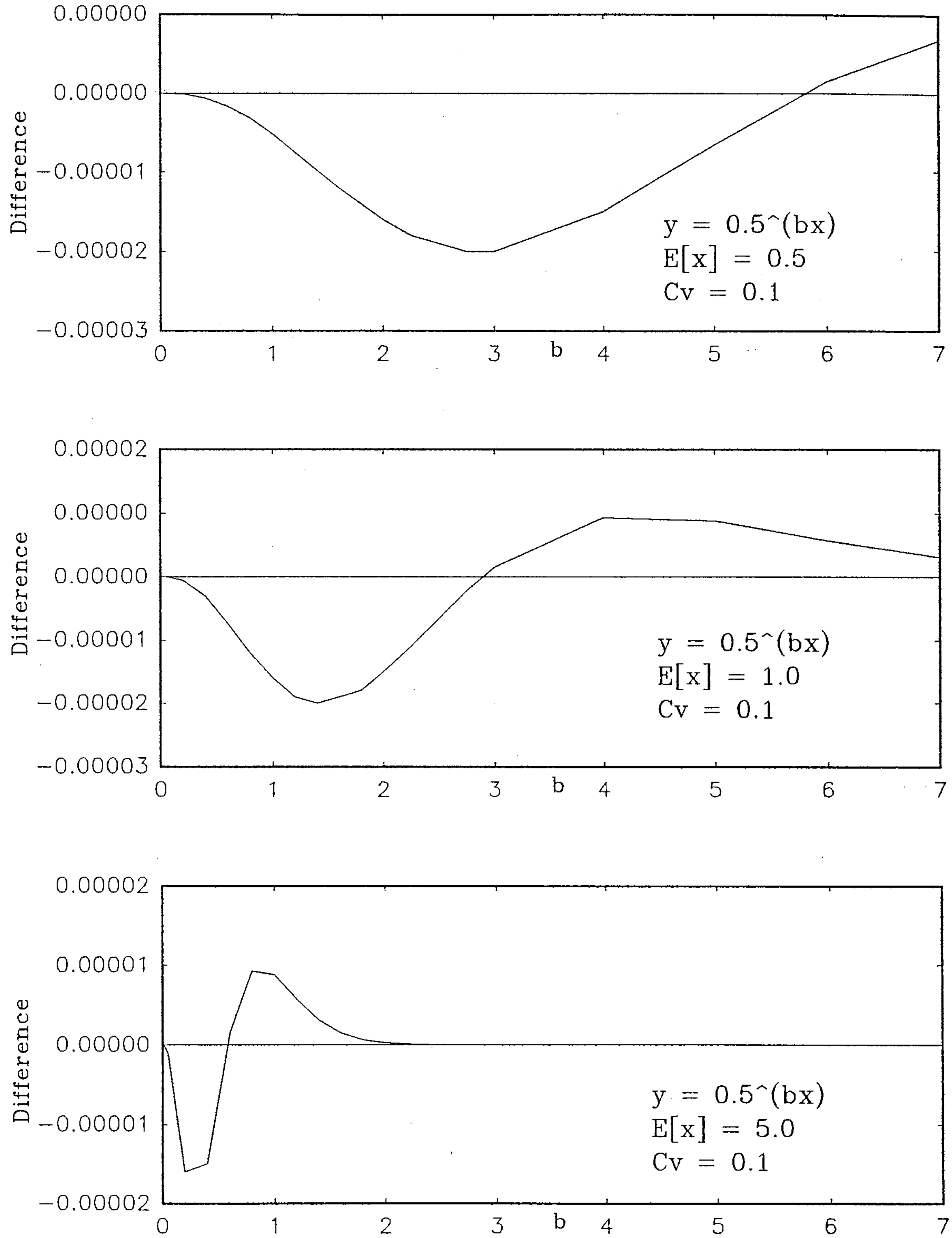

Figure 4–21. Behavior of Difference as E[x] Increases

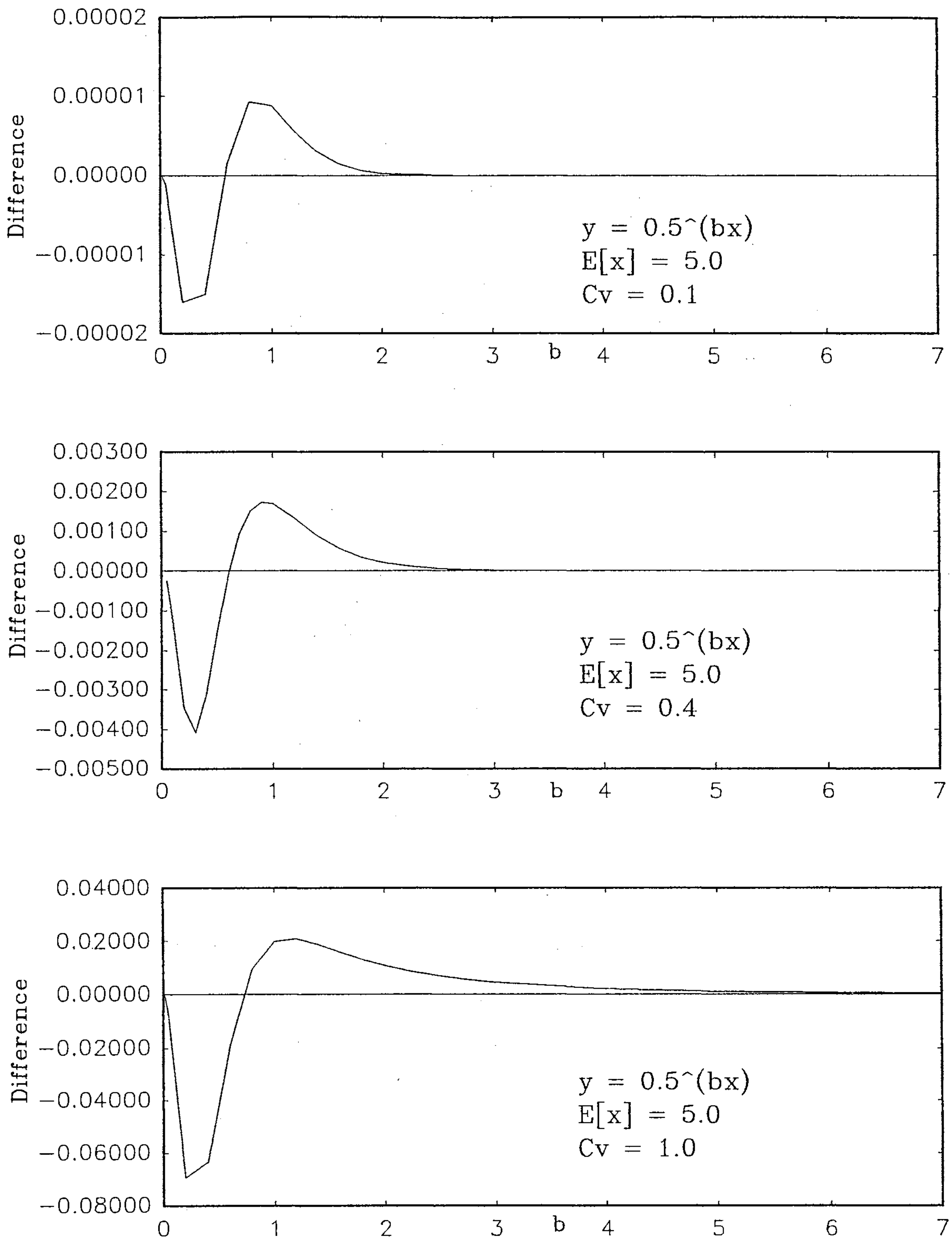

Figure 4−22. Behavior of Difference as Cv Increases

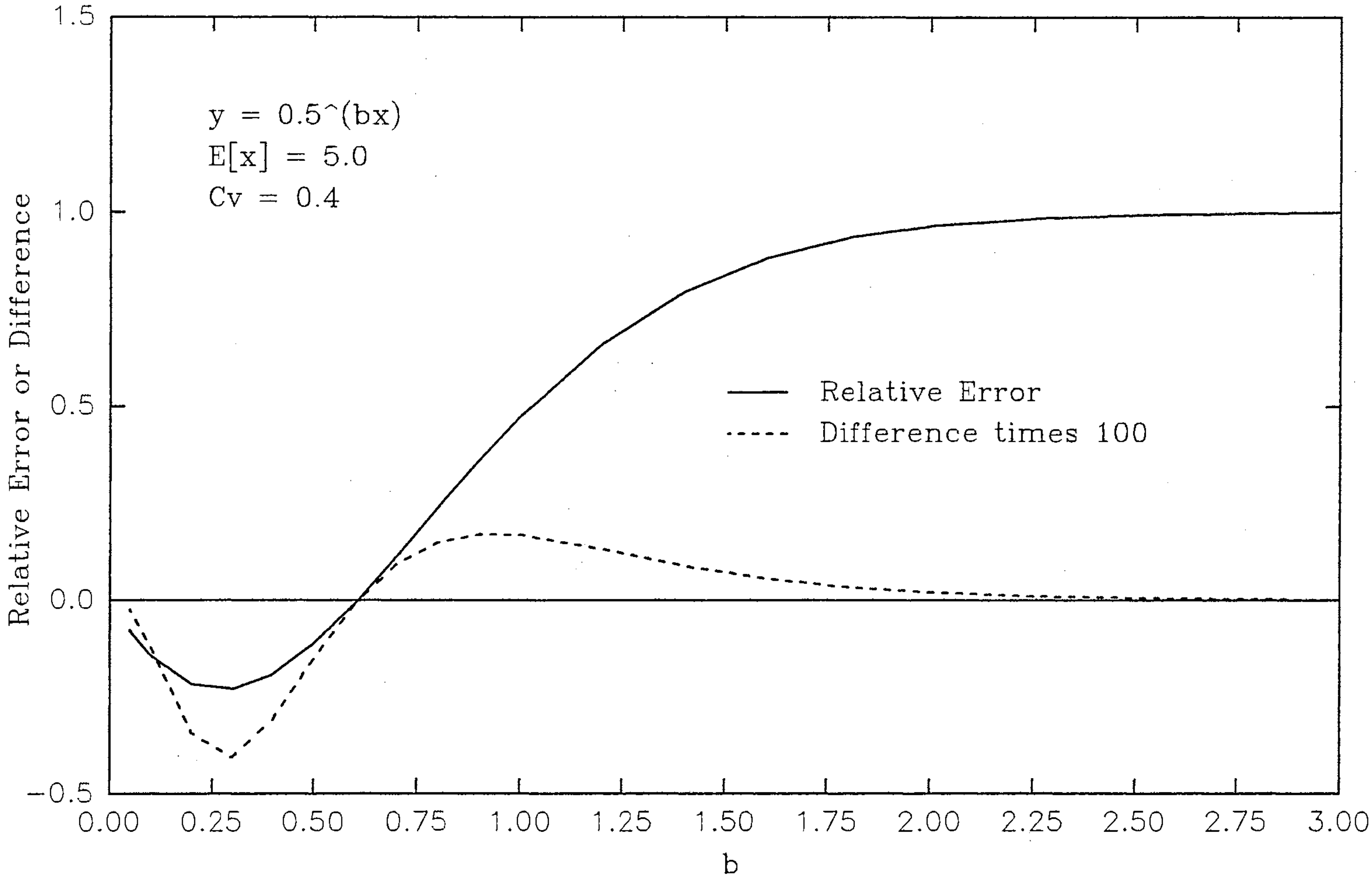

Figure 4−23. Pattern of Relative Error or Difference
as a Function of b

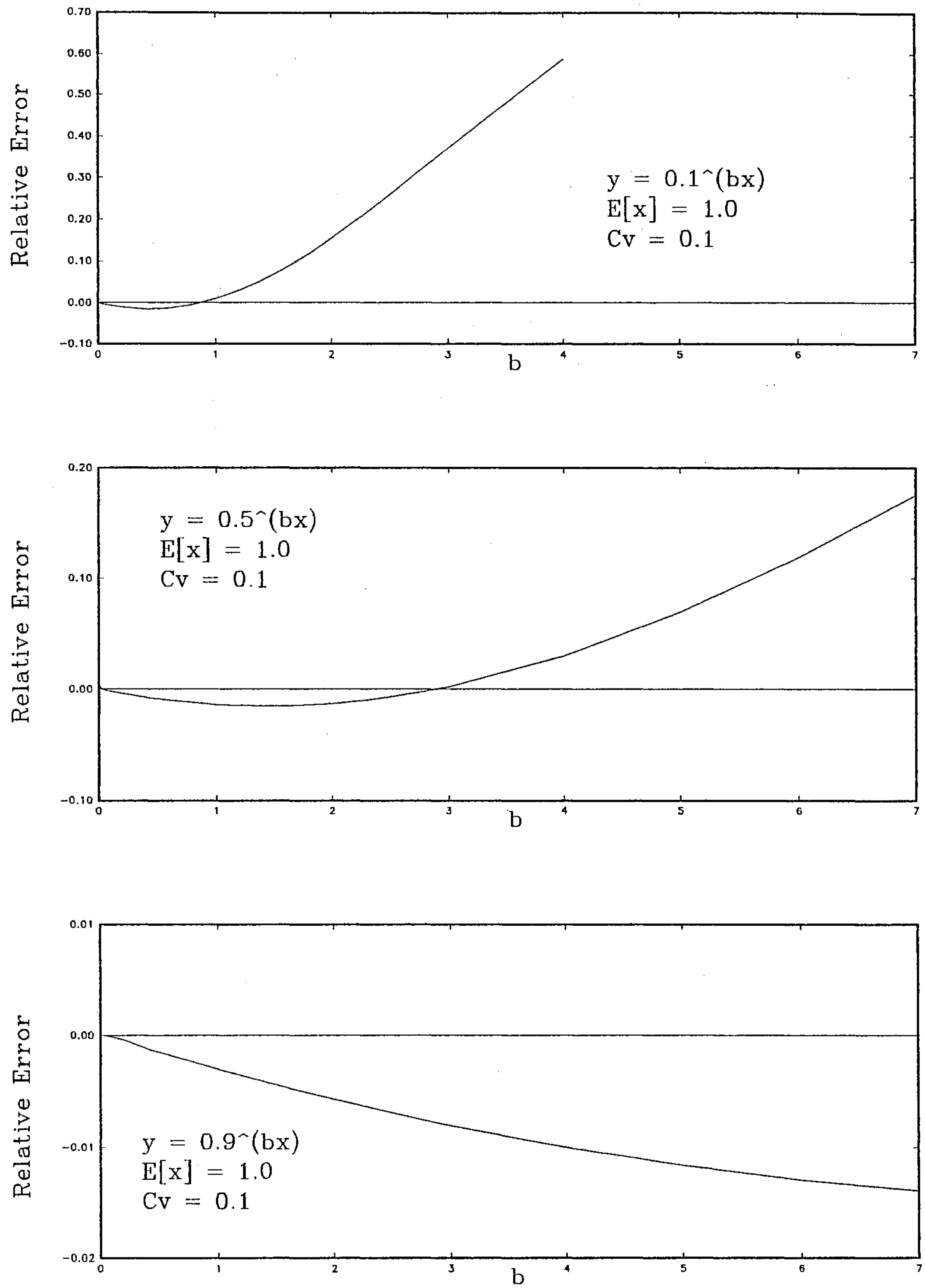

Figure 4–24. Behavior of Relative Error as a Increases

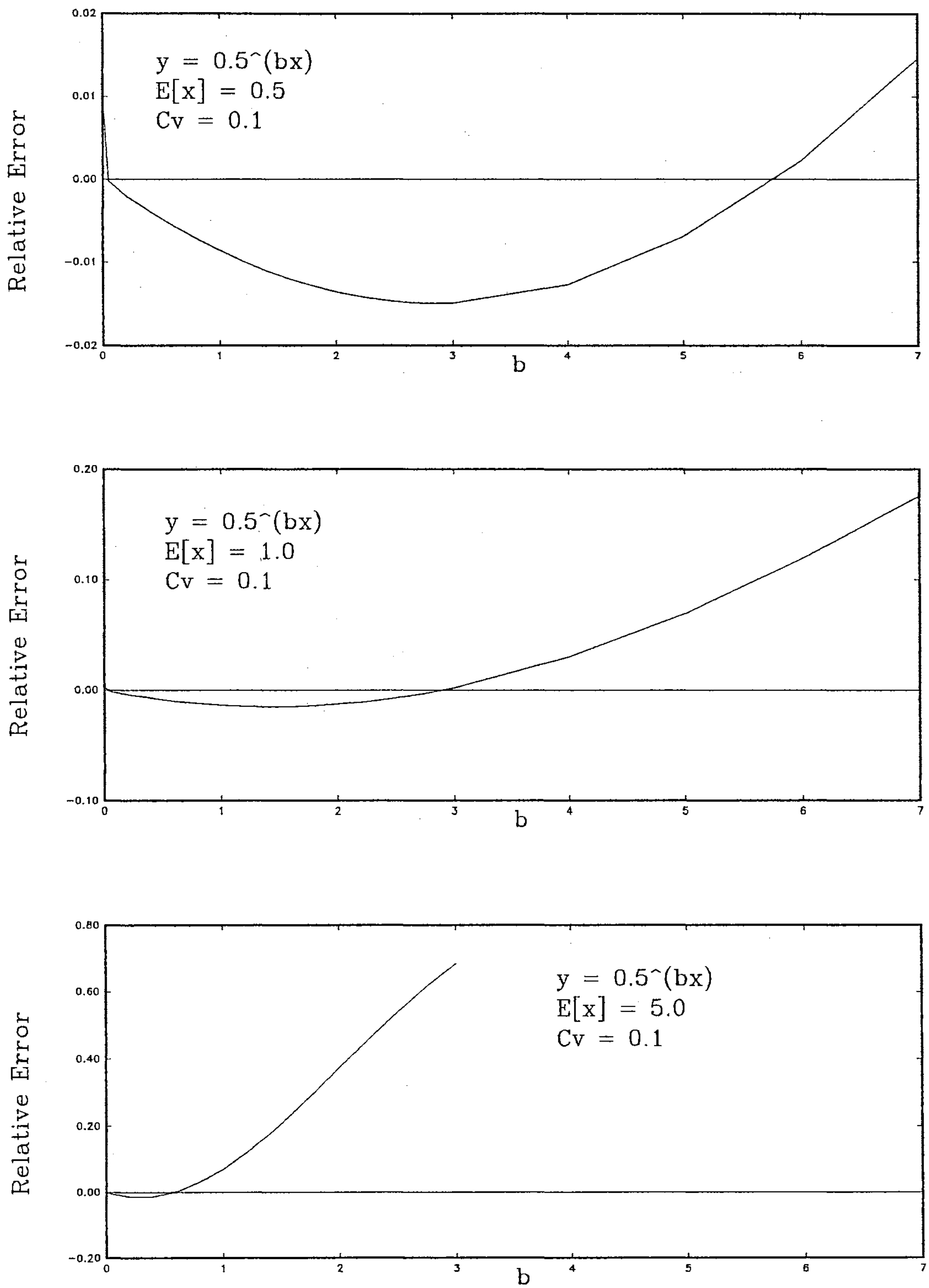

Figure 4–25. Behavior of Relative Error as E[x] Increases

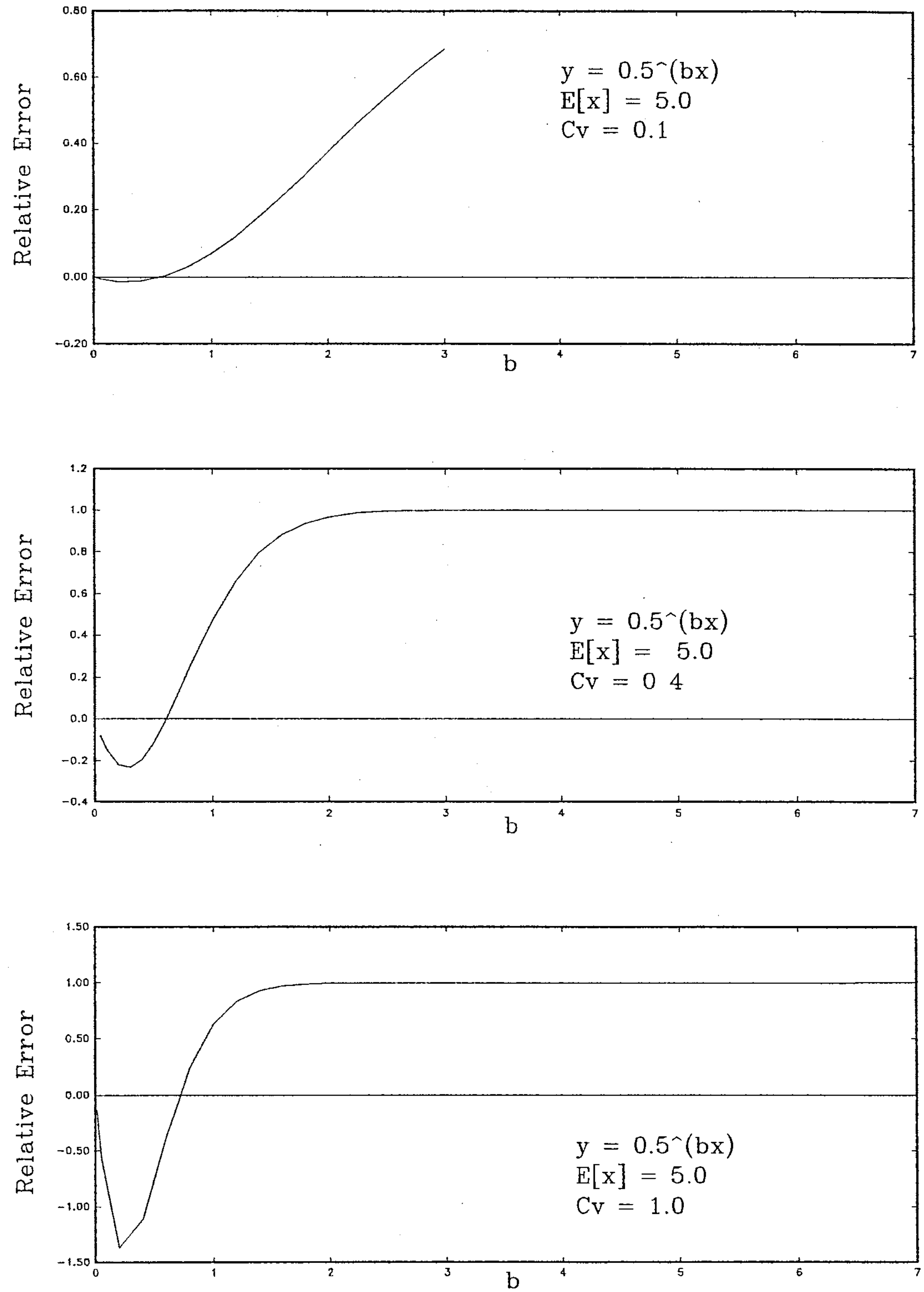

Figure 4-26. Behavior of Relative Error as Cv Increases

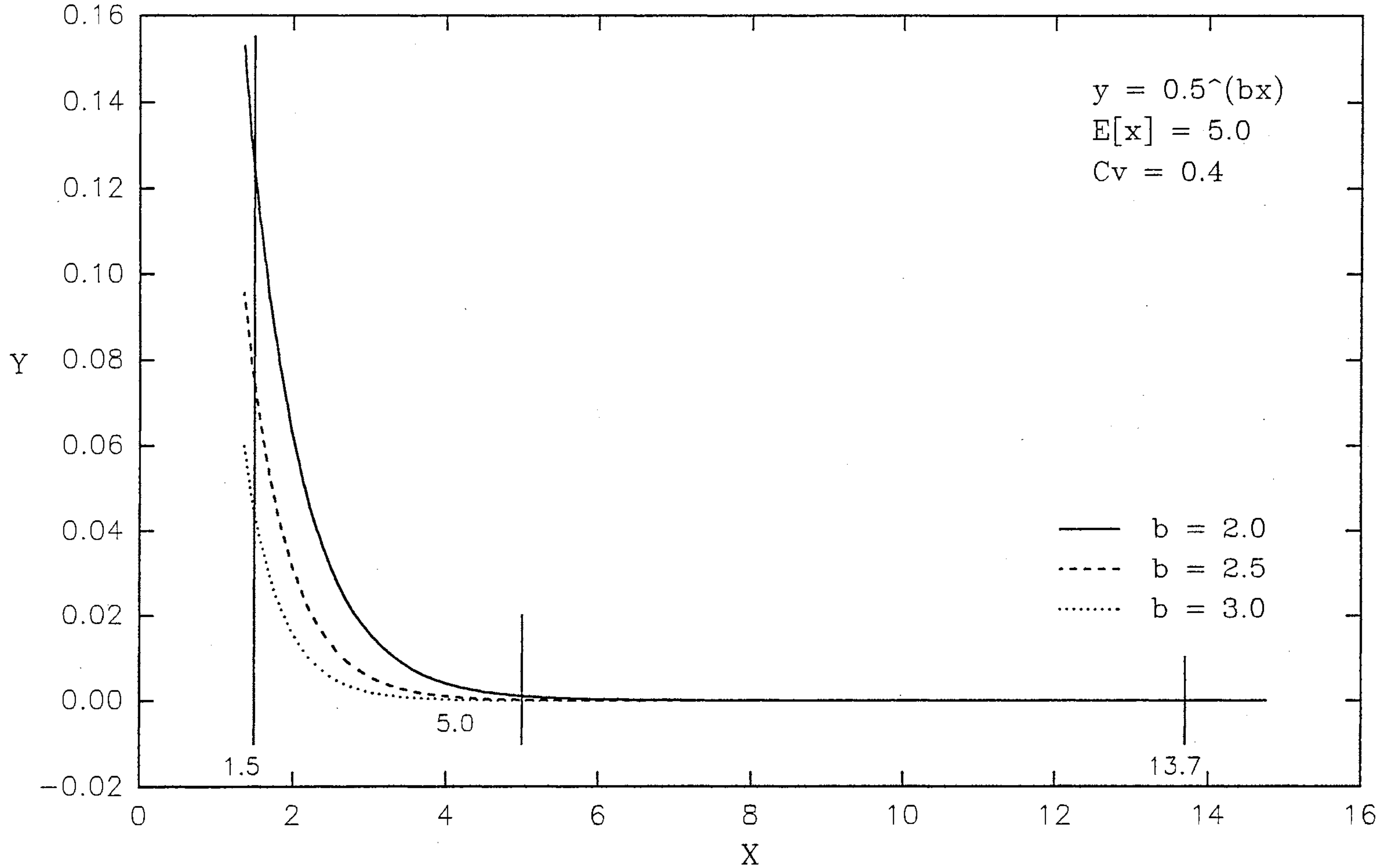

Figure 4−27. Behavior of Slope Evaluated at E[x] as b increases − E[x] Relatively Large

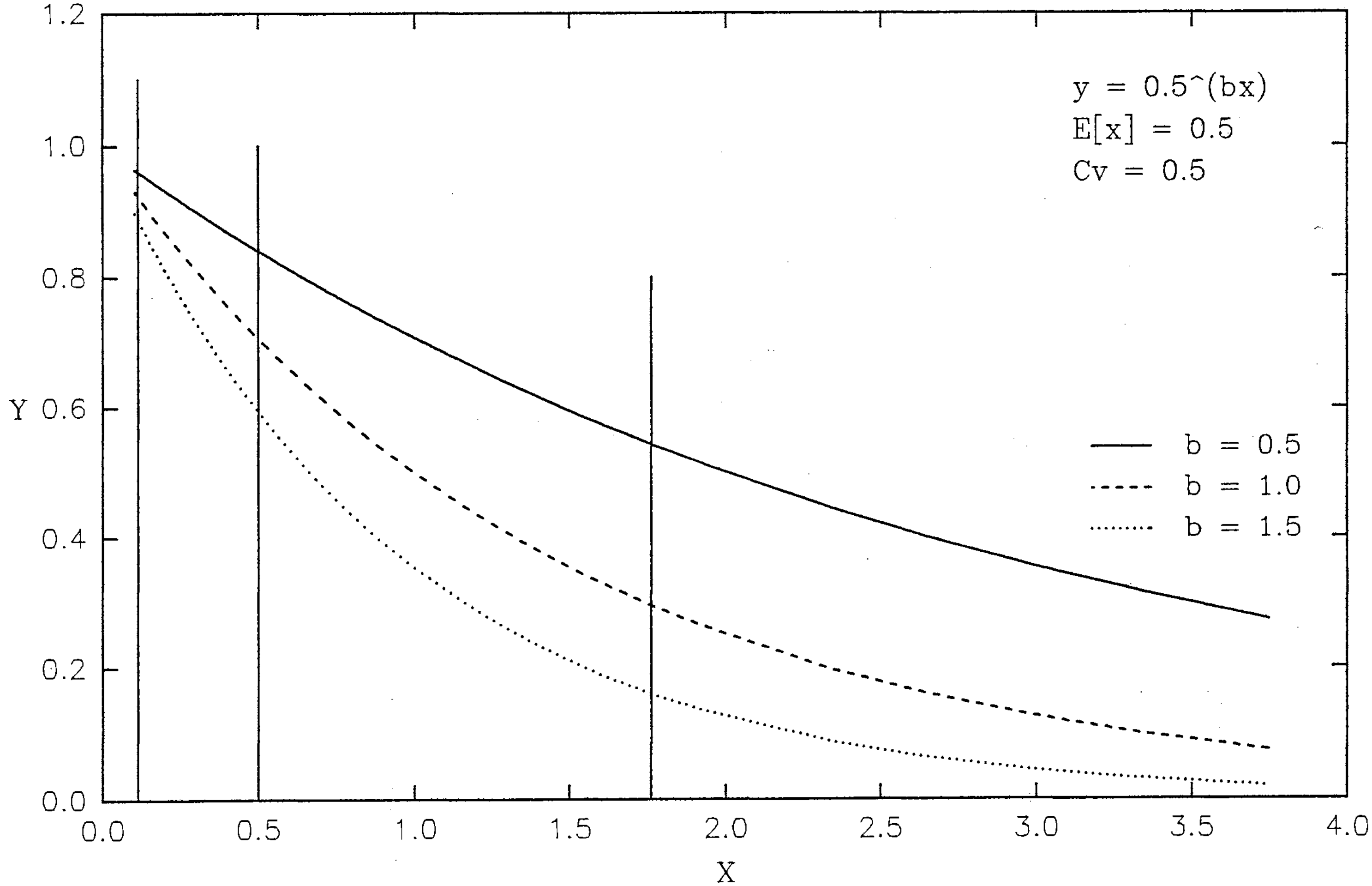

Figure 4-28. Behavior of Slope Evaluated at E[x] as b Increases – E[x] Relatively Small

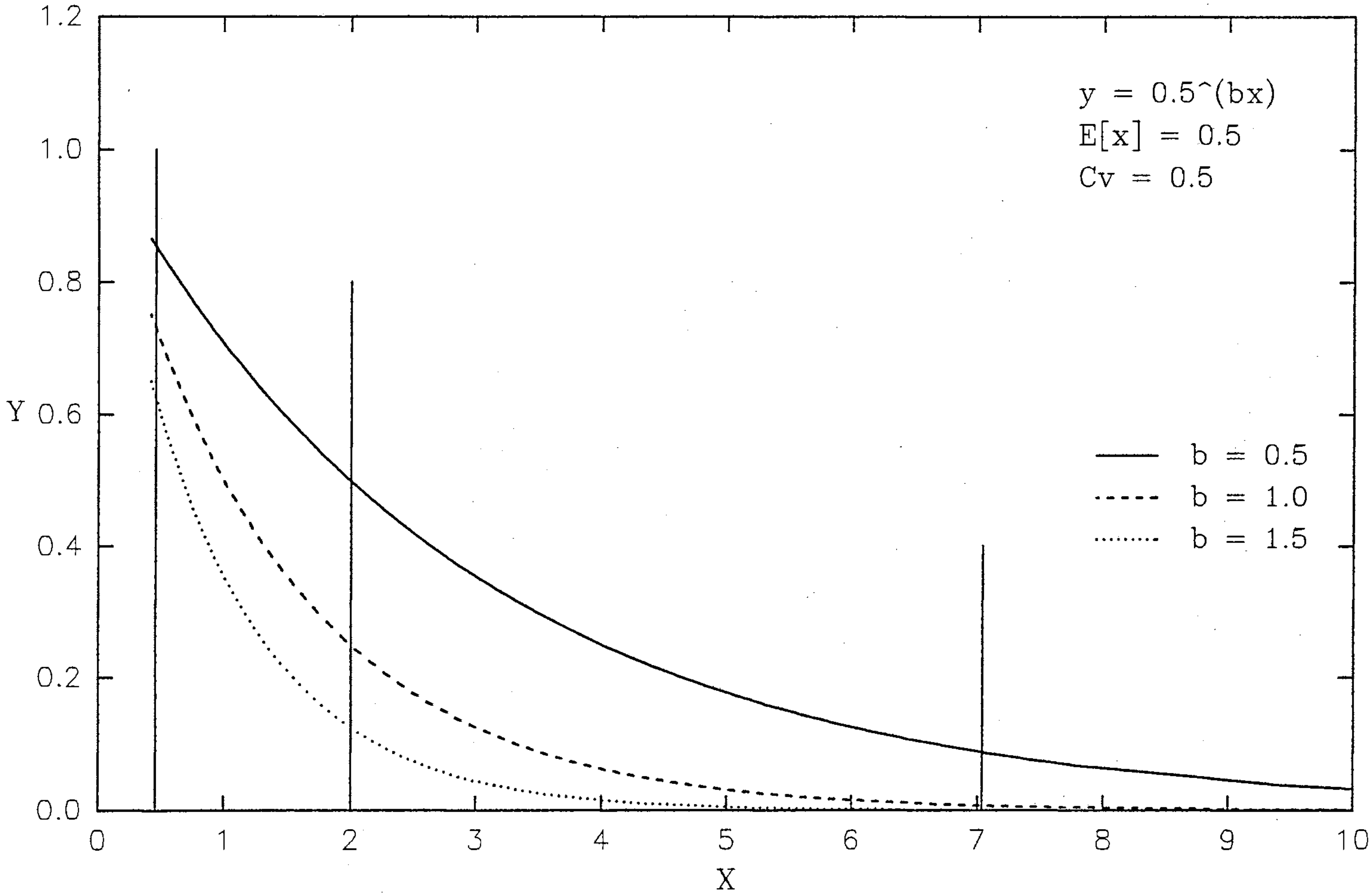

Figure 4–29. Behavior of Slope Evaluated at E[x] as b Increases – E[x] in Region of Maximum Curvature

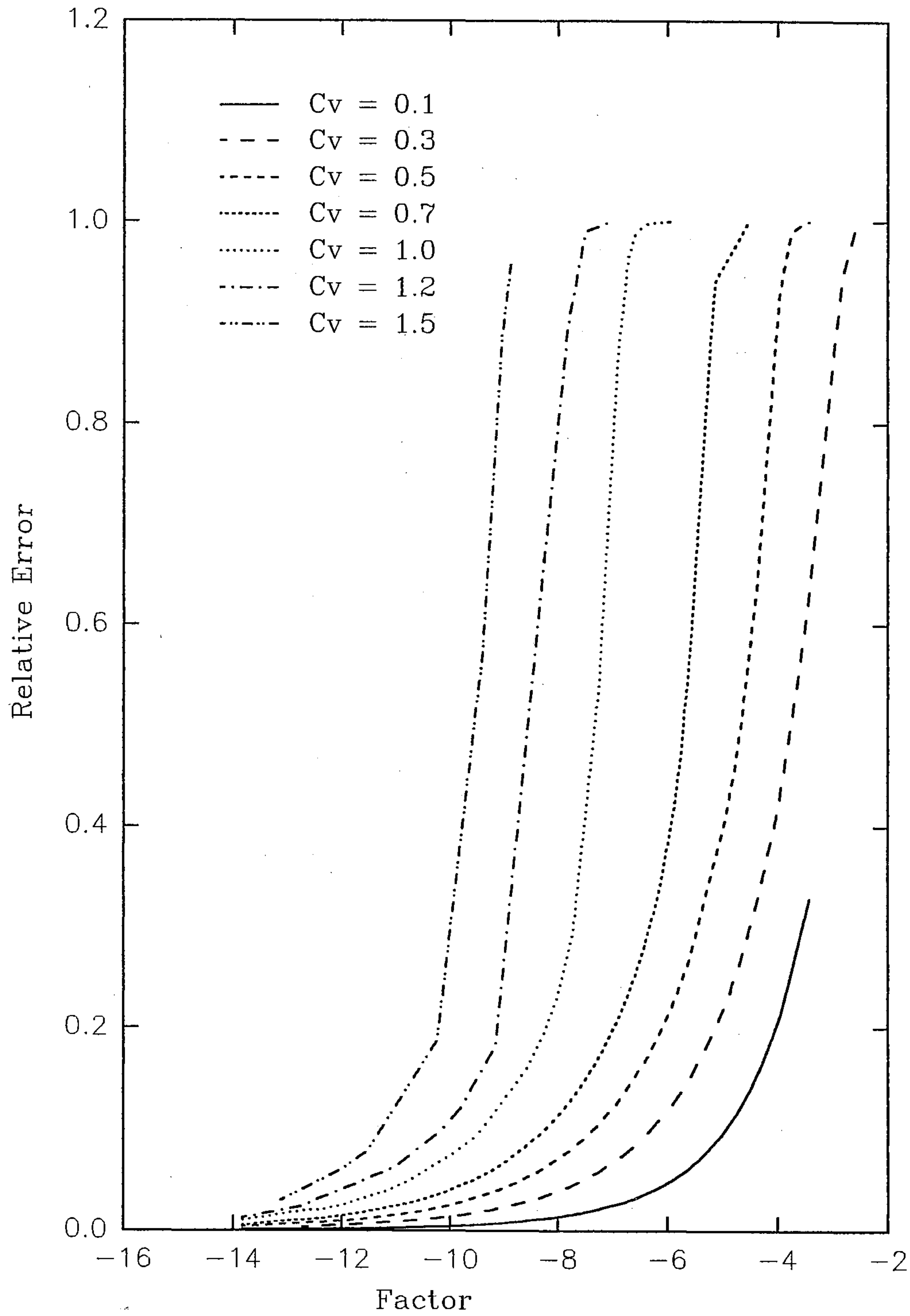

Figure 4−30. Composite Relative Error vs Factor Curve − Type C and D Exponential Models

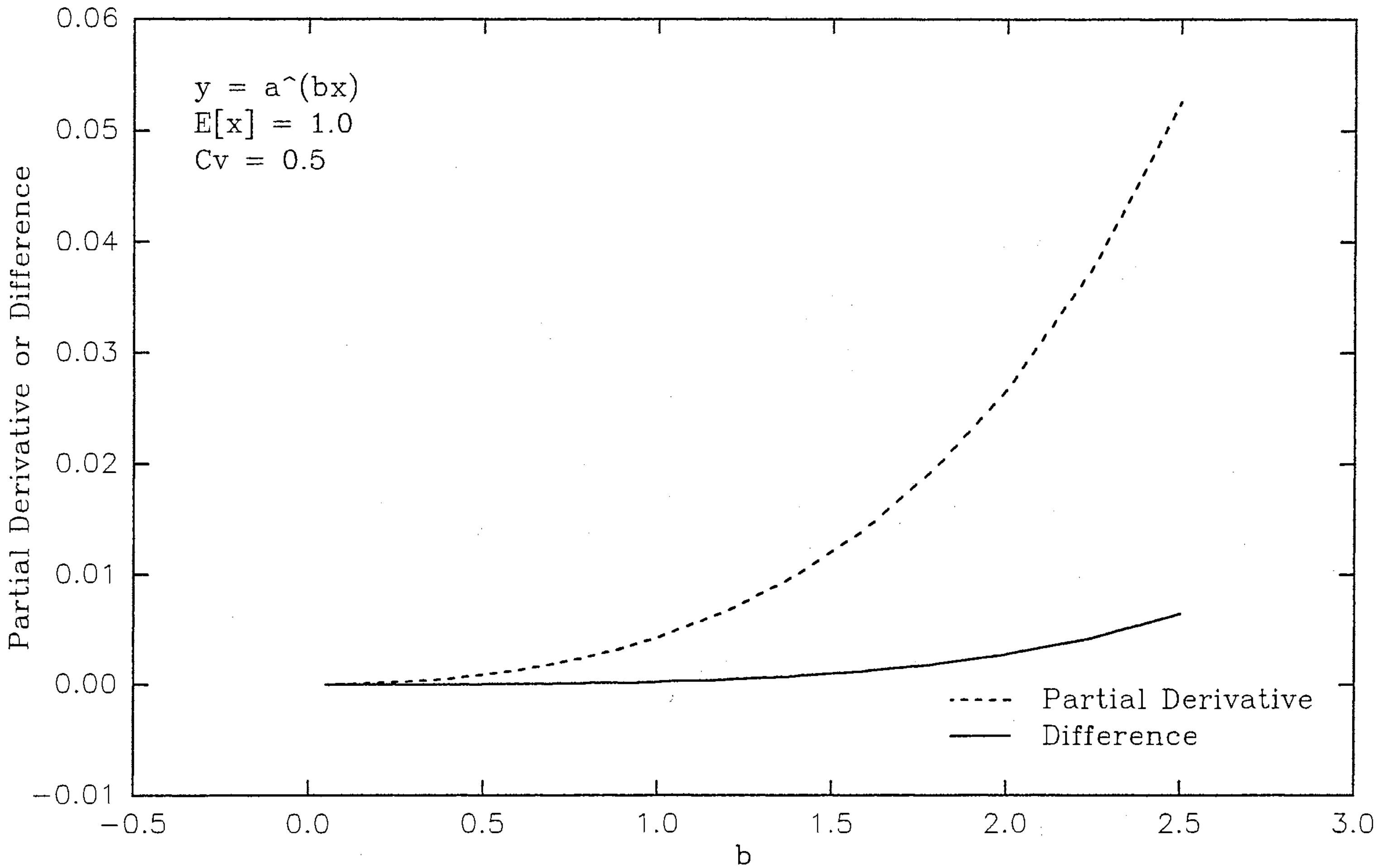

Figure 4-31. Pattern of Partial Derivative and Difference as b Increases

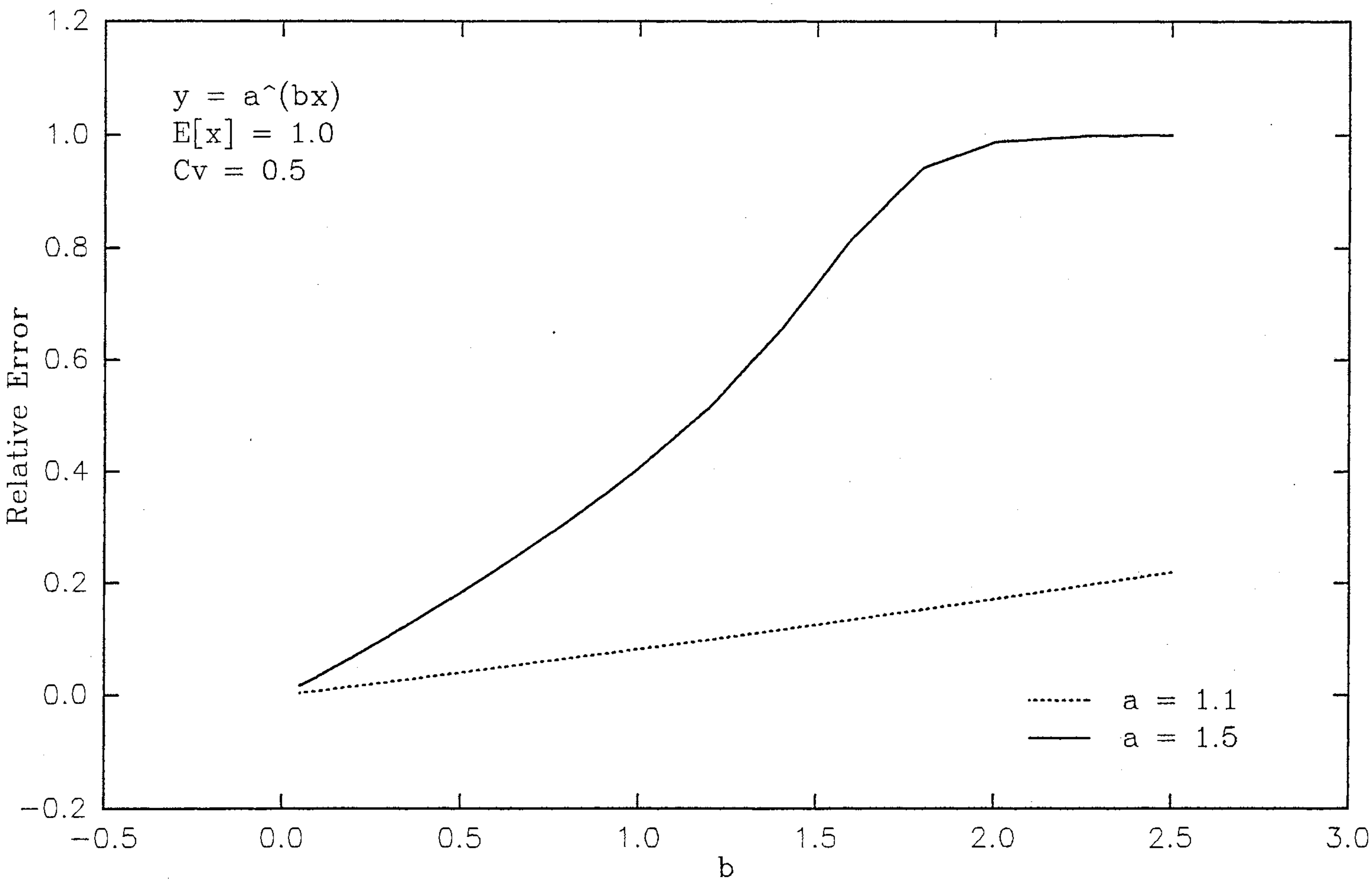

Figure 4-32. Pattern of Relative Error With Respect to b for Selected a's

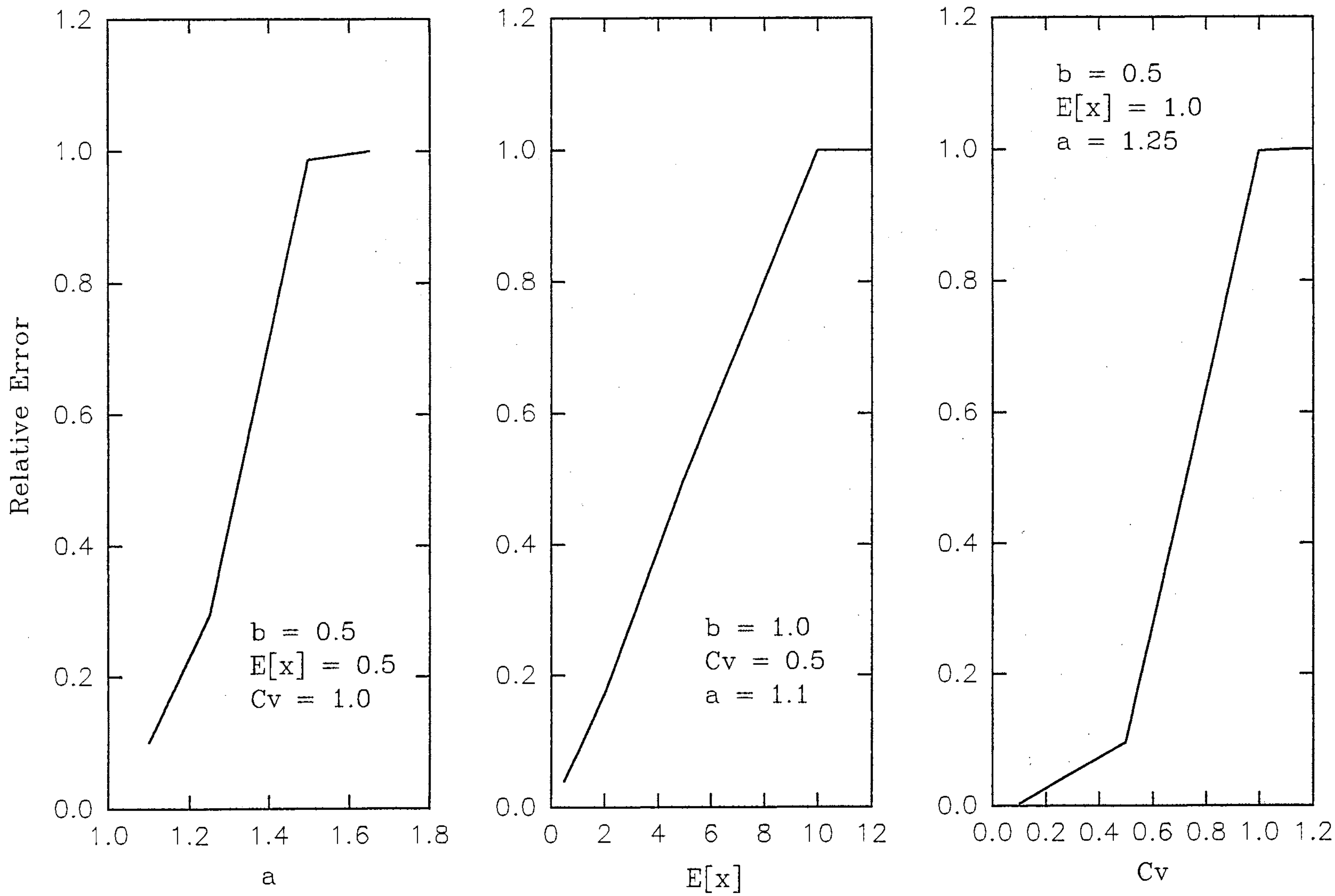

Figure 4-33. Behavior of Relative Error as a Function of a, E[x], and Cv

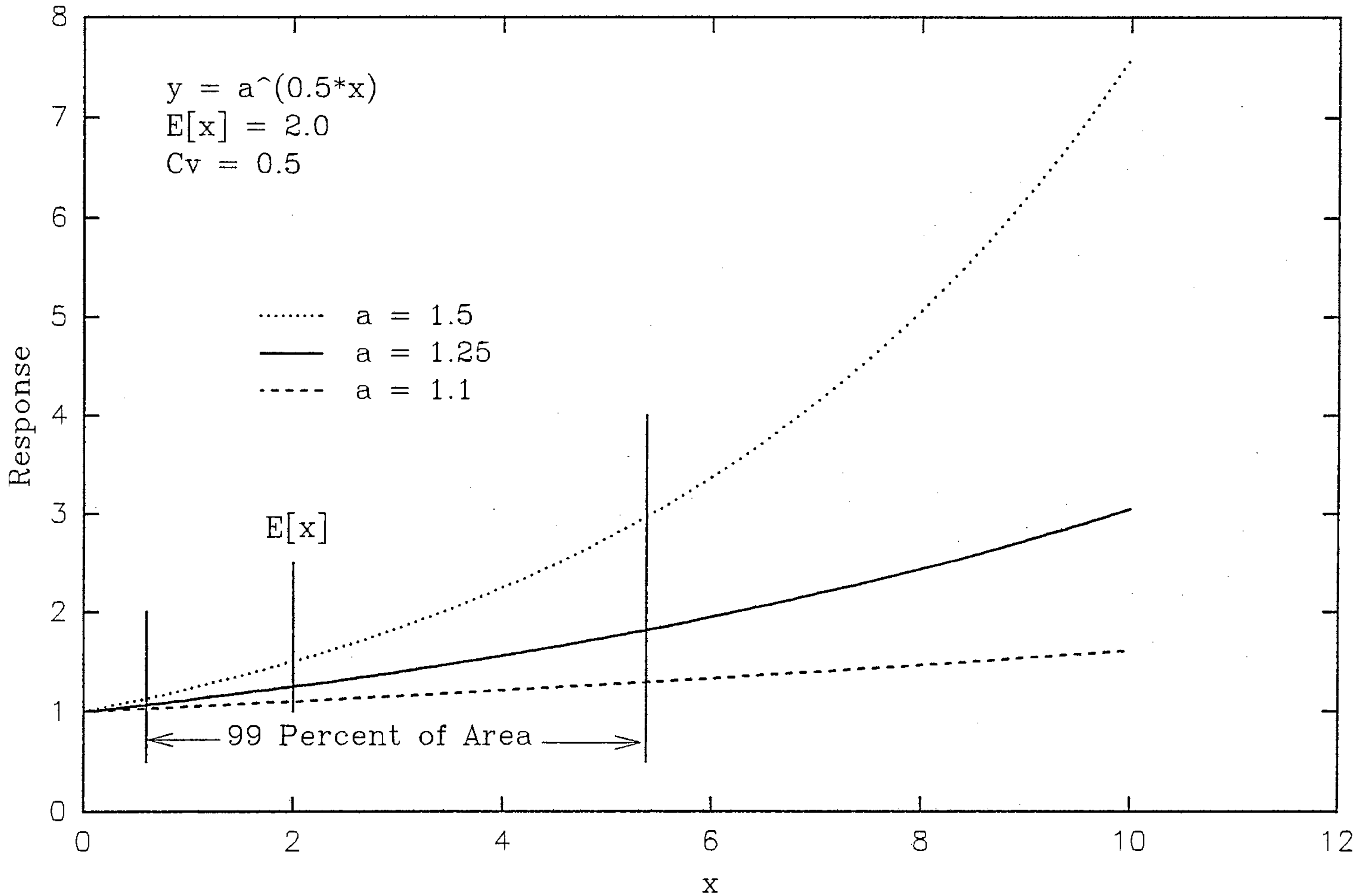

Figure 4-34. Slope of Response as a Increases

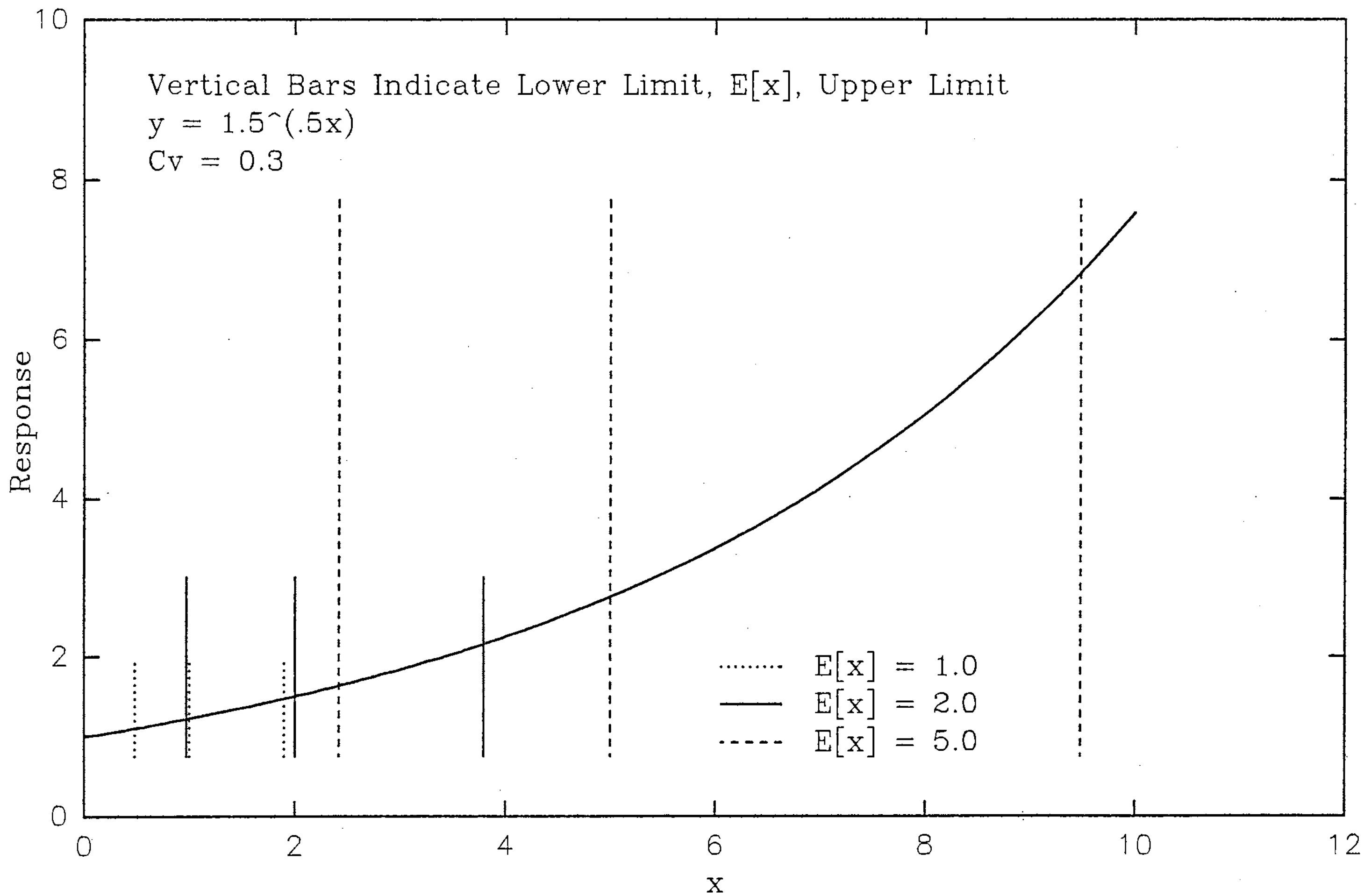

Figure 4–35. Change in Range of Significant Probability as E[x] Increases

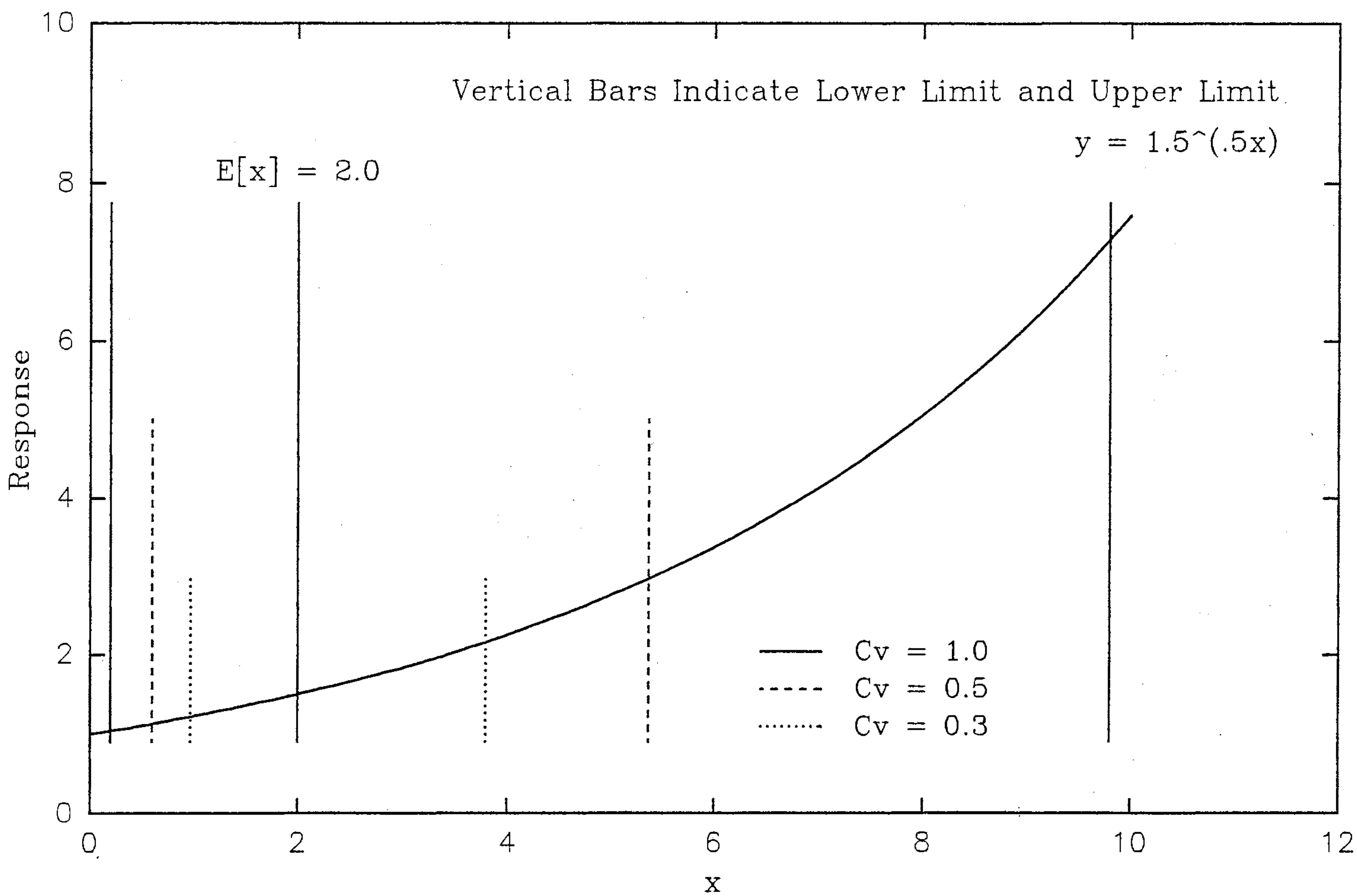

Figure 4–36. Change in Range of Significant Probability as Cv Increases

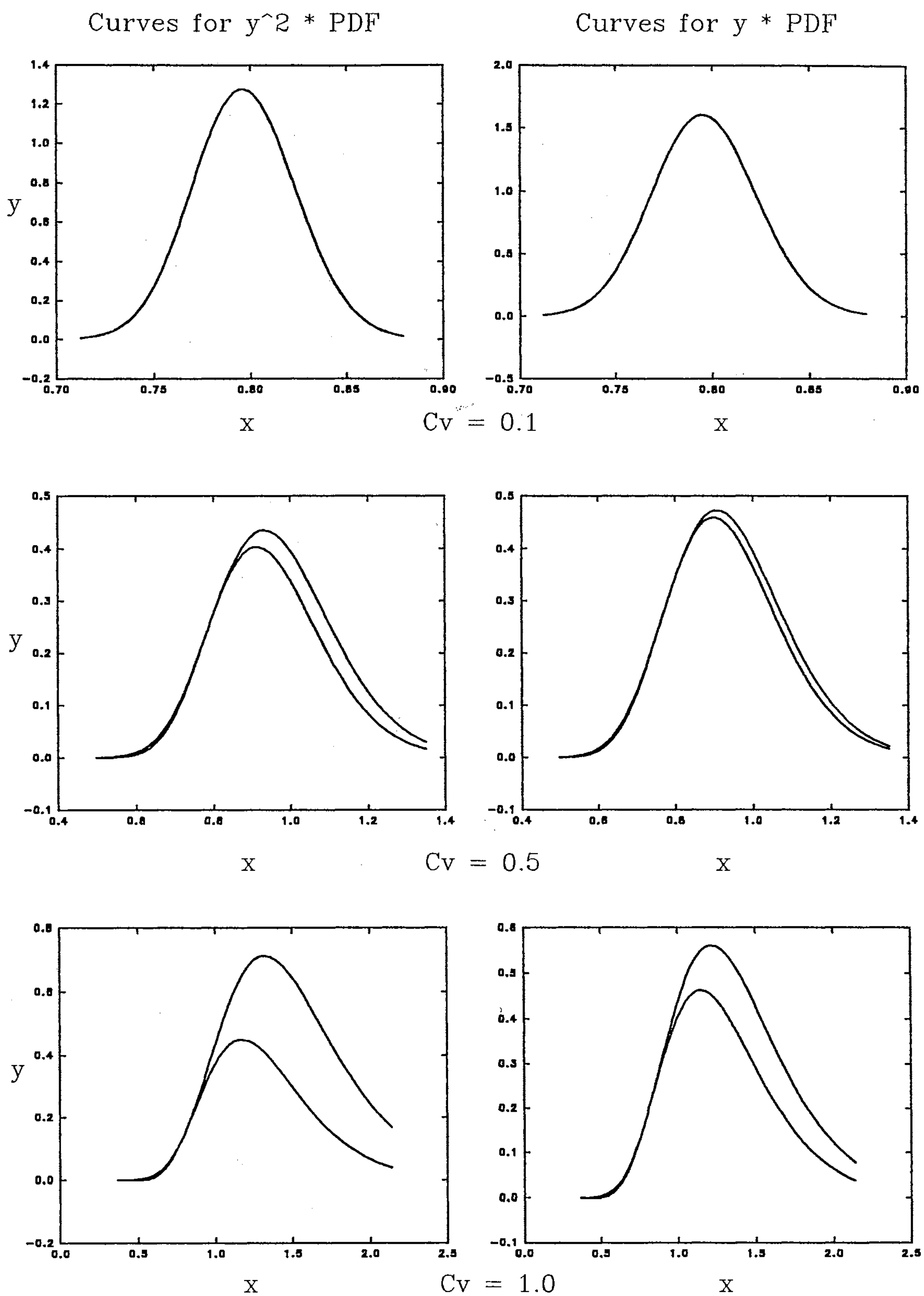

Figure 4–37. Behavior of Response Times PDF as Cv Changes

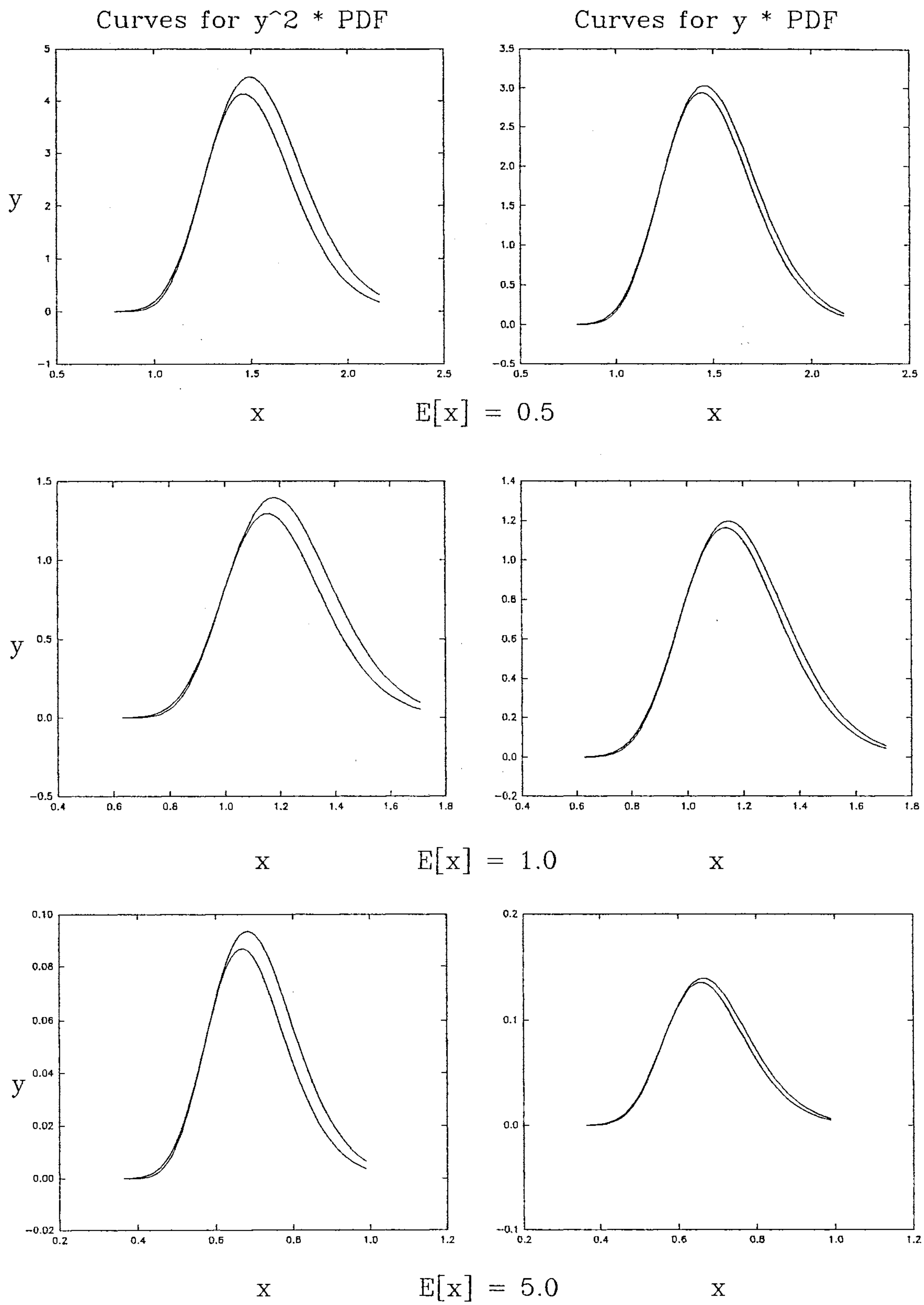

Figure 4–38. Behavior of Response Times PDF as E[x] Changes

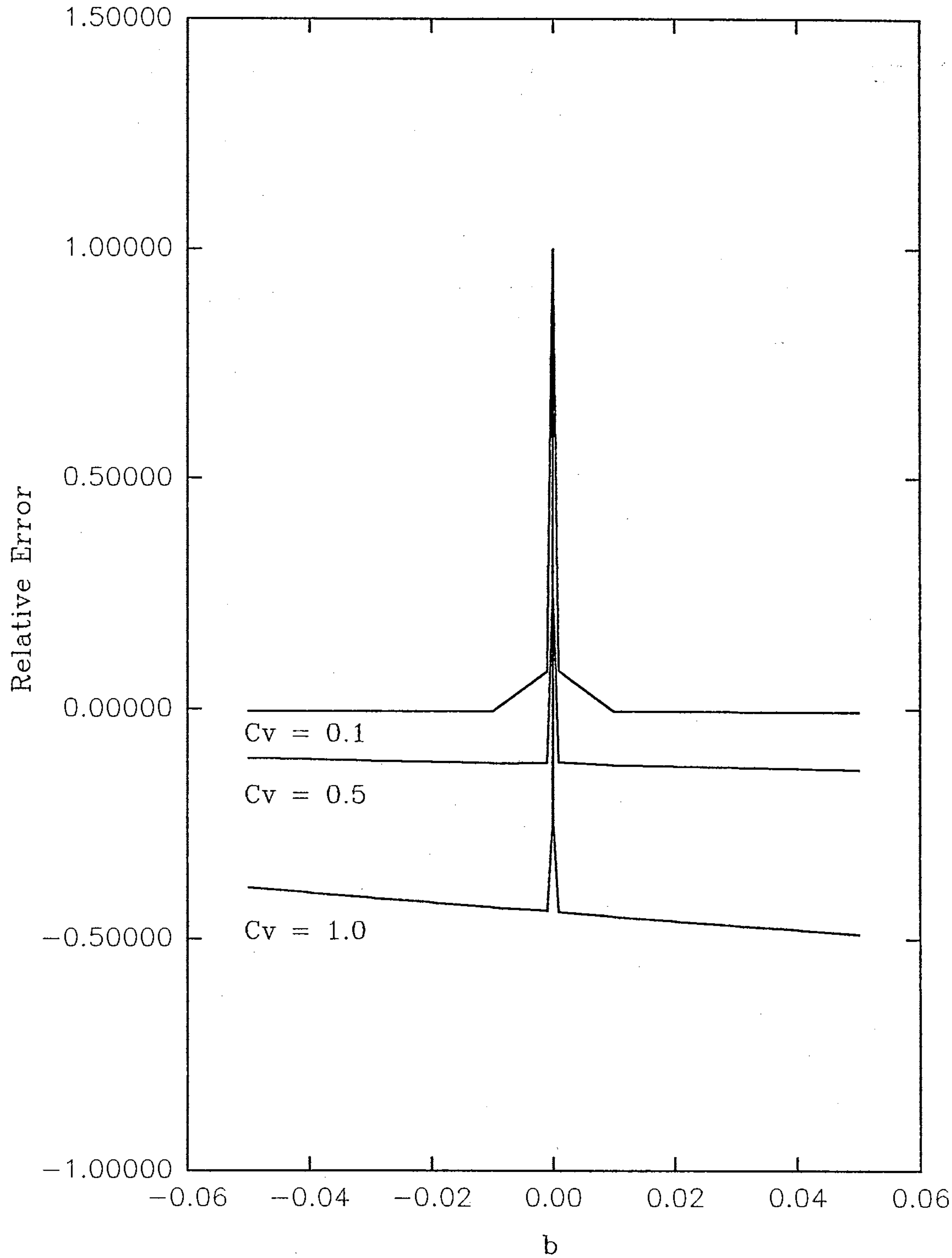

Figure 4−39. Error Curves in the Region of b = 0

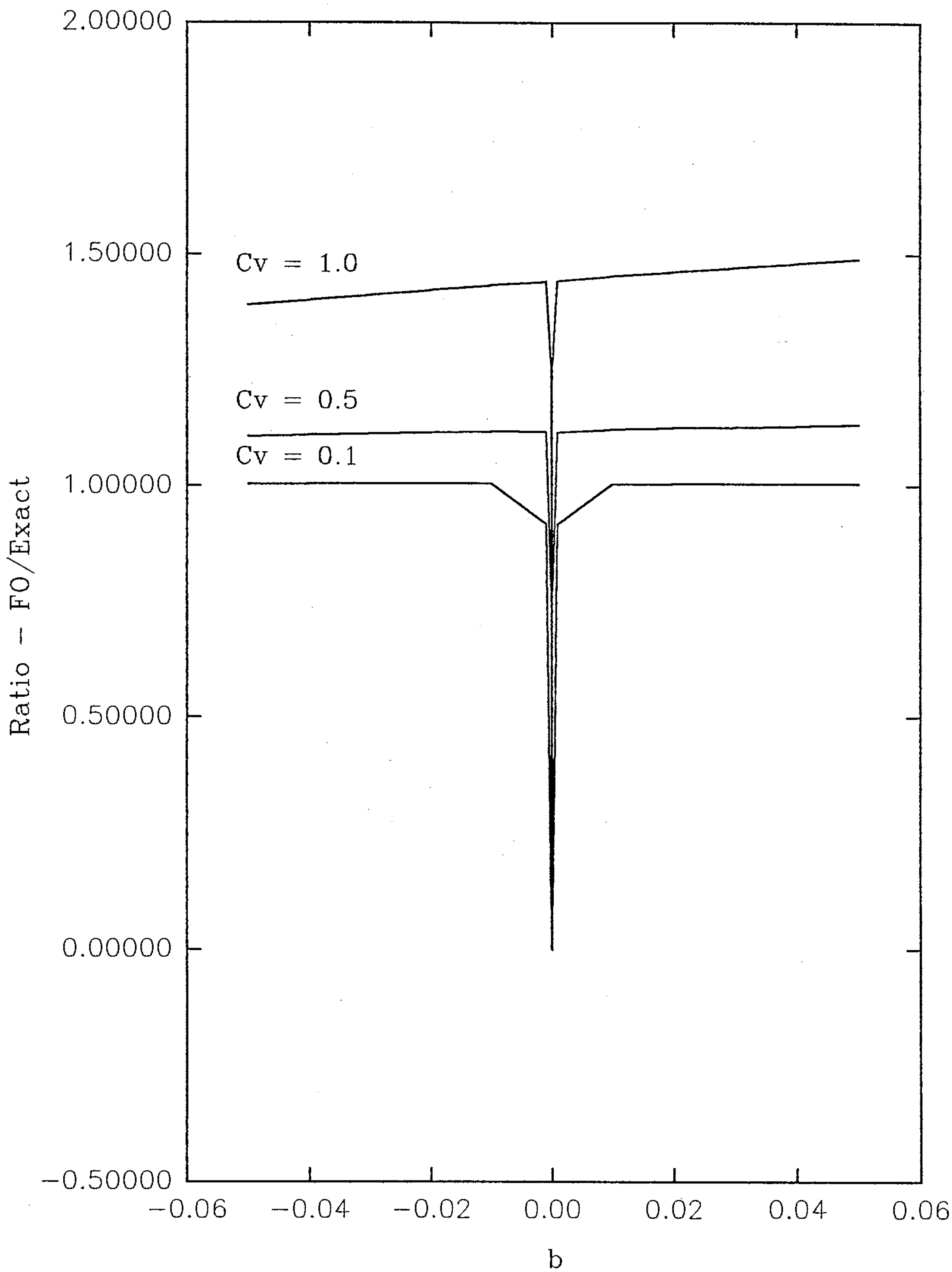

Figure 4-40. Ratio of First Order to Analytical Variance

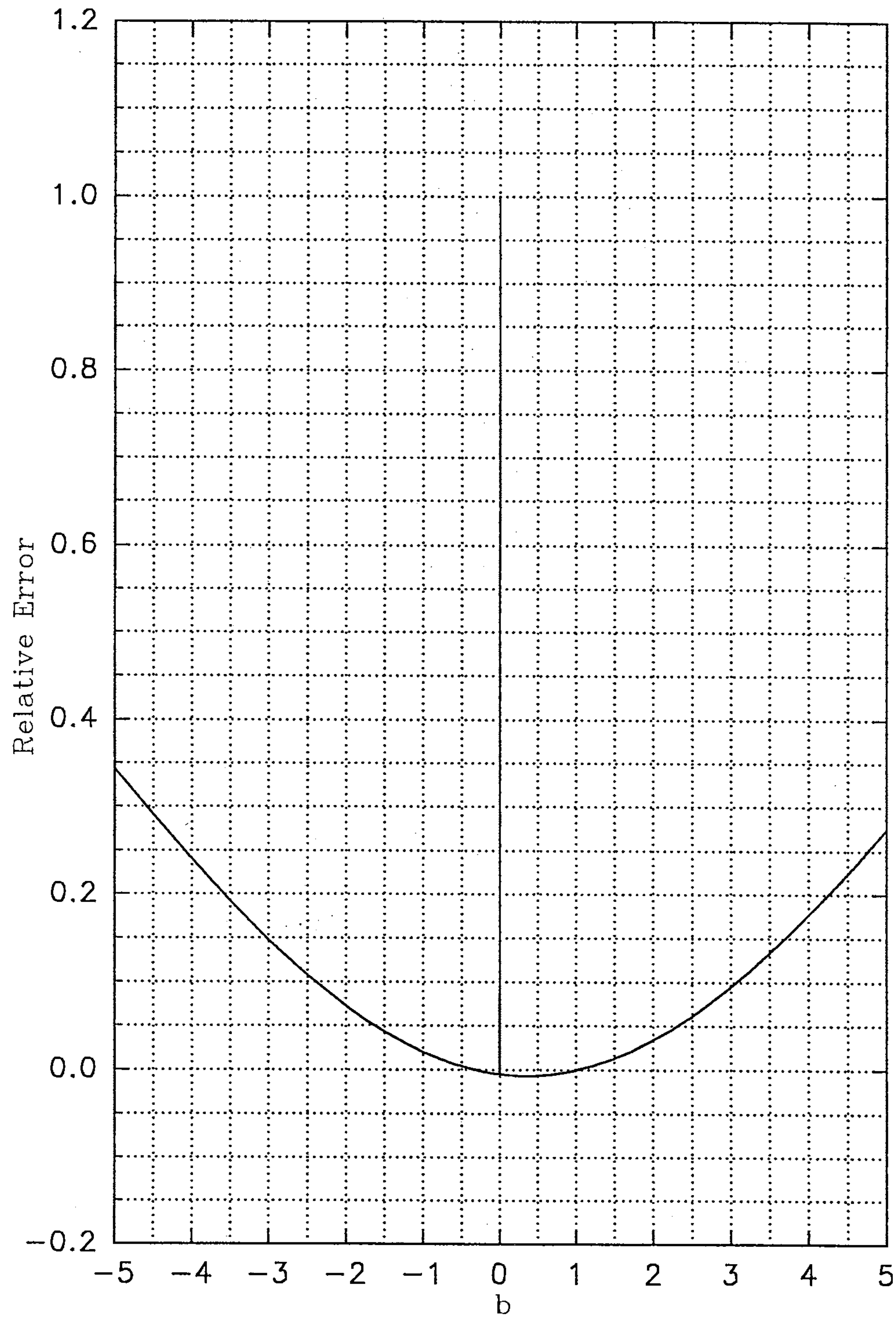

Figure 4−41. Relative Error vs b for Cv = 0.1

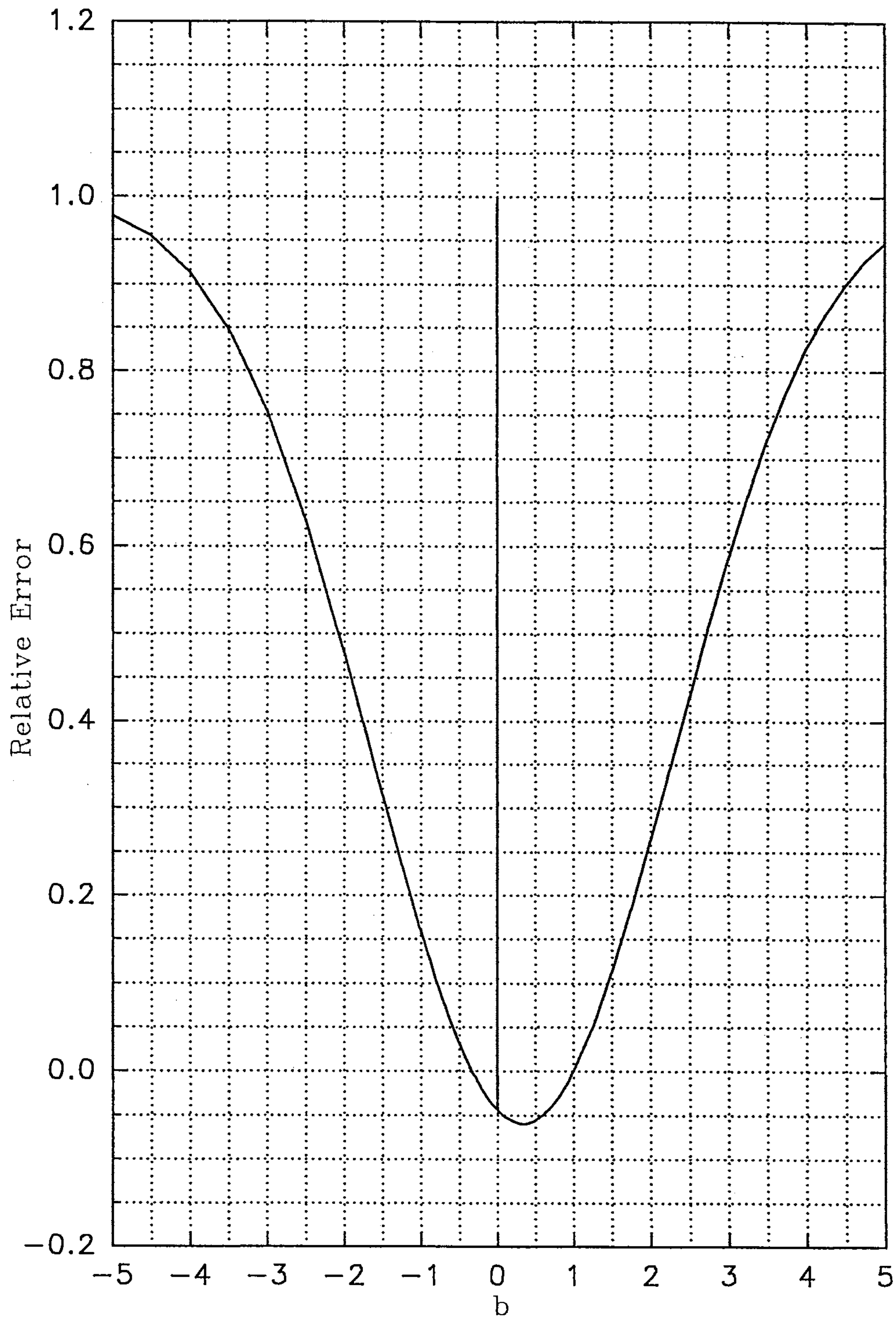

Figure 4−42. Relative Error vs b for Cv = 0.3

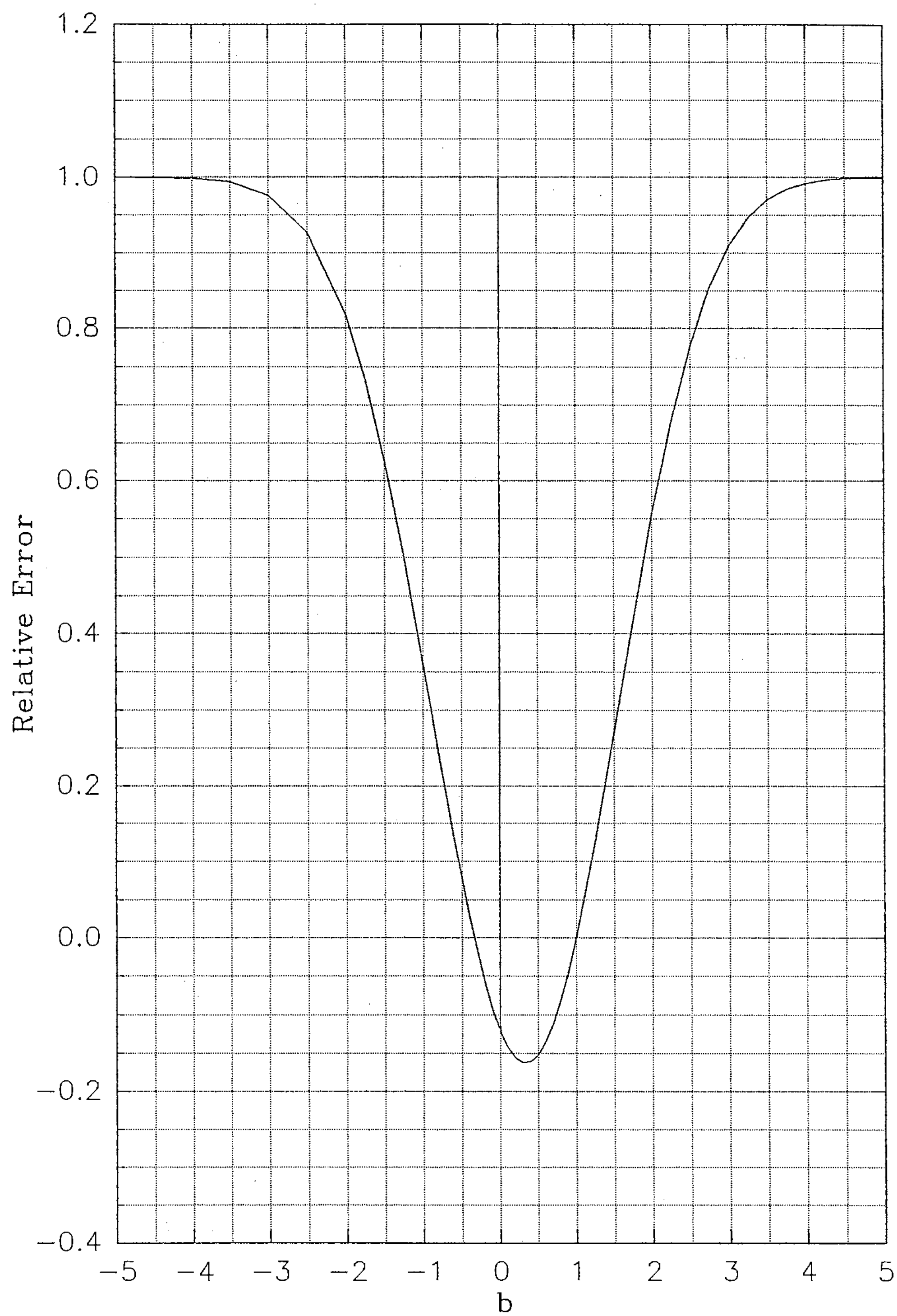

Figure 4−43. Relative Error vs b for Cv = 0.5

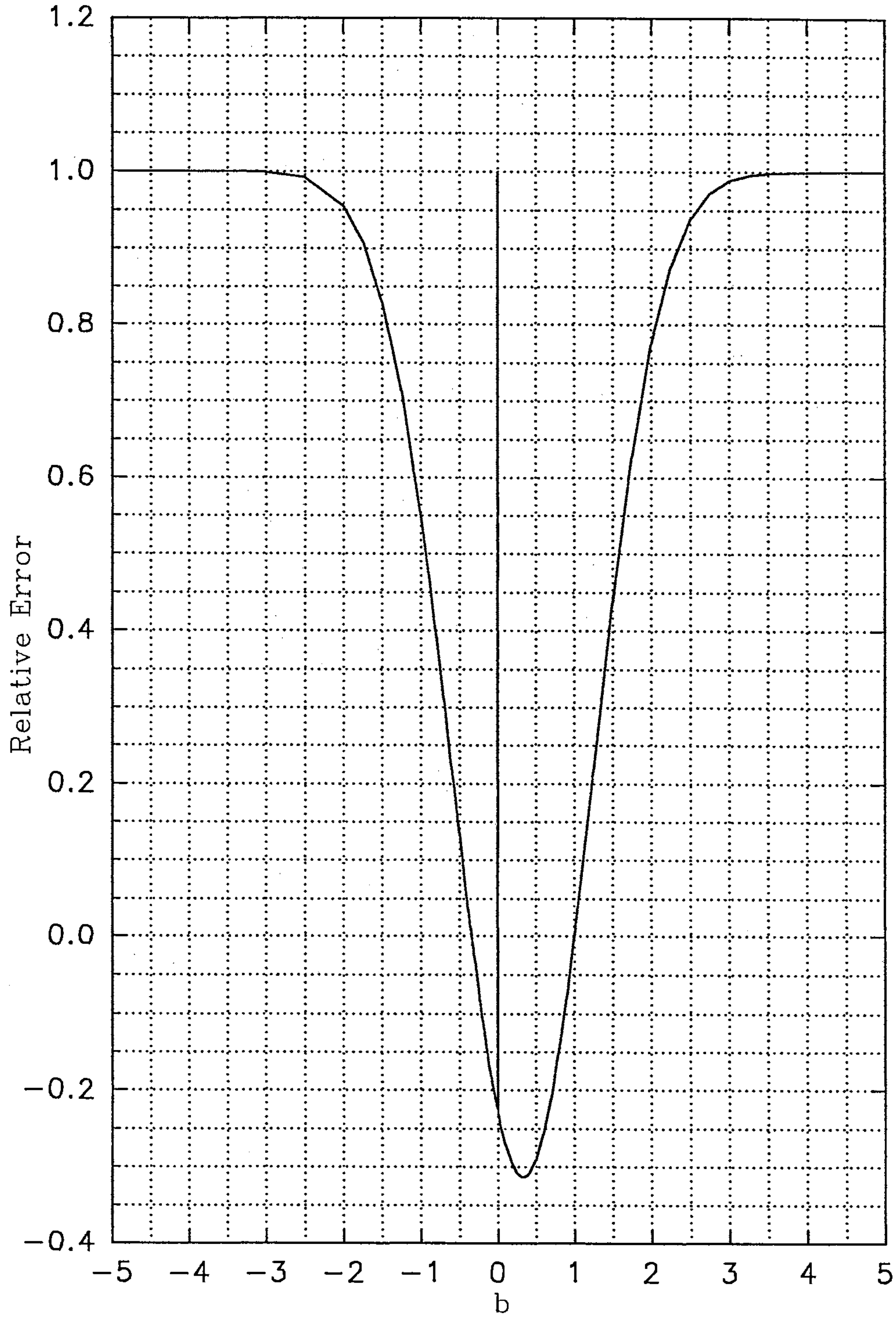

Figure 4−44. Relative Error vs b for Cv = 0.7

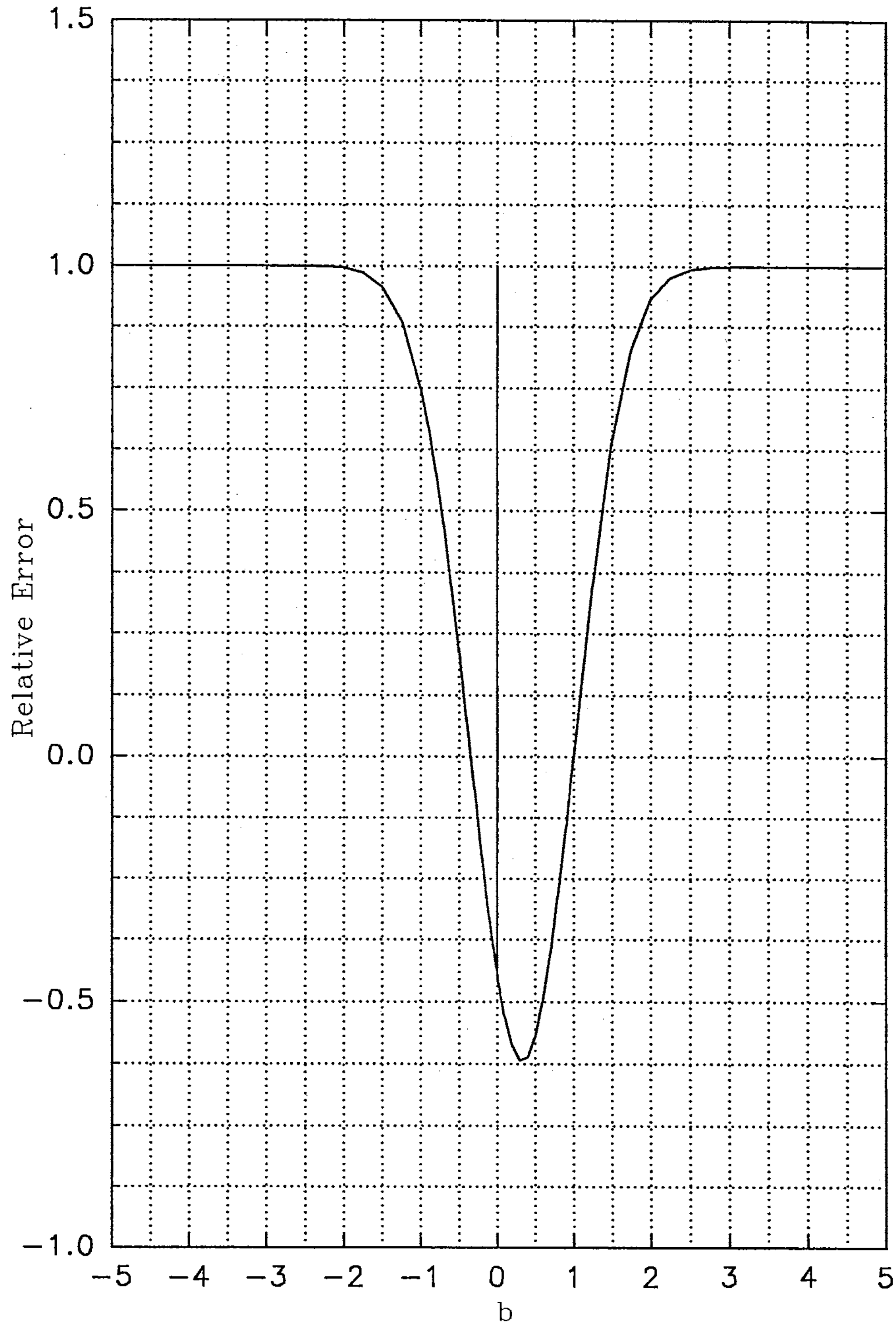

Figure 4−45. Relative Error vs b for Cv = 1.0

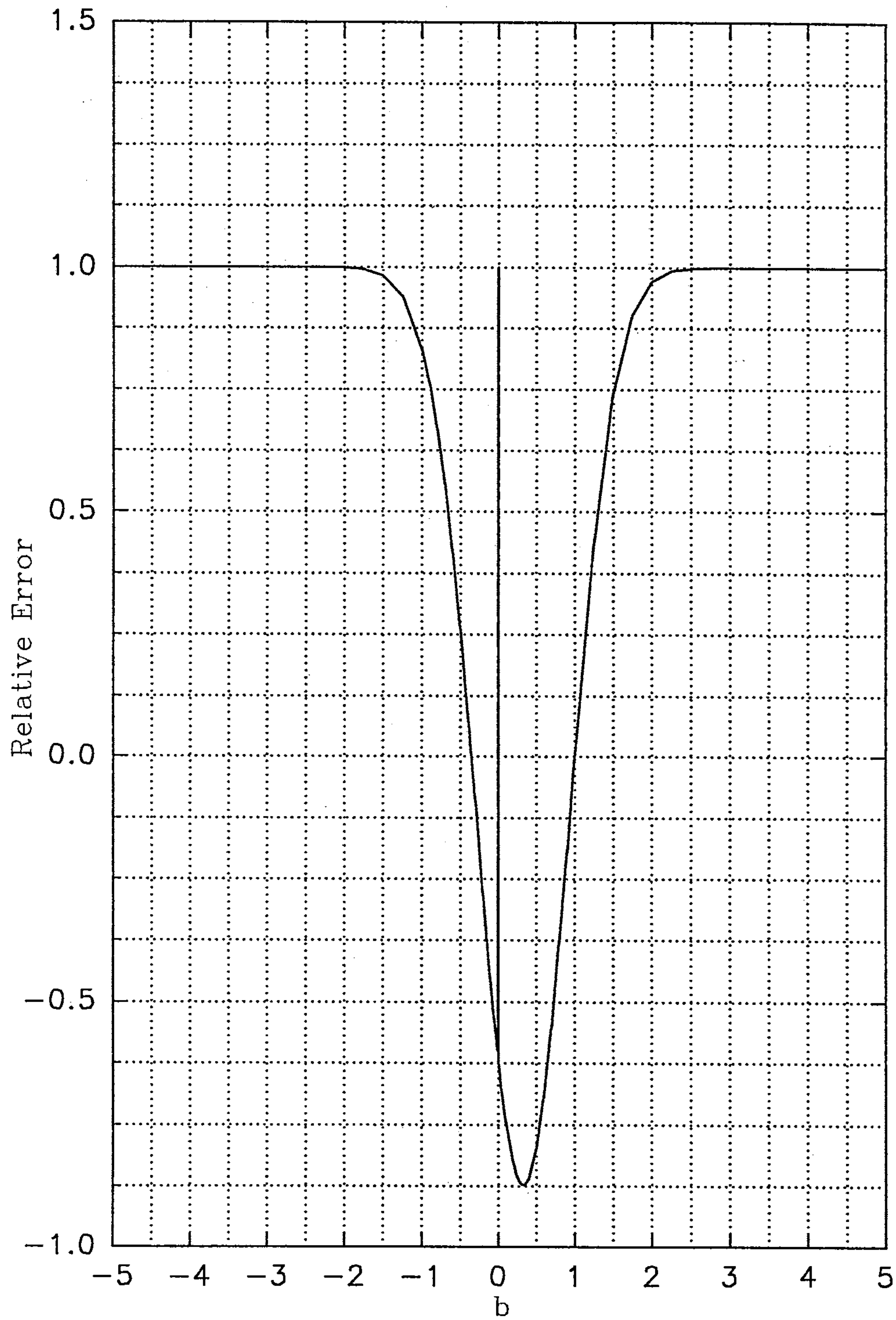

Figure 4−46. Relative Error vs b for Cv = 1.2

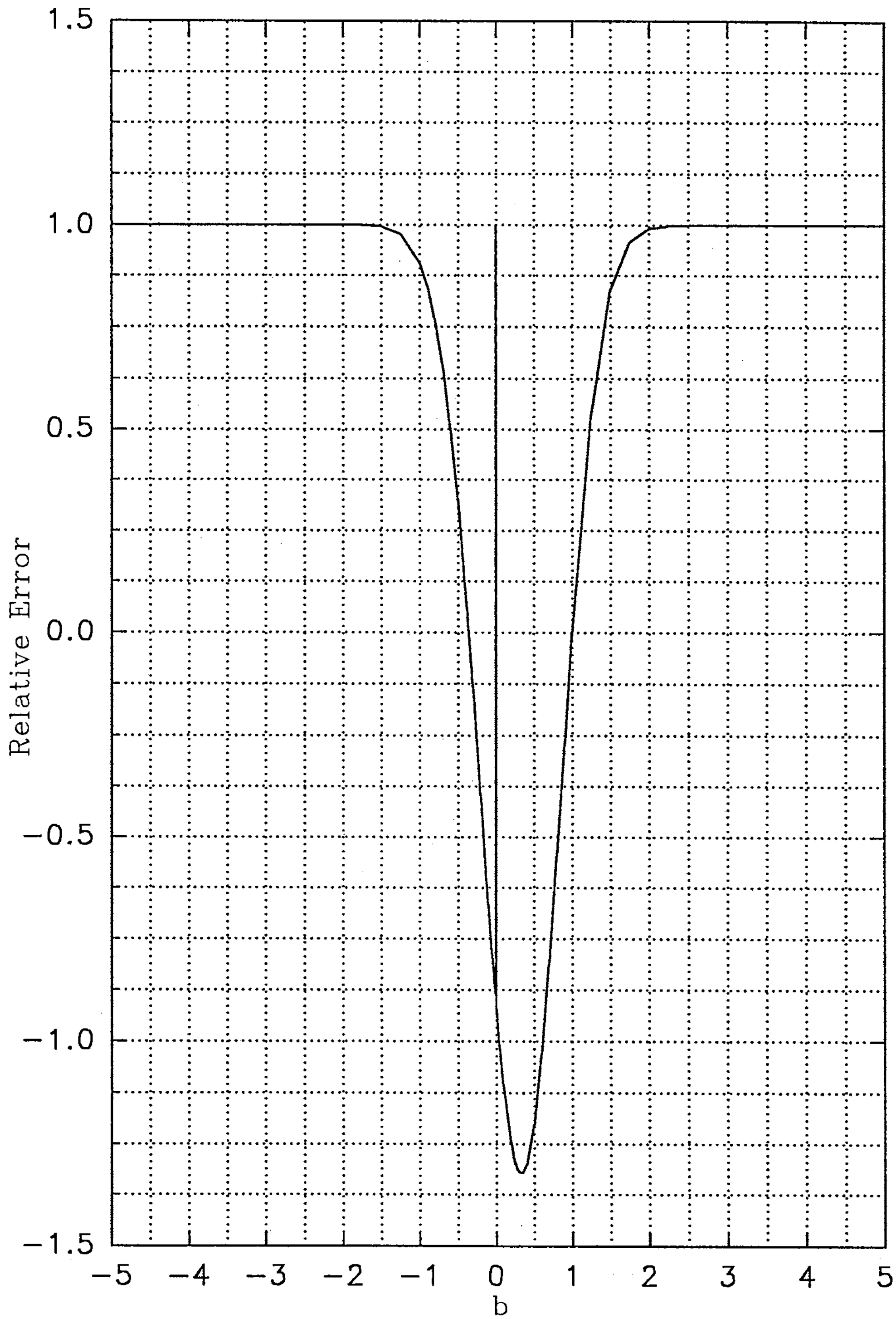

Figure 4−47. Relative Error vs b for Cv = 1.5

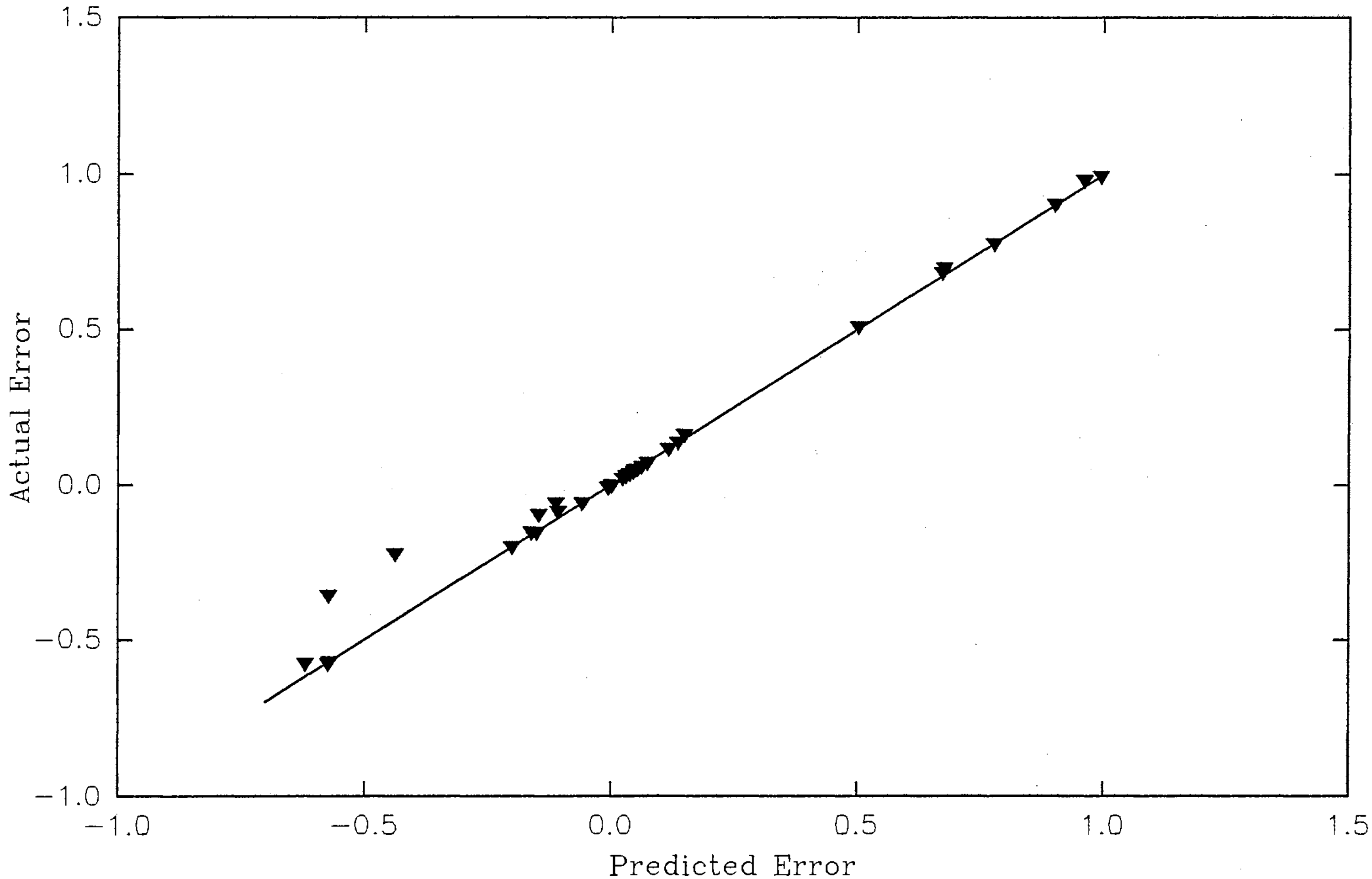

Figure 4-48. Actual vs Predicted Errors for Polynomial Test Runs

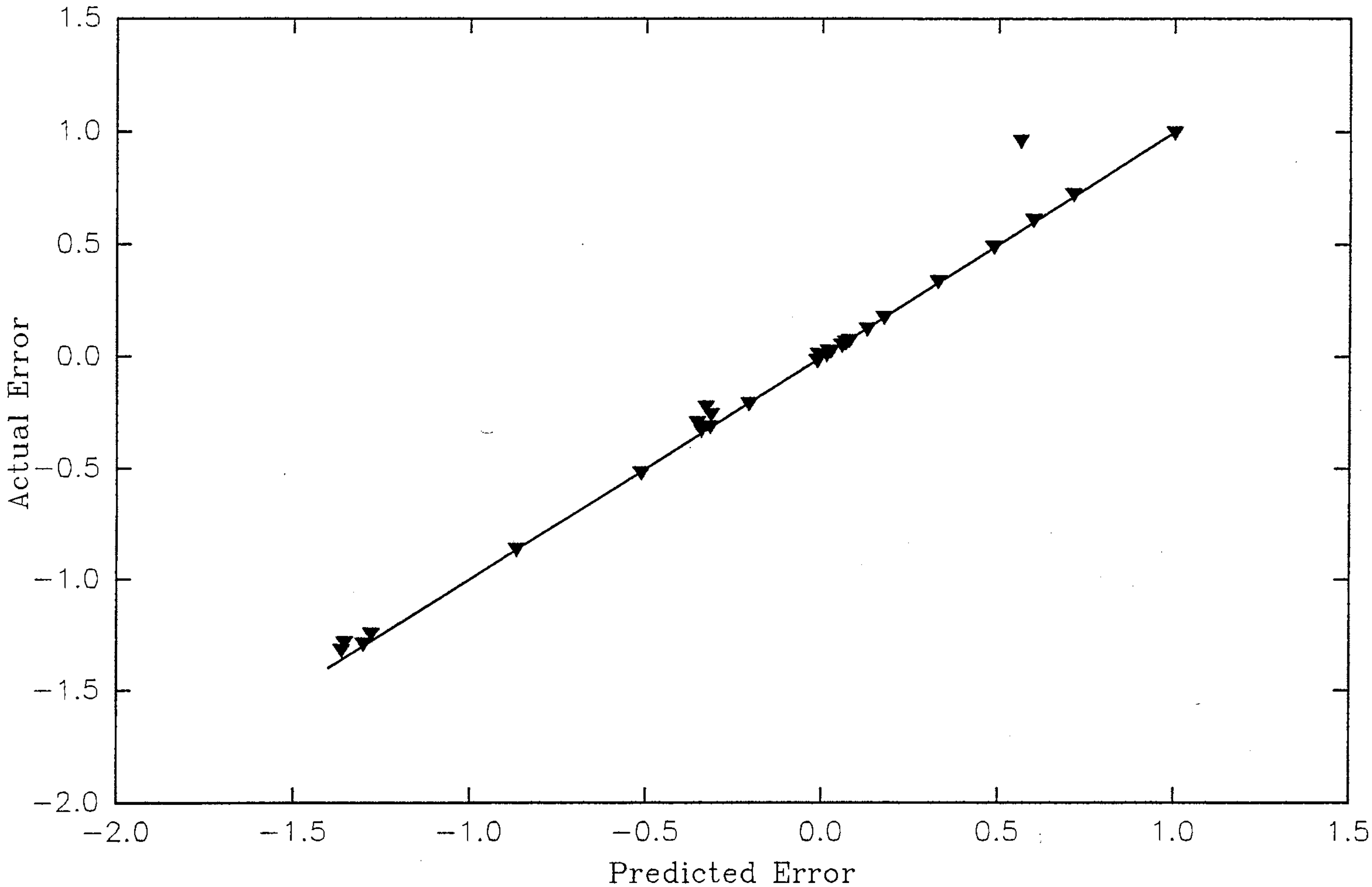

Figure 4−49. Actual vs Predicted Errors for Exponential Test Runs

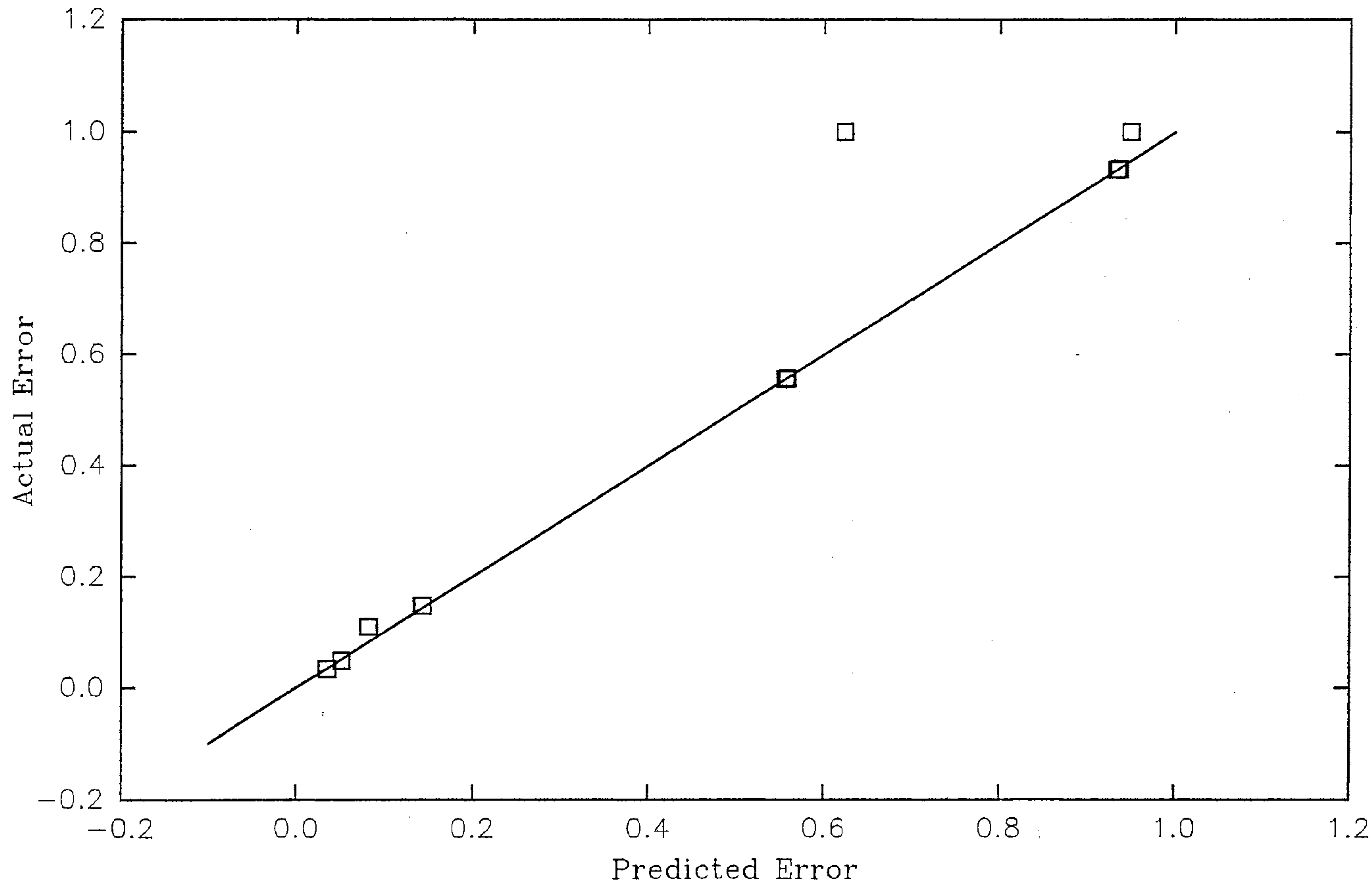

Figure 4−50. Actual vs Predicted Errors for Mixed Model Test Runs

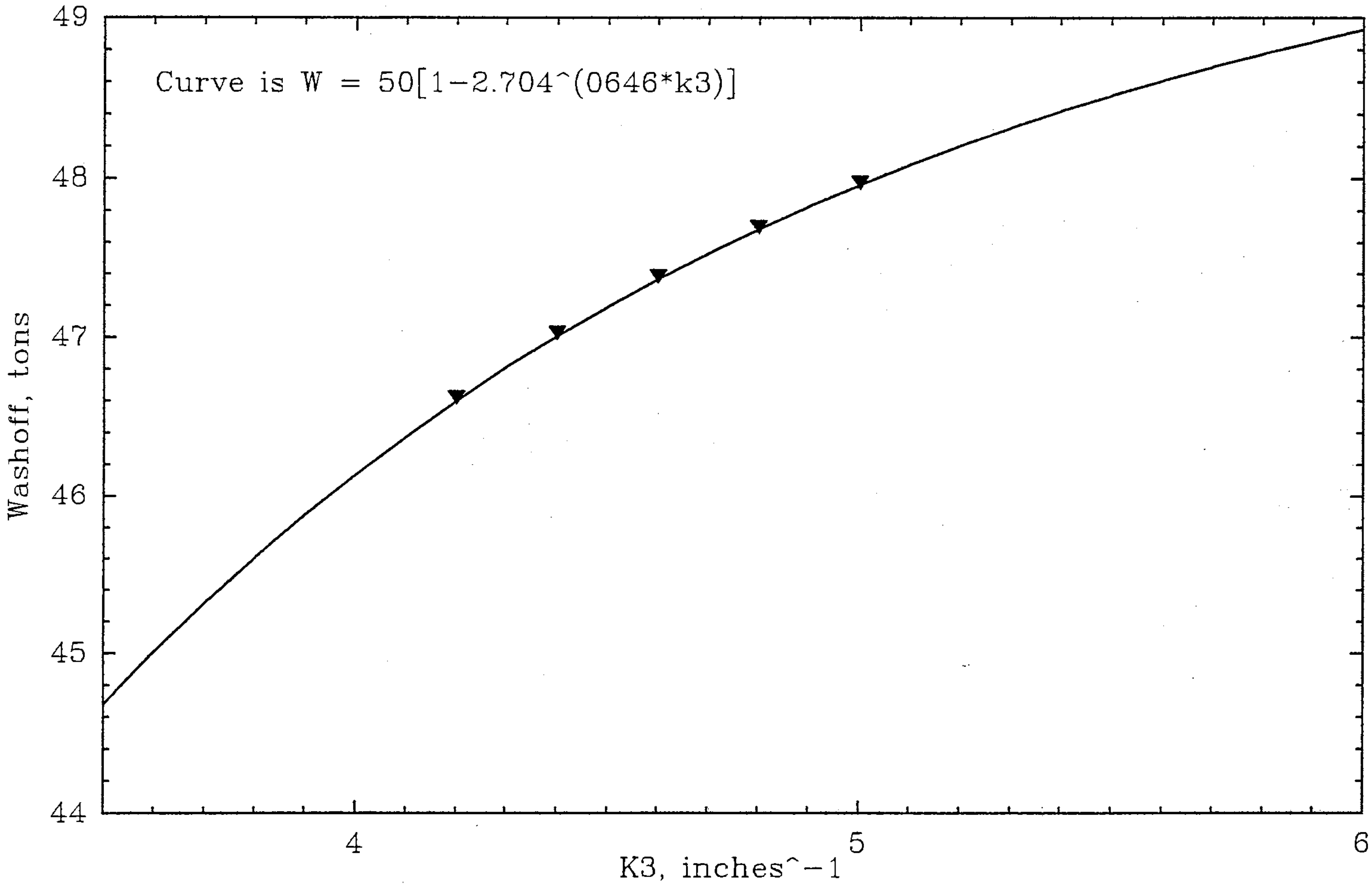

Figure 4-51. Washoff Model Responses and Smooth Curve PLotted Using Estimated Model

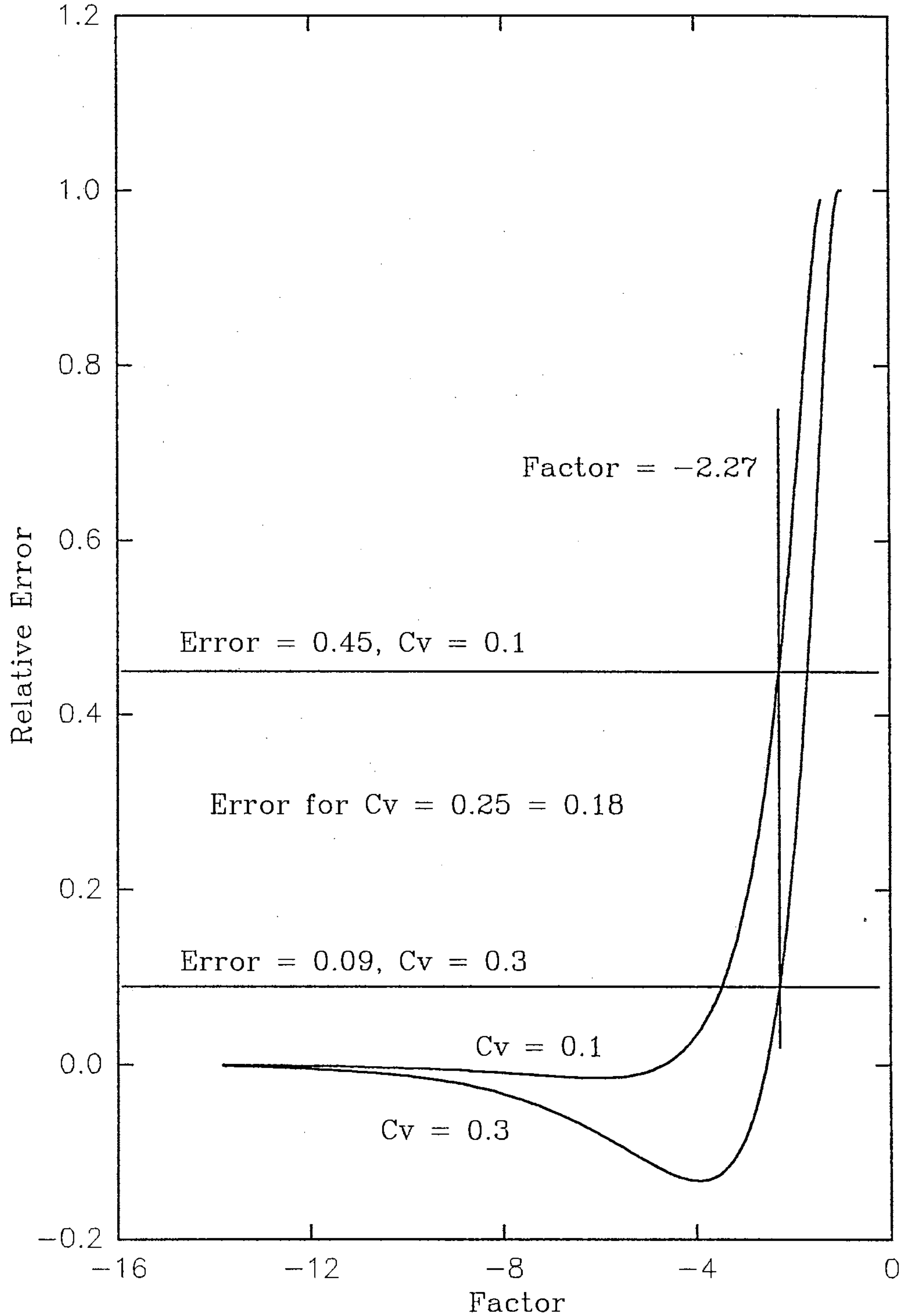

Figure 4−52 Use of Error vs Factor Curves

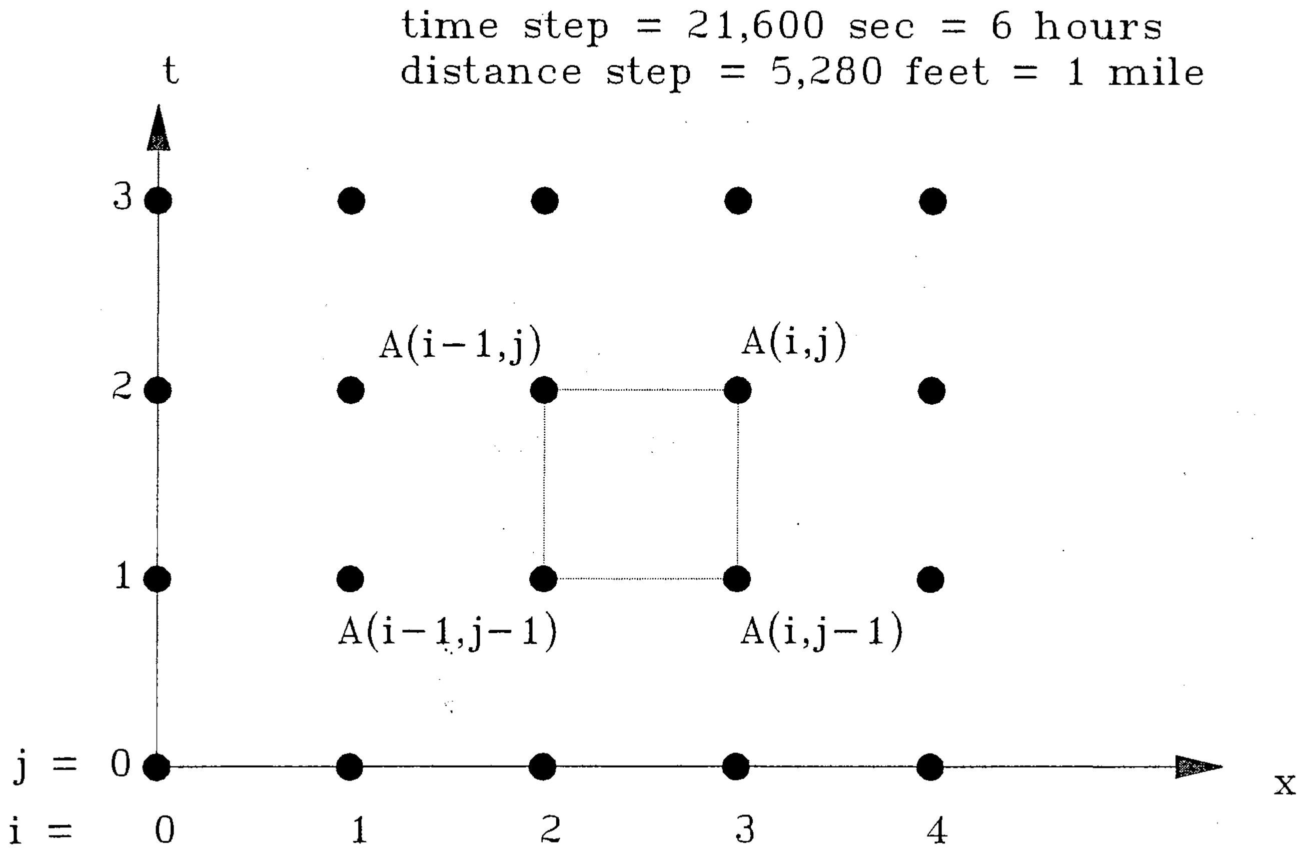

Figure 4-53. Numerical Approximation Grid in x-t Plane

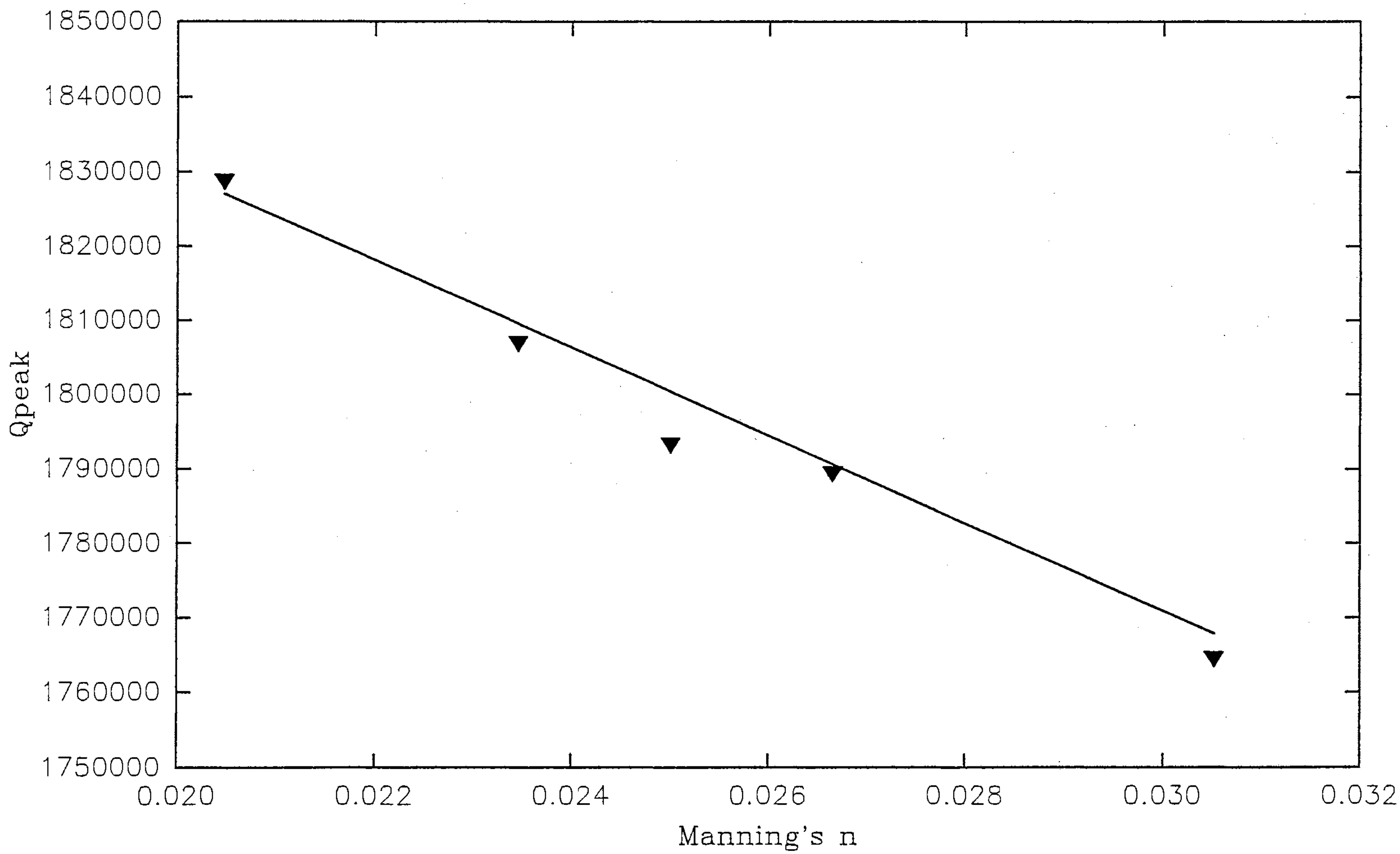

Figure 4–54. Model Response, Qpeak, vs Manning's n

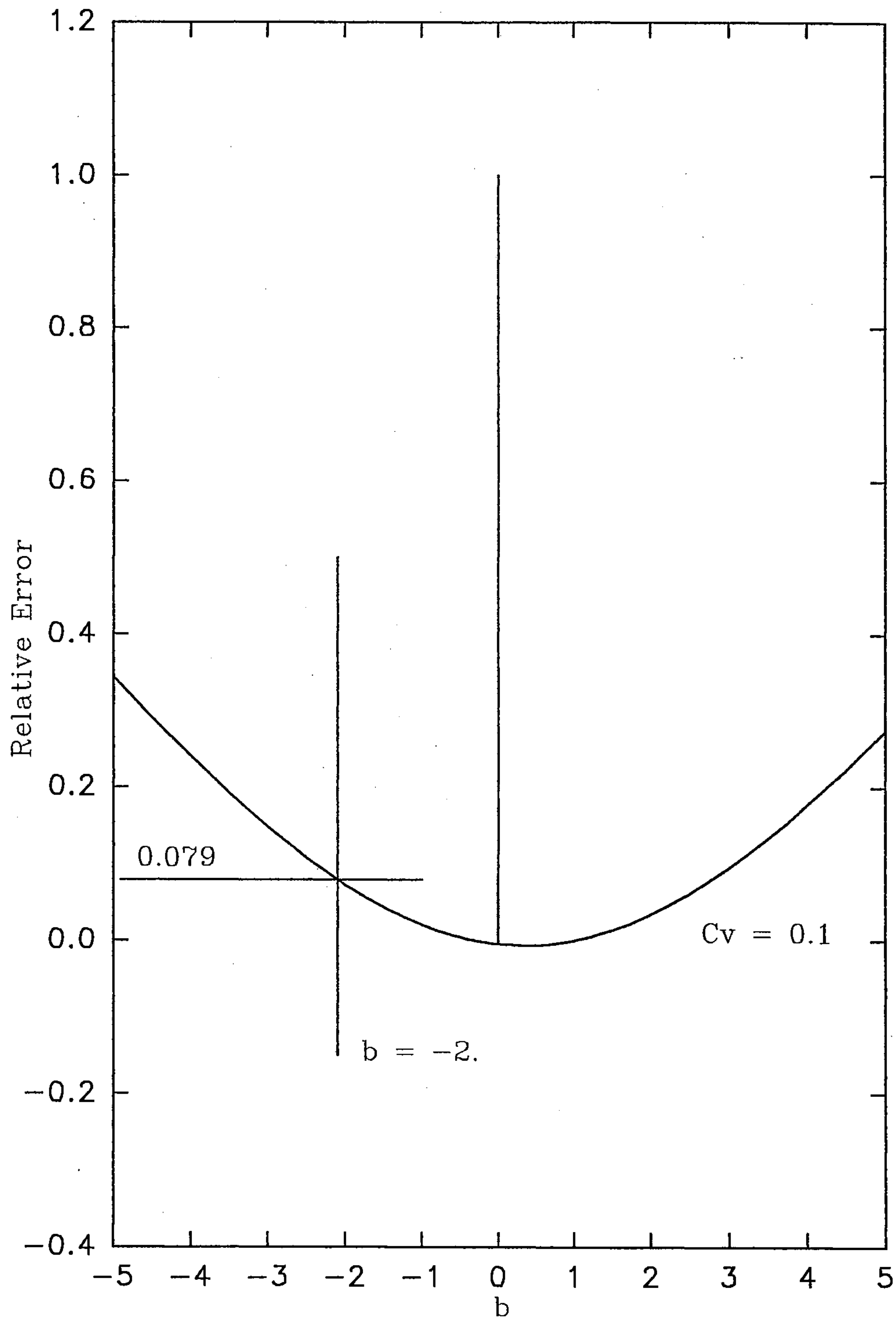

Figure 4–55. Use of Error vs b Curves

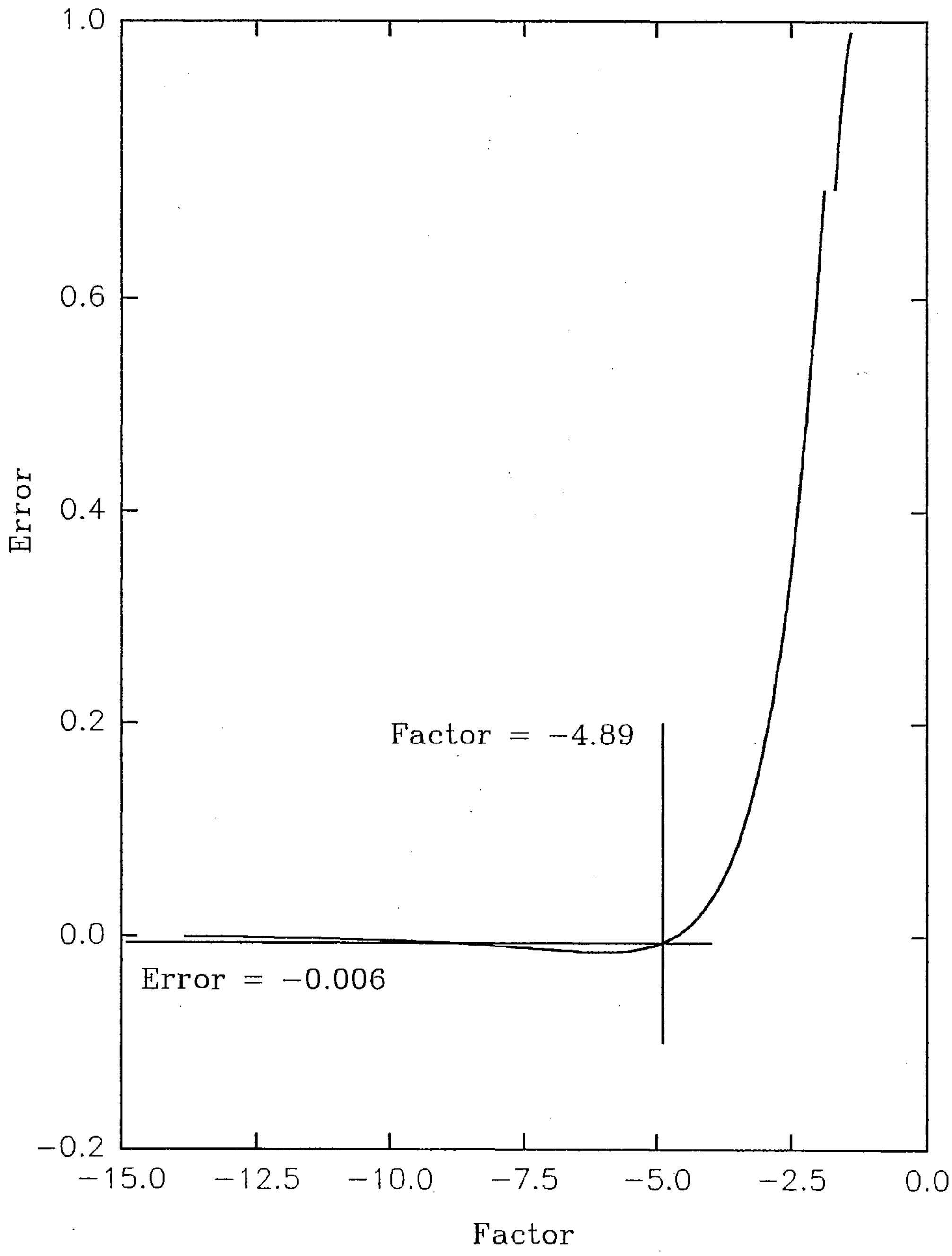

Figure 4-56. Use of Error vs Factor Curves

CHAPTER FIVE

ANALYSIS OF TWO PARAMETER MODELS

Two parameter models with polynomial, exponential, and mixed forms were evaluated. The objective was to find a means of predicting the error in the FOA variance, or, if that was not possible, to find a way to determine a range for the errors.

Given uncertain parameters x and y and constants a, b, c, and d, the models studied were of the forms

Polynomial	$z = x^b y^c$	(5-1)
Exponential	$z = a^{bx} c^{dy}$	(5-2)
Mixed Exponential-Polynomial	$z = a^{bx} y^c$	(5-3)

Note that models with the form of equation 5-2 can be rearranged to have the form

$$z = \exp(c_1 x + c_2 y) \tag{5-4}$$

where $c_1 = b\ln(a)$ and $c_2 = d\ln(c)$.

The uncertain parameters were assumed to be lognormally distributed, and had C_v's of 0.1, 0.5, and 1.0. A variety of means and combinations of constants were used, to form a grid of models with varying degrees of nonlinearity and various combinations of parameters being more or less uncertain. Correlations between the parameters of 0, ± 0.25, ± 0.5, and ± 0.75 were used.

The analytical solutions were obtained by numerically integrating the expression

$$Var(z)=\int_0^\infty\int_0^\infty z^2 f_{XY}(x,y)dxdy-[\int_0^\infty\int_0^\infty z f_{XY}(x,y)dxdy]^2 \qquad (5\text{-}5)$$

where $f_{XY}(x,y)$ was the bivariate lognormal PDF of x and y. For each parameter, the upper limit used for the integration was

$$UL=\exp(\mu+6\sigma) \qquad (5\text{-}6)$$

Since this limit might not be sufficiently high for rapidly increasing functions, any models for which the computed expected values of z or z^2 were larger than 10^6 were eliminated. The double numerical integrations were extremely time consuming to compute, so it was not practical to have a higher upper limit. Each integration took approximately 11 minutes to complete on an Intel 80486 based PC running at 33 MHz. The majority of the integrations were done on a Sun Sparc10 workstation, and these took anywhere from 0.7 to 2.5 minutes, depending on other usage of the equipment.

To ensure that the computer program written to perform the integrations performed properly, the computations were checked using a spreadsheet. Since the strictly increasing exponential models were most likely to "blow up", two of them were used as test cases. A mean of 1 and C_v of 0.1 was chosen for both x and y. These were used because the integrations involving very small numbers seemed more likely to have errors if the step size was too large. Due to limitations of spreadsheet dimensions, the step size used in the spreadsheet was considerably larger than the step size used in the program, so perfect agreement in the results would not be expected. For the model $z = 1.1^{.5x}1.1^{.5y}$, the program result for E[z] was 1.09 and the spreadsheet result was 1.11, indicating that the computations in the program proceeded as they were supposed to. A second model, $z = e^x e^y$ was also checked. The program result was 7.46. The spreadsheet result was 7.625848. Increasing the upper limit to

$$UL = \exp(\mu + 8\sigma) \tag{5-7}$$

for both x and y on the spreadsheet still gave a result of 7.625848, indicating that the upper limit used was appropriate.

The expression for the FOA variance of the output of a two parameter model is

$$Var(z) \approx \left(\frac{\partial z}{\partial x}\right)^2 \Big|_{\bar{x}} Var(x) + \left(\frac{\partial z}{\partial y}\right)^2 \Big|_{\bar{y}} var(y) + 2\frac{\partial z}{\partial x}\Big|_{\bar{x}} \frac{\partial z}{\partial y}\Big|_{\bar{y}} Cov(x,y) \tag{5-8}$$

The term "error" refers to the relative error

$$error = \frac{analytical\ variance - FO\ variance}{analytical\ variance} \tag{5-9}$$

RESULTS FOR POLYNOMIAL MODELS

The first thing investigated for the polynomial forms (equation 5-1) was if, as for the one parameters models, the mean of the uncertain parameter affected the error in the FOA variance, where error is defined by equation 5-9. Through the remainder of this chapter, the term "error" refers to the relative error in the FOA variance computed in this manner. The test cases showed that the error was not a function of the parameter means. This can be shown analytically for the case with b = 1, c = 1, and independent parameters. The exact variance is

$$Var(z) = Var(x)Var(y) + Var(y)(E[x])^2 + Var(x)(E[y])^2 \tag{5-10}$$

and the FOA variance is

$$FOA\ Var(z) = \bar{y}^2 Var(x) + \bar{x}^2 Var(y) \tag{5-11}$$

The error is, then

$$error = \frac{Var(x)Var(y)}{Var(x)Var(y) + Var(y)(E[x])^2 + Var(x)(E[y])^2} \tag{5-12}$$

Substituting the expression $(E[x])^2 = Var(x)/C_{vx}^2$ and the similar expression for y gives

$$error = \frac{1}{1 + \frac{1}{C_{v_x}^2} + \frac{1}{C_{v_y}^2}} \tag{5-13}$$

showing that the error is only dependent on the means of the parameters through C_v. It was found empirically that this result also holds for b's and c's not equal to one and for correlated parameters. It is not possible to prove this analytically. Table 5-1 contains some of these empirical results.

Analysis of this simple example (b = c = 1) also revealed other interesting details. If y is not uncertain, i.e. Var(y) = 0, then the model is equivalent to a constant times x. In this case, the error in the FOA variance would be zero, since the model is linear in x. Throughout this chapter, references to the "error due to x" will mean the error in the FOA variance that would be computed using the one-parameter model methods and considering x the only uncertain parameter. For these computations the y parameter should be replaced by its mean. For example, if Var(y) is equal to 0, then y is a constant and

$$Var(z) = y^2 E[x^2] - (yE[x])^2 = y^2 Var(x) \tag{5-14}$$

Also, $\partial z/\partial x = y$ and the FOA variance is $y^2Var(x)$. The error due to x is zero since the exact and FOA variances are equal. Similarly, if the variance of x is zero, the error due to y is zero.

Comparing equation 5-10 and 5-11 it is apparent that when both parameters are uncertain the analytical solution for the variance is the same as the FOA variance, except that the term Var(x)Var(y) is added to the exact variance. Thus, even though there is no error due to either x or y, there will still be an error in the FOA variance. Since the squared C_v's in equation 5-13 are all positive, the error will always be positive and less than one.

The error in the FOA variance is a function of the C_v's of x and y, the values of b and c, and the correlation coefficient, ρ. Some patterns in the behavior of the error can be identified.

Given C_{vx}, C_{vy}, c and ρ, the behavior of the error as a function of b is similar to the behavior of the error as a function of b for one parameter polynomial models. While the grid of models for which the analytical and approximate variances were computed was not sufficiently dense that a smooth curve could be constructed, the available data exhibited a very consistent error pattern. The error was equal to one for large negative powers, decreasing, and then increasing back to one for large positive powers. The pattern was the same for all values of ρ investigated. Figure 5-1 contains some examples of this pattern. As expected, given C_{vx}, b, and c, the error increased as C_{vx} increased. Figure 5-2 shows this.

The effect of parameter correlation on the error was also investigated. Given C_v's of x and y, b, and c, the error as a function of ρ depended on the form of the model output. For models with z increasing as both x and y increased, or polynomial increasing models (PIMs), and for polynomial models with z decreasing as both x and y increased (PDMs), the error increased as ρ increased. Given a polynomial model with z increasing as either x or y increased and decreasing as the other increased (PMM), the error decreased as ρ increased. Figures 5-3 through 5-5 show results for three combinations of C_v. While the magnitudes of the errors changed as a function of C_v, the pattern followed by the curves did not.

Given a model and the distributions of its parameters, the FOA variance as a function of ρ is a linear function. Note that the first partial derivative of FOA variance with respect to ρ given by

$$\frac{\partial FOVar}{\partial \rho}=2\sqrt{Var(x)Vary(y)}\frac{\partial z}{\partial x}\Big|_{\bar{x}}\frac{\partial z}{\partial y}\Big|_{\bar{y}} \tag{5-15}$$

is not a function of ρ, so the FOA variance is linear in ρ. The first partial derivative of the analytical variance with respect to ρ is

$$\frac{\partial Var(z)}{\partial \rho}=\int_0^\infty\int_0^\infty z^2\frac{\partial f_{XY}(x,y)}{\partial \rho}dxdy-\left[\int_0^\infty\int_0^\infty z\frac{\partial f_{XY}(x,y)}{\partial \rho}dxdy\right]^2 \tag{5-16}$$

The derivative of the PDF with respect to ρ is

$$\frac{\partial f_{XY}(x,y)}{\partial \rho}=\frac{\rho}{\pi\sigma_x\sigma_y xy(1-\rho^2)^{\frac{3}{2}}}\exp\{\frac{-1}{2(1-\rho^2)}[z_x^2-2\rho z_x z_y+z_y^2]\}$$

$$+\frac{1}{2\pi\sigma_x\sigma_y xy\sqrt{1-\rho^2}}\exp\{\frac{-1}{2(1-\rho^2)}[z_x^2-2\rho z_x z_y+z_y^2]\}$$

$$\times\{\frac{\rho}{(1-\rho^2)^2}[z_x^2-2\rho z_x z_y+z_y^2]+\frac{1}{(1-\rho^2)}z_x z_y\} \tag{5-17}$$

where $z_p = (\ln(p)-\mu_p)/\sigma_p$.

It is obvious that the partial derivative of the analytical variance with respect to

ρ will be a highly nonlinear function of ρ, although the form it will take is a function of all the parameters and is not possible to predict without evaluating the integrals, which have no analytical solution.

An intuitive argument for how the variance behaves with respect to ρ can be formulated. Consider finding the mean and variance by simulation. If the parameters are positively correlated, then it is likely that the sampled parameters will either both be above or below the mean value of the parameter. If the model is a PIM, a model result computed from two parameters which are both above or below the mean will be further away from the FOA mean (equation 3-4), than a model result using a parameter above the mean and a parameter near the mean. The more highly correlated the parameters are, the more likely they are to be the same relative distance from the mean. In this sense, relative distance refers to the number of standard deviations away from the mean. Thus, there will be a wider spread of model results away from the FOA mean, and consequently a larger variance.

If the parameters are negatively correlated, then the sampled parameters are more likely to be one above and one below the mean. This would tend to bring the model result closer to the mean. Here, there would be a smaller spread and a smaller variance. The effect of correlation is the same for models decreasing in both parameters.

With PMMs, if the parameters are negatively correlated and one is above and one below the mean, this will cause a larger spread in the results. Consider a PMM where z increases as x increases and decreases as y increases. If the sampled x parameter is above the mean and the sampled y parameter is below the mean, then the model result is an above FOA mean value divided by a below FOA mean value, which will give an even relatively higher above FOA mean result. This will yield a larger spread and higher variance. For positively correlated parameters, the sampled values are likely to be either both above or below the mean. The effect of having the model output decreasing as one parameter increases and increasing as the other increases will tend to bring the model result closer to the mean. Thus, the variance will decrease as the parameters become more highly positively correlated.

Figure 5-6 is a plot of the analytical and FOA variances as a function of ρ. The PIM used was $z = x^{1.5}y^{1.5}$, with -1.5 being the exponent for the PDM and $z = x^{1.5}y^{-1.5}$ was the PMM. This plot shows the divergence of the analytical variance away from the FOA variance as ρ increases or decreases. While the analytical variance curves may not look nonlinear in the plot, they actually are. Numerical derivatives of the analytical variances with respect to ρ were taken at points along the curve and found to range between 0.046 and 0.054 for the PIM, between 0.048 and 0.057 for the PDM, and between -0.055 and -0.047 for the PMM. This confirms that the curves are nonlinear and diverge away from the linear FOA variance function, which has a constant slope of 0.045 for the PIM and PDM and -0.045 for the PMM.

Figures 5-7 through 5-9 show error as a function of ρ for one type of model (PIM, PDM, or PMM) and three combinations of C_v's. These curves show that as the C_v's increase, the function becomes more nonlinear. Figure 5-10 displays the analytical and FOA variances for the increasing model. This plot illustrates that the analytical variance diverges from the FOA variance at a much faster rate for higher C_v's resulting in the error function (Figure 5-7) being more nonlinear for higher C_v's.

It would be possible to construct error vs power (b or c in equation 5-1) plots similar to the plots constructed for one parameter polynomial models. Constructing these plots would require holding the C_v's of x and y and the value of b fixed and plotting the error as a function of c. For an example of what constructing these curves would require, assume that a range of useful values of C_{vx} and C_{vy} is between 0.1 and 1 and a range of useful values of c is between -3.5 and 3.5. Since the error is highly nonlinear with respect to C_v and c, the grid of C_v's and c would have to be fairly dense for interpolation between curves to be accurate. If C_v's of 0.1, 0.3, 0.5, 0.7, and 1 are used with c having increments of 0.5, then 375 plots are needed. Given that these 375 plots were available, using them to predict errors could be an arduous task since up to five interpolations may be required.

A search was therefore made for a factor (or factors) which would be a function of the sources of error and could be used to predict the error. A factor which seemed promising was the error due to x and the error due to y, along with ρ. Using data for $\rho = 0$, a plot of error due to x and error due to y vs FOA variance error was constructed by assigning different symbols to ranges in the error (Figure 5-11). There was very little overlap of different symbols, indicating that a valid contour plot or regression could potentially be formulated. The pattern of the symbols indicated that contours would be nearly circular, suggesting a quadratic model.

Denoting the error due to x as errx and the error due to y as erry, an error-predicting model of the form

$$error=CONSTANT+A1*(errx+erry)+A2*(errx^2+erry^2)+A3*errx*erry \tag{5-18}$$

was estimated using the SYSTAT (Wilkinson, 1990) statistical software. A total of 354 errx-erry-variance error triples were used in the estimation. The R^2 was 0.9966, indicating a good fit. The standard deviation of the residuals was 0.046, another indication of a good predictive model. Model parameters CONSTANT, A1, A2, and A3 were found to be 0.0610, 0.854, 0.0939, and -0.929, respectively. A plot of the residuals (Figure 5-12) indicated that while they may not have uniform variance throughout, there was no definable pattern to suggest a way the error-predicting model could be modified. Figure 5-13 is a plot of actual vs predicted errors. The data clusters well around the line of equality.

Note that even if the errors due to x and y are zero, the error-predicting model will still estimate some error due to the constant. The previous simple example of z = xy illustrated that there will always be some error, even when errors due to x and due to y are zero. The model z = xy is the only model for which these errors are exactly zero. (In reality, the error in the FOA variance for the model z = xy is not a constant, but depends on the C_v's of x and y. However, it is not necessary to use the model to make predictions for z = xy, since an analytical solution is available.) The simple example illustrates, however, that it is appropriate to formulate the error-predicting model to predict an error, even when the errors due to x and y are zero.

A similar symbol plot was constructed using the data for ρ equal to 0.25 (Figure 5-14). Again, there was not too much overlap in the data, and it appeared that contours would be nearly circular. The same form of error-predicting model was estimated, this time having an R^2 of 0.97. The standard deviation of the residuals was 0.067, indicating a good predictive model. Model parameters CONSTANT, A1, A2, and A3 were estimated as 0.0859, 0.119, 0.810, and -0.911, respectively. The residuals had a reasonably uniform variance (Figure 5-15), and again did not have any pattern which would suggest a modification to the error-predicting model. Figure 5-16 is a plot of actual vs predicted errors. The data cluster fairly well about the line of equality. The same procedure was attempted for ρ equal to 0.5. The symbol plot (Figure 5-17) showed some overlap in the data. The model was estimated, and the R^2 was 0.91. A plot of the actual vs predicted errors (Figure 5-18) showed a significant divergence from the line of equality. This would not appear to be a particularly good model. Since it appeared that the scatter became greater as ρ increased, an error-predicting model for ρ equal to 0.75 was not even attempted.

The symbol plot for ρ equal to -0.25 (Figure 5-19) did not show much overlap and it appeared that contours would be circular contours, so the error-predicting model was estimated for this data. The R^2 was 0.980 and the standard deviation of the residuals was 0.058, indicating a good model. Model parameters CONSTANT, A1, A2, and A3 were computed as 0.0265, 0.0848, 0.884, and -0.950, respectively. The residuals had a reasonably uniform variance (Figure 5-20) and they did not exhibit any pattern which would indicate that the error-predicting model should be reformulated. The estimated vs actual data clustered well about the line of equality (Figure 5-21). Similar to the results for $\rho = 0.5$, the data for $\rho = -0.5$ (Figure 5-22) had considerable scatter and the estimated model had an R^2 of 0.899. The actual vs estimated data diverged considerably from the line of equality (Figure 5-23). Again, an error-predicting model for ρ equal to -0.75 was not attempted.

Another approach tried was to plot the error which would occur if the parameters were uncorrelated against the error which occurred with the correlation. The scatter in the data was reduced if the models were separated into the categories - PDM, PIM, and PMM. These curves are shown in Figures 5-24 through 5-41. The plots suggested that it might be possible to formulate linear models to predict the errors with correlated parameters as a function of the errors with uncorrelated parameters.

Linear models of the form

$$error_{\rho} = CONSTANT + slope \times error_{0} \tag{5-19}$$

where $error_{\rho}$ is the error for the given ρ corresponding to the error when $\rho = 0$, were estimated for the PDMs. Table 5-2 gives ρ, R^2, the model parameters (CONSTANT and slope), and the standard error of the estimate (SEE) for all the models. Figures 5-42 through 5-47 are plots of the residuals. These exhibited reasonably uniform variance and did not indicate that the error-predicting model should be reformulated. Figures 5-48 through 5-53 are plots of the predicted vs actual errors. With the exception of the model for $error_{-.75}$, the data clusters well about the line of equality. Actual vs predicted error data for this model indicates that if the predicted error is 0.4 or less, the actual error will be even smaller.

Linear models were estimated for the PIMs. The R^2 was close to unity and the SEE was reasonable small for ρ equal to -0.25, 0, 0.25, 0.5 and 0.75. Figures 5-30 through 5-35 are plots of $error_{\rho}$ vs $error_{0}$. It was clear there was too much scatter in the data for ρ equal to -0.5 or -0.75 to find an accurate model. Table 5-3 gives the R^2, model parameters, and standard error of the estimate for the models successfully estimated. Figures 5-54 through 5-57 are plots of the residuals, and exhibit satisfactory characteristics. Figures 5-58 through 5-61 show the predicted vs actual values, which cluster fairly well about the line of equality.

Figures 5-36 through 5-41 are $error_{\rho}$ vs $error_{0}$ plots for the PMMs. Estimation statistics (R^2 and SEE) were satisfactory for all values of ρ, with the exception of 0.75. Table 5-4 gives the R^2, model parameters, and standard error of the estimate. Plots of the residuals (Figures 5-62 through 5-66) were acceptable. Figures 5-67 through 5-71 display actual vs predicted errors, and the points are all close to the line of equality. For $\rho = 0.75$, the data appeared to have too much scatter for an acceptable linear model. The estimated model had an R^2 of 0.78, confirming this.

An attempt was made to estimate a quadratic model for increasing models with ρ equal to -0.5 or -0.75. This was not successful, with the R^2's being 0.85 and 0.24 respectively. The plots of error_ρ vs error_0 for these two correlations indicated that the error with the correlated parameters is always less than the error with the uncorrelated parameters. This may be useful information, since it indicates that the error in FOA variances estimated for correlated parameters will be no larger than the error which would be present if the parameters were uncorrelated. Thus, if the FOA variance would be acceptable had the parameters been uncorrelated, the FOA variance with the correlated parameters will be a more conservative estimate.

For ρ equal to 0.75, the error with correlated parameters was always larger than the error which would have been present had the parameters been uncorrelated. In fact, for all positive values of ρ evaluated here, given a PDM or PIM, error_ρ was larger than error_0. Given a PDM or PIM, if ρ were negative, error_ρ was smaller than error_0. The reverse was true for PMMs. For positive ρ, error_ρ was smaller than error_0. For negative ρ, error_ρ was larger than error_0.

For purely polynomial forms, the procedure is to first confirm that the model has the correct form. One way to do this is to compute the first and second partial derivatives with respect to x and y, numerically if necessary, at points on the response surface. The recommended points are $x = E[x]$, $y_i = \exp(\mu_y + \sigma_y^2/2 + z_i\sigma_y)$, where $\mathbf{z} = \{0, \pm0.64, \pm2\}$, and $x_i = \exp(\mu_x + \sigma_x^2/2 + z_i\sigma_x)$, $y = E[y]$. While any points on the response surface will work, these points are recommended because the model evaluations at these points will be used later to compute errors (assuming the model has the correct form). If the ratio

$$\frac{\partial^2 z/\partial x^2}{\partial z/\partial x} \div x \tag{5-20}$$

is a constant regardless of the values of x at which the derivatives were evaluated, then the model has the correct form with respect to x. The same procedure can be applied to determine if the model has the correct form with respect to y.

An alternative procedure is to use the five x_i - model response pairs and estimate models of the forms

$$\hat{z} = constant + ax^b \tag{5-21}$$

and

$$\hat{z} = constant + ka^{bx} \tag{5-22}$$

If the R^2 obtained from estimating the polynomial model is much closer to one than the R^2 obtained from estimating the exponential model, then the model can be accepted as being polynomial in x. Similar models

$$\hat{z} = constant + dy^c \tag{5-23}$$

and

$$\hat{z} = constant + kc^{dy} \tag{5-24}$$

can be estimated and compared to determine if the model is polynomial in y.

Once it is confirmed that the model has the correct polynomial form, the error due to x can be found by using the five recommended x and model output pairs and following the procedure for one parameter models. First, find the b power considering the model to be $z = x^b E[y]^c$, then using b and C_{vx} and the curves for one parameter polynomial models, find the error due to x. The error due to y is found in the same manner, using the five recommended y and model output pairs.

The error due to y and the error due to x are then used to predict the error which would be present if x and y were uncorrelated. The model for this is

$$error = 0.061 + 0.0939(errx^2 + erry^2) + 0.854(errx + erry) - 0.929 \times errx \times erry \quad (5\text{-}25)$$

Once the error for uncorrelated parameters is known, the error corresponding to the correct type of model (PDM, PIM, or PMM) and correct ρ can be found using one of the linear models, unless ρ is less than -0.25 or greater than 0.5. If necessary, the errors can be interpolated between values of ρ. How accurate a straight line interpolation will be is a function of the C_v's of the parameters, the nonlinearity of the model (by how much b or c differ from unity), and whether the model is a PDM, PIM, or PMM. While this was not evaluated in detail, Figures 5-7 through 5-9 may provide some guidance as to the nonlinearity of the error vs ρ function.

A grid of models not used in the error-prediction model estimation process was created to validate the model. The test grid contained 64 models, with C_v's of 0.1 and 0.5, E[x] and E[y] equal to 2, and combinations of b and c equal to ± 0.25 and ± 0.5. The ρ values used were 0 and ± 0.25. The models with ρ equal to ± 0.25 will also be used to test whether the quadratic error-predicting model or the linear $error_\rho$ as a function of $error_0$ model makes better predictions.

For ρ equal to zero, there were 32 models in the test grid. The difference between the actual FOA error and the error predicted with the quadratic error-predicting model (equation 5-18) ranged between -0.07 and 0.02. The mean of the differences was

-0.03. Figure 5-72 shows the actual vs predicted errors. The data clusters well around the line of equality.

There were 16 models with ρ equal to 0.25. Using the quadratic error-predicting model, the difference between the actual and predicted errors was between -0.12 and 0.06. The mean of the differences was -0.04. Figure 5-73 displays the actual vs predicted errors. The data show that the model performed well. Using the linear $error_{.25}$ vs $error_0$ model resulted in differences between -0.15 and 0.10, with their mean being -0.02. Figure 5-74 shows actual vs predicted errors using this model. This model performed well, also. The absolute value of the difference was larger when the quadratic error-predicting model was used for 9 out of 16 models.

With ρ equal to -0.25, there were also 16 models. The difference between the actual and predicted errors when the quadratic error-predicting model was used ranged between -0.11 and 0.09, with a mean of 0.01. Figure 5-75 contains the actual vs predicted error data. The data cluster well about the line of equality. Using the linear $error_{-.25}$ vs $error_0$ model resulted in differences between -0.09 and 0.11, having a mean of -0.01. Figure 5-75 displays the actual vs predicted errors. The data cluster well about the line of equality. The absolute value of the difference between predicted and actual errors was greater when the linear model was used in 9 out of 16 cases.

Another test grid of models was generated, this set having C_{vx} equal to 0.3 and C_{vy} equal to 0.7. The means of x and y were both 2, combinations of ± 0.25 and ± 2 were used for b and c, and ρ was 0 or ± 0.25. There were 16 models with ρ equal to zero. The quadratic error-predicting error model was used to predict errors. The model did not perform particularly well with the new C_v's. Three predicted errors were within ± 0.05 of the actual error, one predicted error was within ± 0.15, and the remainder differed from the actual by more than ± 0.3.

Although the errors in the predictions were relatively large, if a relative error with absolute value greater than 0.2 is grounds for rejecting a FOA variance, there were only two cases in which an underestimated variance would be accepted. There were also only two cases in which an overestimated variance would be accepted. There was one case in which an acceptable variance would be rejected.

The conclusions based on the empirical data for polynomial models are as follows. The quadratic model performs well for predicting errors when the C_v's of x and y are equal to the C_v's in the data set used to estimate the model, but does not perform well when x and y have different C_v's. If the C_v's of x and y are some combination of 0.1, 0.5, and 1, the model will perform acceptably. Even though the model did not estimate the errors particularly accurately with C_v not equal to 0.1, 0.5, or 1, there were only 4 out of the 16 cases where a model would have been accepted which should have been rejected. There was only one case in which a model which should have been accepted would have been rejected. It is not recommended that the model be used with parameter C_v's not equal to 0.1, 0.5, or 1.

RESULTS FOR EXPONENTIAL MODELS

Strictly exponential models (equation 5-2) were also evaluated. A model that is exponential in both x and y can be identified by finding the ratio of the first and second derivatives with respect to x and y. If the ratio

$$\frac{\partial^2 z/\partial x^2}{\partial z/\partial x} \tag{5-26}$$

is constant regardless of the value of x used to evaluate the derivatives, the model is exponential in x. The same procedure is used to determine if it is exponential in y.

The grid of models consisted of all combinations of a or c equal to 1.1 or e (2.71828), b or d equal to ± 0.5 or ± 1 (including combinations of positive and negative powers), E[x] or E[y] equal to 1 or 5, and C_{vx} or C_{vy} equal to 0.1, 0.5, and 1. The values of ρ used were 0, ± 0.25, ± 0.50, and 0.75. For each value of ρ, the combinations of bases, exponents, means, and C_v's resulted in 1152 models. After the models with E[z] or E[z^2] greater than 1e+06 were eliminated, there were approximately 850 models available for analysis with each value of ρ.

The error in the FOA variance for two parameter exponential models is a function of the model constants a, b, c, and d, and of the parameter means, C_v's and correlation. Using equation 5-4 to rewrite the model, a and b can be combined as bln(a) and c and d can be combined as dln(c).

The behavior of the error in the FOA variance as a function of these various factors was examined. The error was seldom monotonic with respect to any of the factors. Given a mean and C_{vy} and dln(c) combination, the error as a function of bln(a) decreased to a minimum and then started rising again. This was the case for all values of ρ. Figure 5-77 shows examples of this behavior. In these plots, E[y] equalled 1, C_{vy} was 0.5 and dln(c) was -0.5. Based on the behavior of the one parameter models, the curve would most likely start out at 1 for large negative values of bln(a), decrease to a minimum, and then increase back to 1. The minimum point was in the vicinity of bln(a) equal to zero. It should be noted that for bln(a) to be exactly equal to zero, either b has to be zero or a has to be 1. For either case, the model is then not a function of x. The error may then exhibit similar behavior to the error in one parameter polynomial models as the power approached zero. It will be shown later that the bln(a) factor is not useful for predicting the error, so it was not considered worthwhile to investigate this behavior in detail.

Given all factors but the C_v of one parameter, the error was generally larger if the C_v was larger. This is also shown in Figure 5-77. This is the expected result, but since the error is not a monotonic function of any of the factors, it is not entirely unexpected that there would be cases of smaller C_v's being associated with larger errors. Given all factors but the mean of one parameter, the error tended to be larger for larger mean. This is also shown in the figure.

Given parameter means and C_v's, the behavior of the error as a function of dln(c) depended on the value of bln(a). No useful trends or consistent patters could be identified. Figure 5-78 presents examples. Here, E[x] and E[y] are equal to 1 and the C_v's of x and y and 0.5.

As a function of ρ, the error tended to decrease as ρ increased for models where z increased as both x any y increased (EIMs) and for models where z decreased as both x and y increased (EDMs). For models where z increased as either x or y increased and decreased as the other increased (EMMs), the error increased as ρ increased. There were exceptions to this, however. Figures 5-79 through 5-81 display this data. Figures 5-82 through 5-84 show the models by category. Larger errors were found with C_v's equal to 0.1. This is possible given the nonlinear, non-monotonic behavior of the errors as functions of bln(a) and dln(c), so the error as a function of C_v depends on the choices of bln(a) and dln(c). Here, the a's and c's were 1.1 and b and d were either 0.5 or -0.5, depending on whether the model was an EIN, EDM, or EMM.

An attempt was made to identify a factor or combination of factors which could be used to predict the error for exponential functions. Since it had been successful for polynomial models, an attempt was made to use the error due to x and the error due to y. The error due to x is found by evaluating the model at five points with x_i equal to $\exp(\mu_x+\sigma^2_x/2+z_i\sigma_x)$ where $\mathbf{z} = \{0, \pm0.64, \pm2\}$ and y equal to E[y], then finding the "factor" as described for one parameter exponential models. The one parameter model error vs factor curves are then used to predict the error due to x. The error due to y is found in the same manner.

Figure 5-85 displays the data for ρ equal to 0. The figure shows that there is too much scatter and overlap in the data to construct a model, or even to make a contour plot. Since this approach was not successful for ρ equal to 0, it was not considered worthwhile to investigate any other ρ's. The data did show, however, that if both the error due to x and error due to y were greater than 0.25, then the error in the FOA variance would be at least 0.3. With an error_0 of at least 0.3 and given and EIM or EDM and negative ρ, error_ρ would be larger than 0.3. Given an EMM and positive ρ, error_ρ would be larger than 0.3.

The factor approach, which had been successful for one parameter models was also tried. To compute the factor, y was set at its mean, the model was evaluated at the five recommended points, and the correlation coefficient between the x's and model outputs was found. The same procedure was repeated for y. The factors were then computed as described for one parameter models. Figure 5-86 shows the error and factor data for C_{vx} and C_{vy} equal to 0.5. The figure shows that there is too much scatter in the data to construct a model or contour plot. Since this approach was not successful for ρ equal to 0 and for parameter C_v equal to 0.5, it was not considered necessary to evaluate other ρ's or C_v's.

The final procedure attempted was to take the data for given parameter means and

C_v's and attempt to relate the error to bln(a) and dln(c). Figure 5-87 shows this data for ρ equal to zero. Again, there was too much scatter in the data to construct a model. In this plot, E[x] and E[y] are equal to 1 and their C_v's are 0.5.

As a final check, the decreasing models were separated out, and a factor vs error plot (Figure 5-88) was made. Even with just decreasing models, there was still too much scatter to construct a model or contour plot. A plot like Figure 5-87 was also constructed, using just the decreasing models (Figure 5-89). Again, there was too much scatter to construct a model.

The conclusion for exponential models is, therefore, that none of the approaches which worked for one parameter models or for two parameter polynomial models can be used to predict the error in the FOA variance. In some cases, it is possible to establish that the error will be at least 0.3.

RESULTS FOR MIXED EXPONENTIAL-POLYNOMIAL MODELS

Models containing an exponential and polynomial component (equation 5-3) were also evaluated. Since it was not possible to identify an error predictor for exponential models, it was not known if this effort would be successful. Accordingly, a smaller grid of model - parameter combinations was generated first, to be examined for any potential predictive factors. If it appeared that there might be something which could be used, the grid could then be expanded and a methodology developed.

A model can be checked to determine if it has the mixed exponential-polynomial (EP) form by setting the x parameter equal to its mean and finding the first and second partial derivatives with respect to the y parameter at several points. If the ratio of second derivative to first derivatives is constant regardless of the value of y, then the model is exponential in y. If the ratio divided by y is constant, the model is polynomial in y. Whether the model is polynomial or exponential in x is found in the same manner. If the model contains a polynomial and exponential component, then it fits into the mixed EP category.

The model (equation 5-3) can also written as

$$z=e^{b_2 x}y^{c} \tag{5-27}$$

where b_2 is equal to bln(a). The model grid contained all combinations of E[x] equal to 1 and 5, E[y] equal to 1, C_{vx} or C_{vy} equal to 0.1, 0.5 and 1, b equal to ± 1, ± 0.5, and ± 0.1, and c equal to ± 0.5 and ± 1.5. Values of ρ used were 0, ± 0.25, ± 0.5, and ± 0.75. As before, if the expected value of z or z^2 was greater than 1e+06, those results were eliminated from the data set. There were originally 2016 model - parameter combinations, with 1690 remaining after the questionable ones were eliminated.

The first analysis done was to determine if the error in the FOA variance could be predicted using the error due to x and the error due to y. The error due to the exponential component is found using the procedure outlined for the two parameter exponential models. The error due to the polynomial component is found by using the procedure described for two parameter polynomial models.

Figure 5-90 shows the results for ρ equal to zero. There is considerable scatter and overlap in the data, indicating that a good model, or even a contour plot, could not be constructed. The available data shows that if the error due to x and error due to y are both greater than 0.25, then the error in the FOA variance will be at least 0.3. The plot also indicates that if both the error due to x and error due to y are less than zero, the error in the FOA variance will be less than 0.3.

The models for which z decreased as both x and y increased (EPDMs) were then separated from the rest, to determine if any consistent patterns could be found by separating the models into categories. Figure 5-91 shows these results, and it appeared that there might be somewhat circular contours. A model with the form of equation 5-18 was estimated. Model parameters CONSTANT, A1, A2, and A3 were estimated to be 0.150, 0.204, 0.610, and -0.531, respectively. The R^2 was 0.92 and the standard deviation of the residuals was 0.10. This would not appear to be a particularly accurate model. A plot of actual vs predicted errors (Figure 5-92) confirmed this. Since this approach did not work for EPDMs with ρ equal to 0, it was not considered worthwhile to pursue it for other values of ρ or other types of models.

For the mixed EP models, a potential predictor for the error due to the exponential component is the correlation factor and a potential predictor for the error due to the polynomial component is the power, c. Taking the data for ρ equal to zero, a plot using the factor and the power for C_{vx} and C_{vy} equal 0.5 was constructed (Figure 5-93). There was considerable overlap in the data, so neither a model or contour plot could be constructed using these data. Again, the EPDMs were evaluated separately (Figure 5-94). The figure shows that there was too much overlap in the data to construct a model.

Finally, a plot using bln(a) and c, with E[x] and E[y] equal to 1 and C_{vx} and C_{vy} equal to 0.5 was constructed (Figure 5-95). There was no overlap, so it might have been possible to construct a contour plot. There were no obviously circular contours or contours which would suggest any other type of function to fit to the data. The data was somewhat sparse, and it is entirely possible that addition of more points would result in scatter or overlap. This approach was not carried any further since application of the method would require generating plots for all combinations of useful values of ρ, E[y],

C_{vx}, and C_{vy}. This would be a massive effort to compile, and would not be particularly useful, since interpolations between four sets of curves would be required.

The behavior of the error with respect to ρ exhibited the same trends as found in polynomial models, i.e., error increasing as a function of ρ for EPDMs and for models in which z increased as both x and y increased (EPIMs). For models where z increased as either x or y increased and decreased as the other increased (EPMMs), the error decreased as ρ increased. Figures 5-96 through 5-98 show error as a function of ρ. For a given type of model, error with C_v's of x and y equal to 0.1 were smaller than errors with higher C_v's for either parameter. This is the expected result, but again, is dependent on the choices of b, c, and E[y]. Figures 5-99 through 5-101 contain this data.

For the cases where it can be established that $error_0$ is at least 0.3, given an EPDM or EPIM and positive ρ, $error_\rho$ will be larger than 0.3. Also, given that $error_0$ is at least 0.3, with an EPMM and negative ρ, $error_\rho$ will be larger than 0.3. If it can be established that $error_0$ is less than 0.3, given an EPDM or EPIM and negative ρ, $error_\rho$ is also less than 0.3. For EPMMs, if $error_0$ is less than 0.3 and ρ is positive, then $error_\rho$ is also less than 0.3.

The conclusion for mixed models is, therefore, that no reliable method for predicting the error in the FOA variance could be identified. In some cases, it is possible to predict if the error is less than or greater than 0.3.

TWO PARAMETER EXAMPLE APPLICATION

A model for which the response is not an explicit function of the parameters was used to demonstrate the error predicting procedure. The model finds the runoff hydrograph resulting from a 24-hour rainstorm. The SCS curve number method is used to find the rainfall excess. The SCS unit hydrograph is used to compute the runoff hydrograph. The response of interest is the peak discharge, Q_p, of the runoff hydrograph.

Model parameters with no uncertainty were the watershed area and 24-hour rainfall depth. For this example, the watershed area was 2 square miles (1280 acres) and the 24-hour rainfall was taken as the 10-year storm in Stillwater, Oklahoma, which is approximately 6 inches. The uncertain parameters were the SCS curve number and the time increment for the computations. The time increment determines the time to peak of the unit hydrograph.

The model first takes the total rainfall and divides it up into incremental amounts. The equation

$$P_i = P_{24}[0.5 + \frac{t_i - 12}{24}(\frac{24.04}{2|t_i - 12| + .04})^{.755}] \qquad (5\text{-}28)$$

(Barfield, et al, 1981) approximates the SCS Type II mass rainfall curve. In equation 5-28, P_{24} is the 24-hour rainfall, P_i is the accumulated rainfall at the end of the ith time increment in inches, and t_i is the time in hours at the end of the ith time increment.

The SCS curve number method (SCS, 1972) was used to find the cumulative rainfall excess, R_i, in inches at the end of each time period. This is computed as

$$R_i=\frac{(P_i-.2S)^2}{P_i+.8S} \tag{5-29}$$

where S is a parameter computed from the curve number, CN, as

$$S=\frac{1000}{CN}-10 \tag{5-30}$$

The rainfall excess for time period i is given by $r_i = R_i - R_{i-1}$. The contribution to runoff from that rainfall excess is found by applying the SCS unit hydrograph. The ordinates of the unit hydrograph can be approximated by

$$UHG_i=q_p[\frac{t_i}{t_p}\exp(1-t_i/t_p)]^{3.77} \tag{5-31}$$

(Barfield, et al, 1981) where t_p is the time to peak in hours which is taken as 4 times the time increment and q_p is the peak flow rate of the unit hydrograph. This is estimated as

$$q_p=\frac{484A}{t_p} \tag{5-33}$$

where A is the watershed area in square miles.

The ordinate of the total runoff hydrograph in the jth time step is found as the sum

$$q_j=\sum_{i=1}^{j} u_i r_{j-i+1} \tag{5-34}$$

where r_k is the rainfall excess in the kth time step. The discharge at the peak of the runoff hydrograph is then identified and is the response of interest.

For this example, the mean of the curve number was 75 and the C_v was 0.1. Corresponding lognormal distribution parameters are μ_c equal to 4.3125 and σ_c^2 equal to

0.00995. Then mean of the time increment was taken as 30 minutes (0.5 hours) and the C_v was 0.1. The lognormal distribution parameters were μ_i equal to 3.3962 and σ_i^2 equal to 0.00995. Two cases were considered. For one, the parameters were assumed to be independent. For the other, they were correlated with ρ equal to -0.25.

Since evaluations of first and second derivatives at the means of the parameters are required for model classification and for computing the FOA variance, an evaluation of the optimum step size was needed. For the partial derivative with respect to curve number, both the two-point and four-point central difference approximations were equal to 30.64 cfs/unit of CN for step sizes of 0.001, 0.005, 0.01, 0.05, 0.1, 0.3. This was accepted as the correct result. As a check, a linear model was estimated using curve number - model response pairs found at the 5 recommended points. The slope of this model was found to be 29.3, indicating that 30.64 is a reasonable estimate of the first derivative at the curve number mean.

The results were not as clear for the derivative with respect to the time increment. The two- and four-point derivatives did not exhibit the pattern found in the one-parameter example of being different, coming closer in value, and then starting to diverge as the step size increased. For this case, it was decided that the best estimate of the first derivative was the one closest to the slope found by estimating a linear model of the form Q_p = CONSTANT + SLOPE * Δt. The slope was found to be -1236. The derivative found using a step size of 2 minutes (0.03333 hours) was -1249.34. The two- and four-point derivatives had only a 0.9 percent difference. This was accepted as the best approximation of the derivative at the mean of the time increment length.

The ratio of second to first derivatives was found and was not constant for either curve number or time increment. Neither was the ratio divided by curve number or time increment. Accordingly, polynomial and exponential models (equations 5-21 through 5-24) were estimated. Polynomial models using curve number and time increment as the dependent variable had R^2's of 0.998 and 0.999 respectively. The exponential models had zero R^2's in both cases. Thus, it was determined that the model could be classified as polynomial in both curve number and time increment and the polynomial error predicting technique could be applied.

The "true" variances to compare the FOA variances against were derived by MCS. A random sample of 10,000 independent curve numbers and time increments was generated and the model run using each pair of parameters. Since the curve number cannot be greater than 100, the samples with curve number greater than 100 were eliminated, leaving 9,991 samples. The distribution of curve number is in reality truncated on the right at curve number equal to 100. This is not particularly significant, since only 0.18 percent of the area under the PDF is eliminated. The sample statistics for curve number showed a mean of 74.86 and a C_v equal to 0.099, which were very close to the intended mean and C_v.

To determine if the 9,991 samples were sufficient, the variance was found using the first 5,000 samples and first 6,000 samples. The percent change was -1.41. The percent changes for 6,000 to 7,000 and 7,000 to 8,000 were 0.5 and -0.03, respectively. This indicates that the simulation had converged to a solution by 8,000 samples, so 9,991 was definitely sufficient.

A sample of 10,000 curve numbers and time increments with a correlation coefficient of -0.25 was also generated. The correlated sample was generated by first generating pairs of independent random normal deviates, z_1 and z_2. These independent random normal deviates were transformed to correlated random normal deviates, f_1 and

f_2 using the equations

$$f_1 = 0.790569z_1 + 0.612372z_2 \tag{5-35}$$

and

$$f_2 = -0.790569z_1 + .612372z_2 \tag{5-36}$$

The constants in these equations were based on the eigenvectors of the 2 $\times$ 2 correlation matrix between CN and time increment. They were found using the SYSTAT computer software (Wilkinson, 1990). The curve number - time increment pairs were then found as

$$\textit{curve number} = \exp(\mu_c + f_1\sqrt{\sigma_c^2}) \tag{5-37}$$

and

$$\textit{increment} = \exp(\mu_i + f_2\sqrt{\sigma_i^2}) \tag{5-38}$$

Once the samples with curve number greater than 100 were eliminated, there were 9,984 samples remaining. The sample mean and C_v of curve number were 74.92 and 0.10, respectively. Sample mean and C_v of time increment were 0.501 and 0.0995. The sample correlation coefficient was -0.255. These samples statistics are very close to the intended values.

A similar analysis was conducted to determine if the number of samples was sufficient. The percent changes in variance between 8,000 and 9,000 and between 9,000 and 9,984 samples were -0.43 and -0.08 respectively. Thus 9,984 was accepted as a sufficient number of samples for the correlated parameter simulation.

With the parameters assumed independent, the sample variance of the model responses was 56,071. The FOA variance was computed (equation 5-8) and found to be

56,710. The relative error (equation 5-9) was -0.011.

To use the quadratic error model to predict the errors, the error due to curve number and error due to increment must be known. Polynomial models estimated using the five recommended points were

$$Q_p = -584.3 + 3.425 \times (curve\ number)^{1.41} \tag{5-39}$$

and

$$Q_p = 535.8 + 116.94 \times (increment)^{-1.85} \tag{5-40}$$

Using the estimated b and c powers gave an error due to curve number of 0.011 and an error due to time increment of 0.06. The quadratic model (equation 5-25) gave a predicted error of 0.12.

With the correlated parameters, the sample variance was 66,857 and the FOA variance (equation 5-8) was 63,888. The relative error was 0.044. Using the quadratic model for the predicted error when ρ is equal to -0.25 gave a predicted error of 0.089.

The linear model for $error_{-.25}$ as a function of $error_0$ for PMMs was also applied. The model is

$$error_{-.25} = .046 + .969 \times error_0 \tag{5-41}$$

and the predicted error was 0.16. Using the actual error for ρ equal to 0 of -0.011 in the linear model gave a predicted error of 0.01.

The example applications showed several things. The error with independent parameters was overpredicted. This resulted in an overprediction of the error with correlated parameters using the linear model. The best results were obtained for the correlated parameters using the quadratic model. If an acceptable range for the error in

FOA variance is ± 0.2, use of the predicted errors would have resulted in the correct accept or reject decisions. As with the one parameter models, the choice of step size can have a great influence on the numerical first derivative. It appears that using a step size which produces a first derivative close in value to the slope of an estimated linear model is a good approach.

TABLE 5-1
EFFECT OF PARAMETER MEAN ON ERROR IN FOA VARIANCE - TWO PARAMETER POLYNOMIAL MODELS

E[x]	E[y]	$C_v[x]$	$C_v[y]$	ρ	b	c	error
1.0	1.0	0.1	0.1	0	-0.5	-0.5	0.017
5.0	1.0	0.1	0.1	0	-0.5	-0.5	0.017
1.0	1.0	0.5	0.1	0	-0.5	-0.5	0.090
5.0	1.0	0.5	0.1	0	-0.5	-0.5	0.090
1.0	1.0	1.0	0.1	0	-0.5	-0.5	0.222
5.0	1.0	1.0	0.1	0	-0.5	-0.5	0.222
1.0	1.0	1.5	0.1	0	-0.5	-0.5	0.327
5.0	1.0	1.5	0.1	0	-0.5	-0.5	0.327
1.0	1.0	0.1	0.5	0	-0.5	-0.5	0.091
5.0	1.0	0.1	0.5	0	-0.5	-0.5	0.091
1.0	1.0	0.5	0.5	0	-0.5	-0.5	0.242
5.0	1.0	0.5	0.5	0	-0.5	-0.5	0.242
1.0	5.0	0.1	0.1	0.5	-0.5	-1.5	0.062
5.0	5.0	0.1	0.1	0.5	-0.5	-1.5	0.062
1.0	5.0	0.5	0.1	0.5	-0.5	-1.5	0.197
5.0	5.0	0.5	0.1	0.5	-0.5	-1.5	0.197

TABLE 5-2
MODEL PARAMETERS - LINEAR MODELS TO PREDICT $ERROR_\rho$ AS A FUNCTION OF $ERROR_0$ - PDMs

ρ	R^2	SEE	const.	slope
-0.75	0.962	0.071	-0.134	1.078
-0.5	0.988	0.039	-0.0853	1.058
-0.25	0.998	0.017	-0.0408	1.030
0.25	0.998	0.014	0.0377	0.970
0.5	0.993	0.026	0.0725	0.941
0.75	0.987	0.036	0.105	0.915

TABLE 5-3
MODEL PARAMETERS - LINEAR MODELS TO PREDICT $ERROR_\rho$
AS A FUNCTION OF $ERROR_0$ - PIMs

ρ	R^2	SEE	const.	slope
-0.25	0.982	0.064	-0.0823	1.035
0.25	0.992	0.039	0.0689	0.956
0.5	0.975	0.067	0.128	0.912
0.75	0.954	0.089	0.180	0.872

TABLE 5-4
MODEL PARAMETERS - LINEAR MODELS TO PREDICT ERROR$_\rho$
AS A FUNCTION OF ERROR$_0$ - PMMs

ρ	R^2	SEE	const.	slope
-0.75	0.977	0.054	0.125	0.909
-0.5	0.988	0.039	0.0872	0.939
-0.25	0.997	0.022	0.0459	0.969
0.25	0.994	0.030	-0.0503	1.027
0.5	0.955	0.098	-0.107	1.013

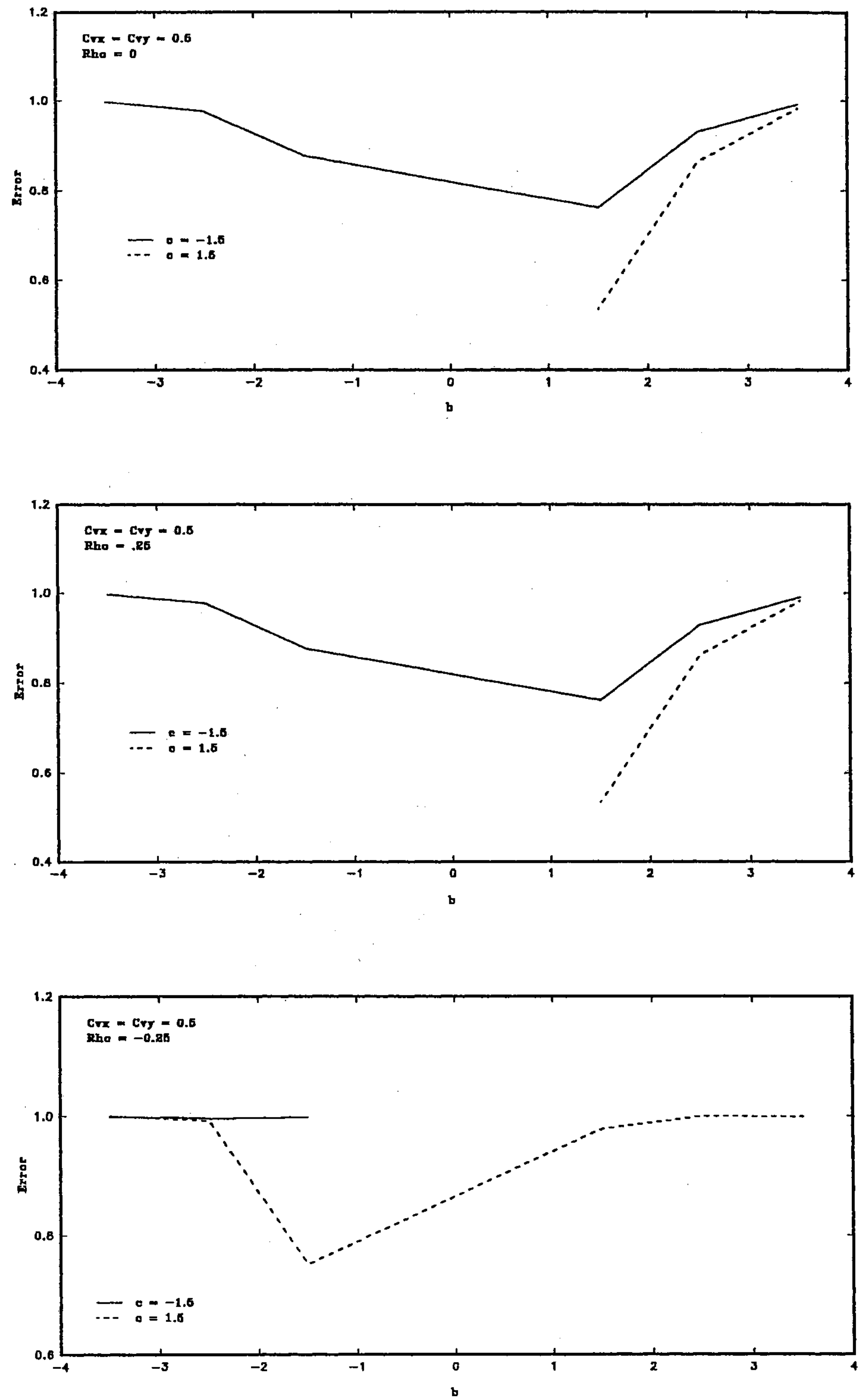

Figure 5−1. Behavior of Error as a Function of b

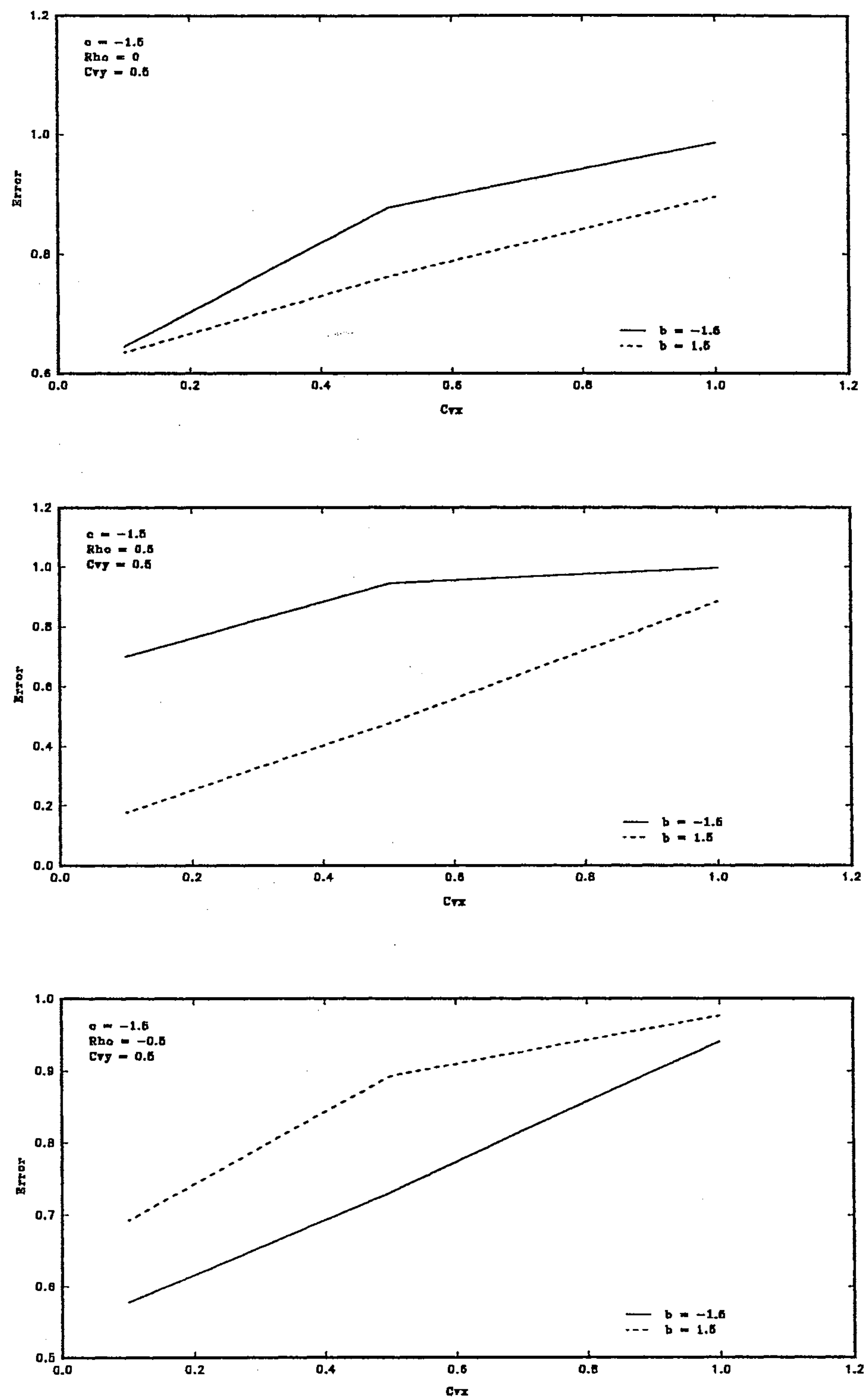

Figure 5–2. Behavior of Error as a Function of Cv

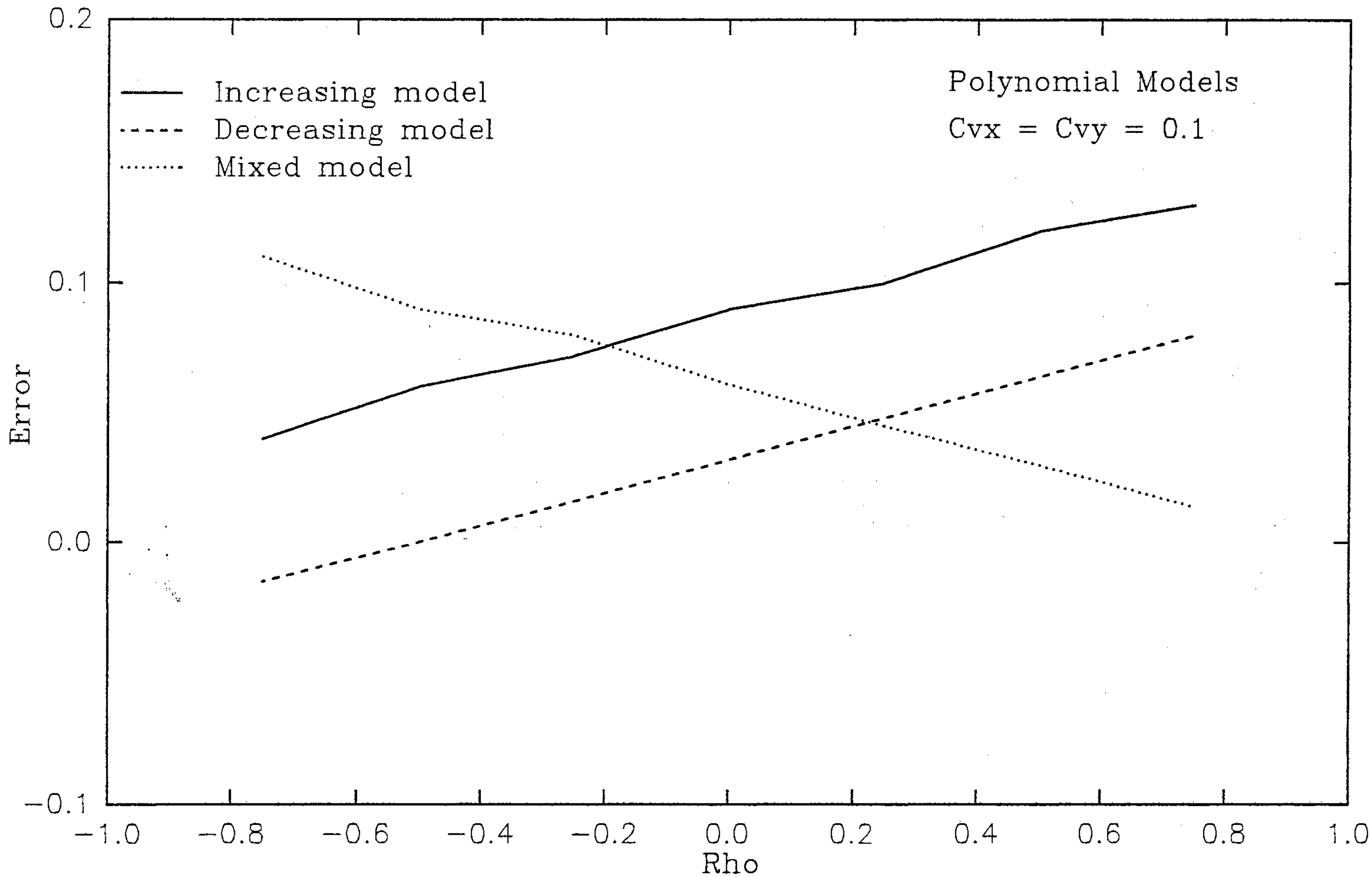

Figure 5−3. Error as a Function of Rho for Cv of x and y Equal to 0.1

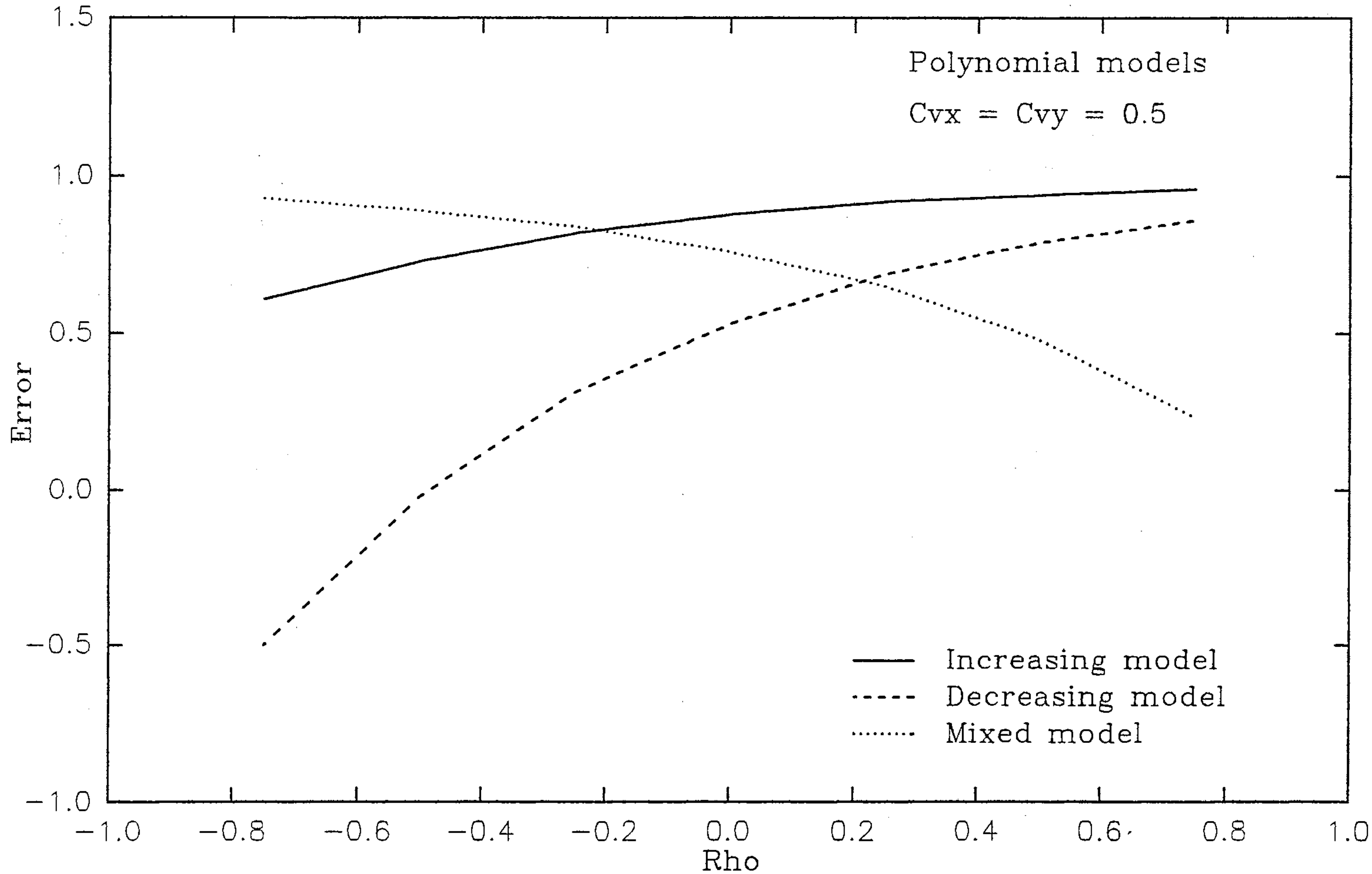

Figure 5−4. Error as a Function of Rho for Cv of x and Cv of y Equal to 0.5

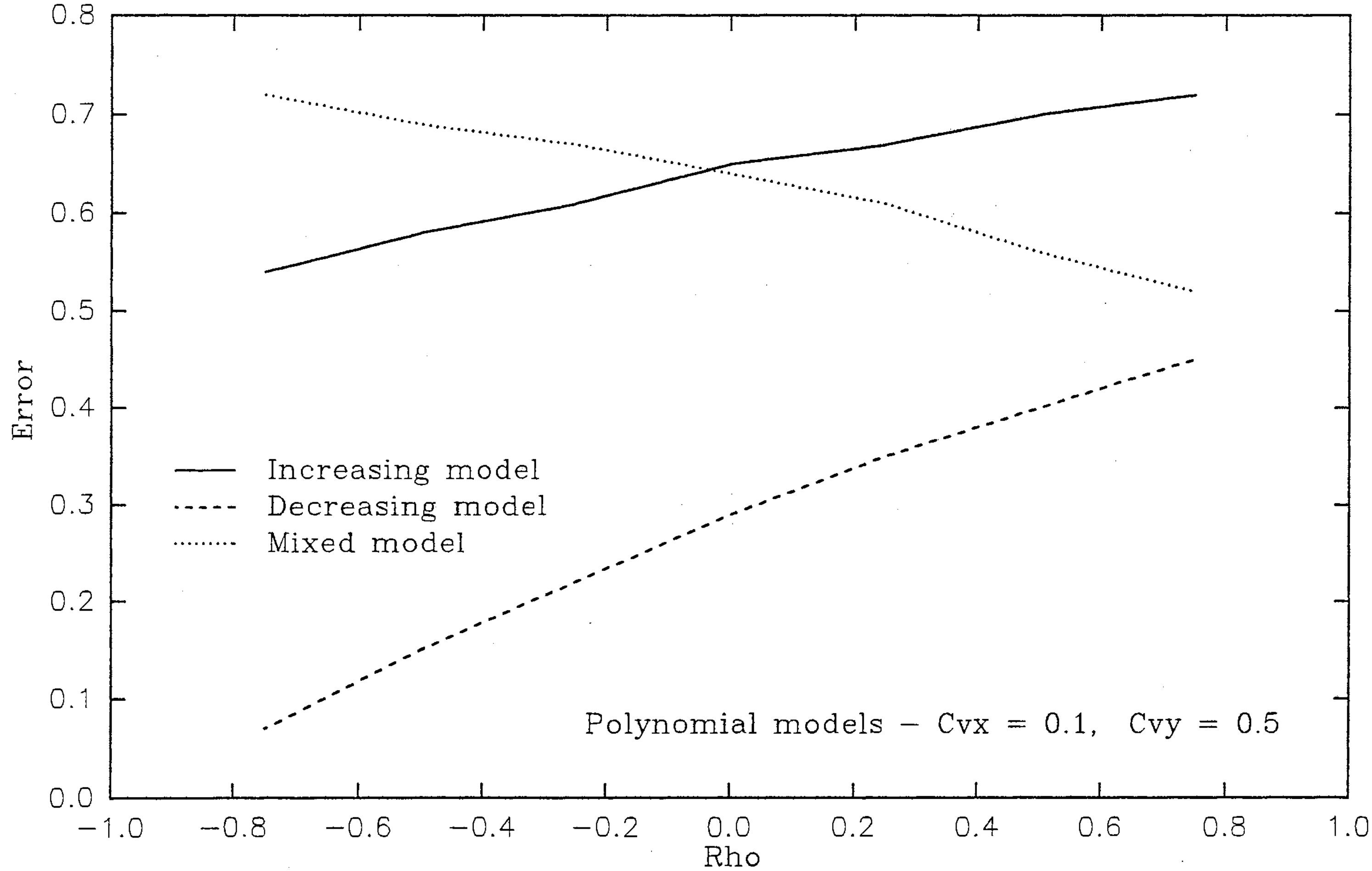

Figure 5–5. Error as a Function of Rho for Cv of x equal to 0.1 and Cv of y Equal to 0.5

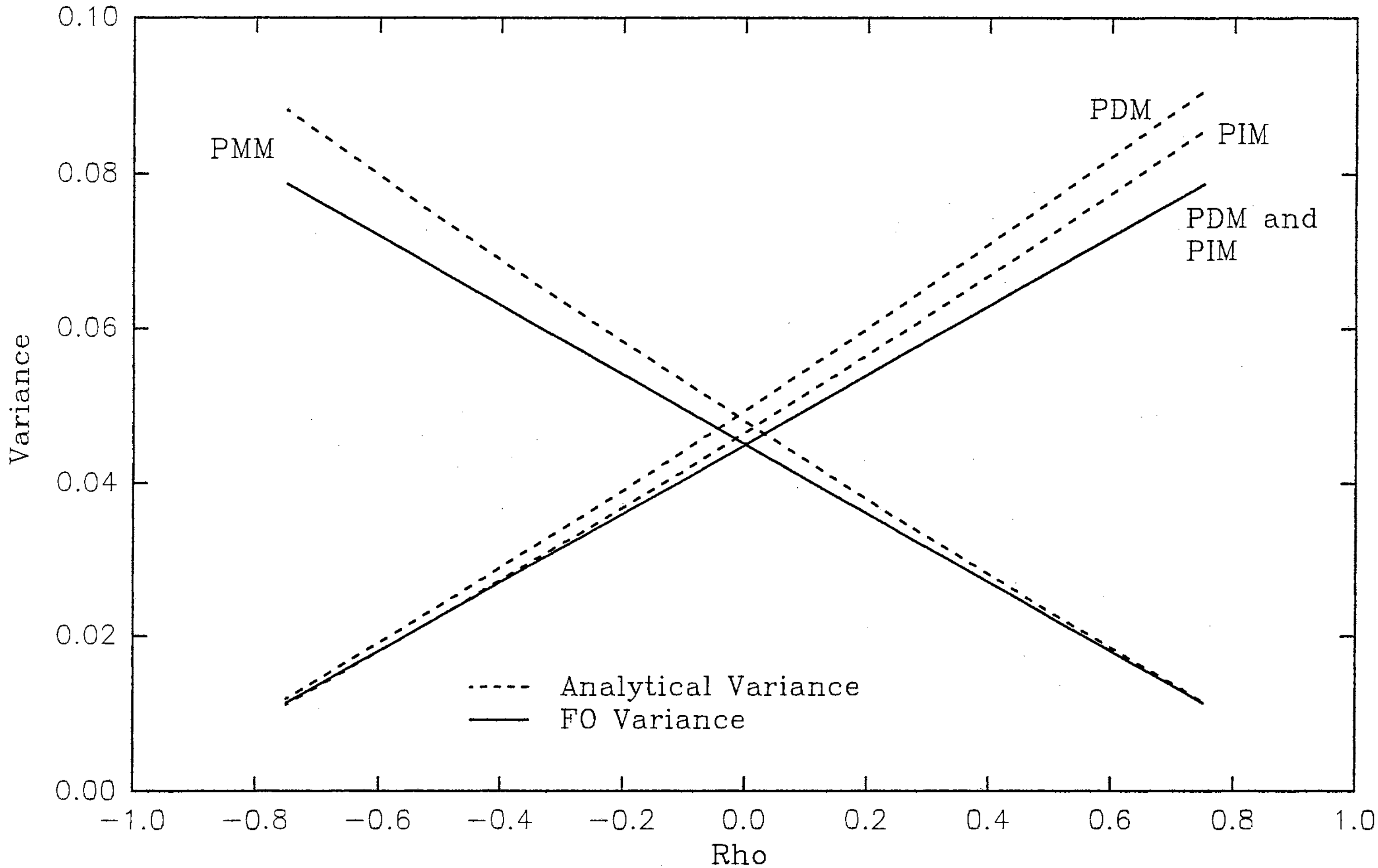

Figure 5−6. Analytical and FOA Variances as a Function of Rho

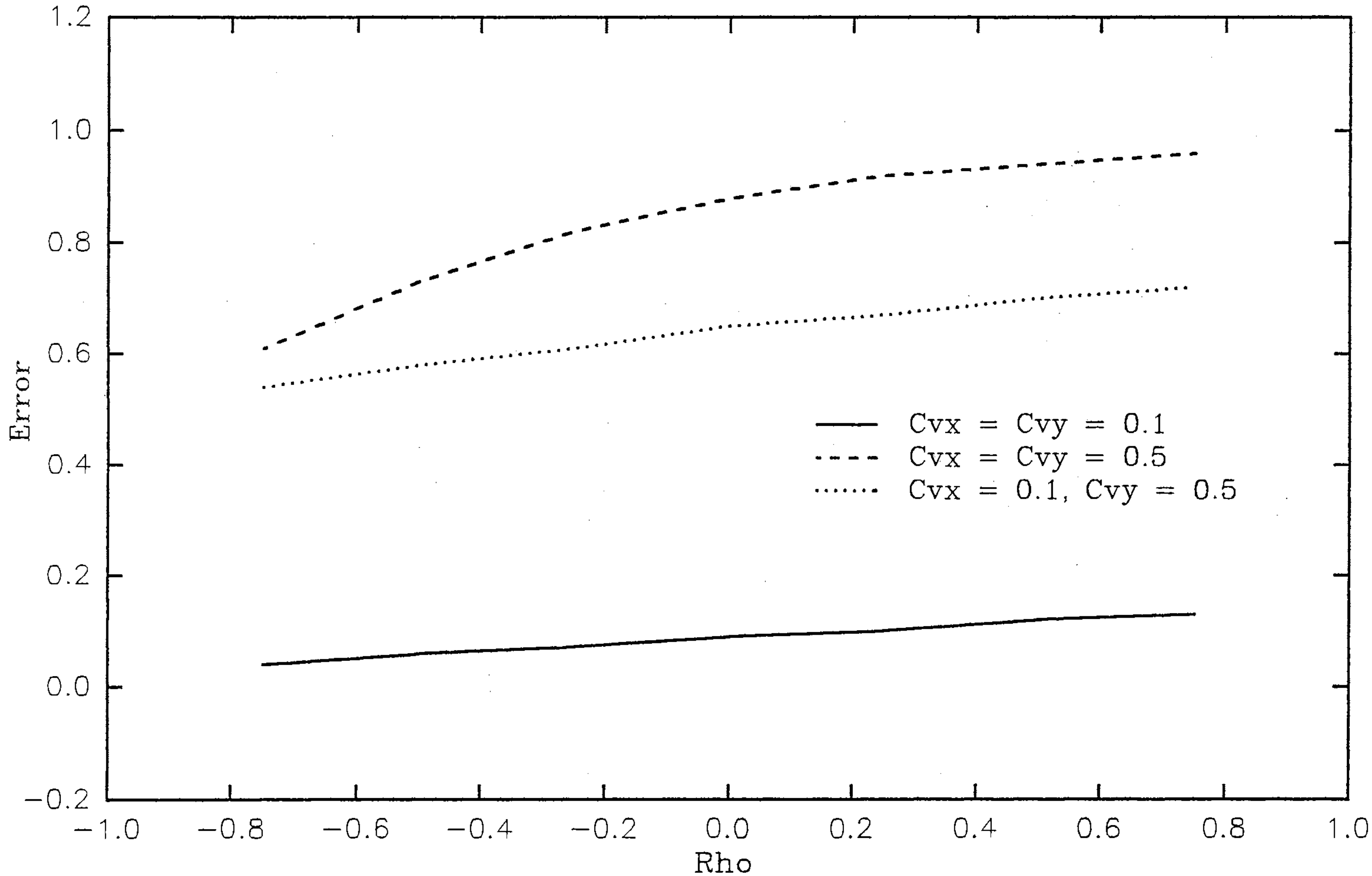

Figure 5−7. Error as a Function of Rho for PIMs

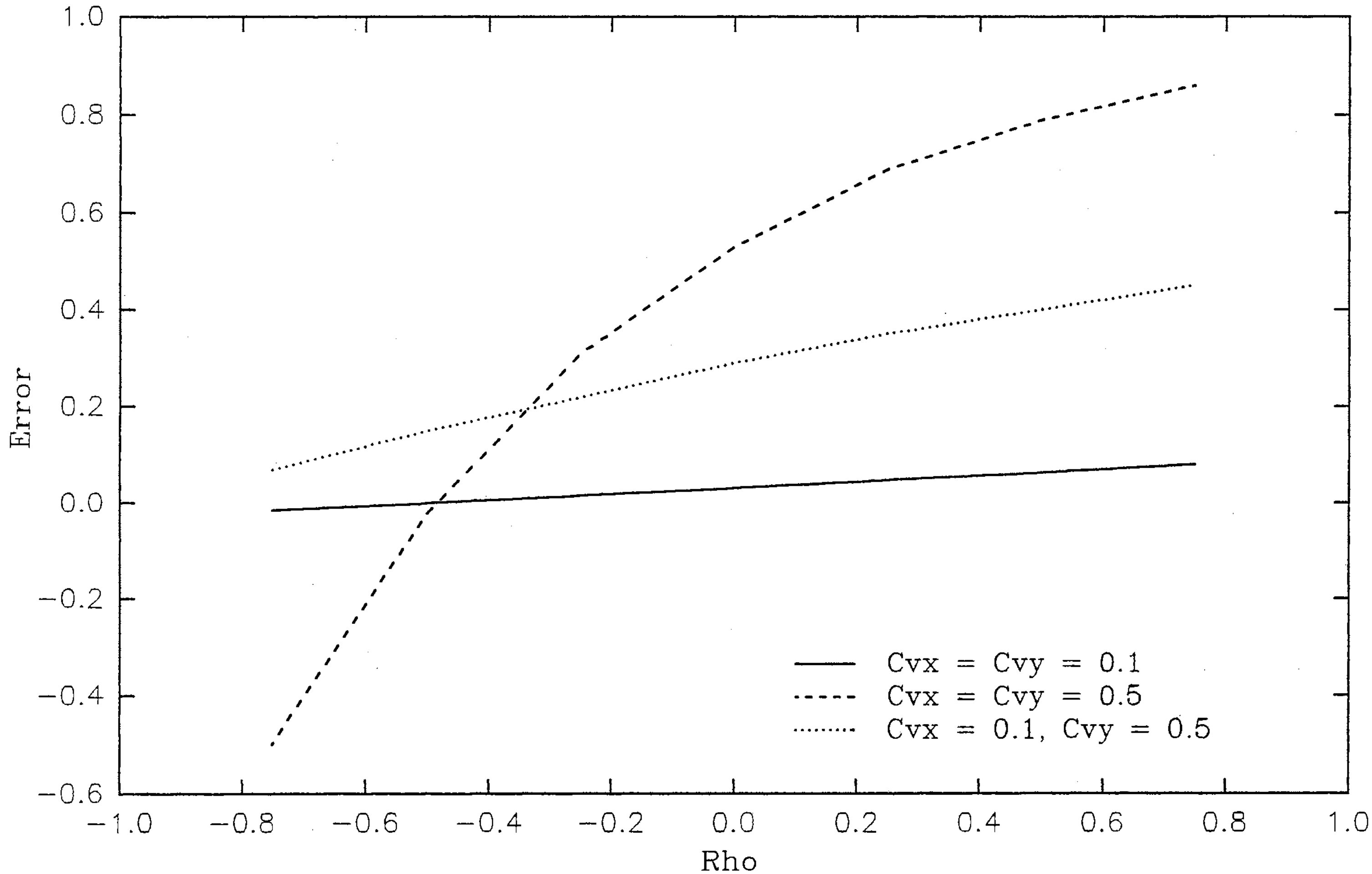

Figure 5–8. Error as a Function of Rho for PDMs

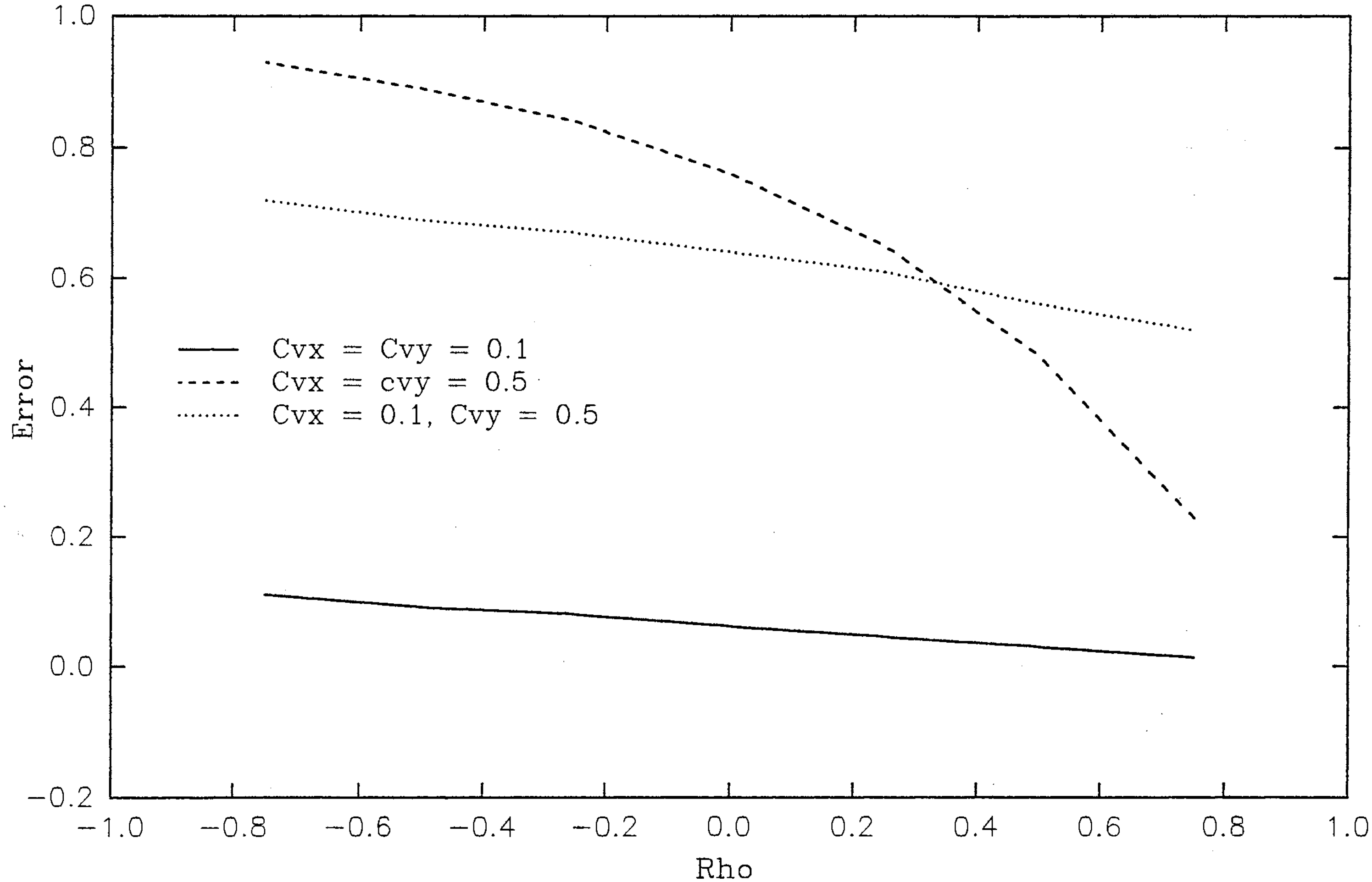

Figure 5−9. Error as a Function of Rho for PMMs

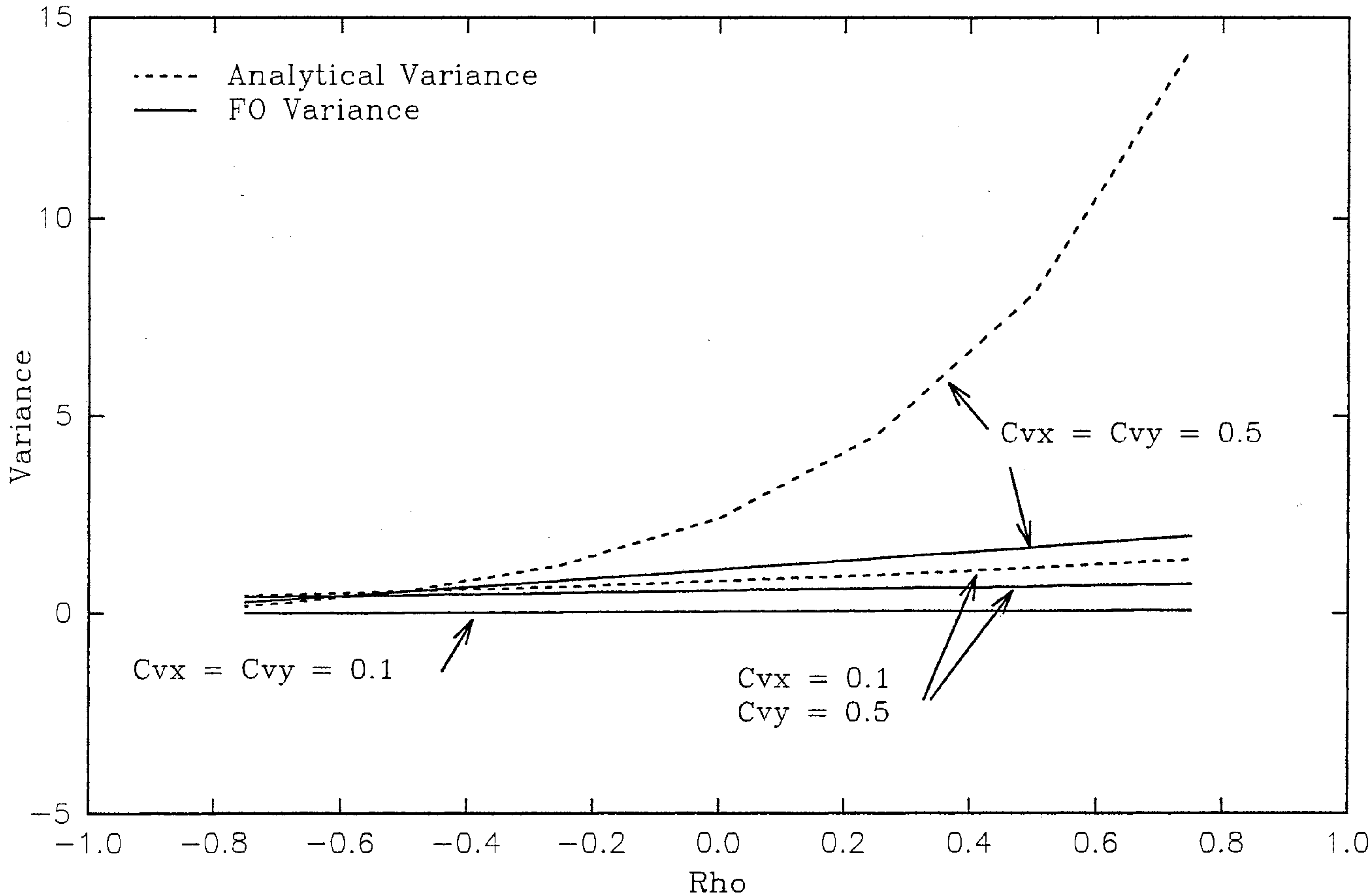

Figure 5–10. Analytical and FOA Variance as a Function of Rho for PIMs

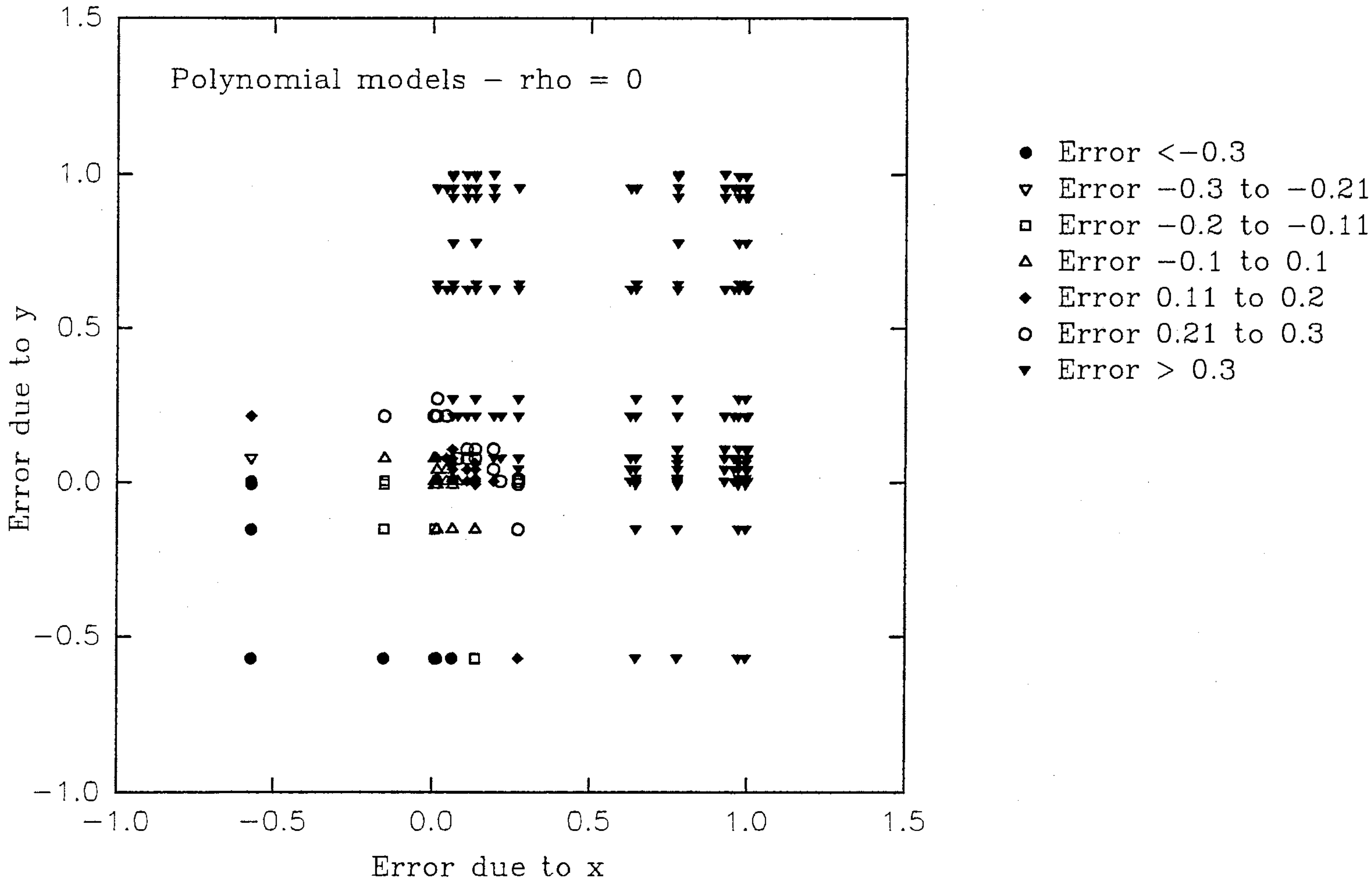

Figure 5–11. Error in FOA Variance vs Error Due to x and Error Due to y, Rho = 0

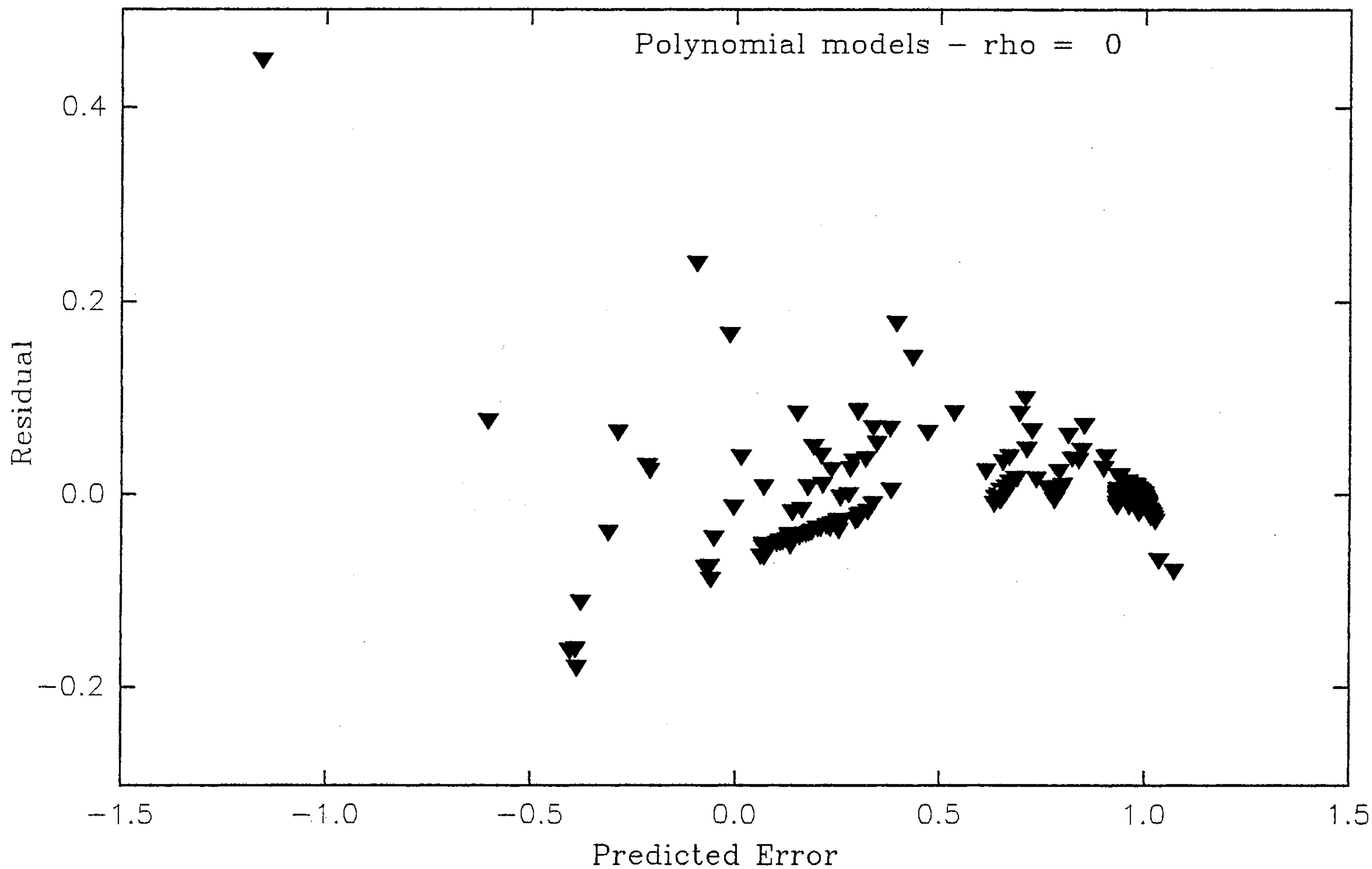

Figure 5-12. Plot of Residuals from Error Predicting Model, Rho = 0

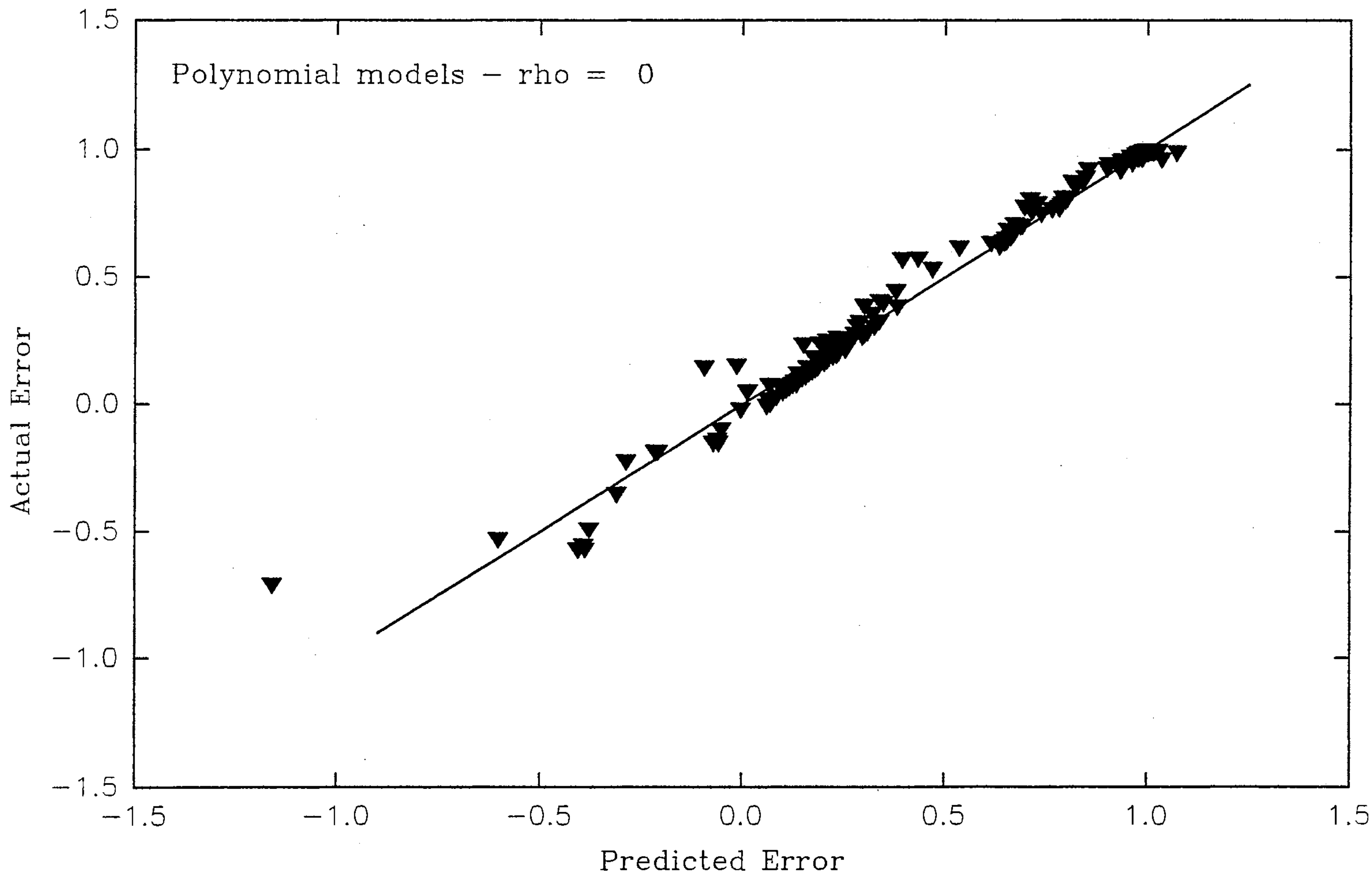

Figure 5-13. Actual vs Predicted Errors, Rho = 0

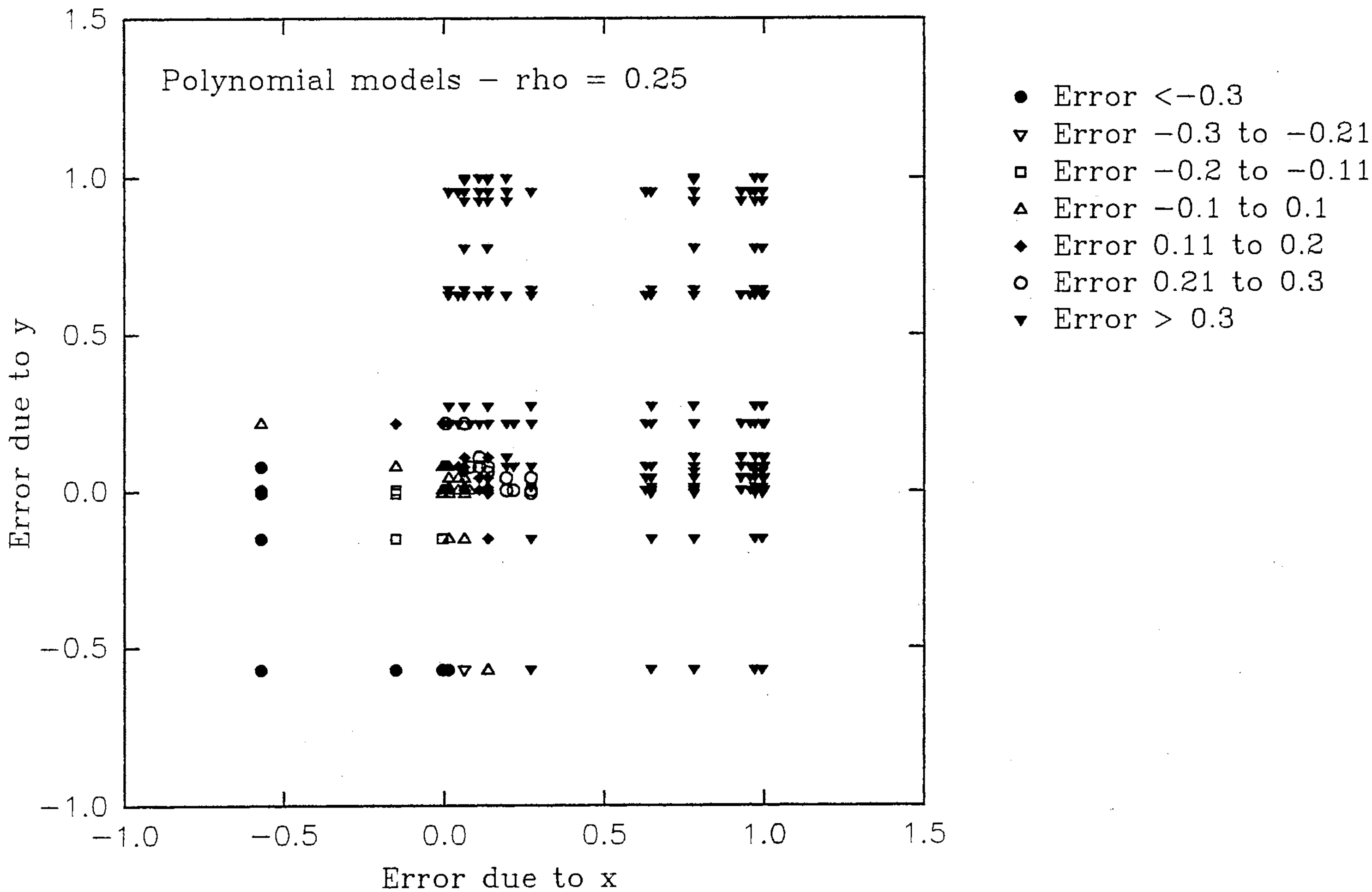

Figure 5–14. Error in FOA Variance vs Error Due to x and Error Due to y, Rho = 0.25

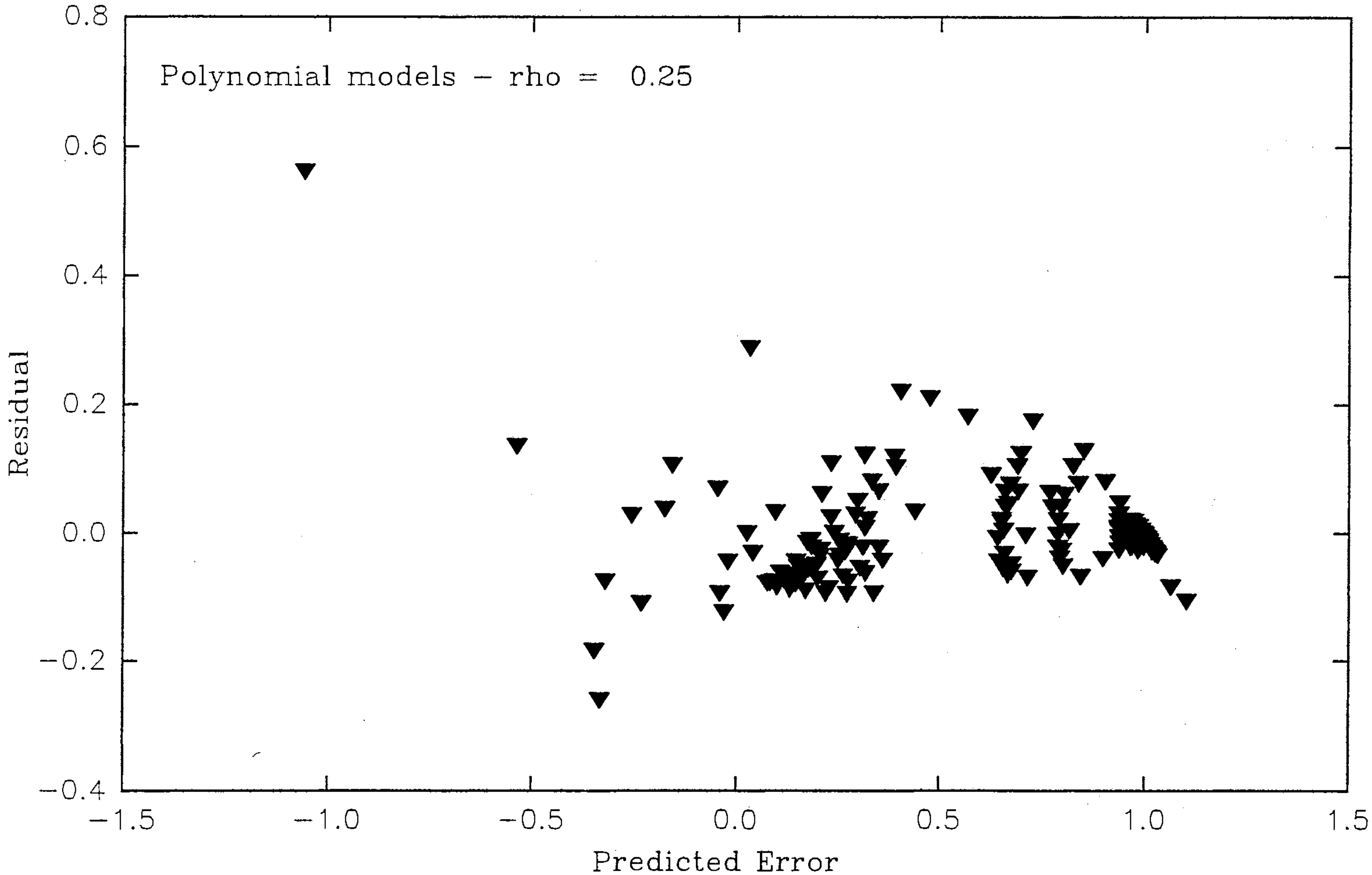

Figure 5–15. Plot of Residuals from Error Predicting Model, Rho = 0.25

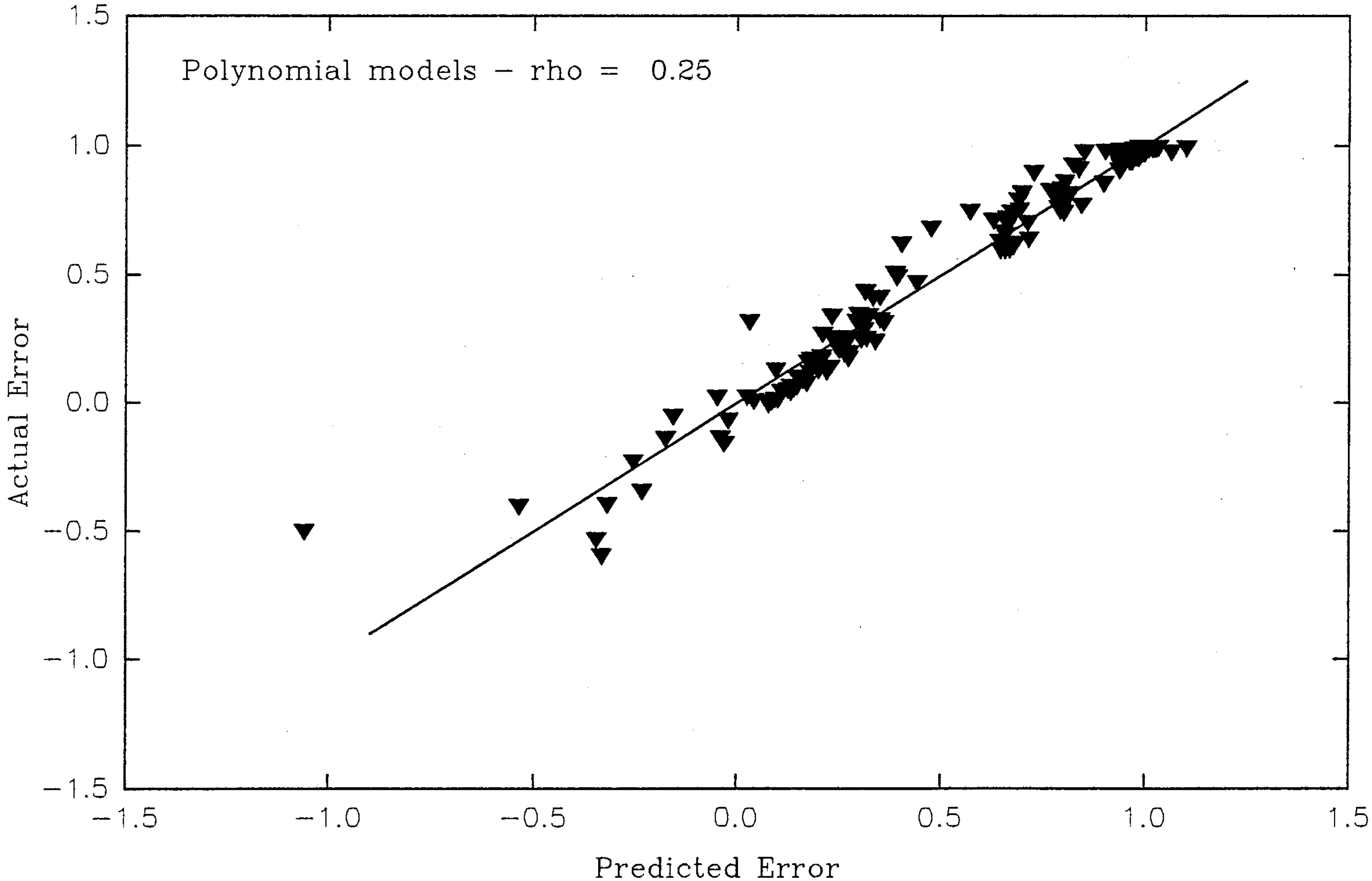

Figure 5-16. Actual vs Predicted Errors, Rho = 0.25

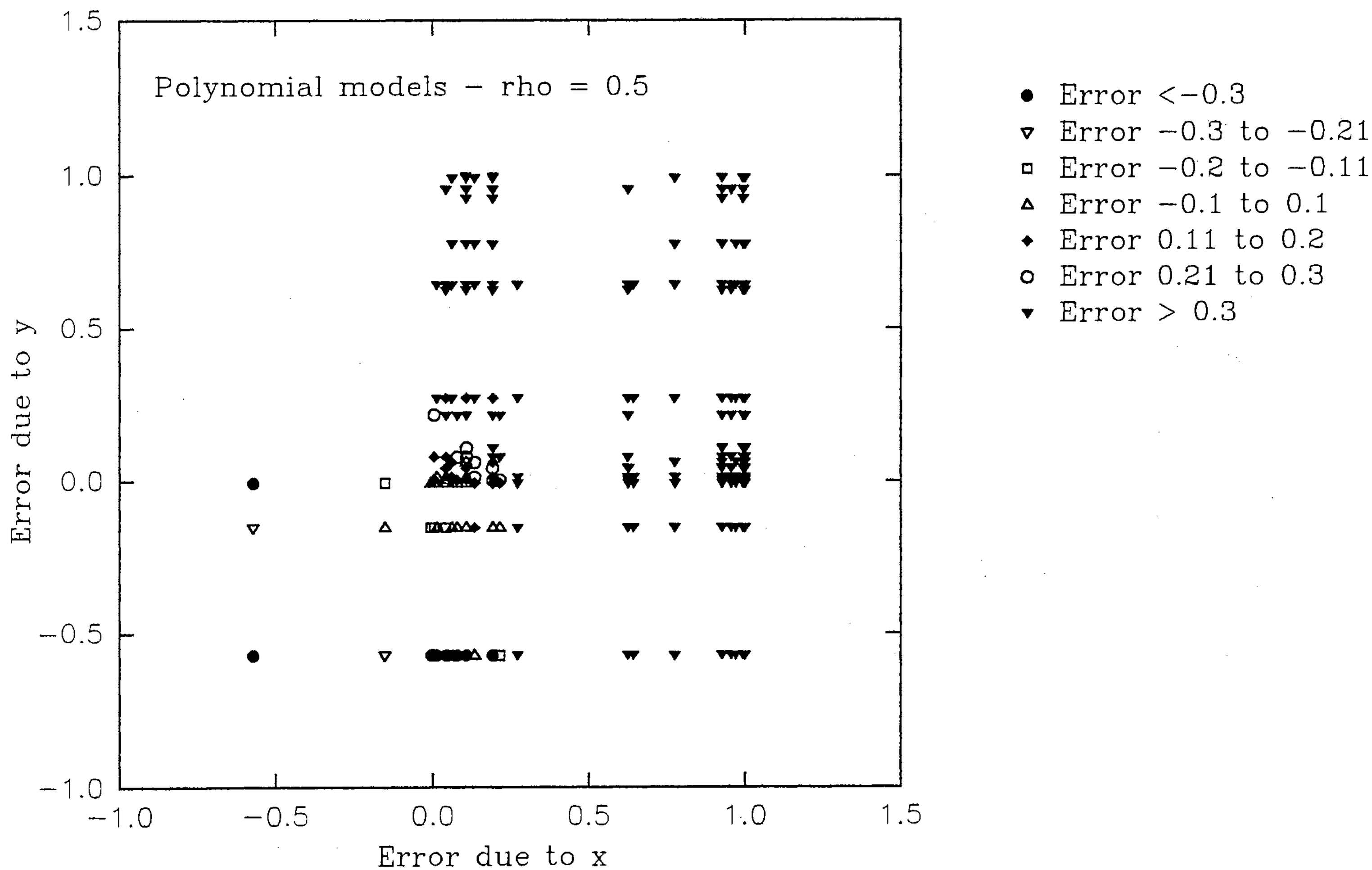

Figure 5−17. Error in FOA Variance vs Error Due to x and Error Due to y, Rho = 0.5

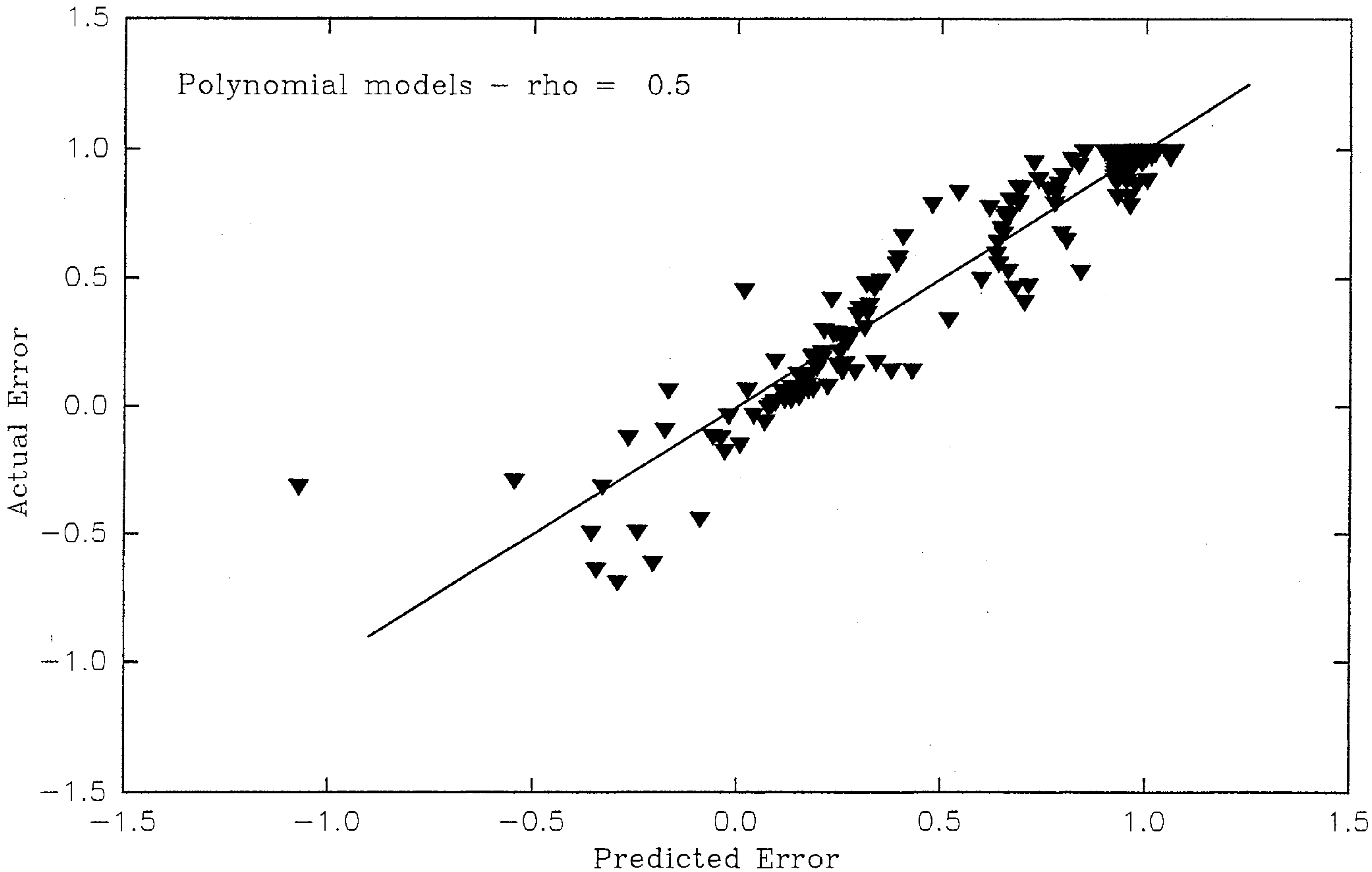

Figure 5-18. Actual vs Predicted Errors, Rho = 0.5

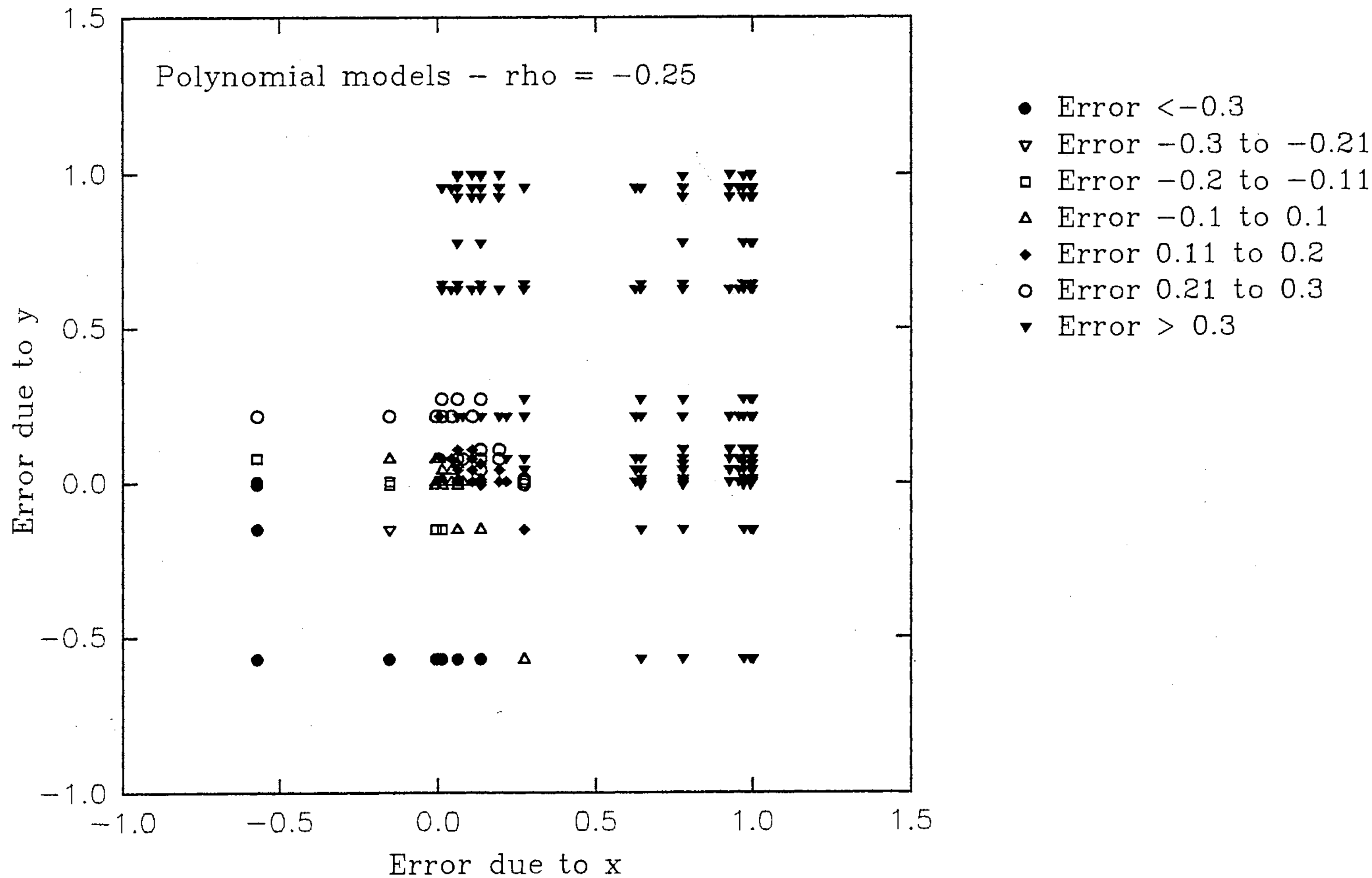

Figure 5−19. Error in FOA VAriance vs Error Due to x and Error Due to y, Rho = −0.25

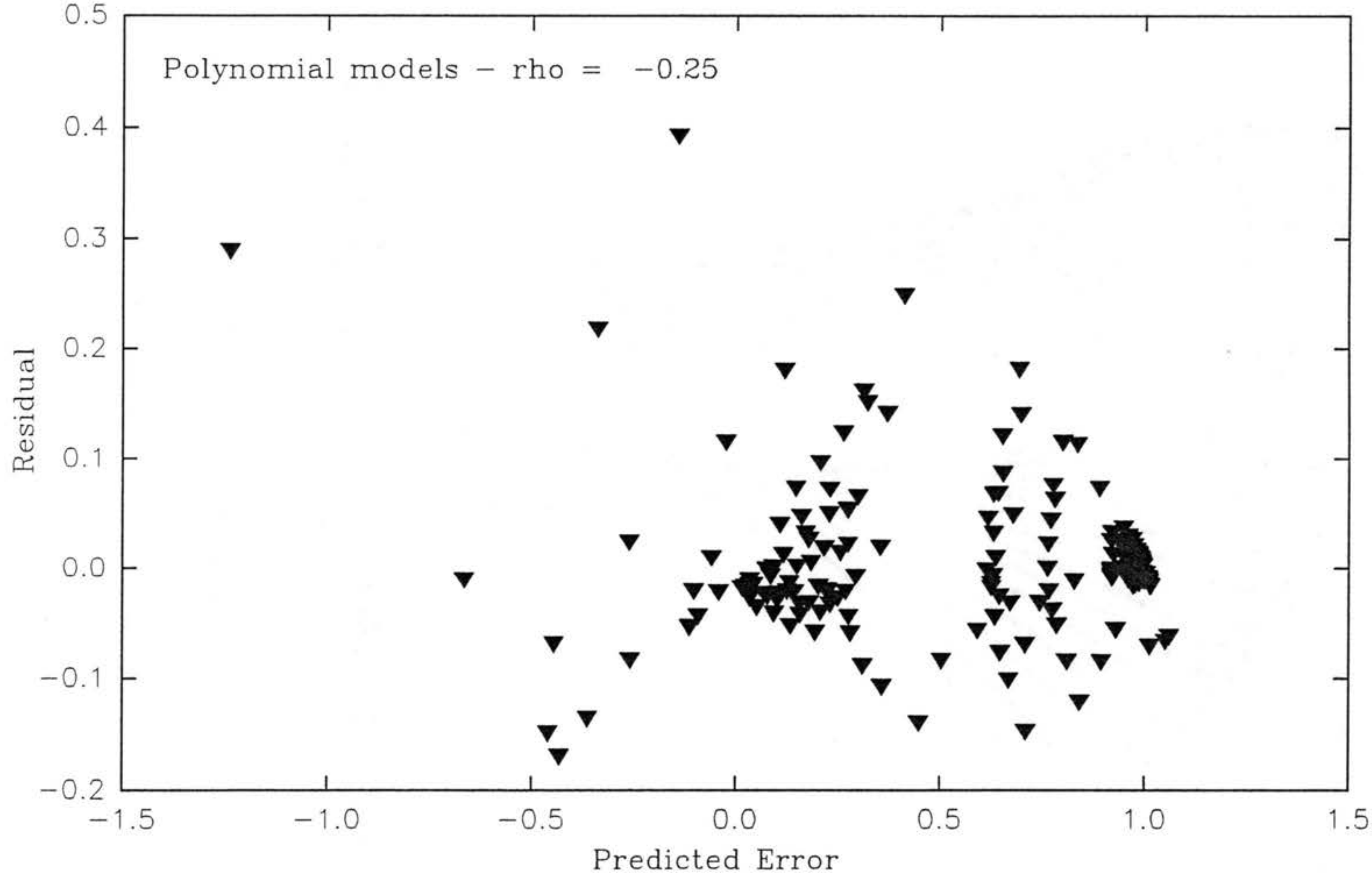

Figure 5−20. Plot of Residuals from Error Predicting Model, Rho = −0.25

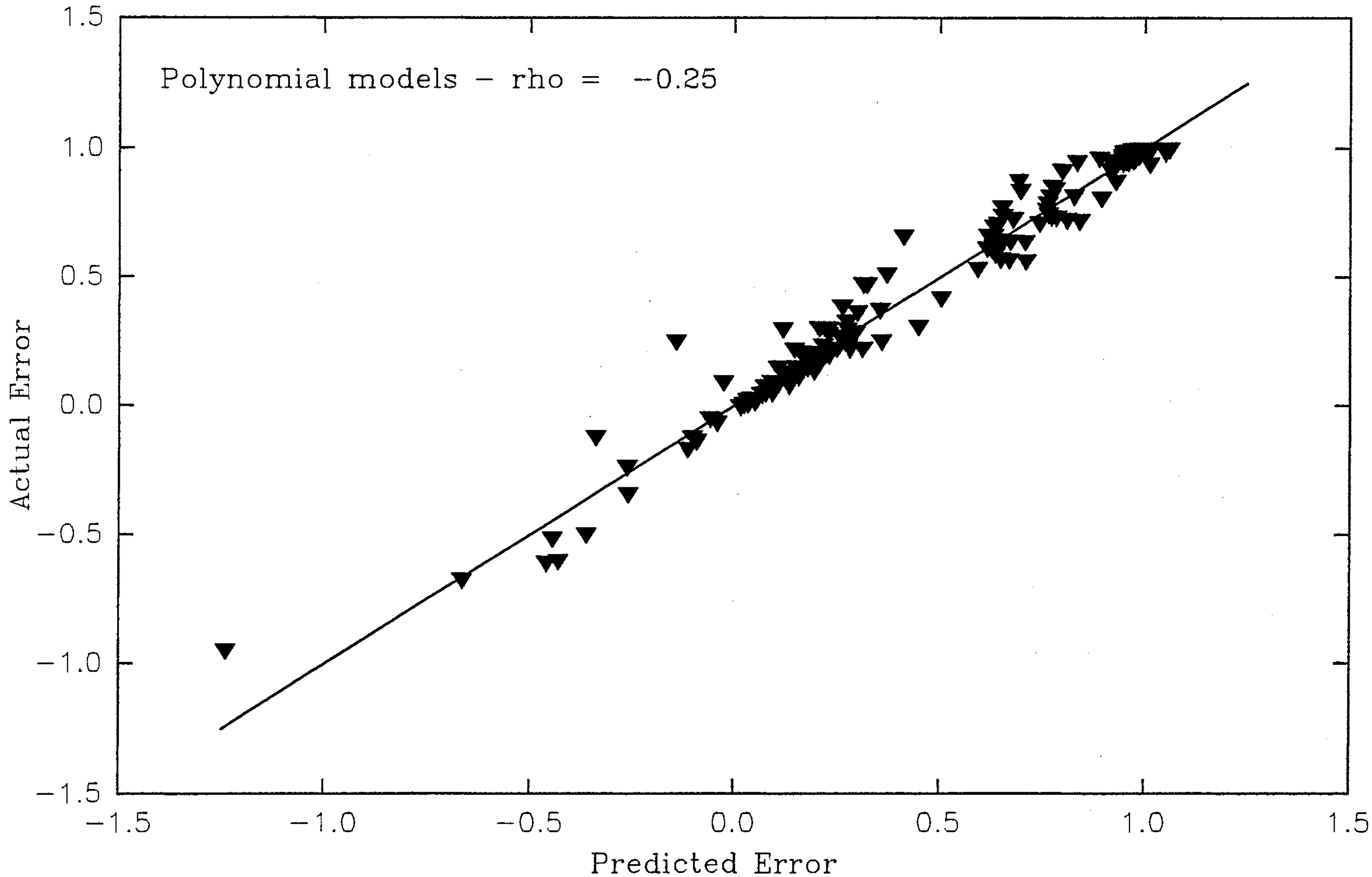

Figure 5-21. Actual vs Predicted Errors, Rho = -0.25

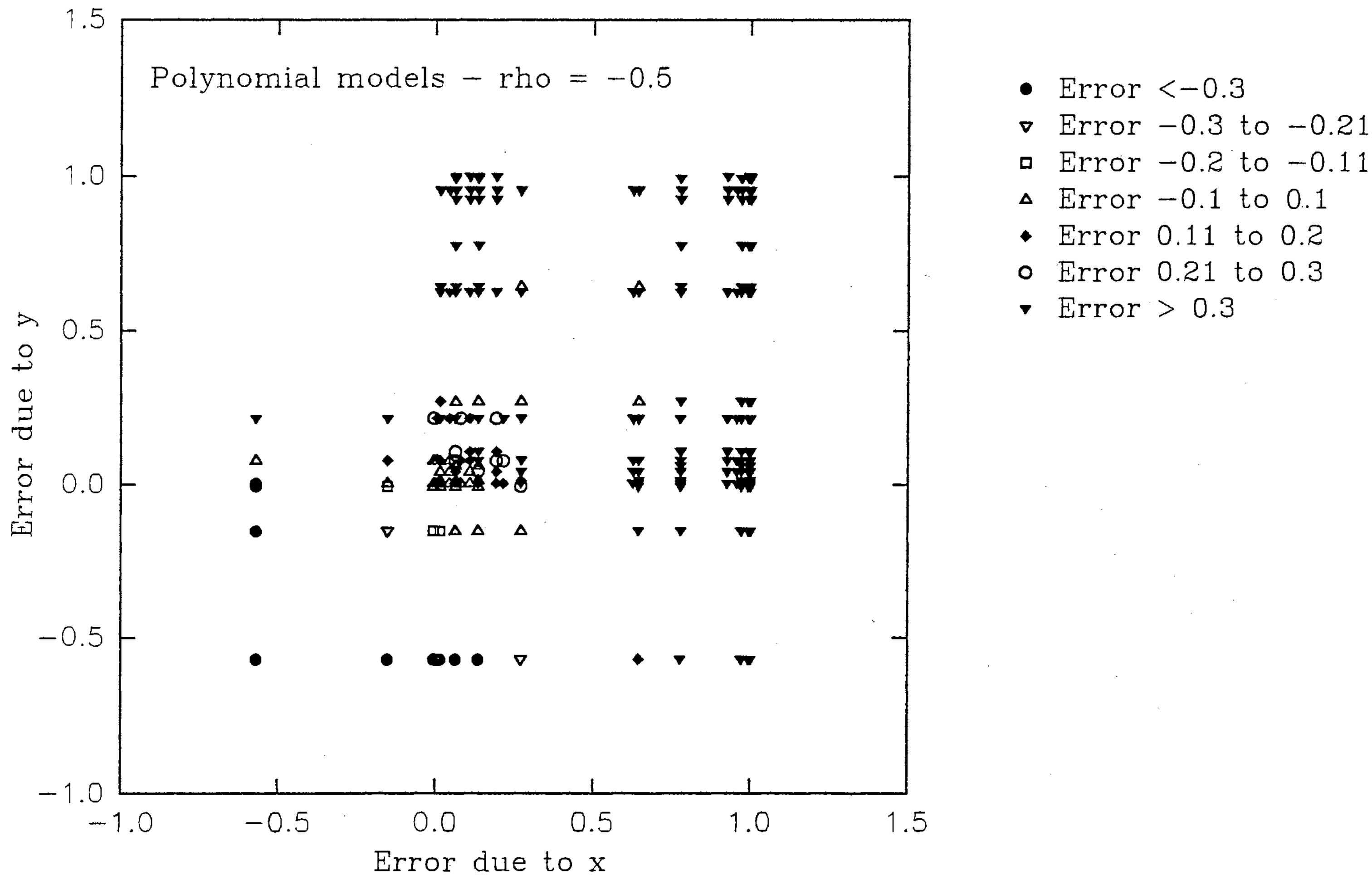

Figure 5–22. Error in FOA Variance vs Error Due to x and Error Due to y, Rho = –0.5

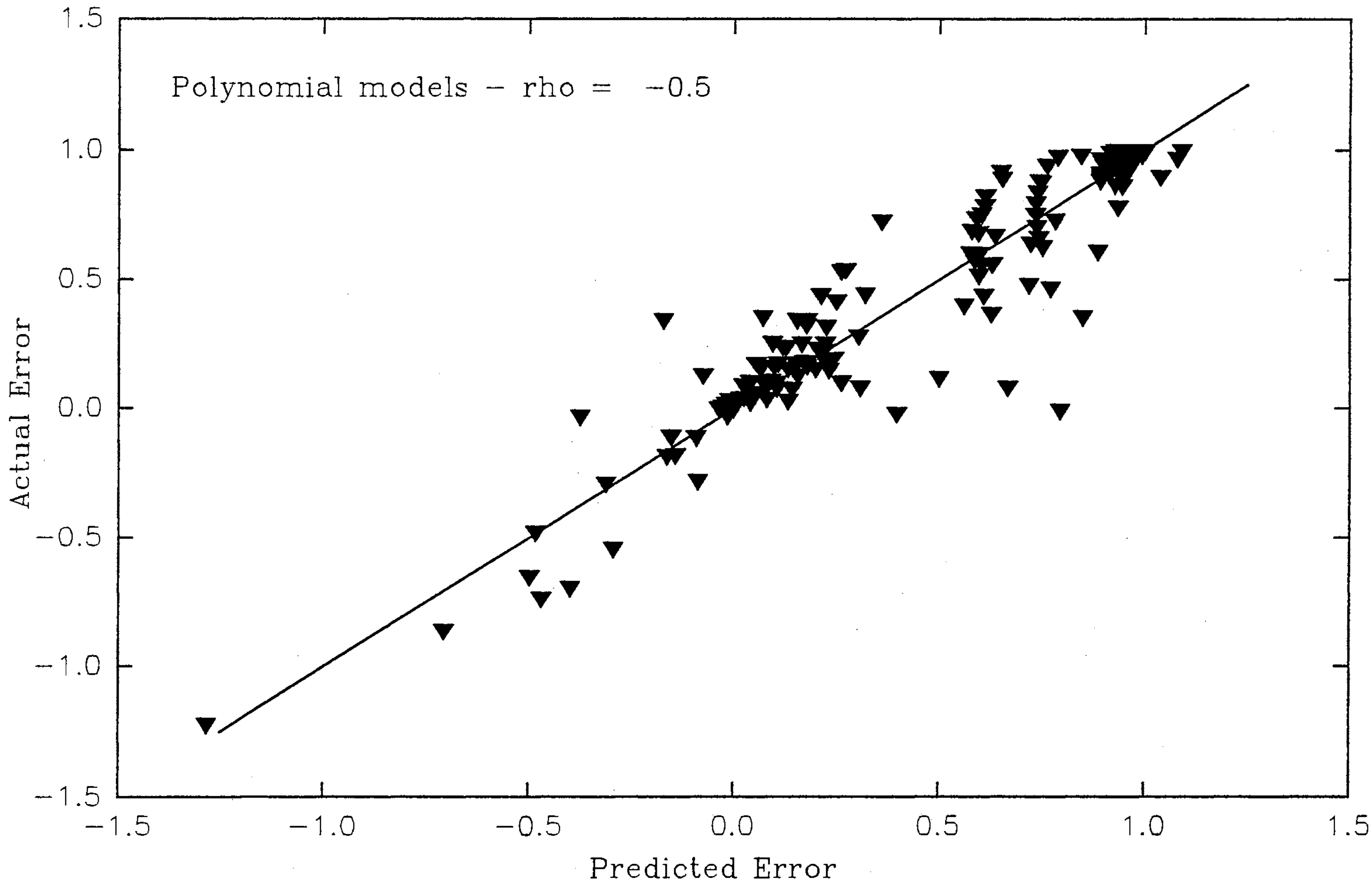

Figure 5–23. Actual vs Predicted Errors, Rho = –0.5

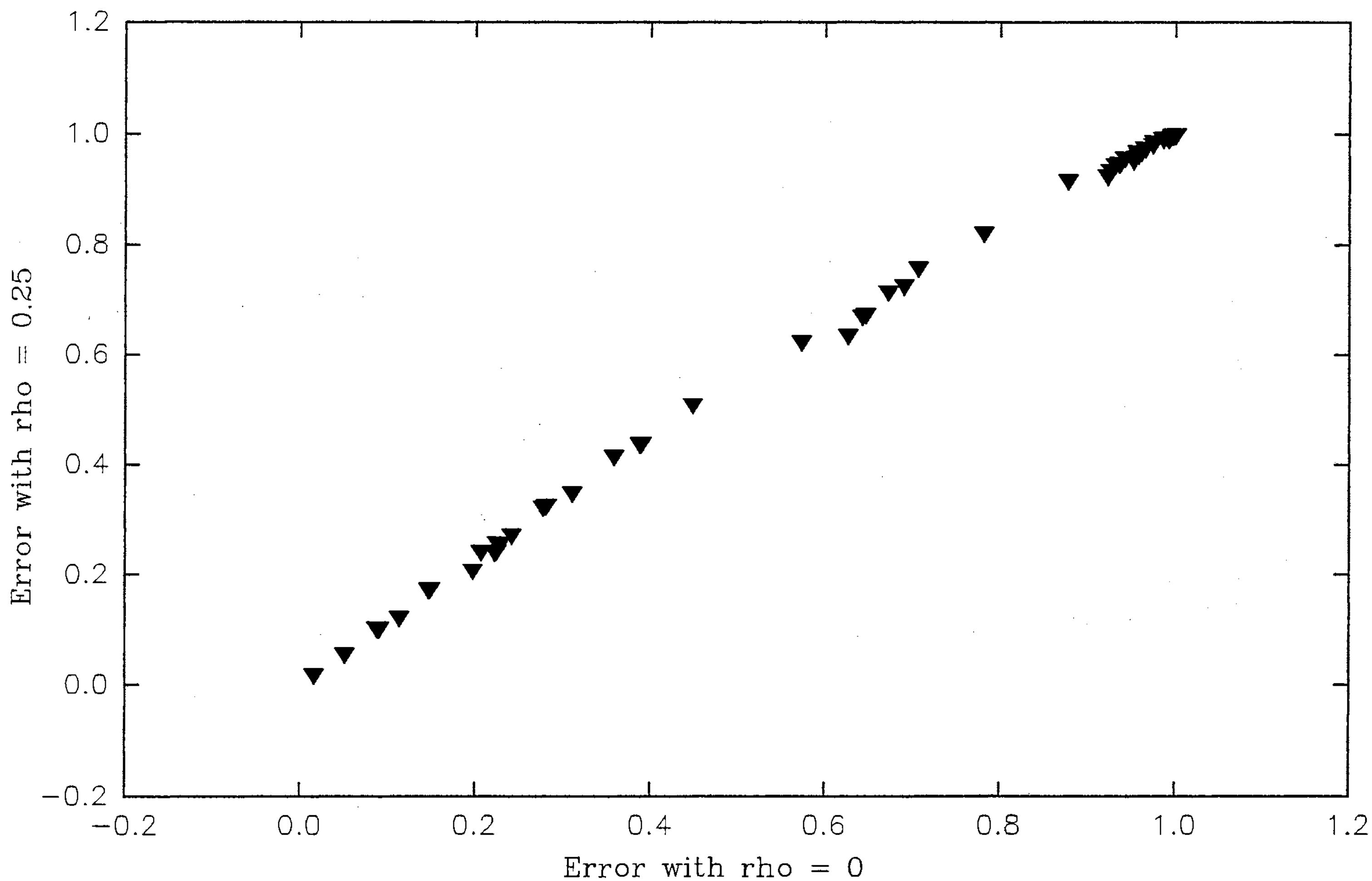

Figure 5−24. Error(.25) vs Error(0) for PDMs

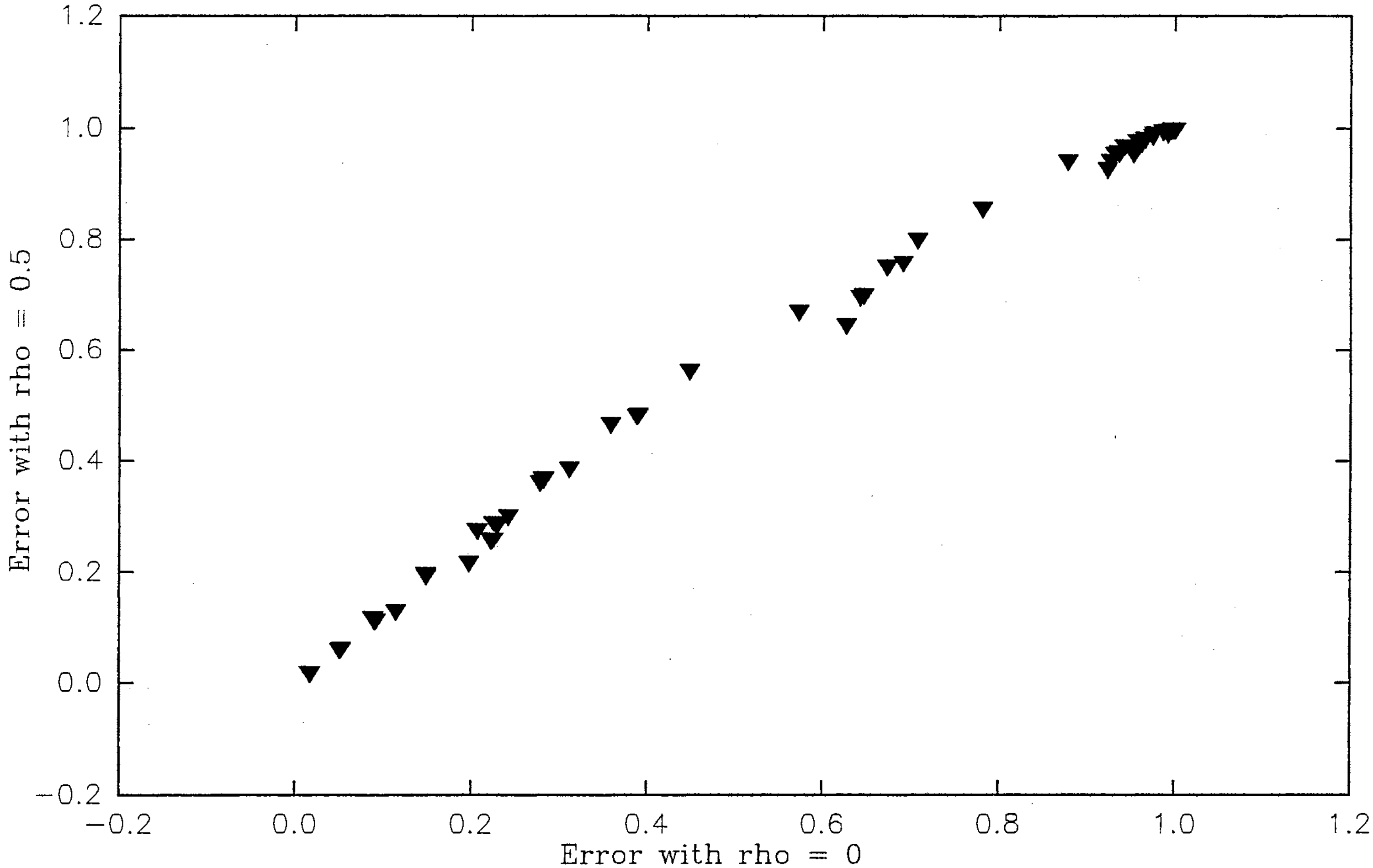

Figure 5−25. Error(.5) vs Error(0) for PDMs

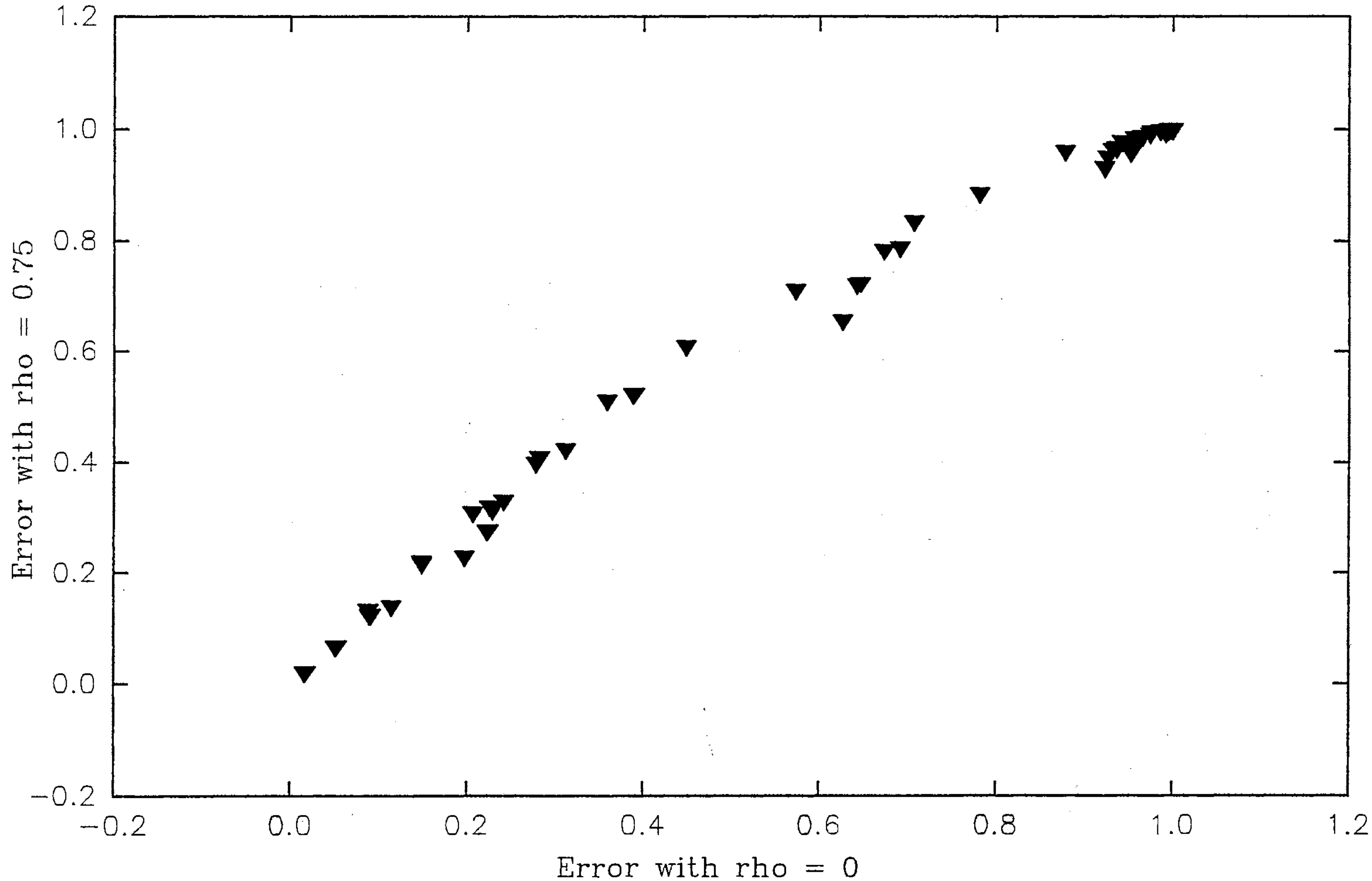

Figure 5-26. Error(.75) vs Error(0) for PDMs

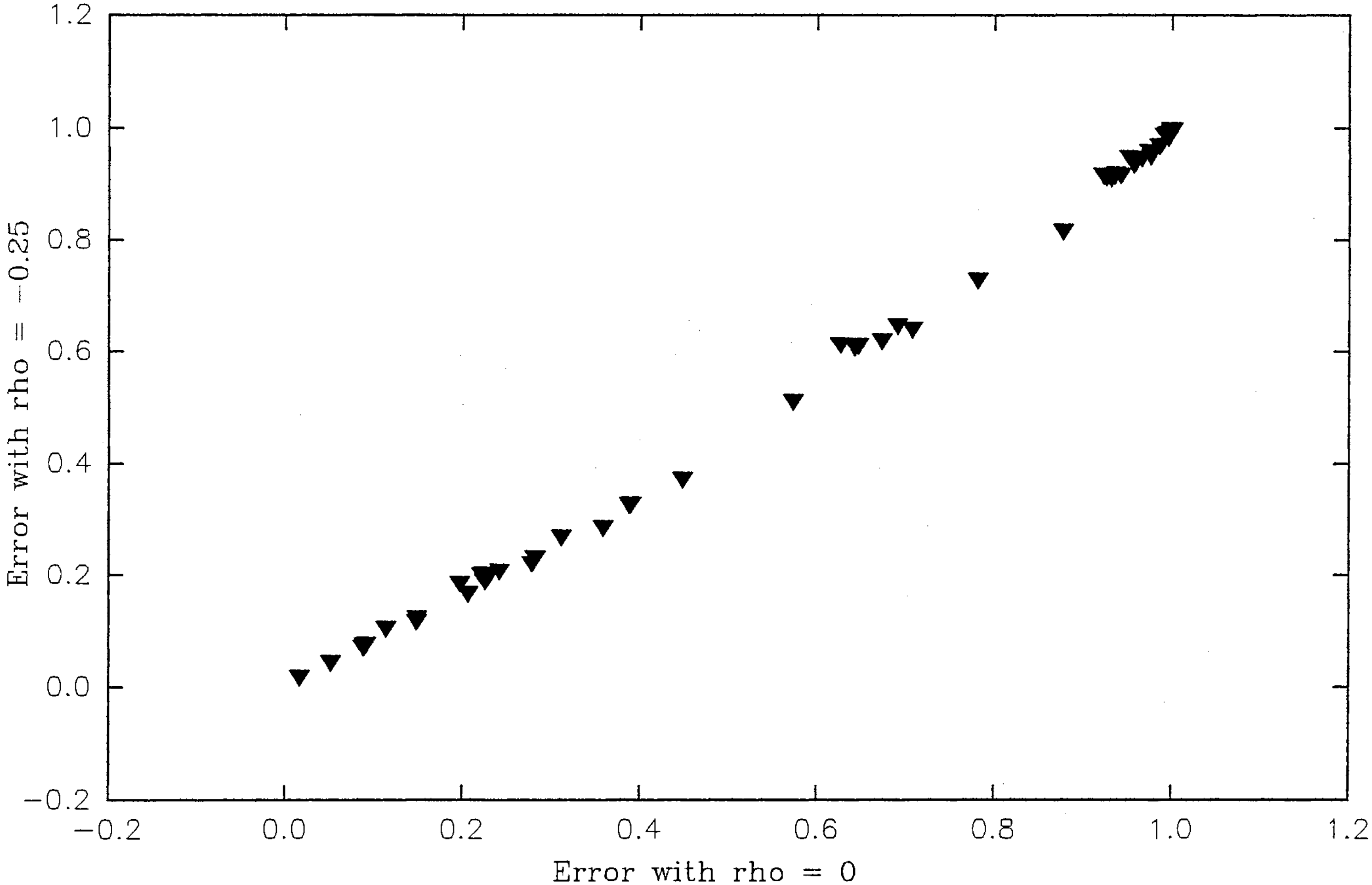

Figure 5-27. Error(−.25) vs Error(0) for PDMs

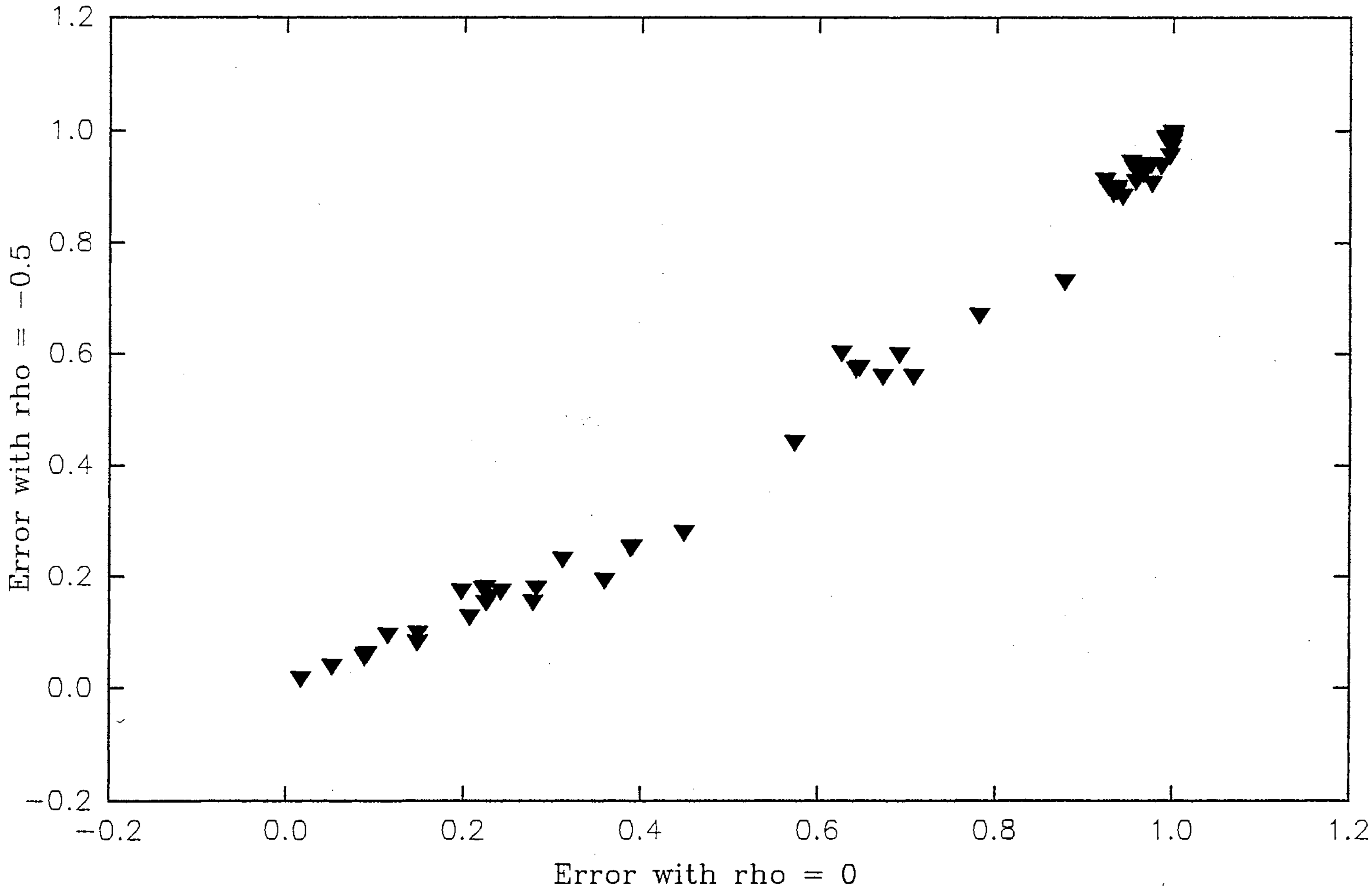

Figure 5−28. Error(−.5) vs Error(0) for PDMs

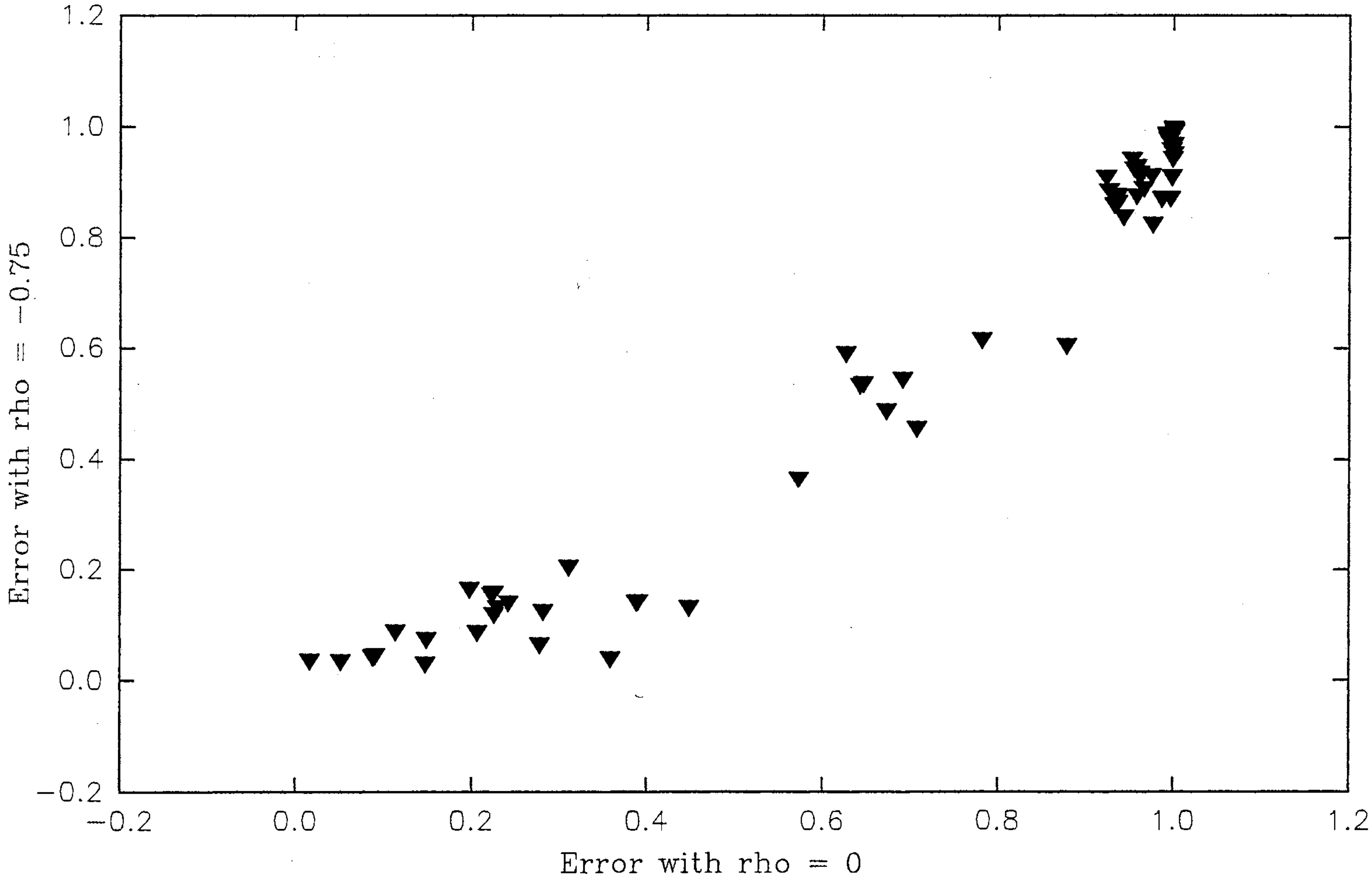

Figure 5−29. Error(−.75) vs Error(0) for PDMs

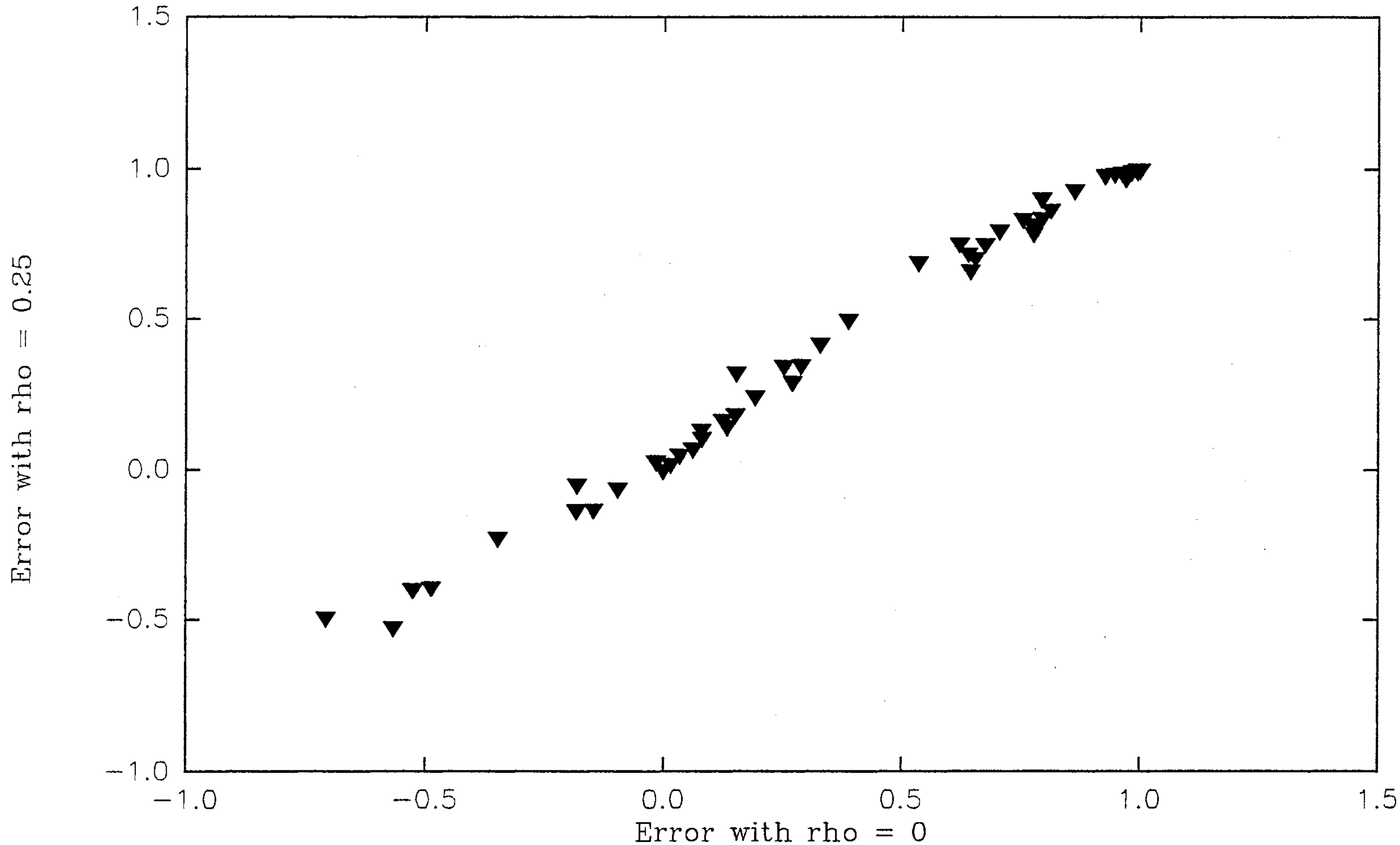

Figure 5−30. Error(.25) vs Error(0) for PIMs

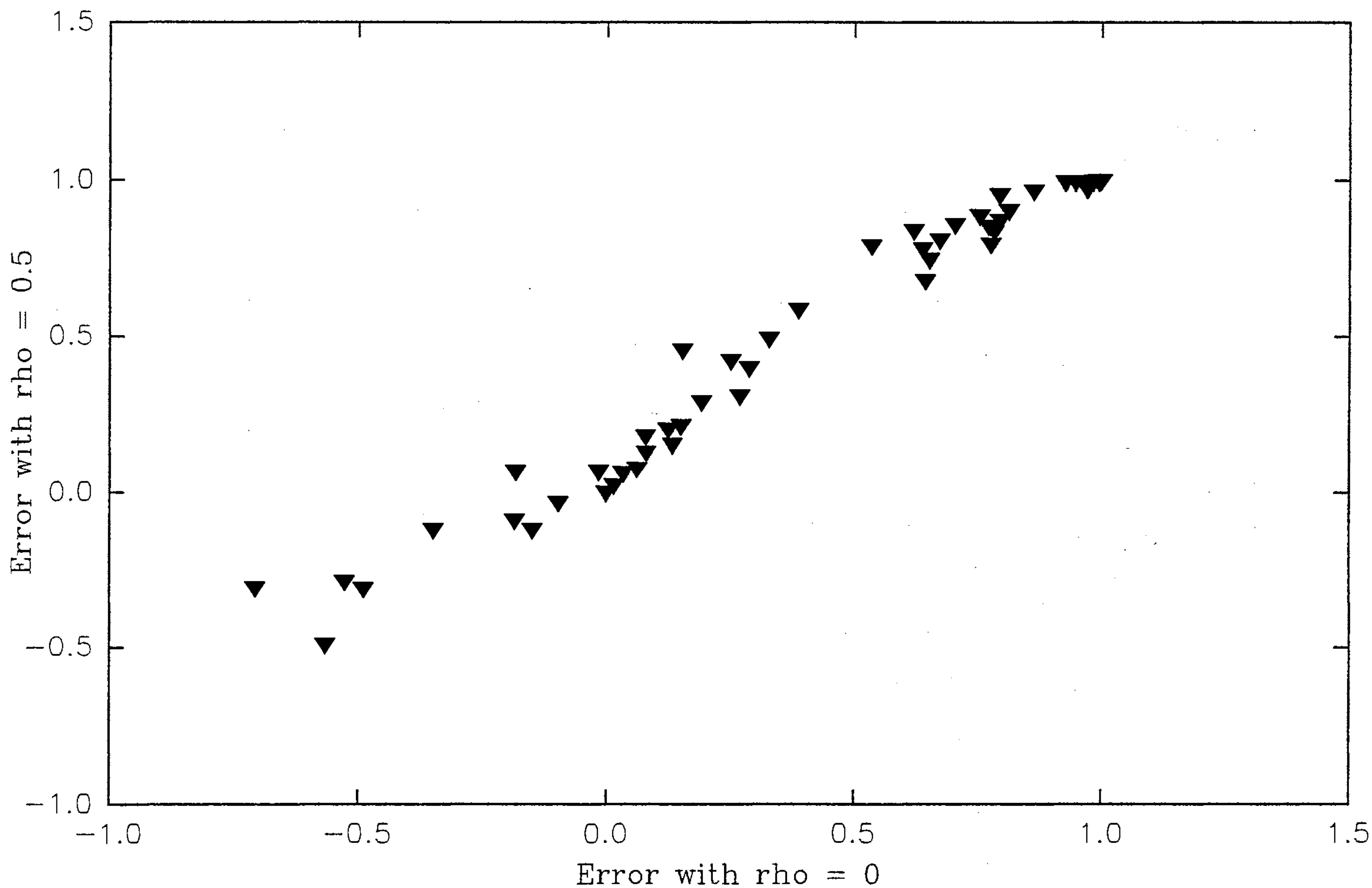

Figure 5−31. Error(.5) vs Error(0) for PIMs

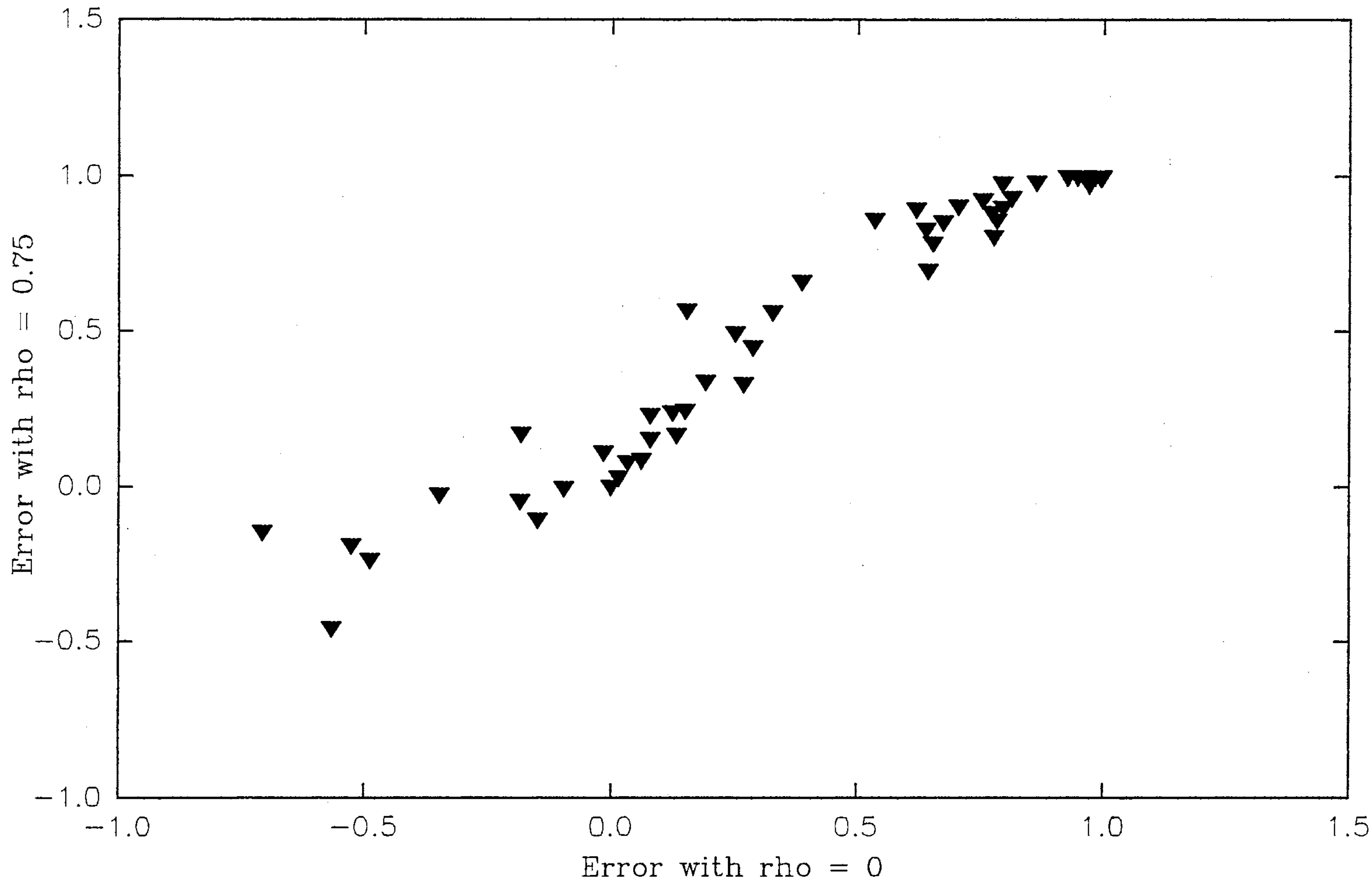

Figure 5−32. Error(.75) vs Error(0) for PIMs

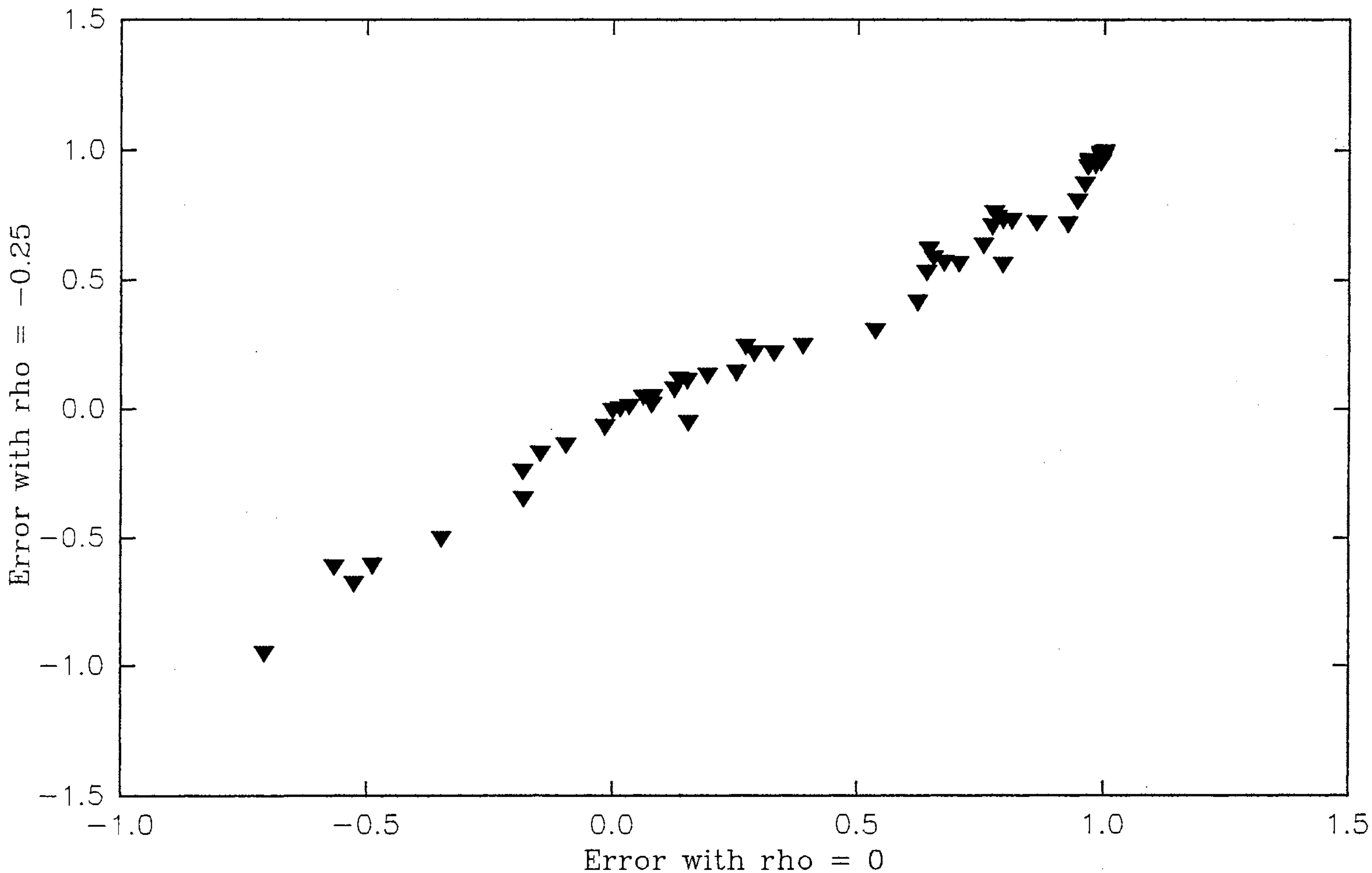

Figure 5−33. Error(−.25) vs Error(0) for PIMs

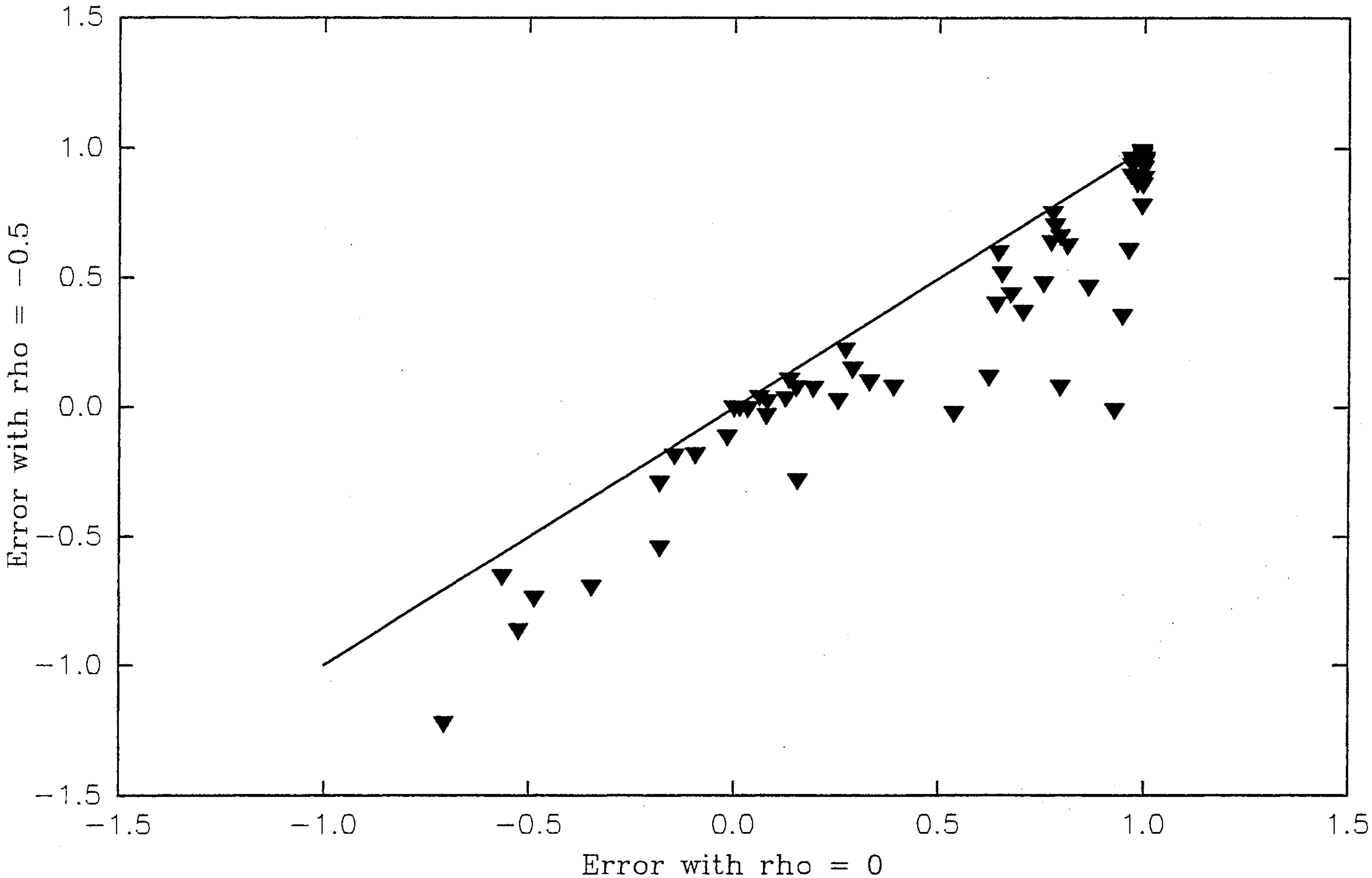

Figure 5−34. Error(−.5) vs Error(0) for PIMs

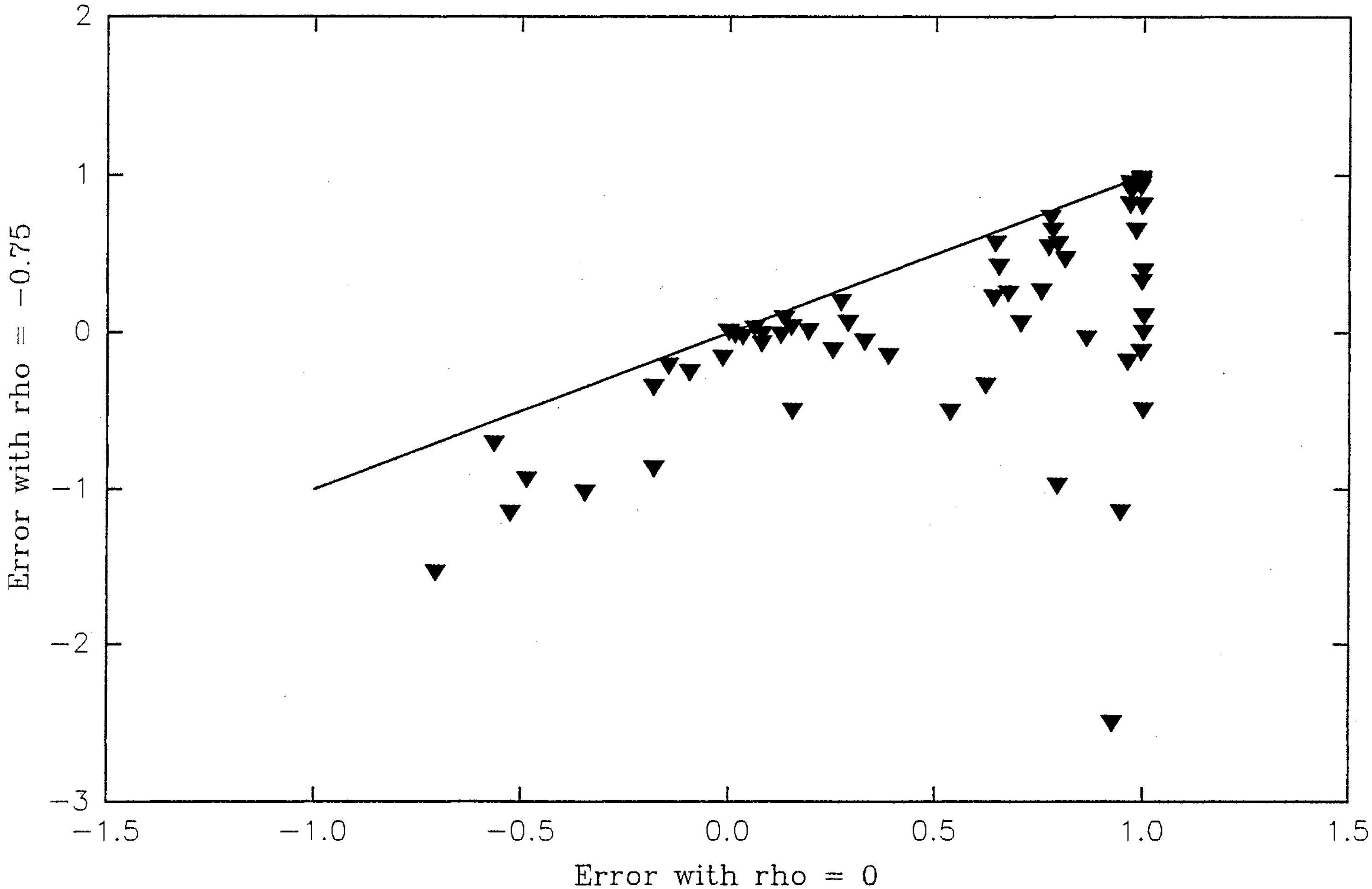

Figure 5−35. Error(−.75) vs Error(0) for PIMs

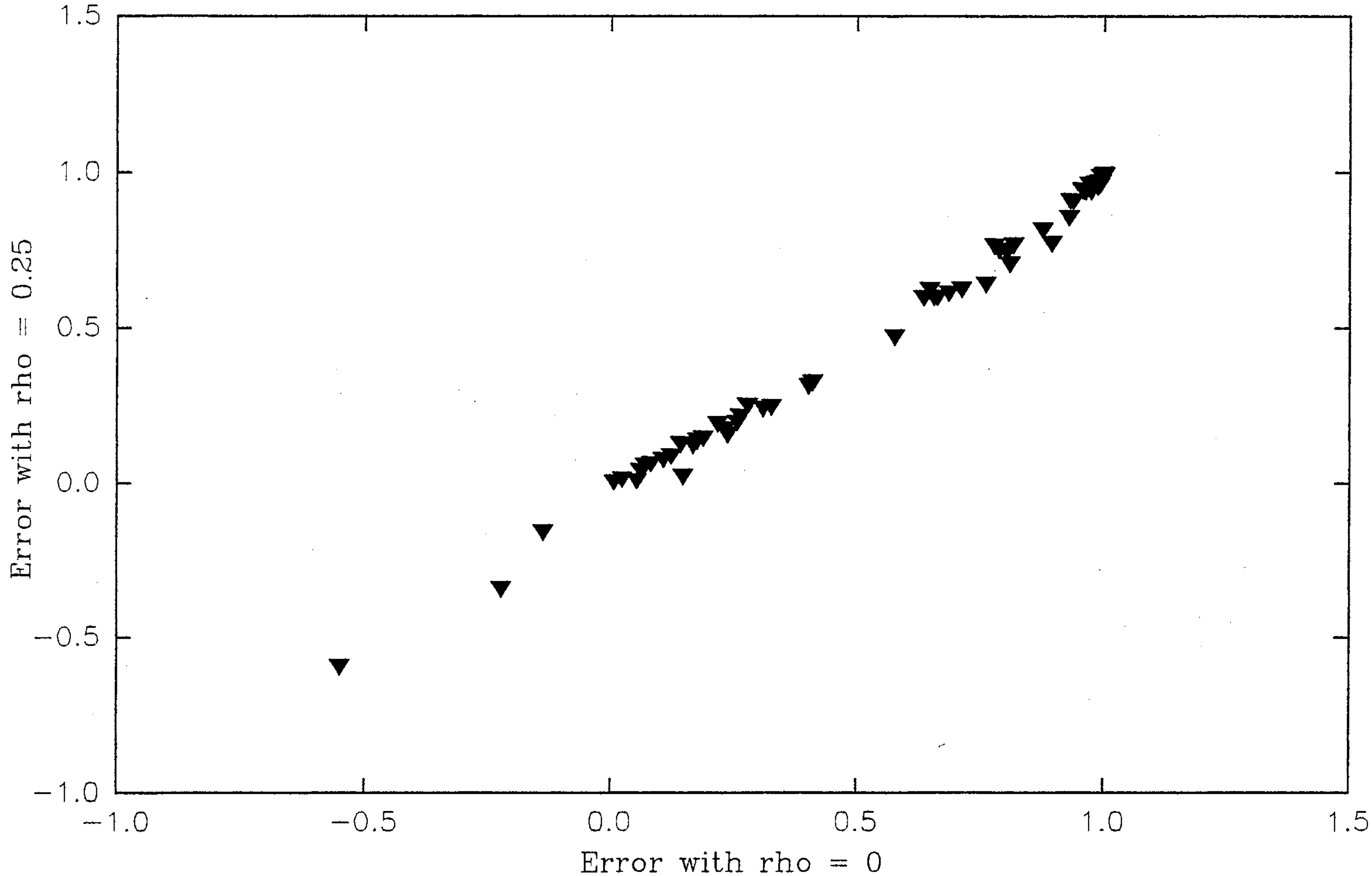

Figure 5–36. Error(.25) vs Error(0) for PMMs

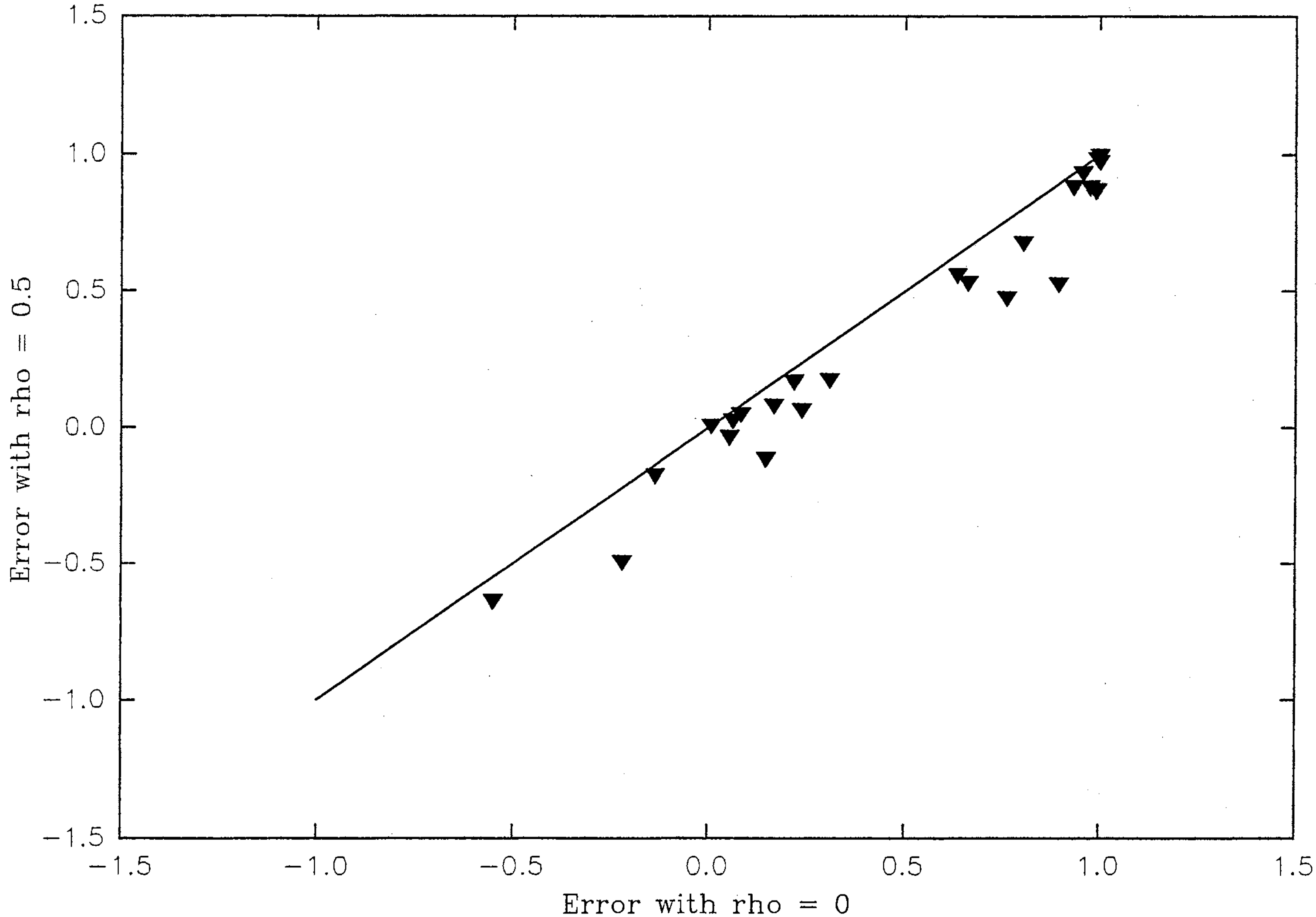

Figure 5−37. Error(.5) vs Error(0) for PMMs

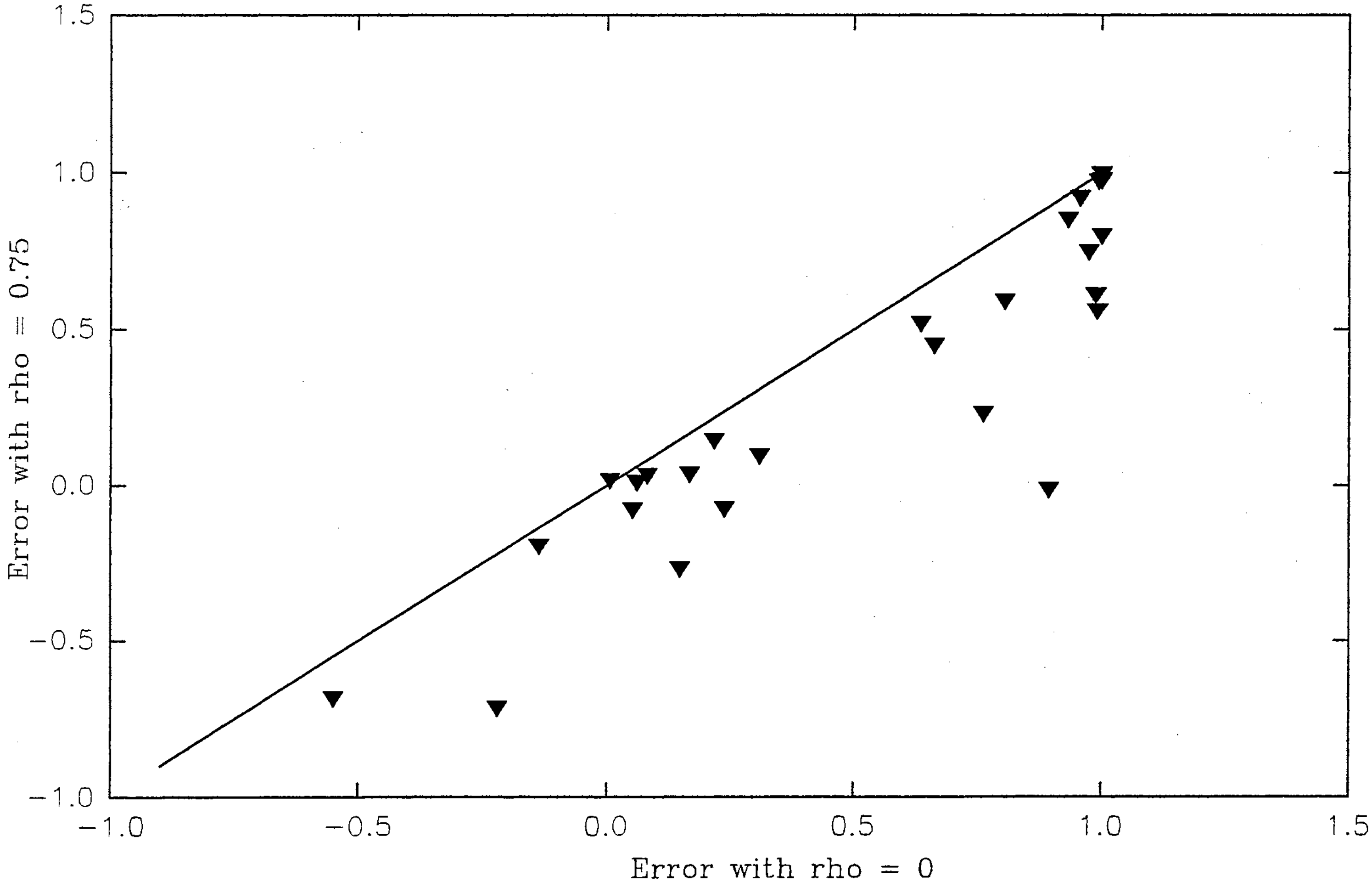

Figure 5-38. Error(.75) vs Error(0) for PMMs

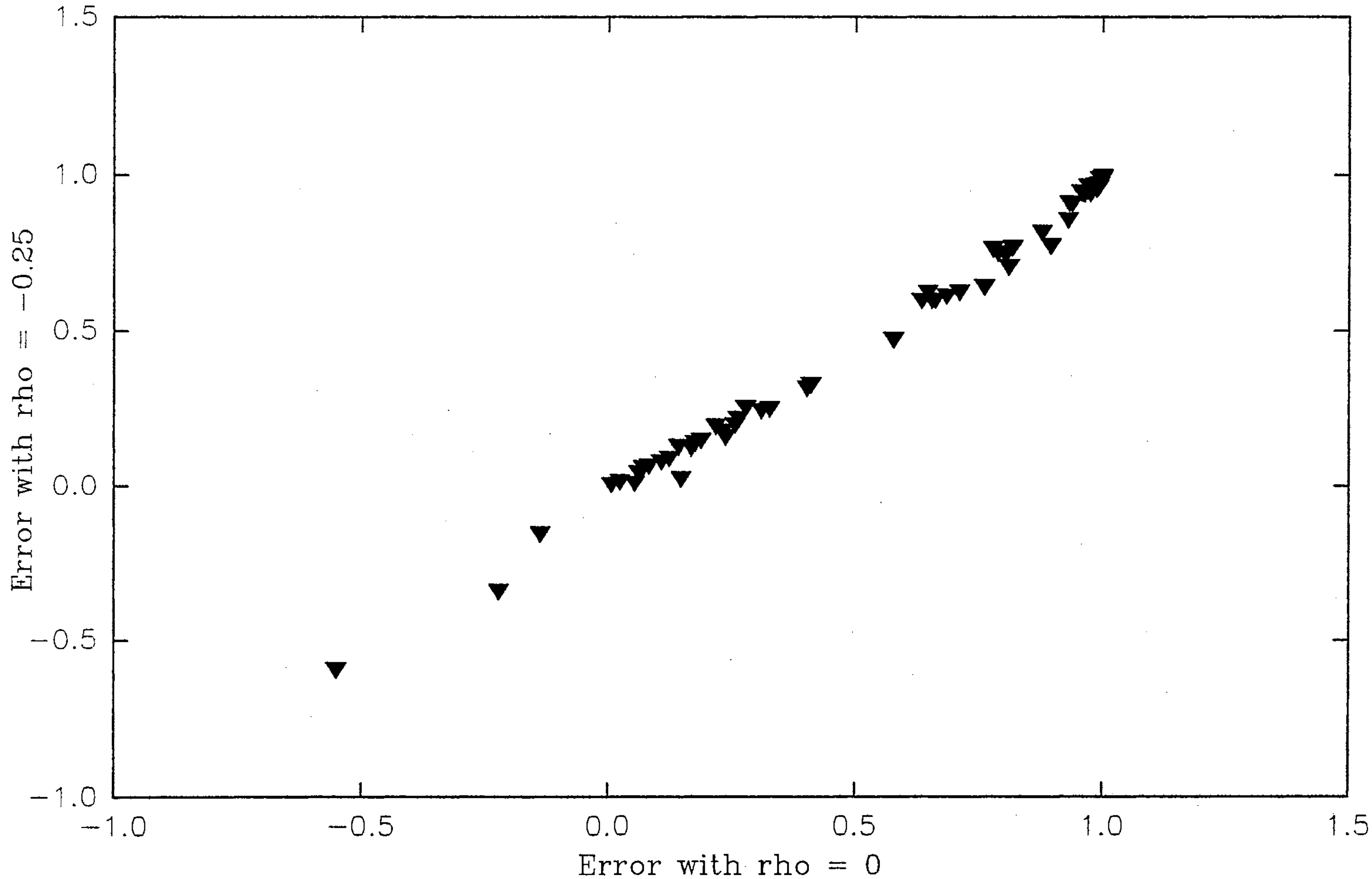

Figure 5-39. Error(-.25) vs Error(0) for PMMs

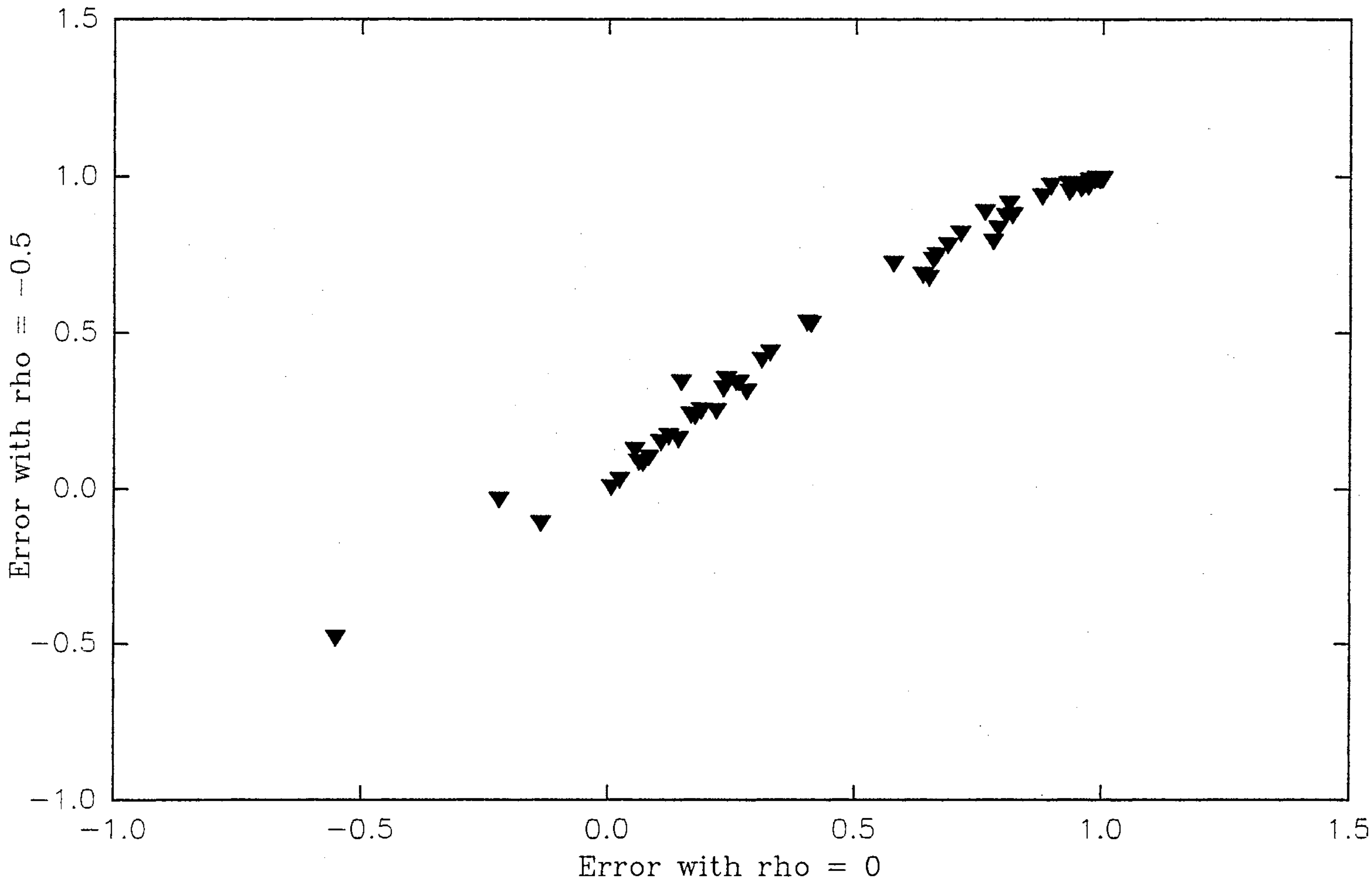

Figure 5−40. Error(−.5) vs Error(0) for PMMs

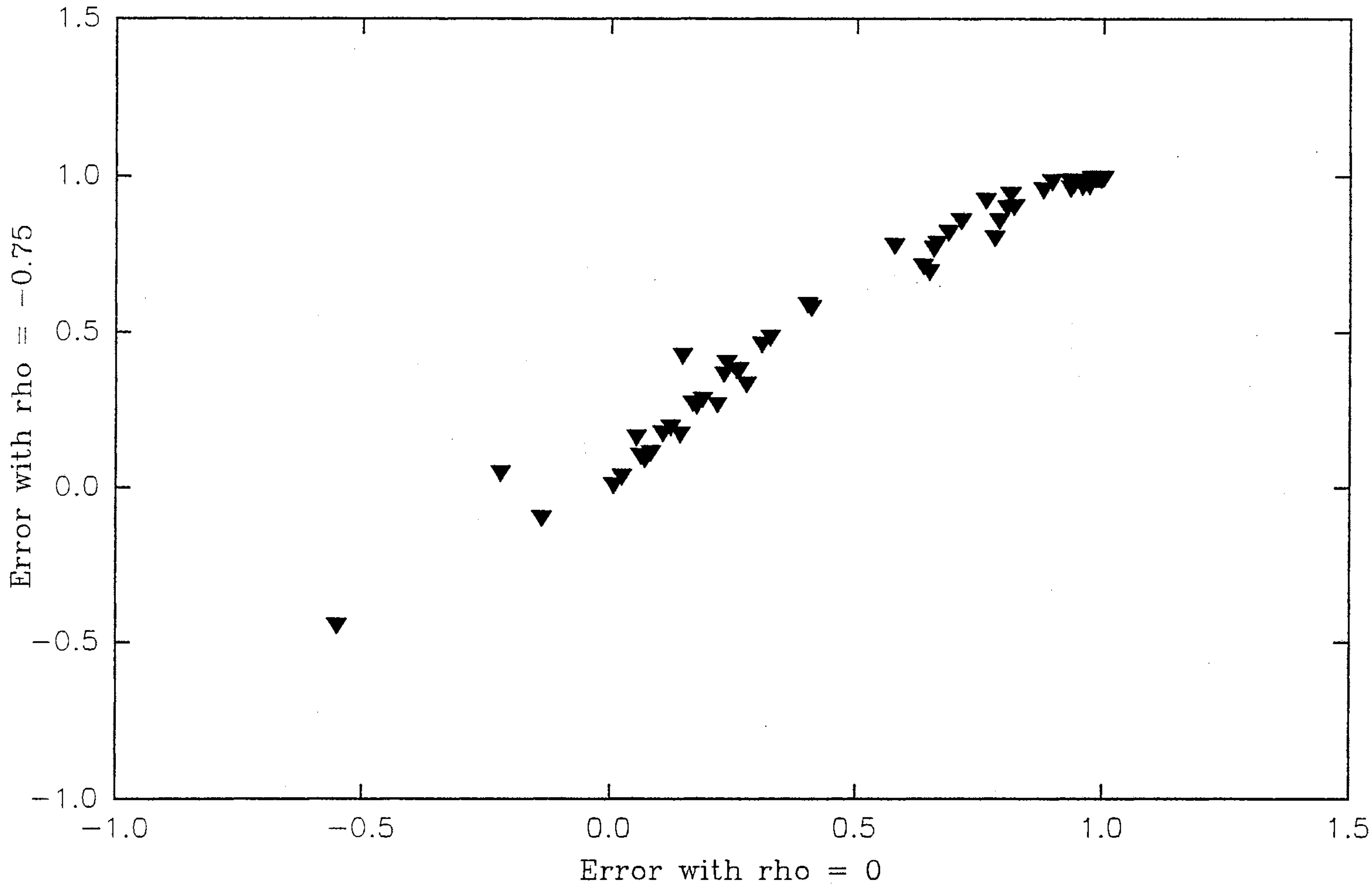

Figure 5-41. Error(-.75) vs Error(0) for PMMs

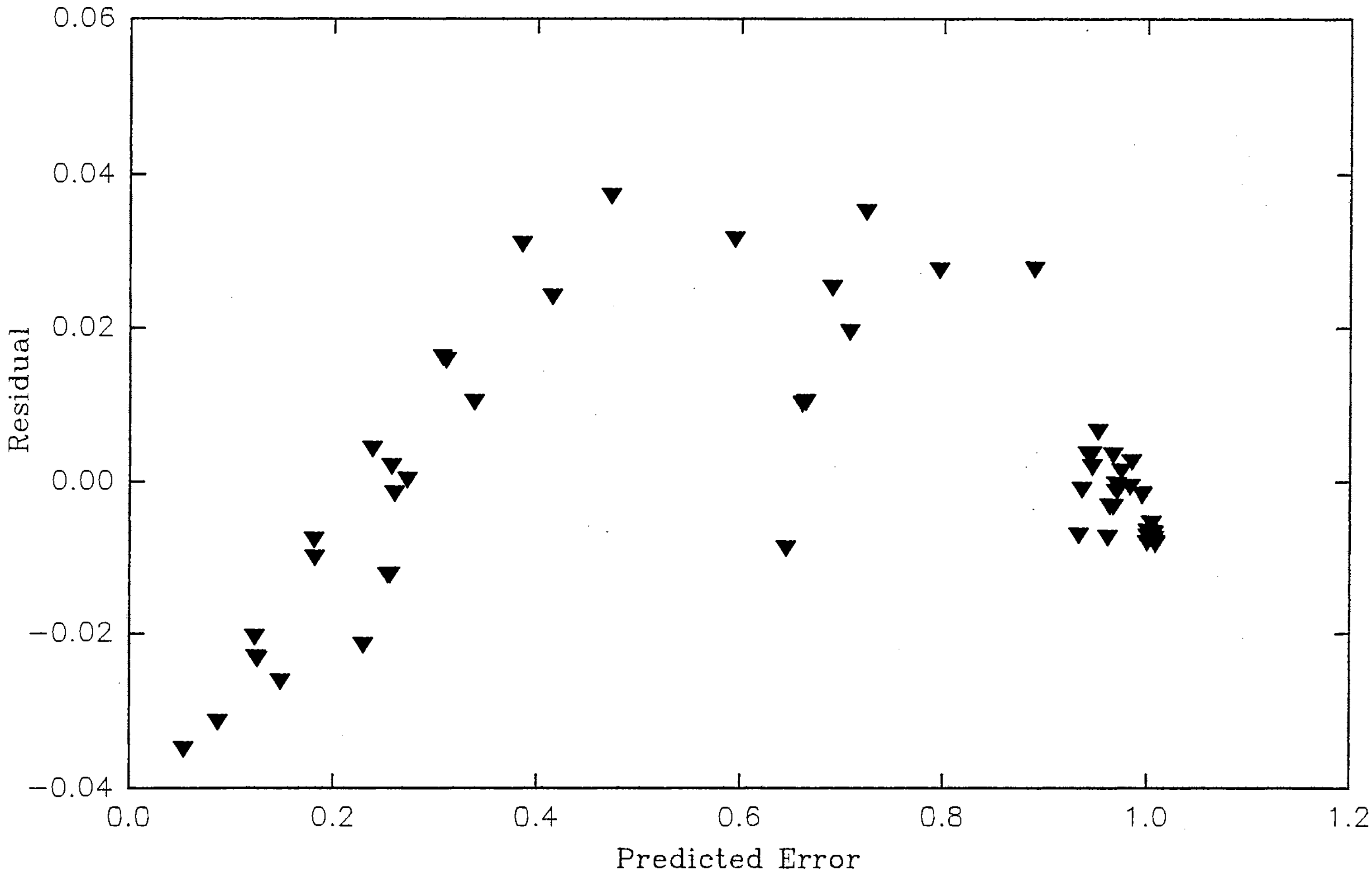

Figure 5−42. Residuals from Linear Model to Predict Error(.25) for PDMs

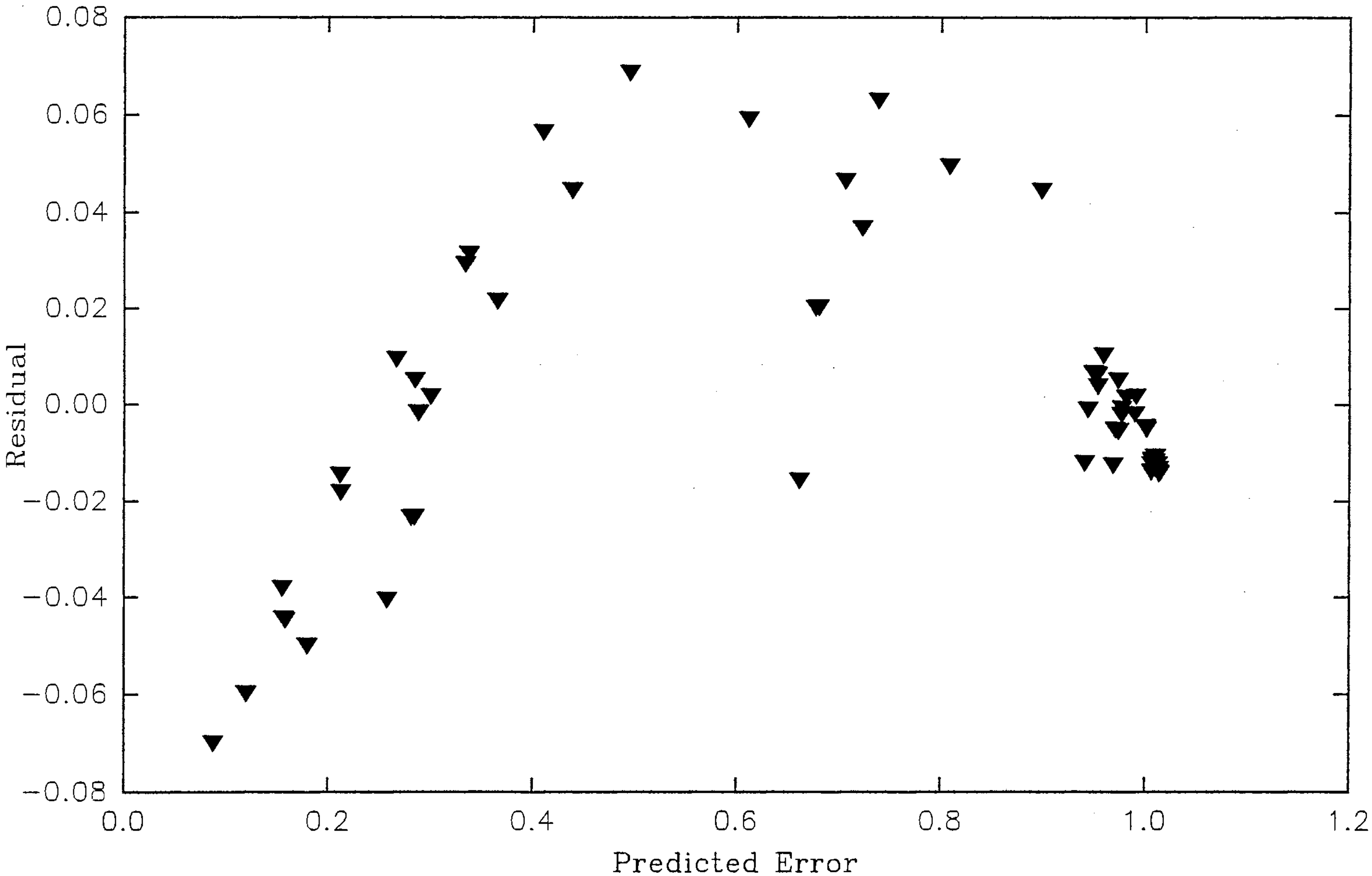

Figure 5−43. Residuals from Linear Model to Predict Error(.5) for PDMs

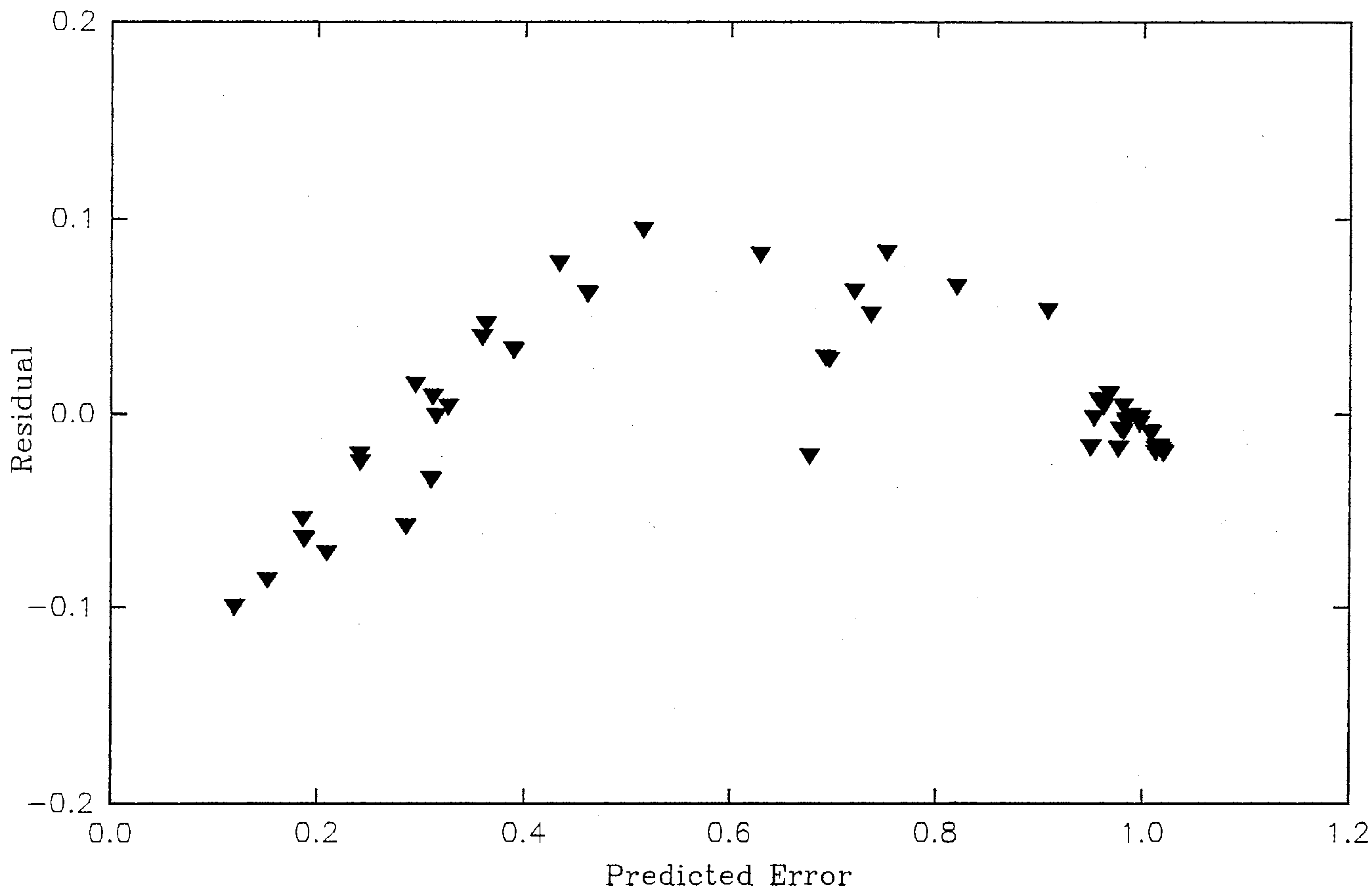

Figure 5−44. Residuals from Linear Model to Predict Error(.75) for PDMs

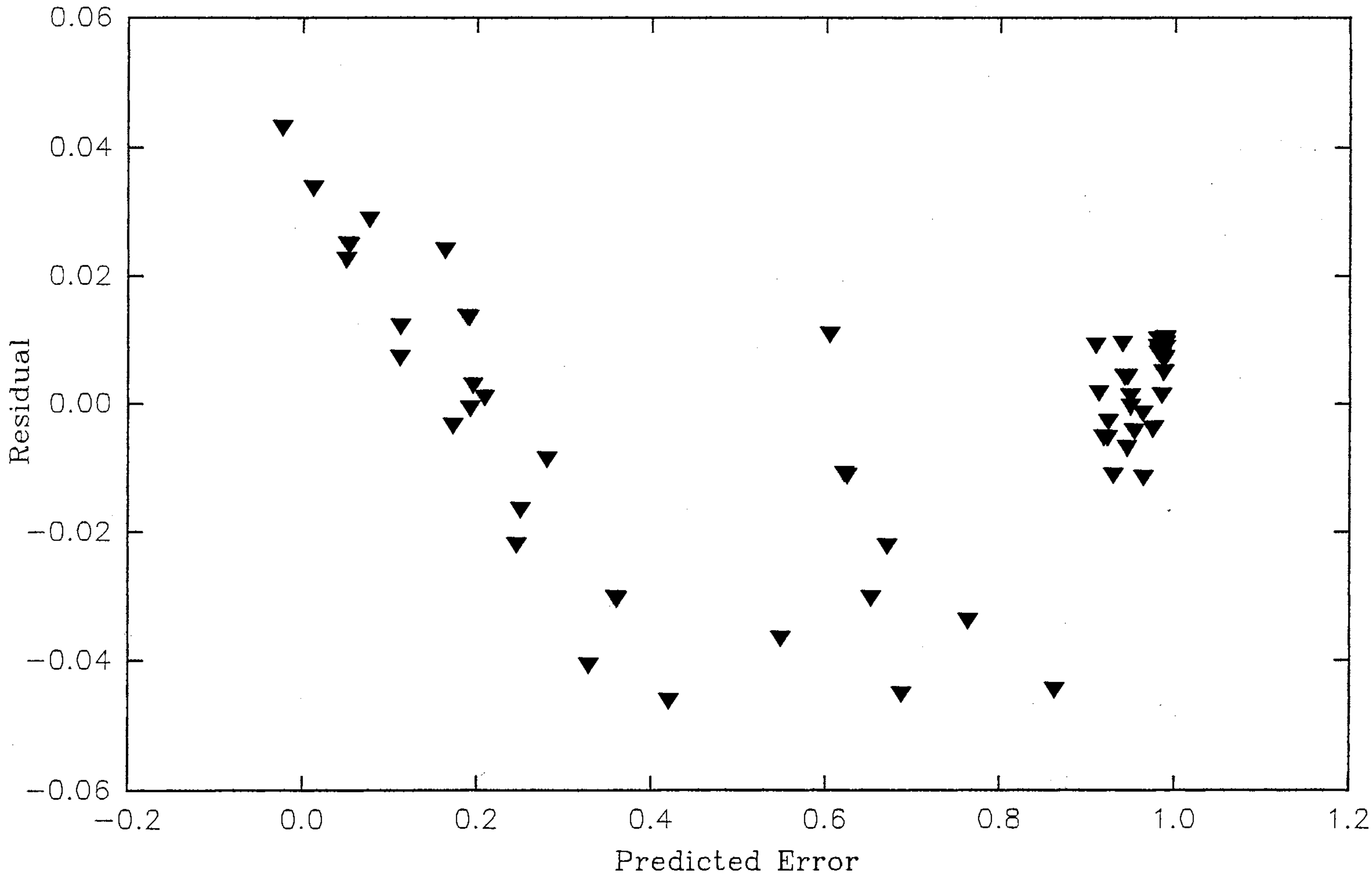

Figure 5−45. Residuals from Linear Model to Predict Error(−.25) for PDMs

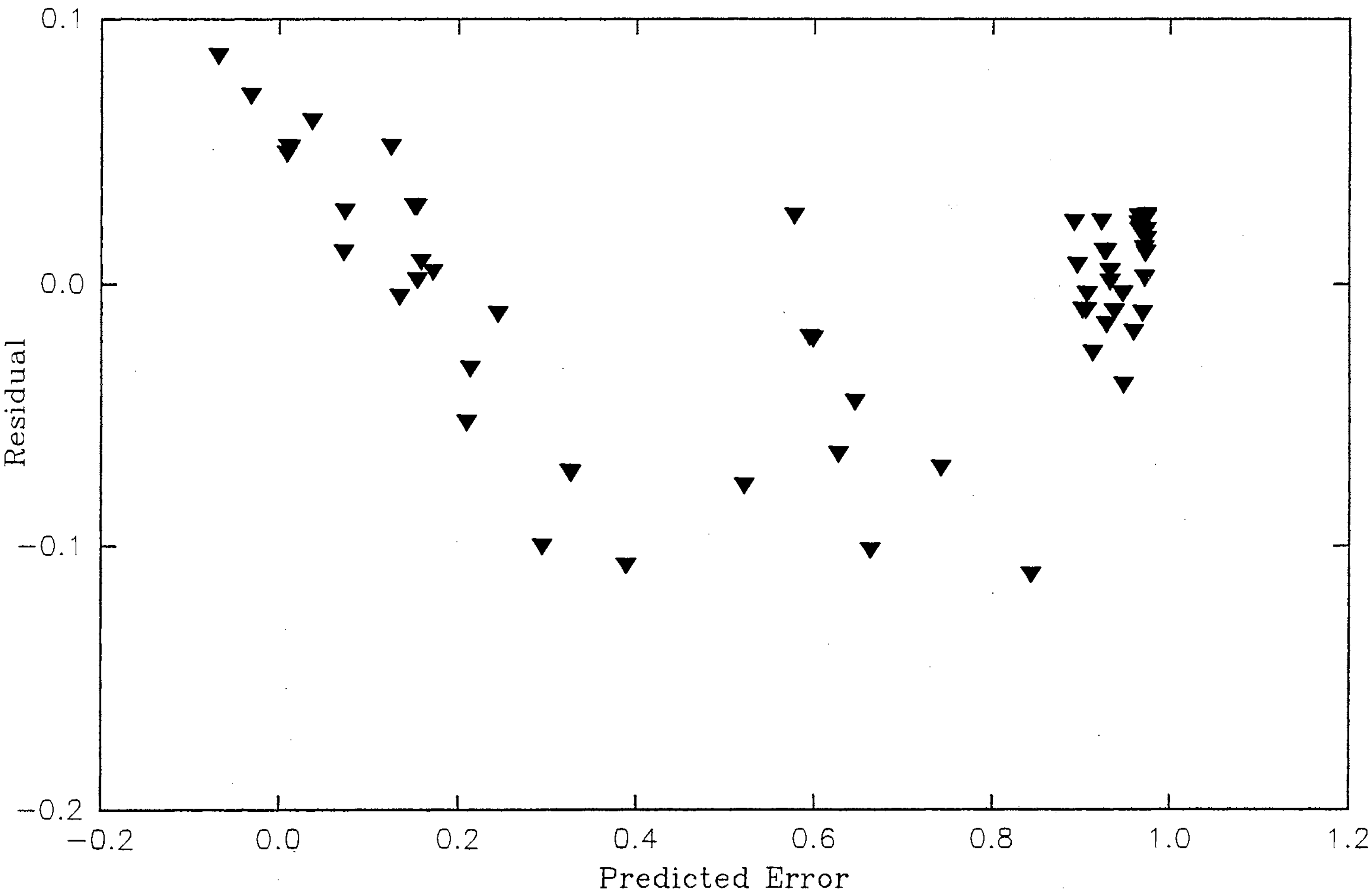

Figure 5−46. Residuals from Linear Model to Predict Error(−.5) for PDMs

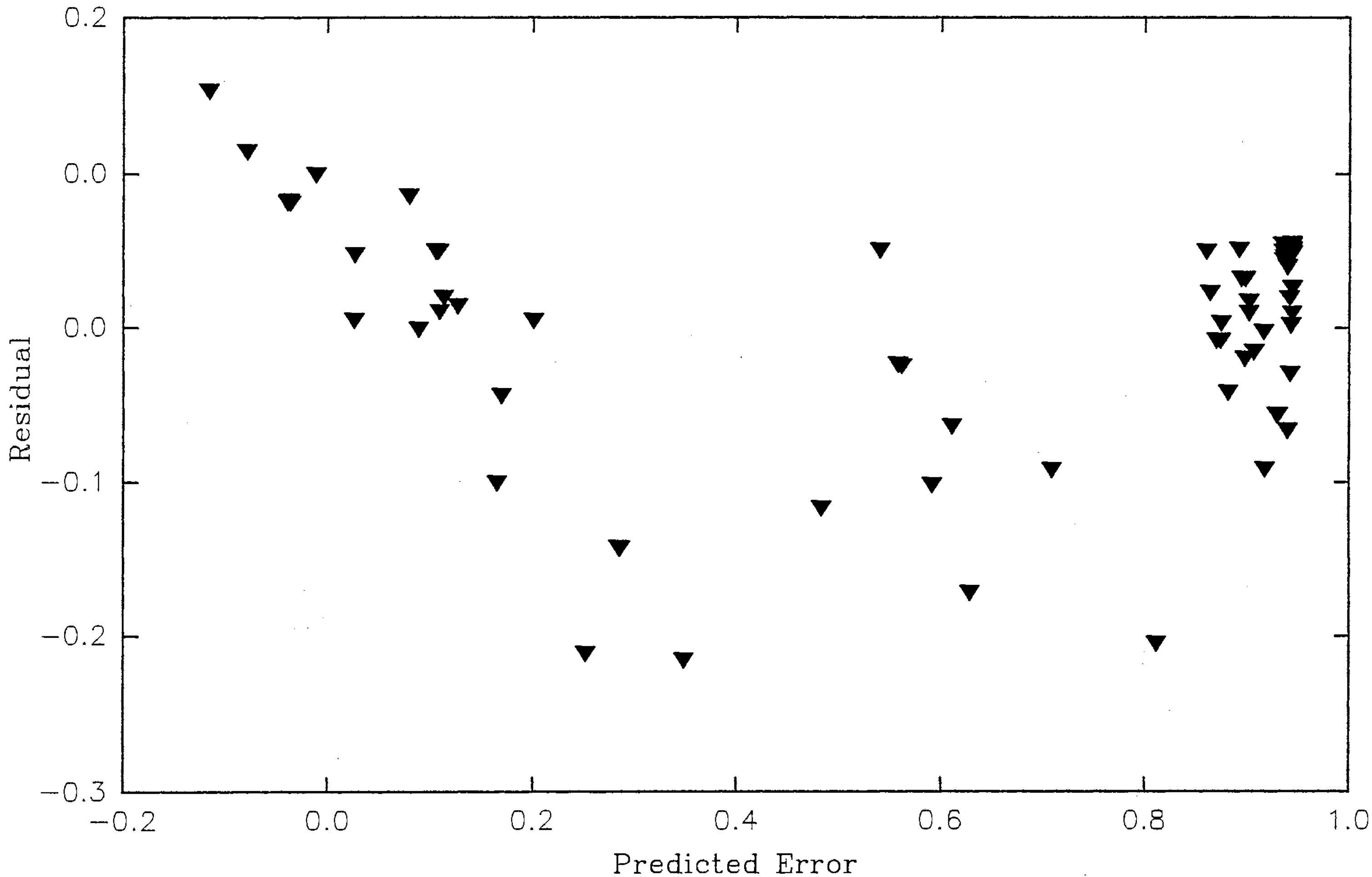

Figure 5−47. Residuals from Linear Model to Predict Error(−.75) for PDMs

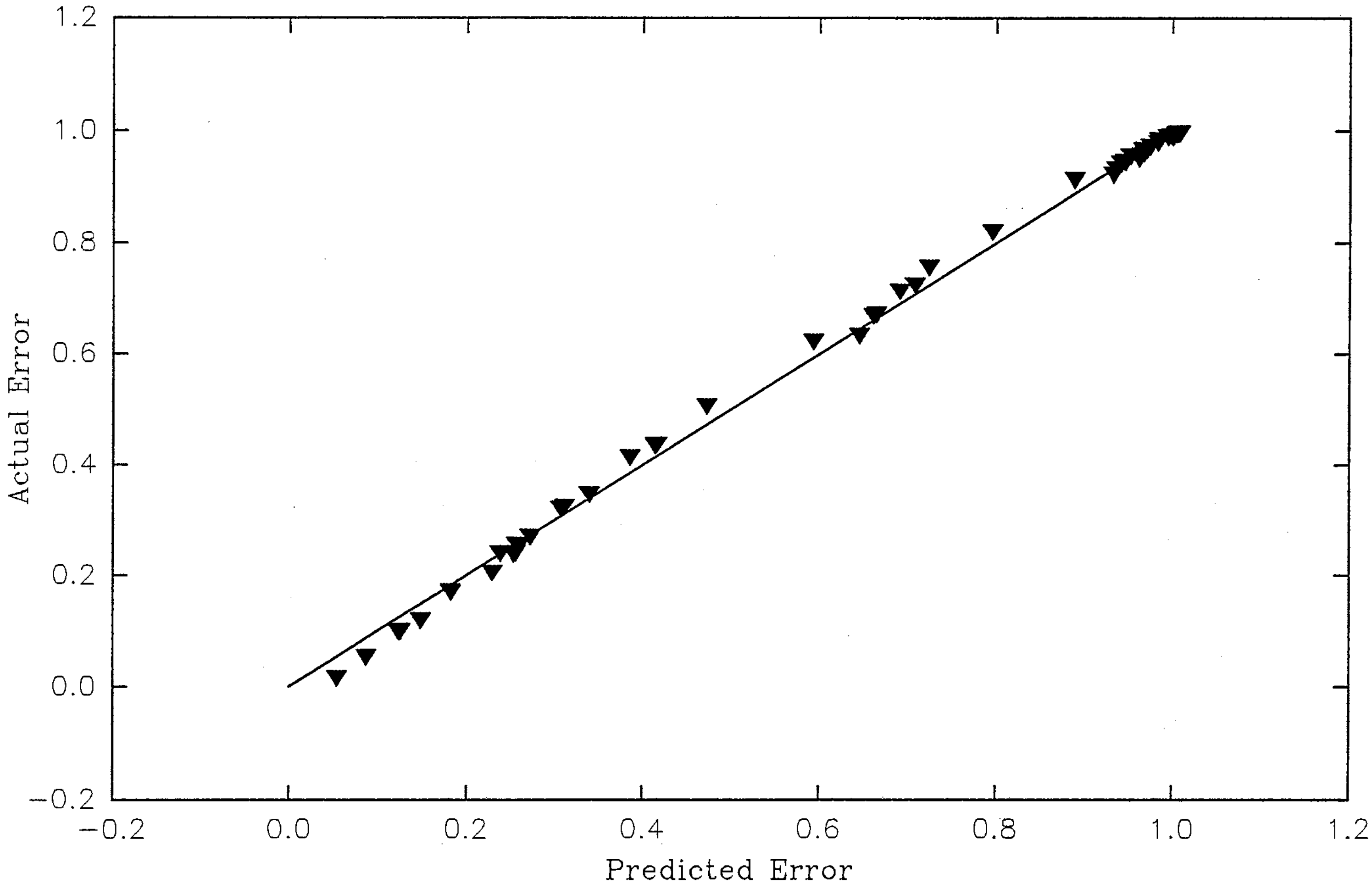

Figure 5−48. Actual vs Predicted Error − Linear Model to Predict Error(.25) − PDMs

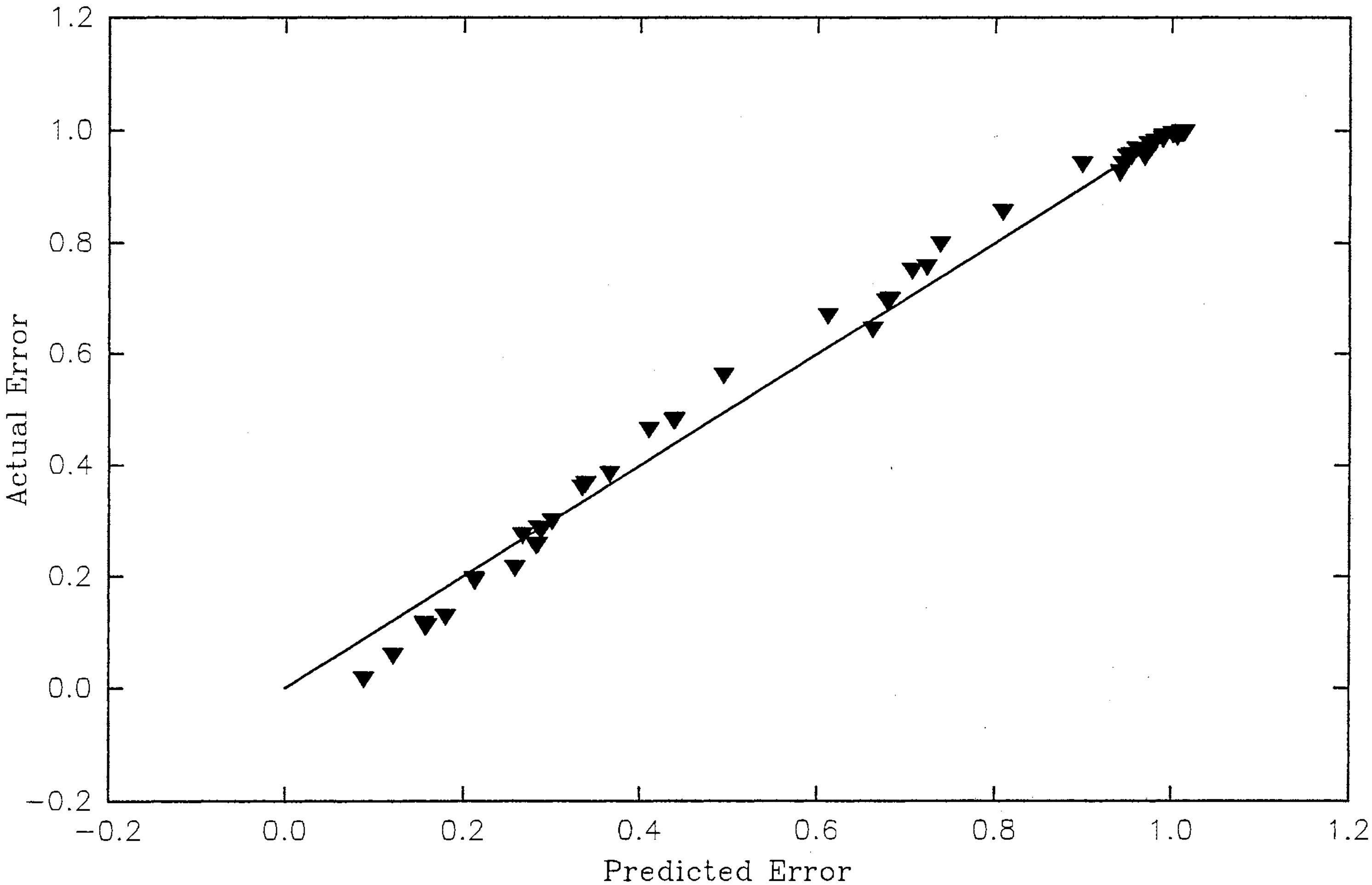

Figure 5−49. Actual vs Predicted Error − Linear Model to Predict Error(.5) − PDMs

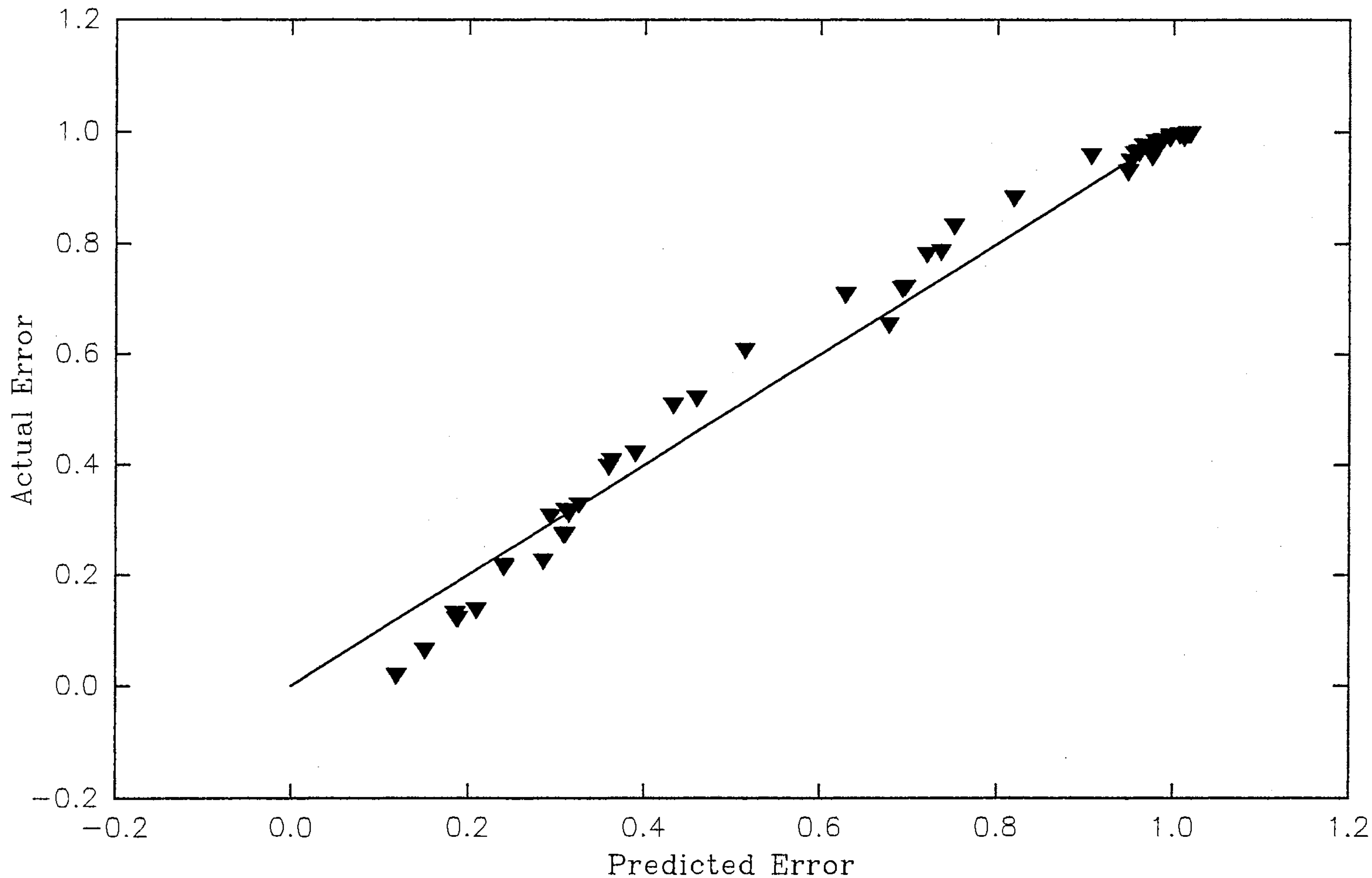

Figure 5−50. Actual vs Predicted Error − Linear Model to Predict Error(.75) − PDMs

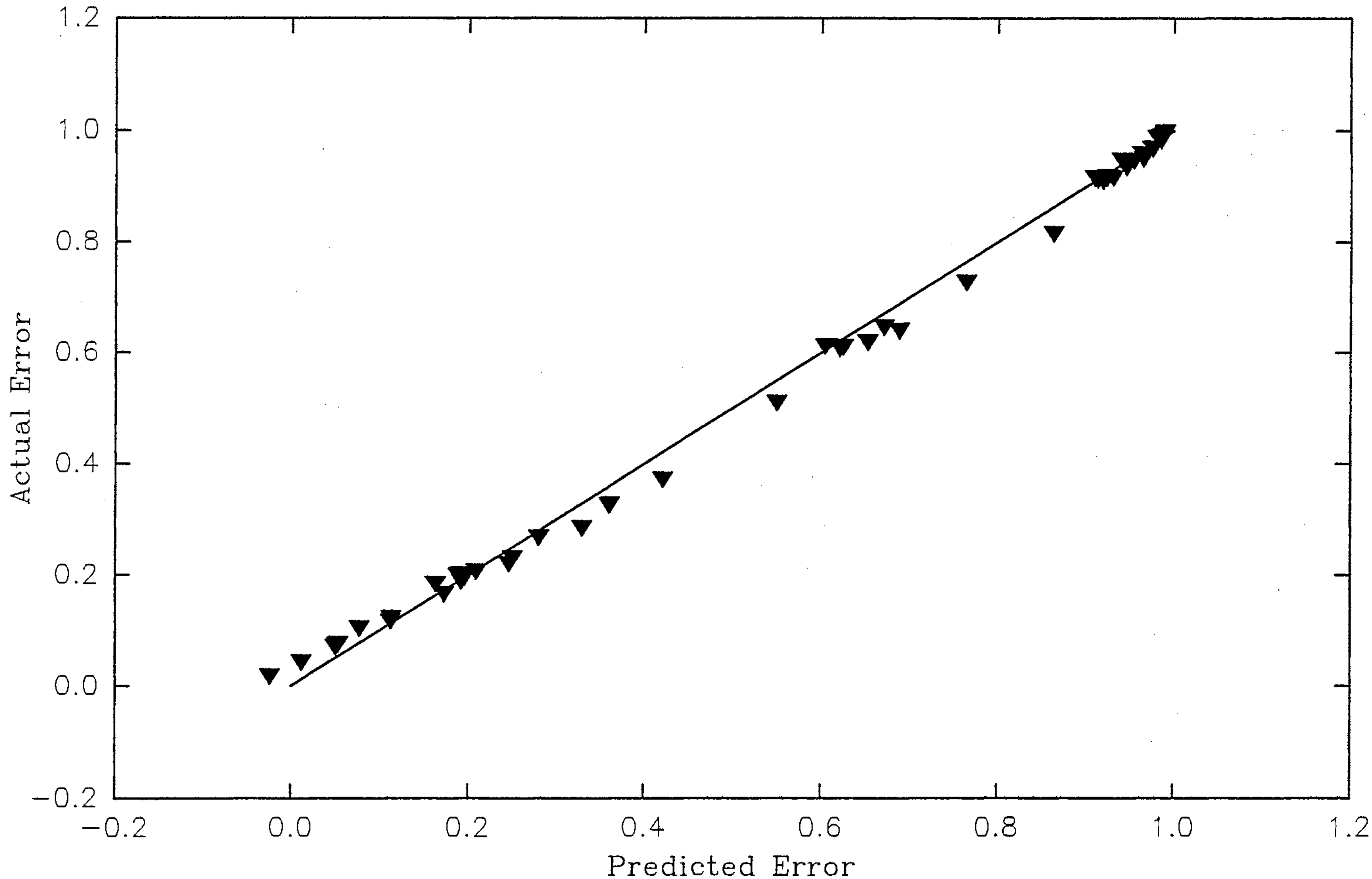

Figure 5−51. Actual vs Predicted Error − Linear Model to Predict Error(−.25) − PDMs

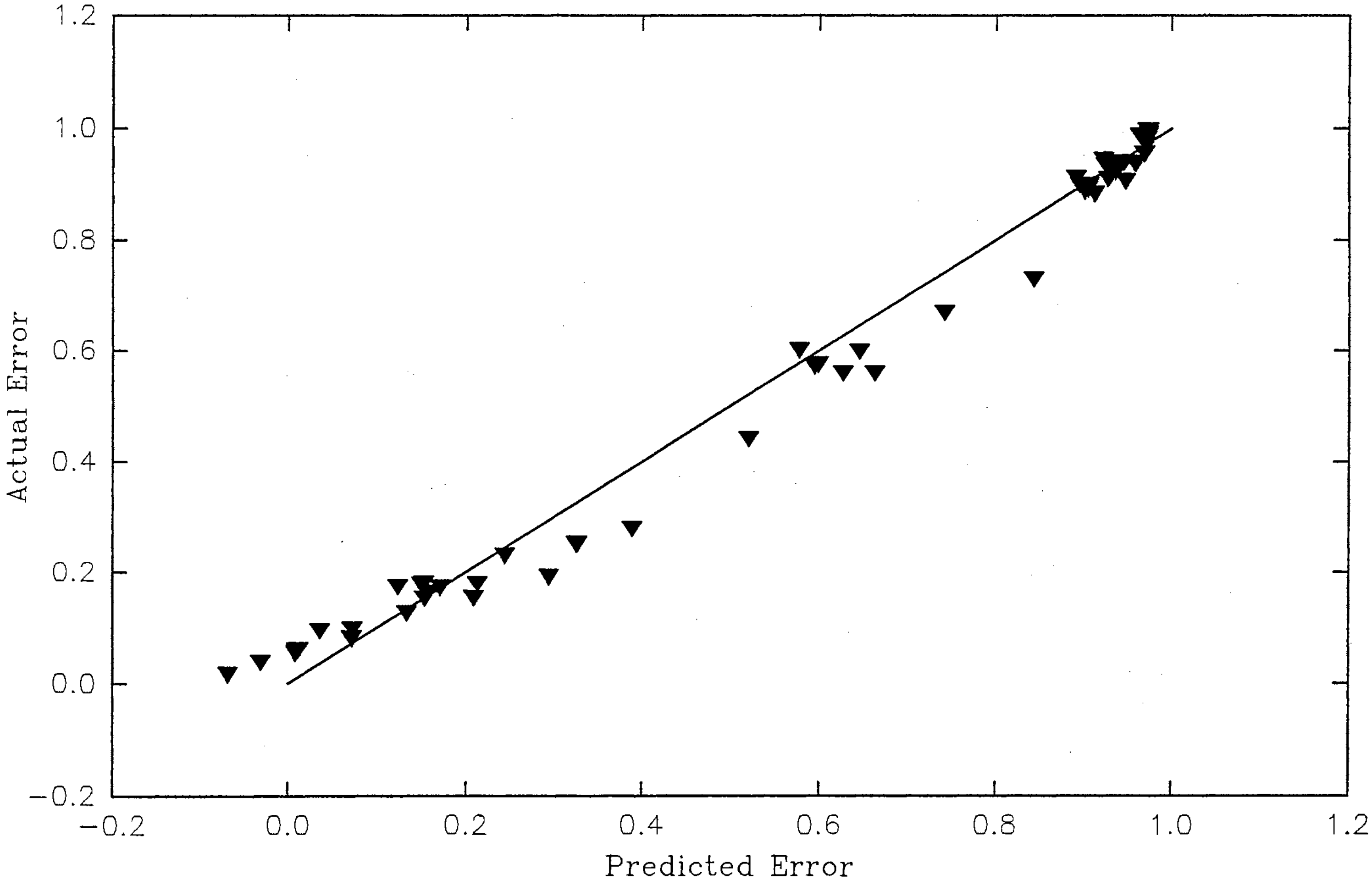

Figure 5−52. Actual vs Predicted Error − Linear Model to Predict Error(−.5) − PDMs

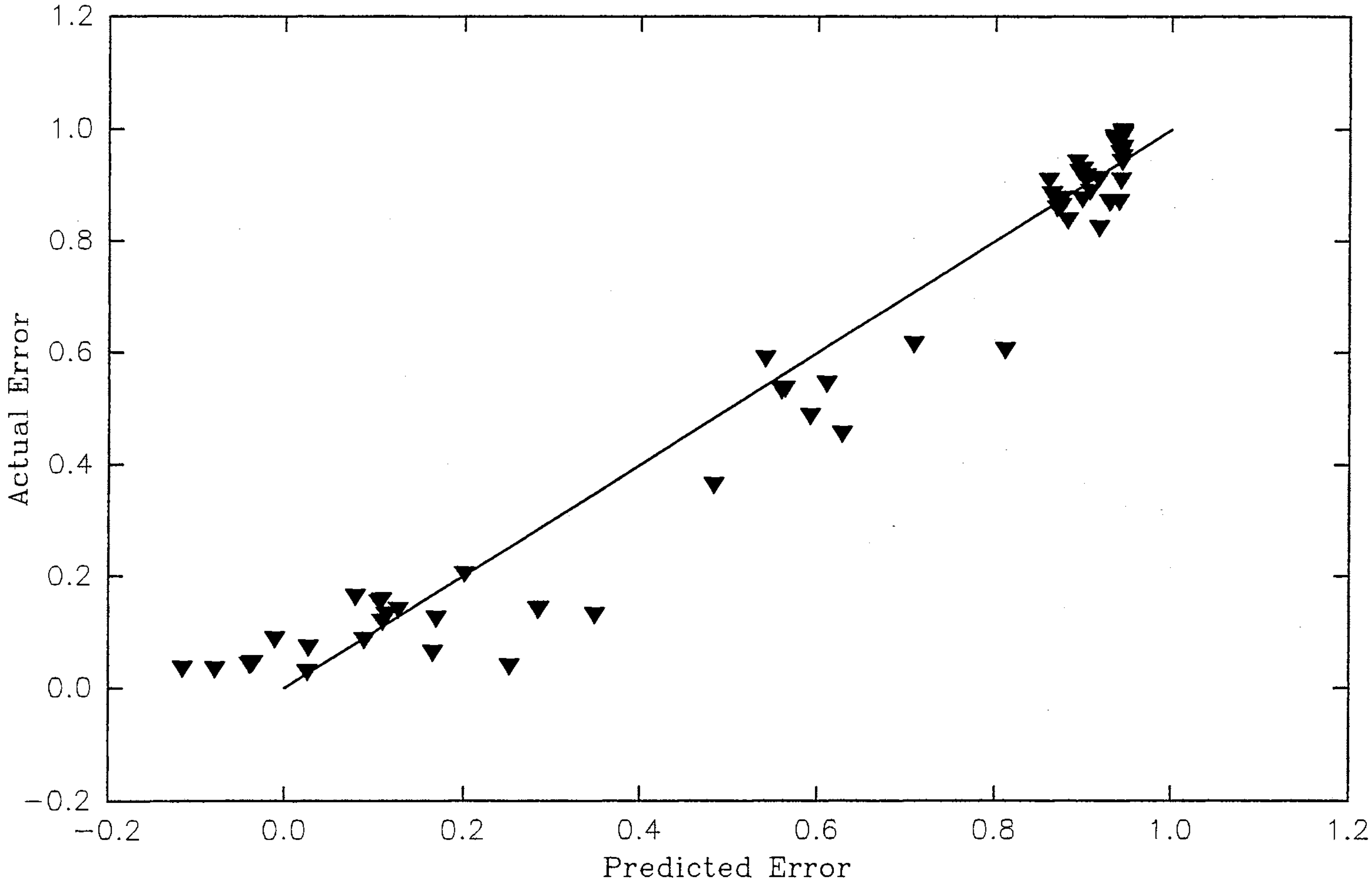

Figure 5−53. Actual vs Predicted Error − Linear Model to Predict Error(−.75) − PDMs

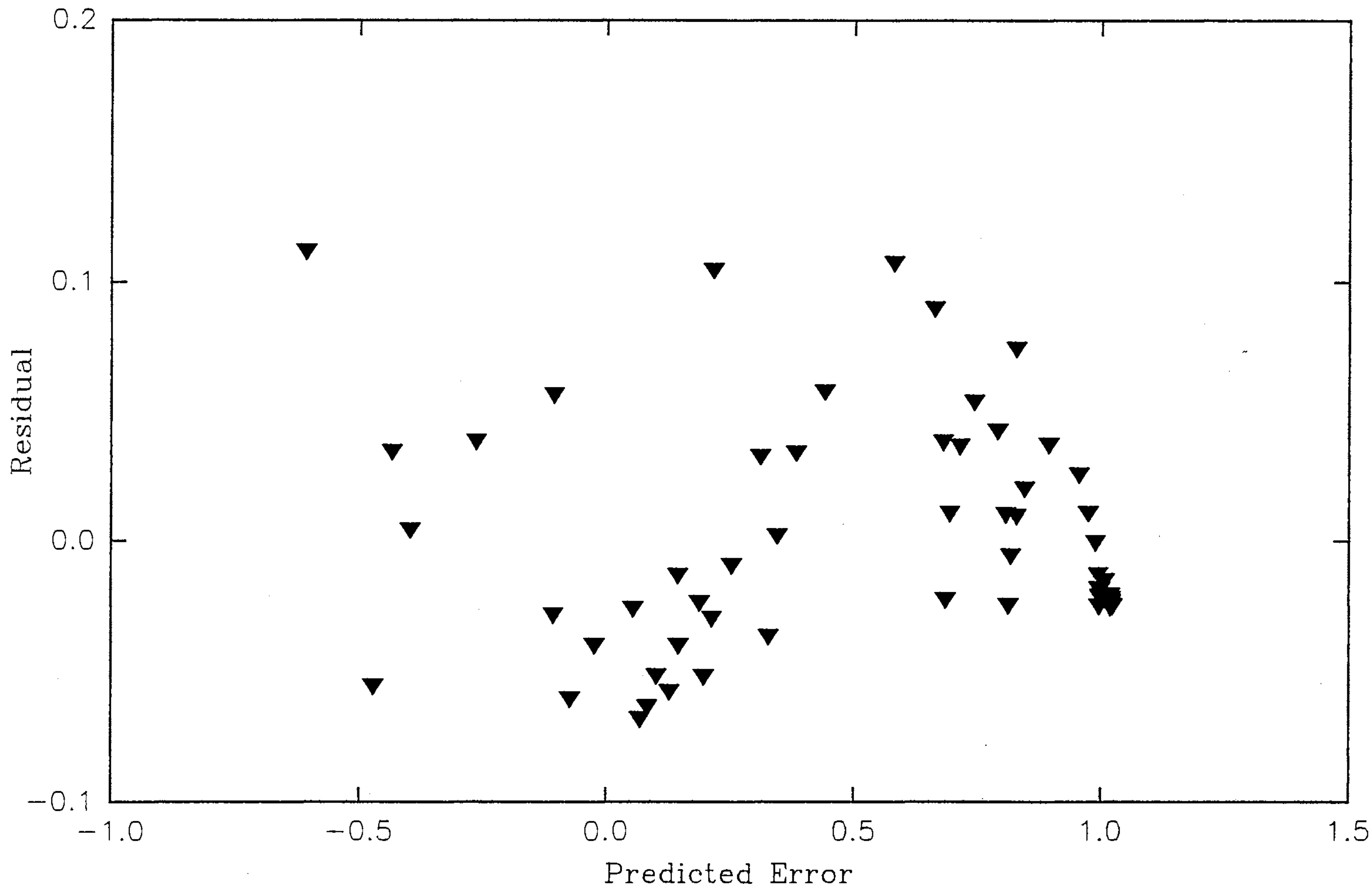

Figure 5−54. Residuals from Linear Model to Predict Error(.25) for PIMs

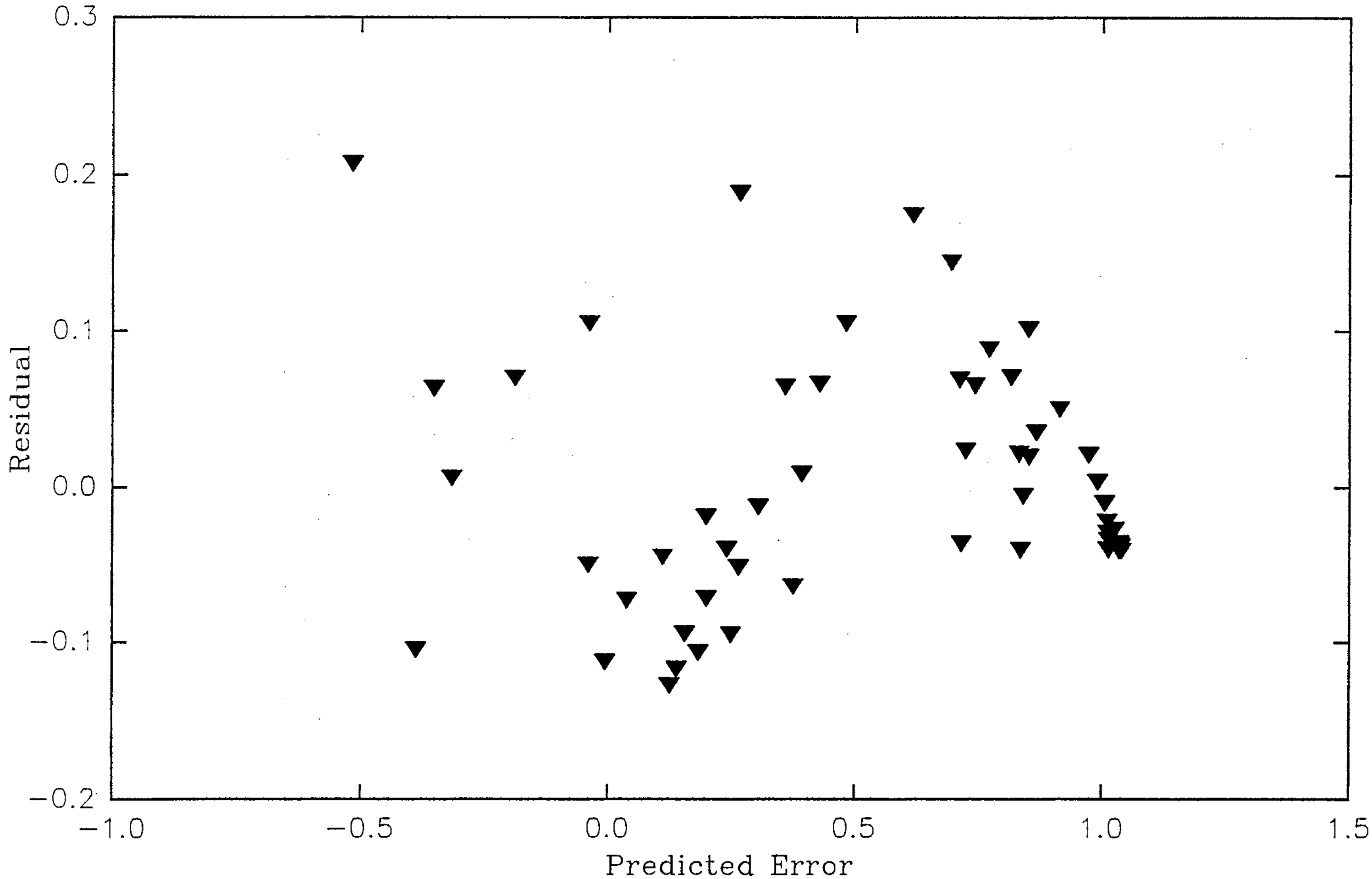

Figure 5−55. Residuals from Linear Model to Predict Error(.5) for PIMs

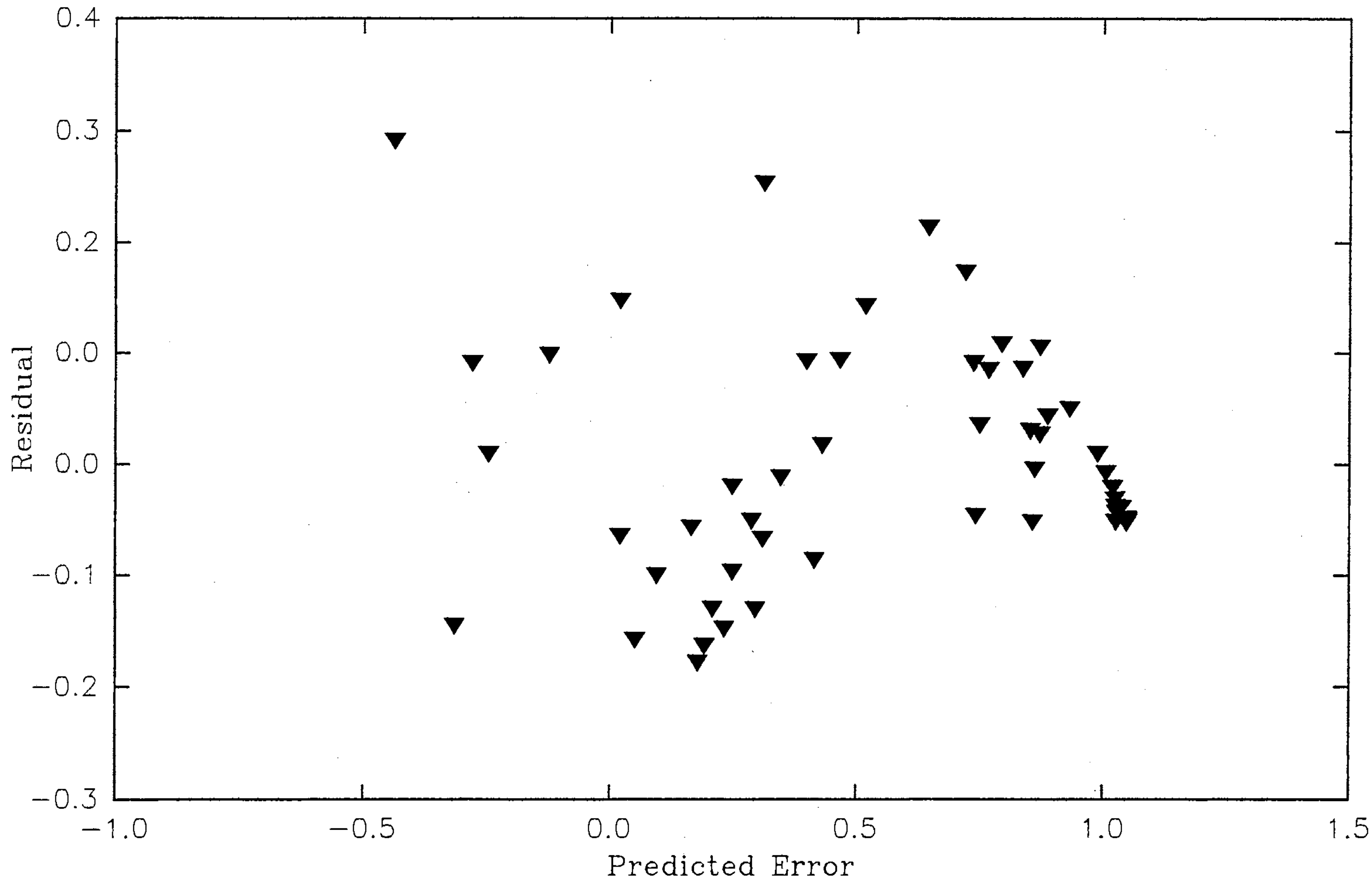

Figure 5−56. Residuals from Linear Model to Predict Error(.75) for PIMs

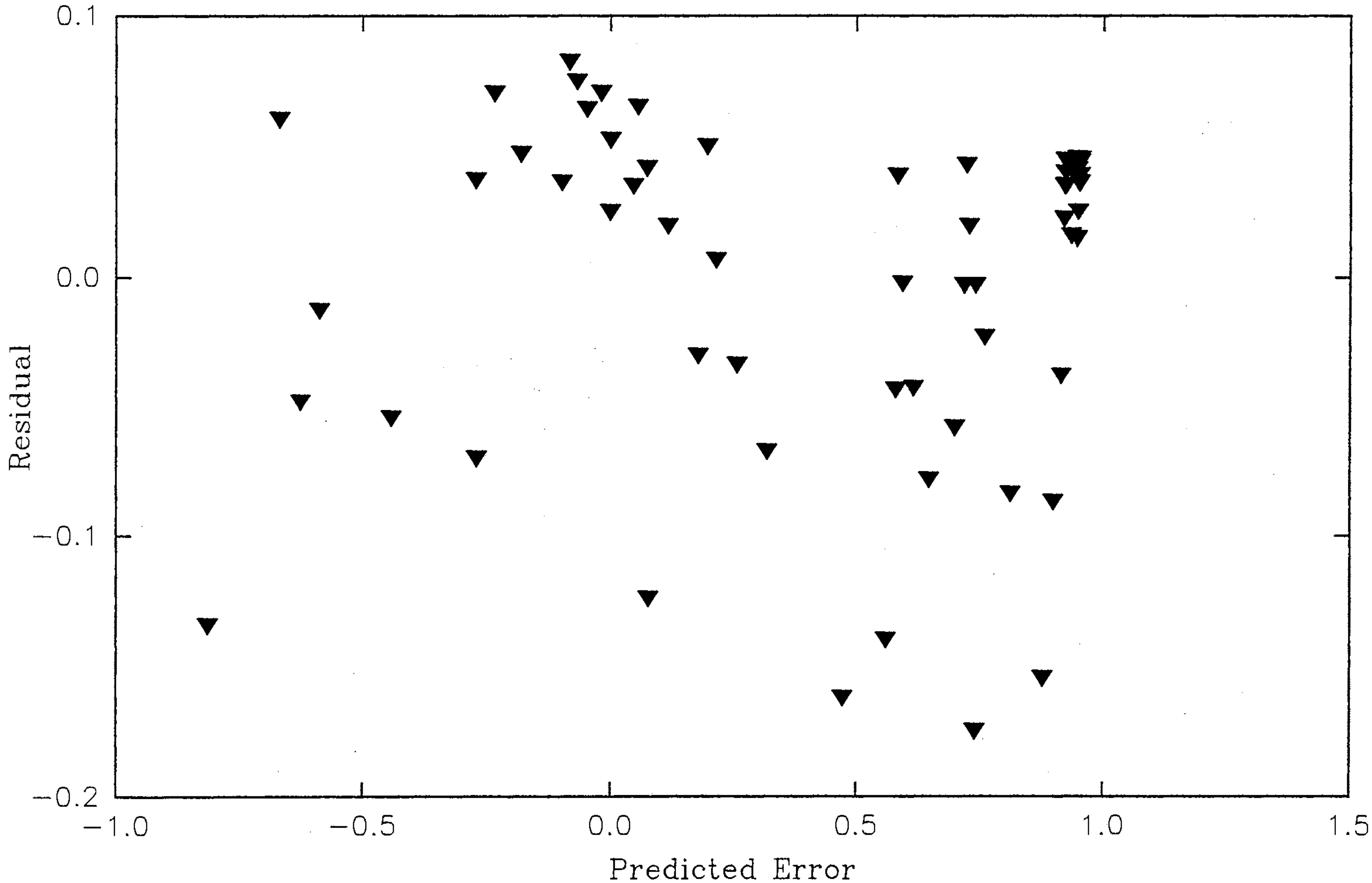

Figure 5−57. Residuals from Linear Model to Predict Error(−.25) for PIMs

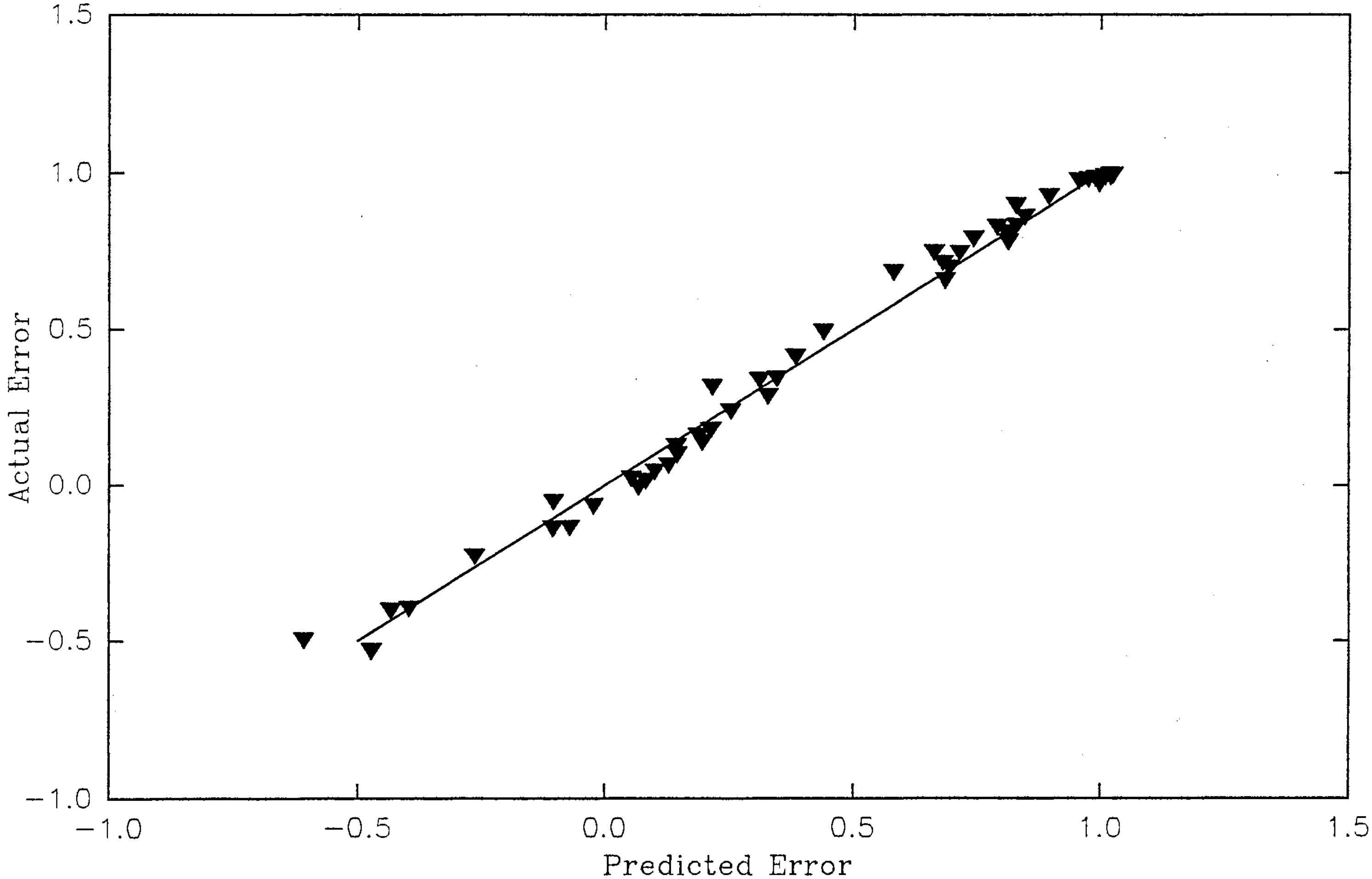

Figure 5−58. Actual vs Predicted Error − Linear Model to Predict Error(.25) − PIMs

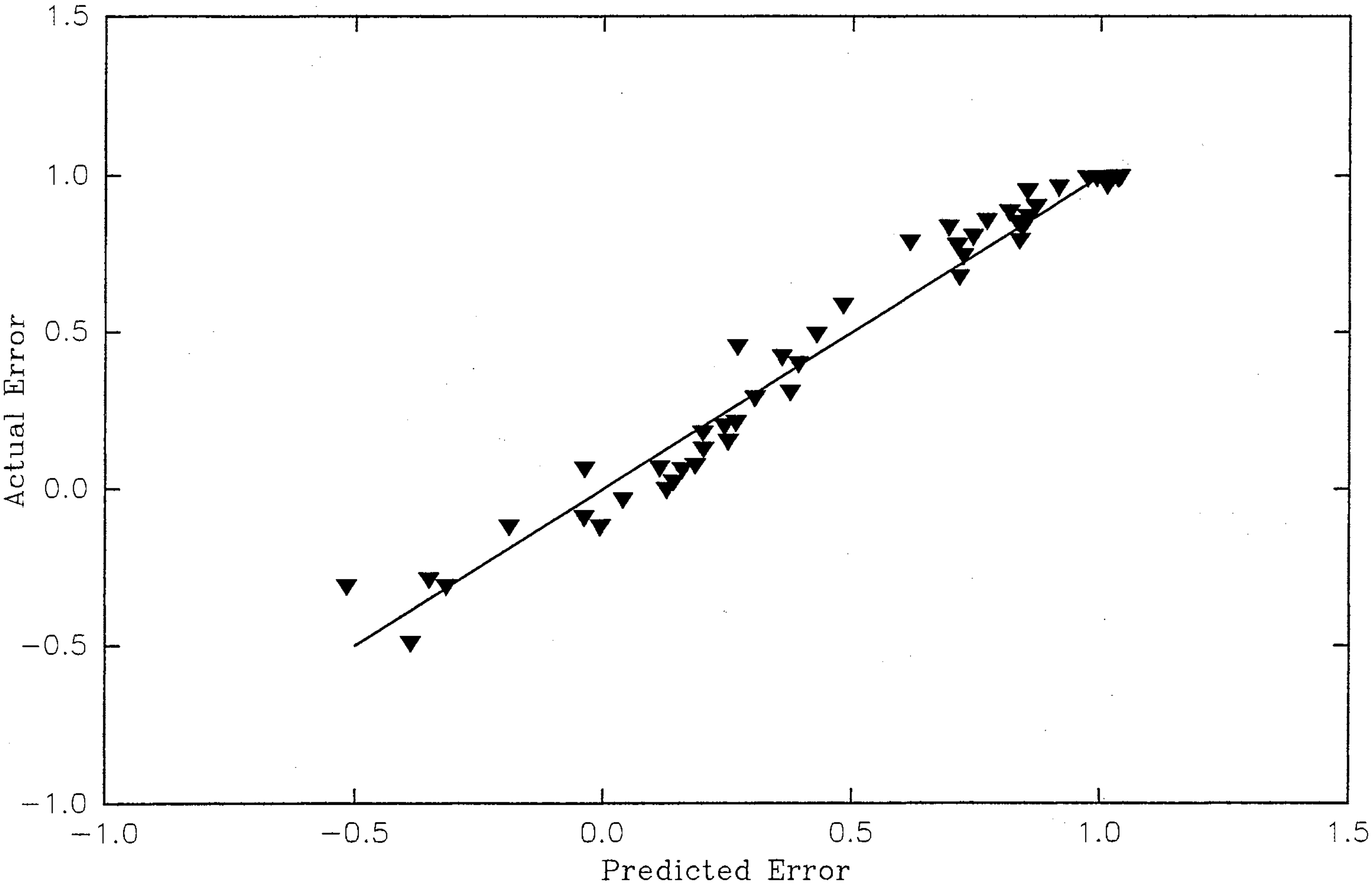

Figure 5−59. Actual vs Predicted Error − Linear Model to Predict Error(.5) − PIMs

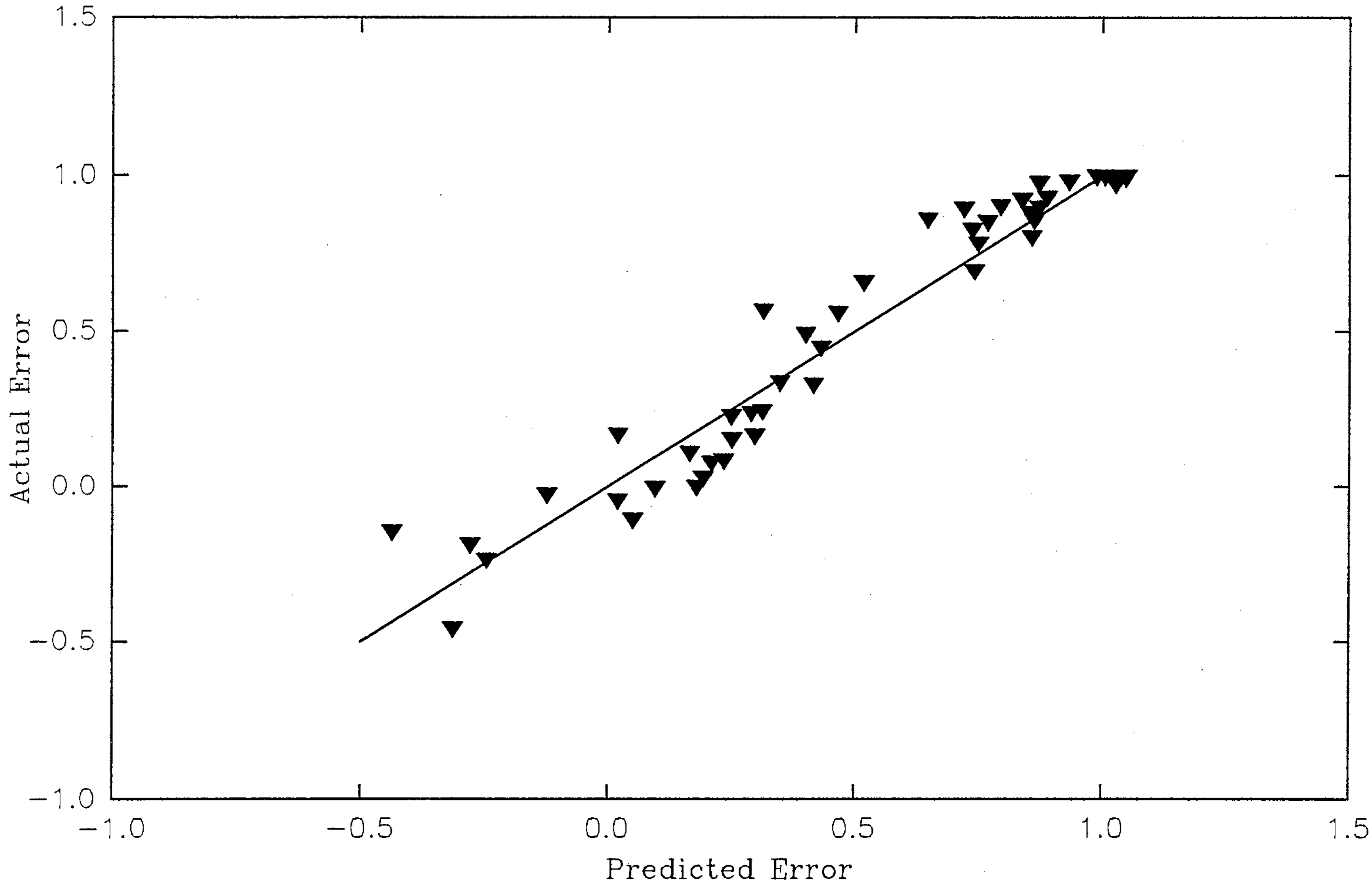

Figure 5−60. Actual vs Predicted Error − Linear Model to Predict Error(.75) − PIMs

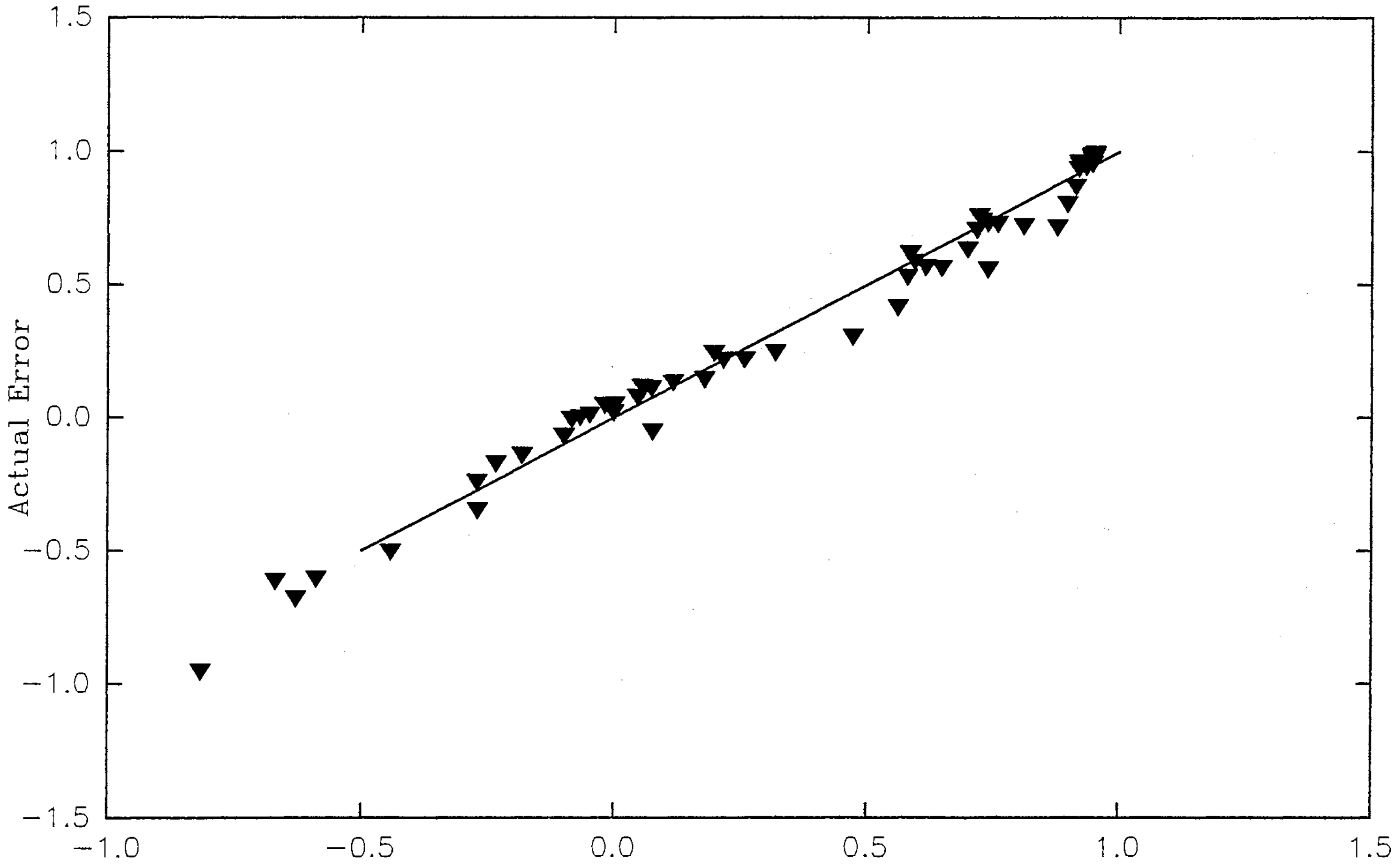

Figure 5−61. Actual vs Predicted Error − Linear Model to Predict Error(−.25) − PIMs

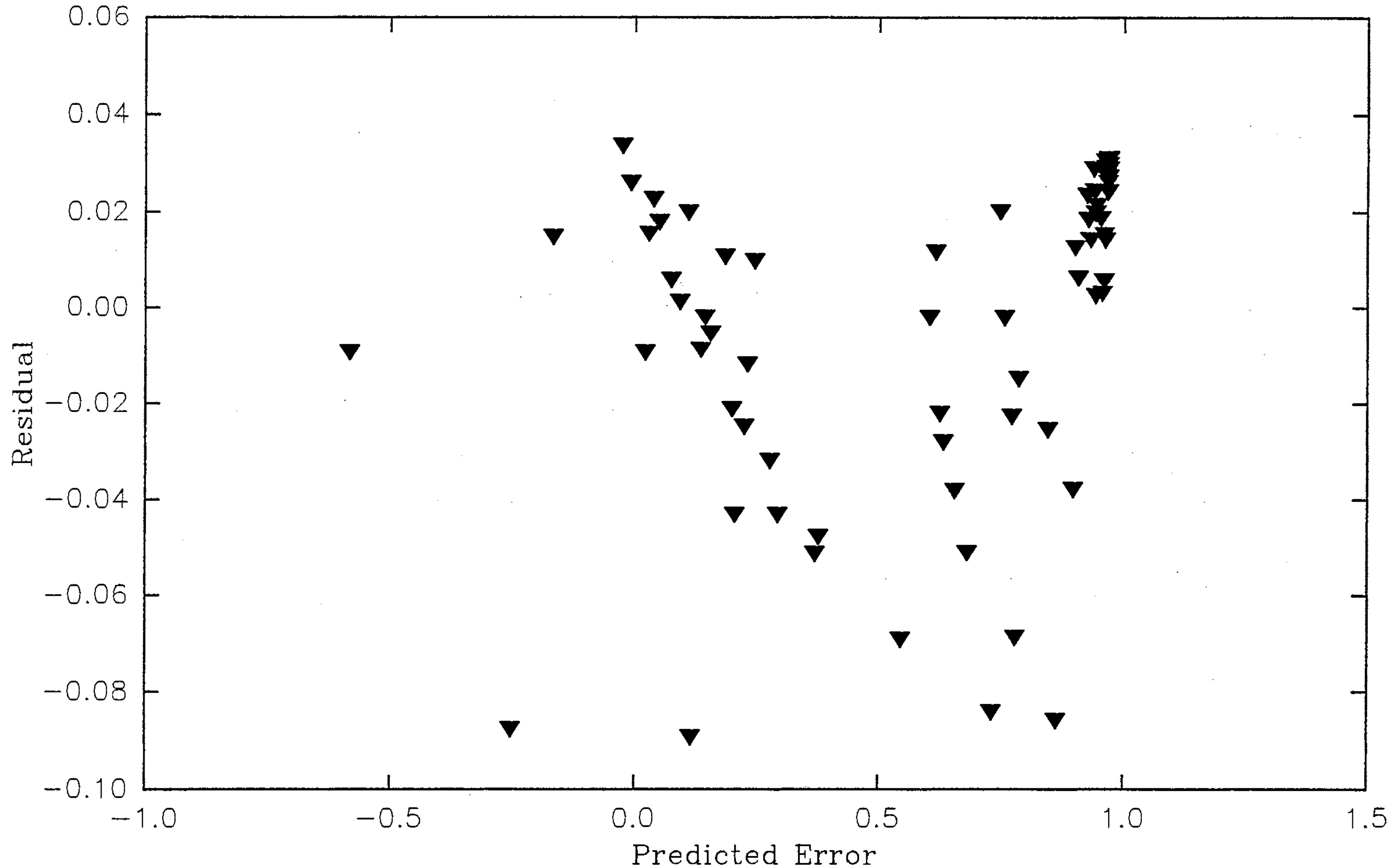

Figure 5−62. Residuals from Linear Model to Predict Error(.25) for PMMs

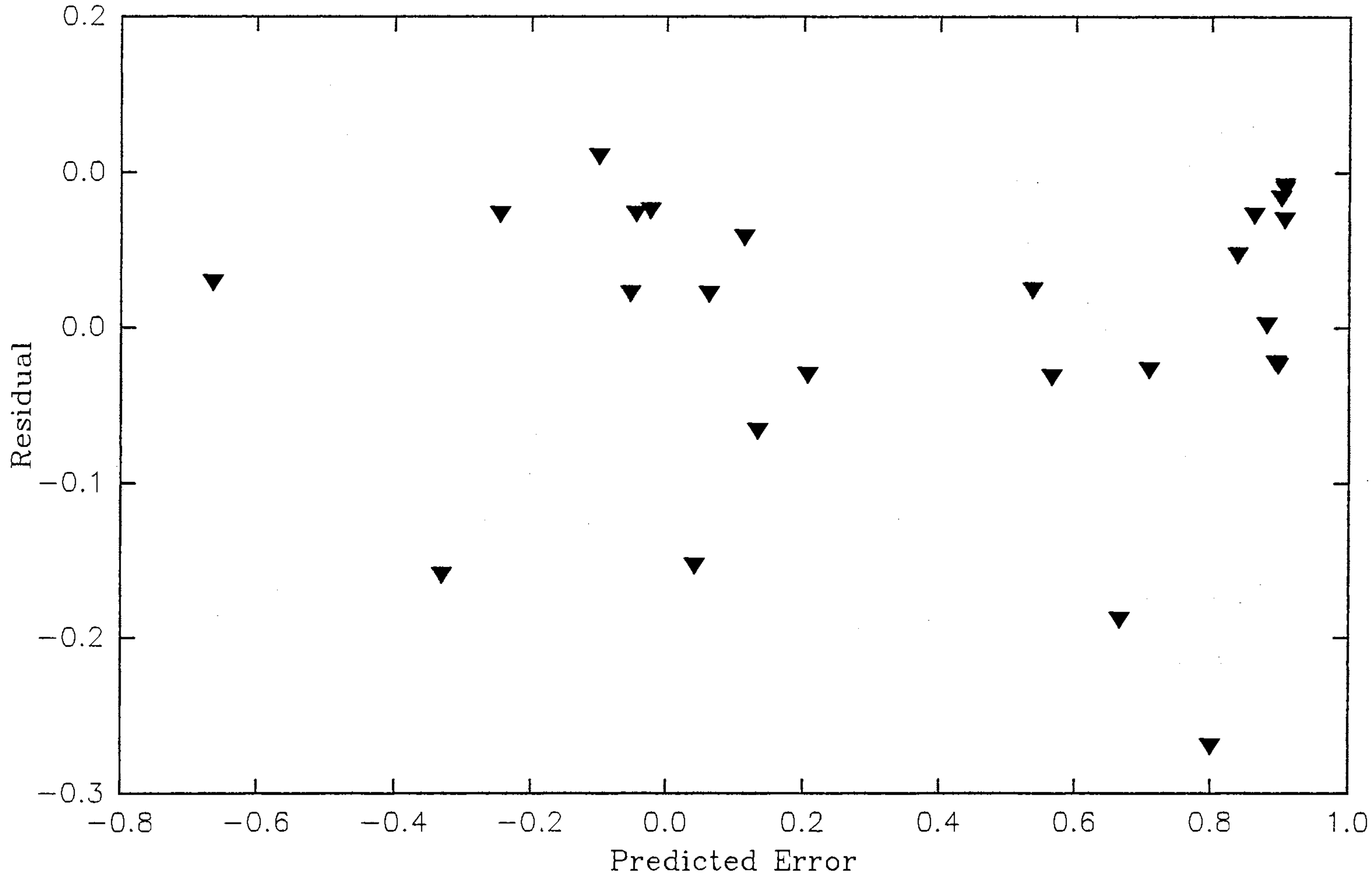

Figure 5−63. Residuals from Linear Model to Predict Error(.5) for PMMs

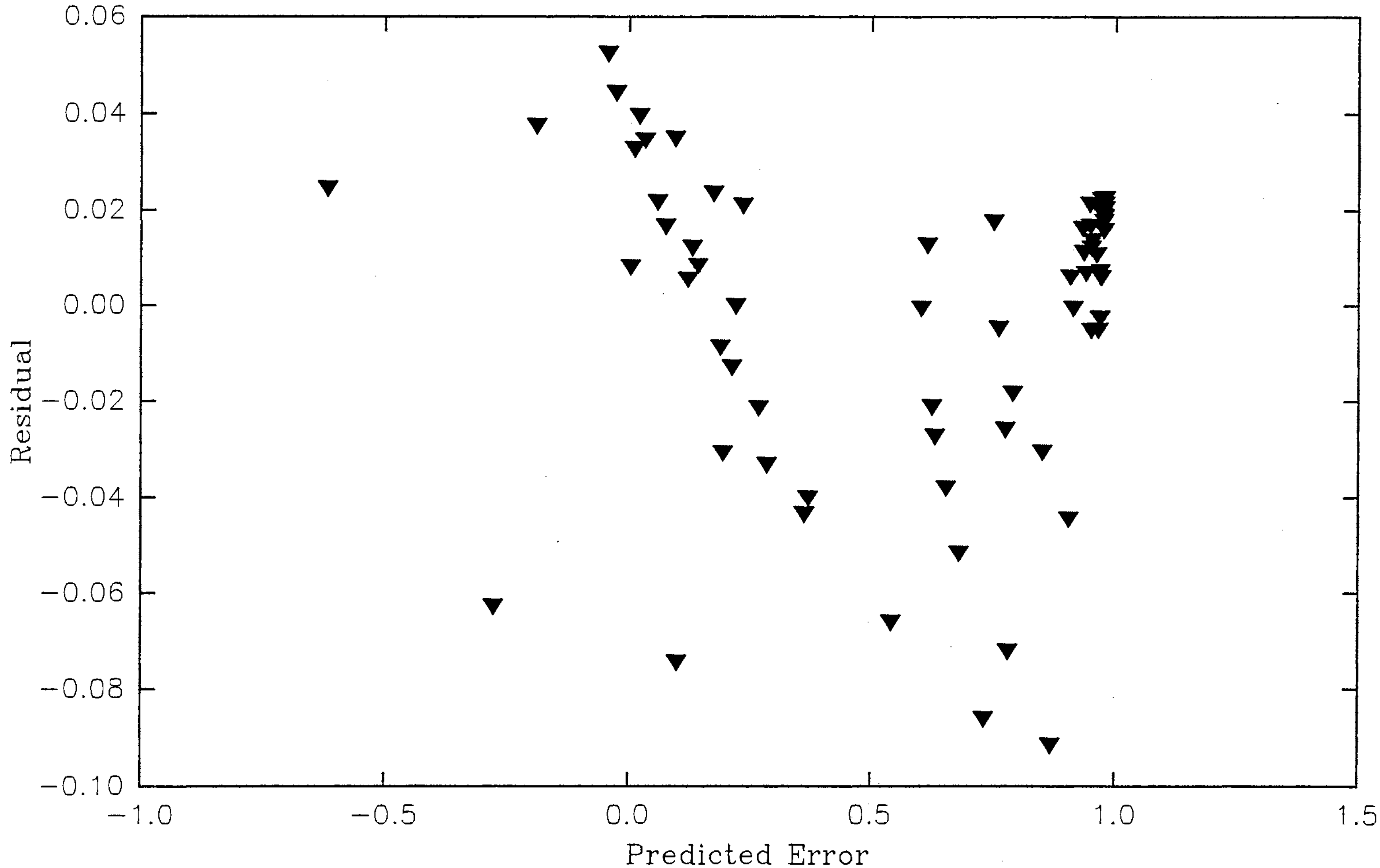

Figure 5−64. Residuals from Linear Model to Predict Error(−.25) for PMMs

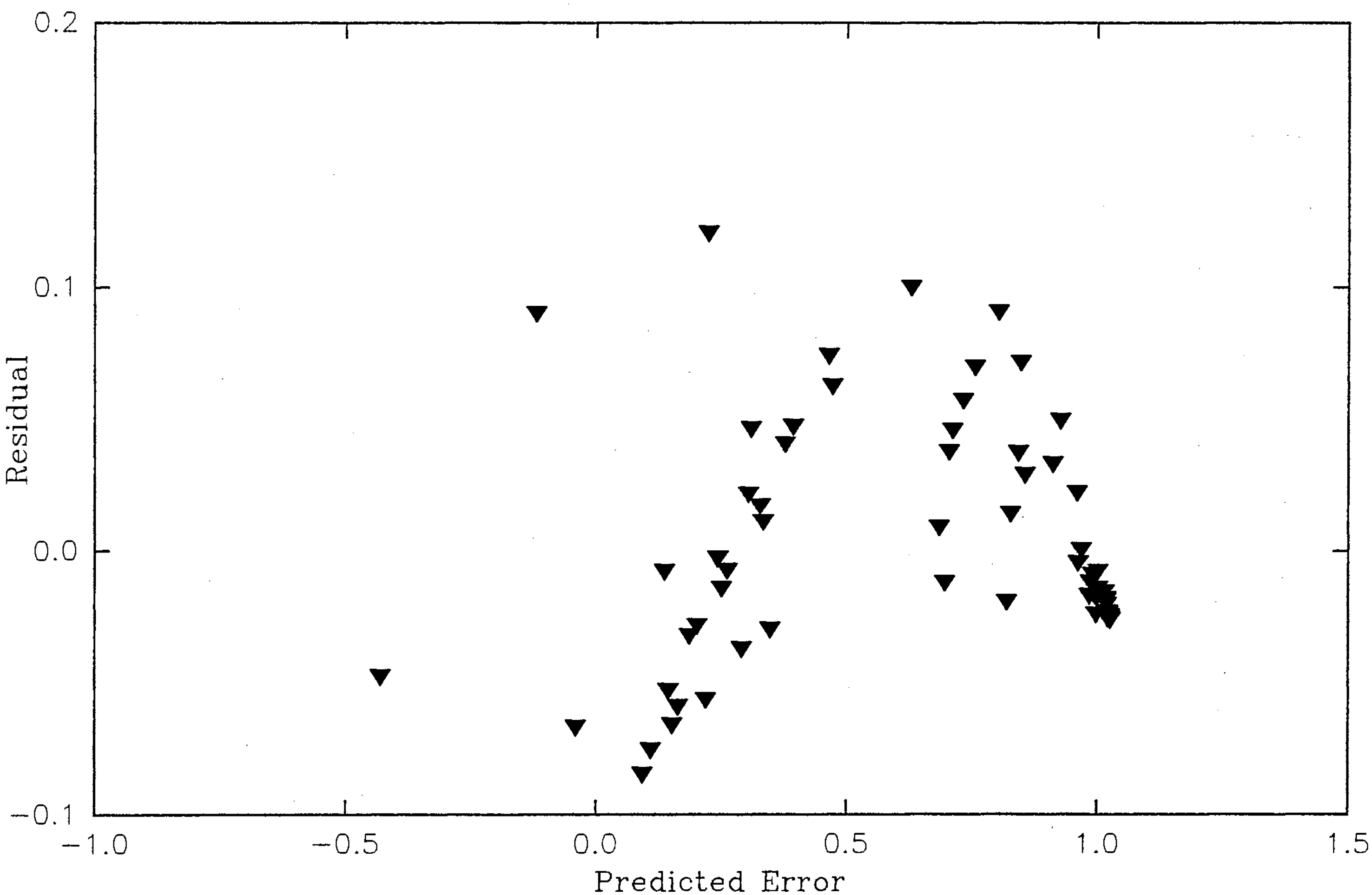

Figure 5−65. Residuals from Linear Model to Predict Error(−.5) for PMMs

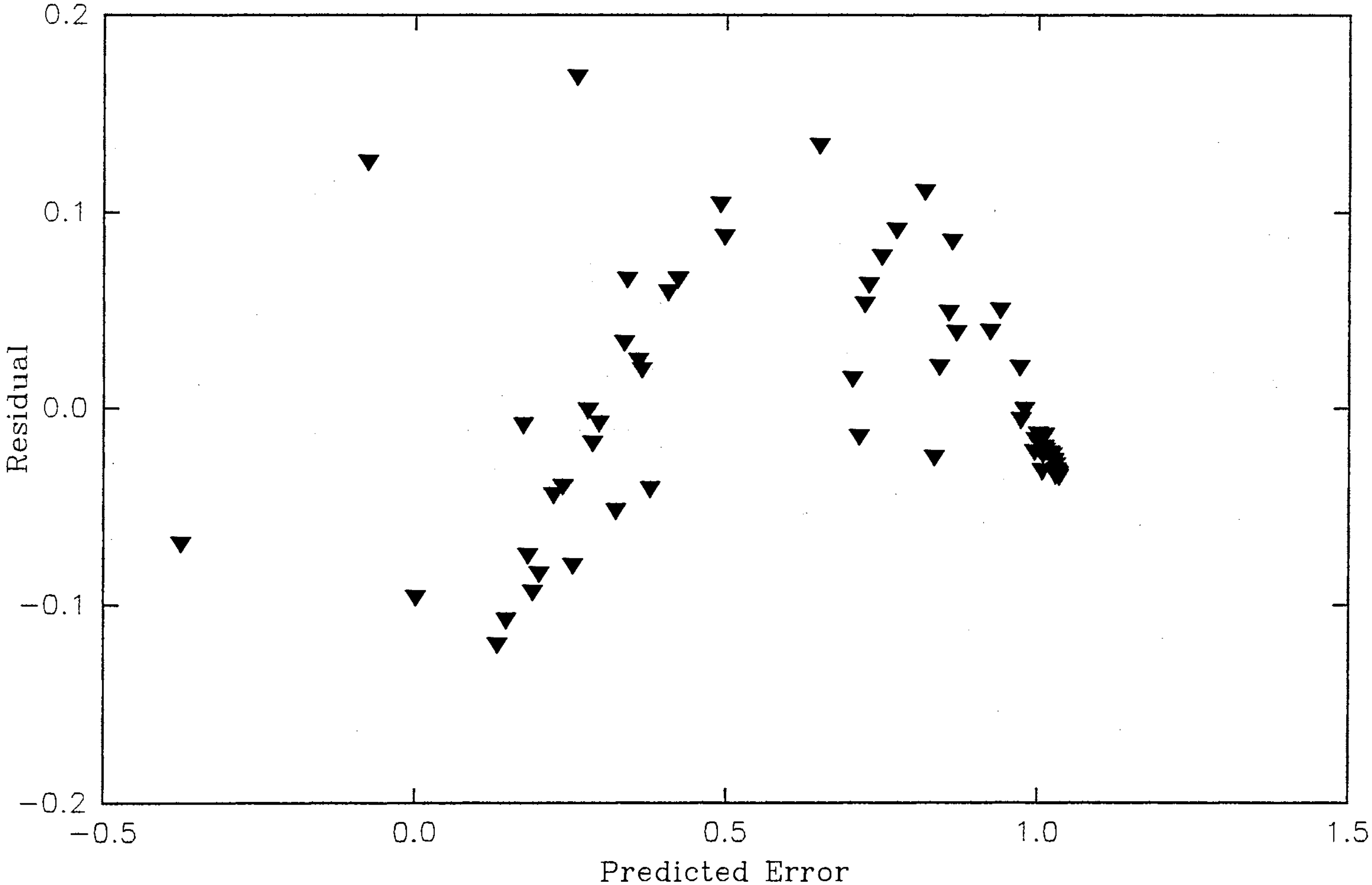

Figure 5−66. Residuals from Linear Model to Predict Error(−.75) for PMMs

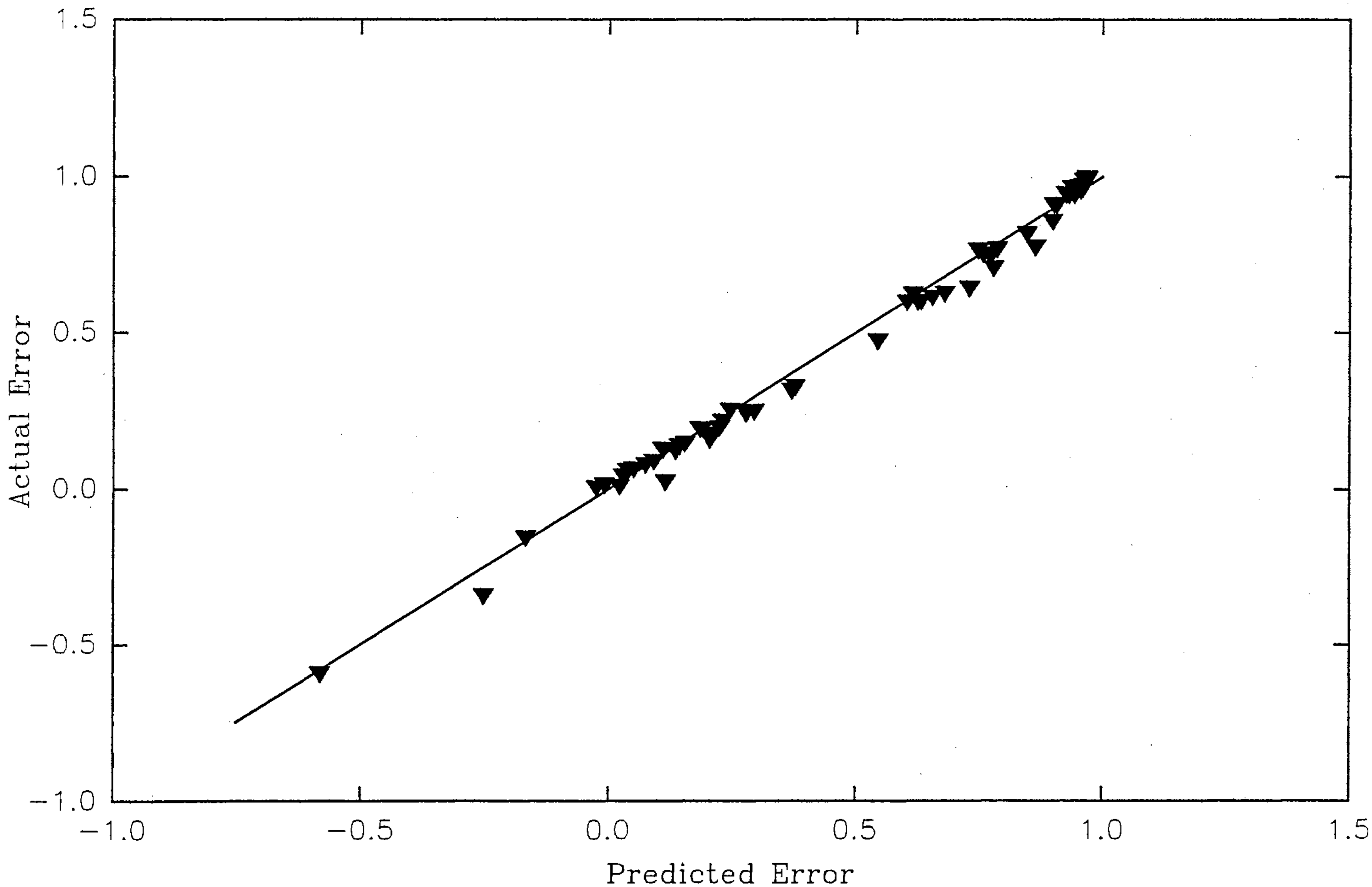

Figure 5–67. Actual vs Predicted Error – Linear Model to Predict Error(.25) – PMMs

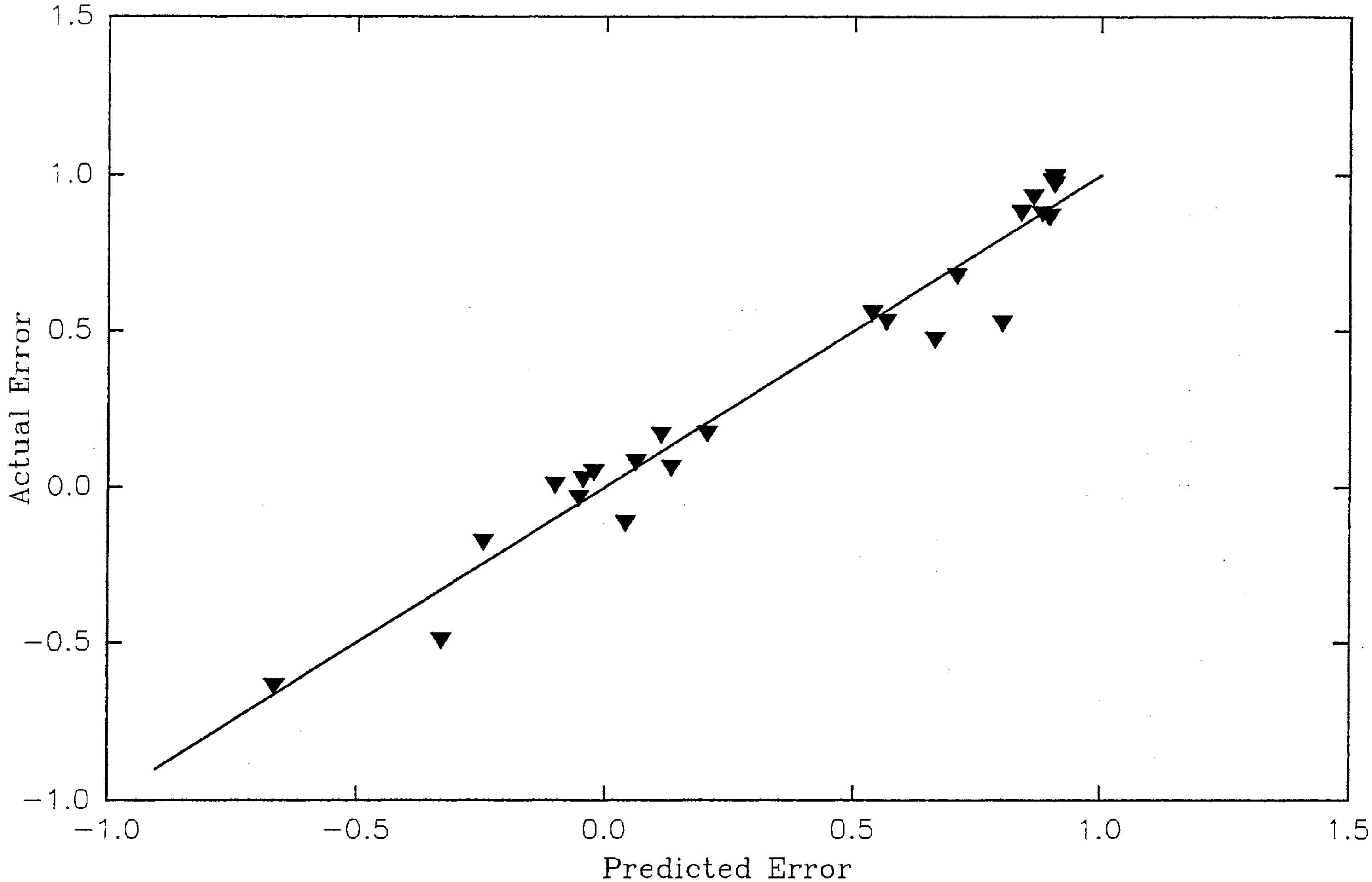

Figure 5−68. Actual vs Predicted Error − Linear Model to Predict Error(.5) − PMMs

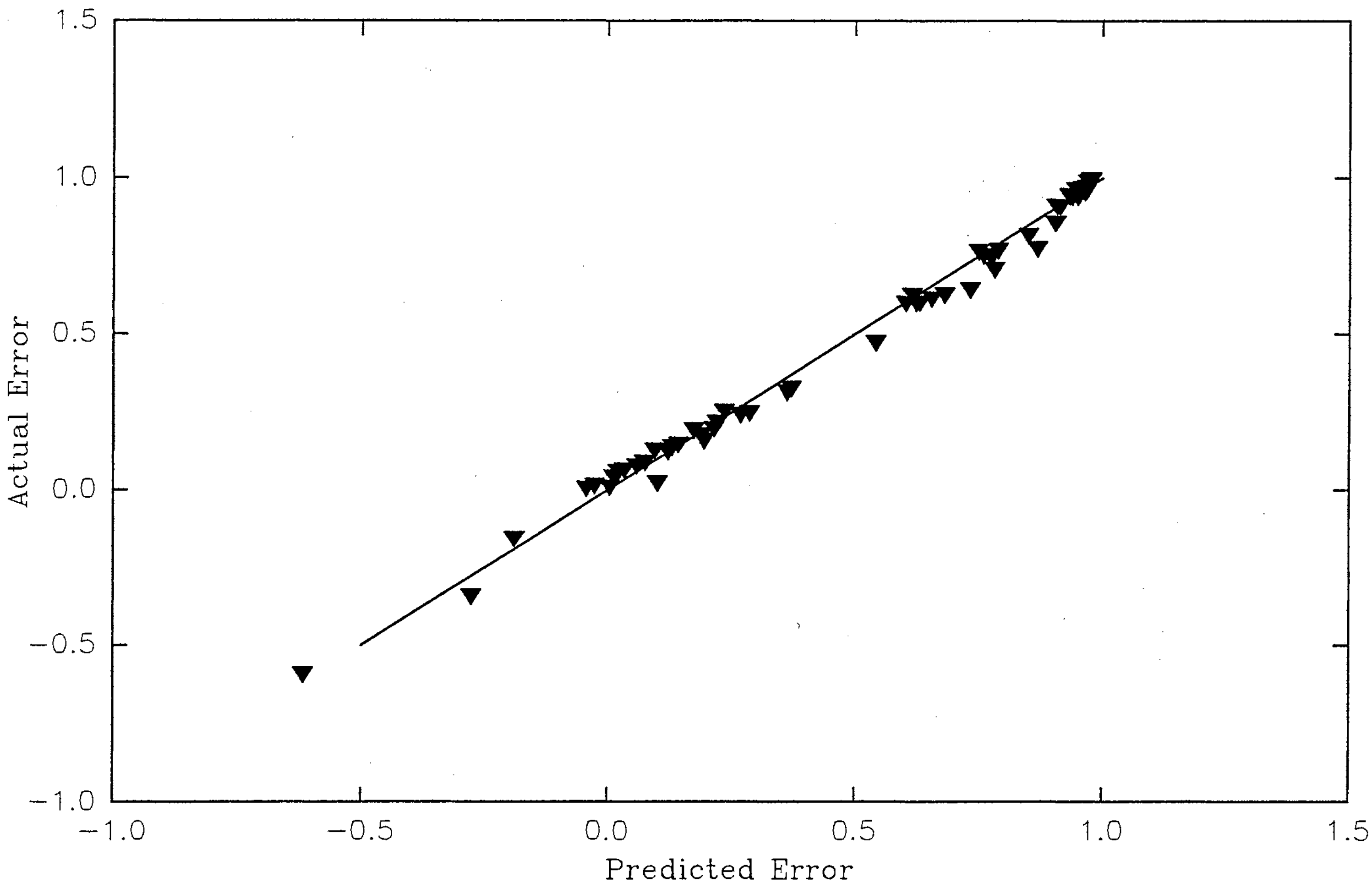

Figure 5−69. Actual vs Predicted Error − Linear Model to Predict Error(−.25) − PMMs

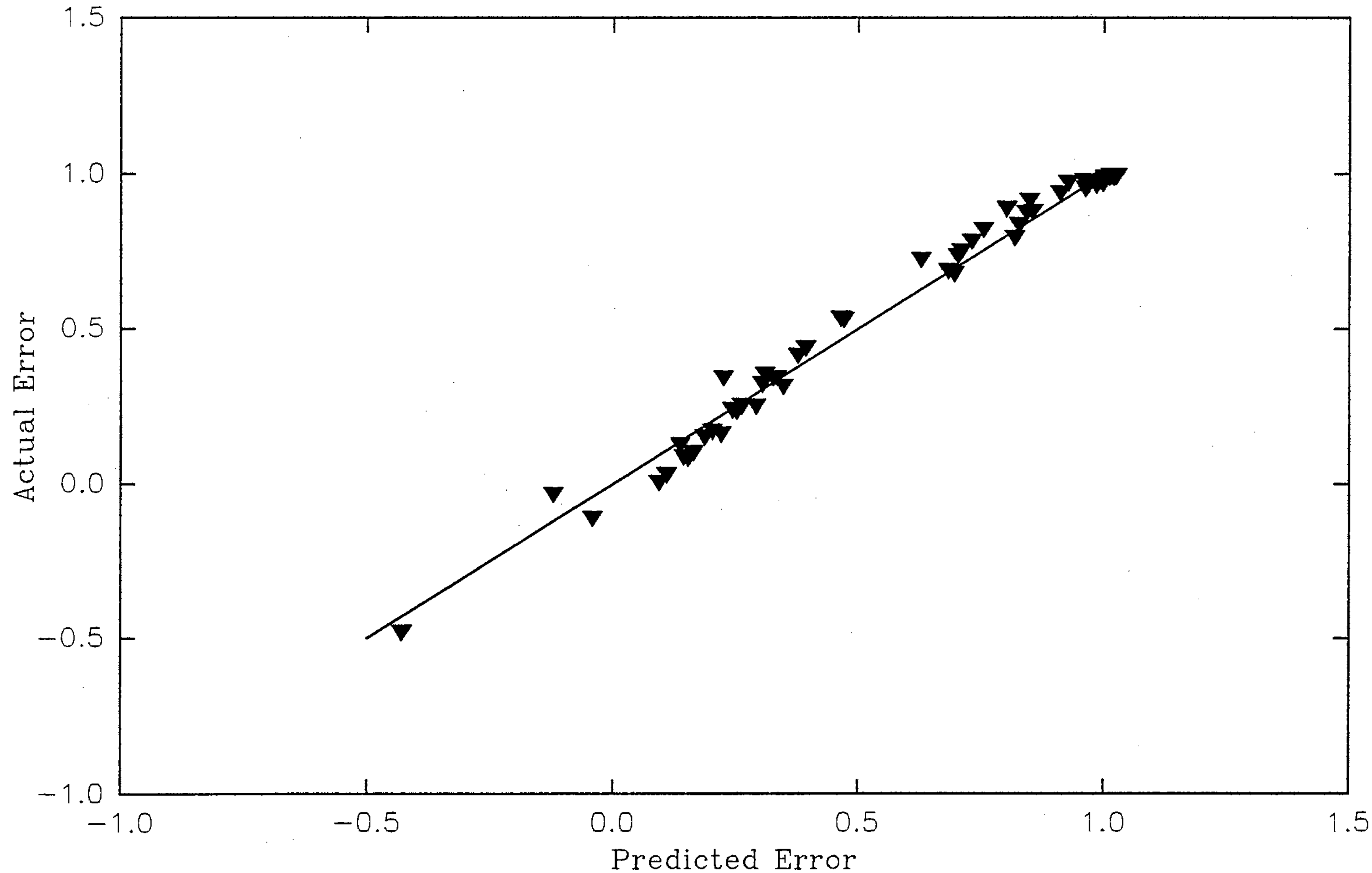

Figure 5−70. Actual vs Predicted Error − Linear Model to Predict Error(−.5) − PMMs

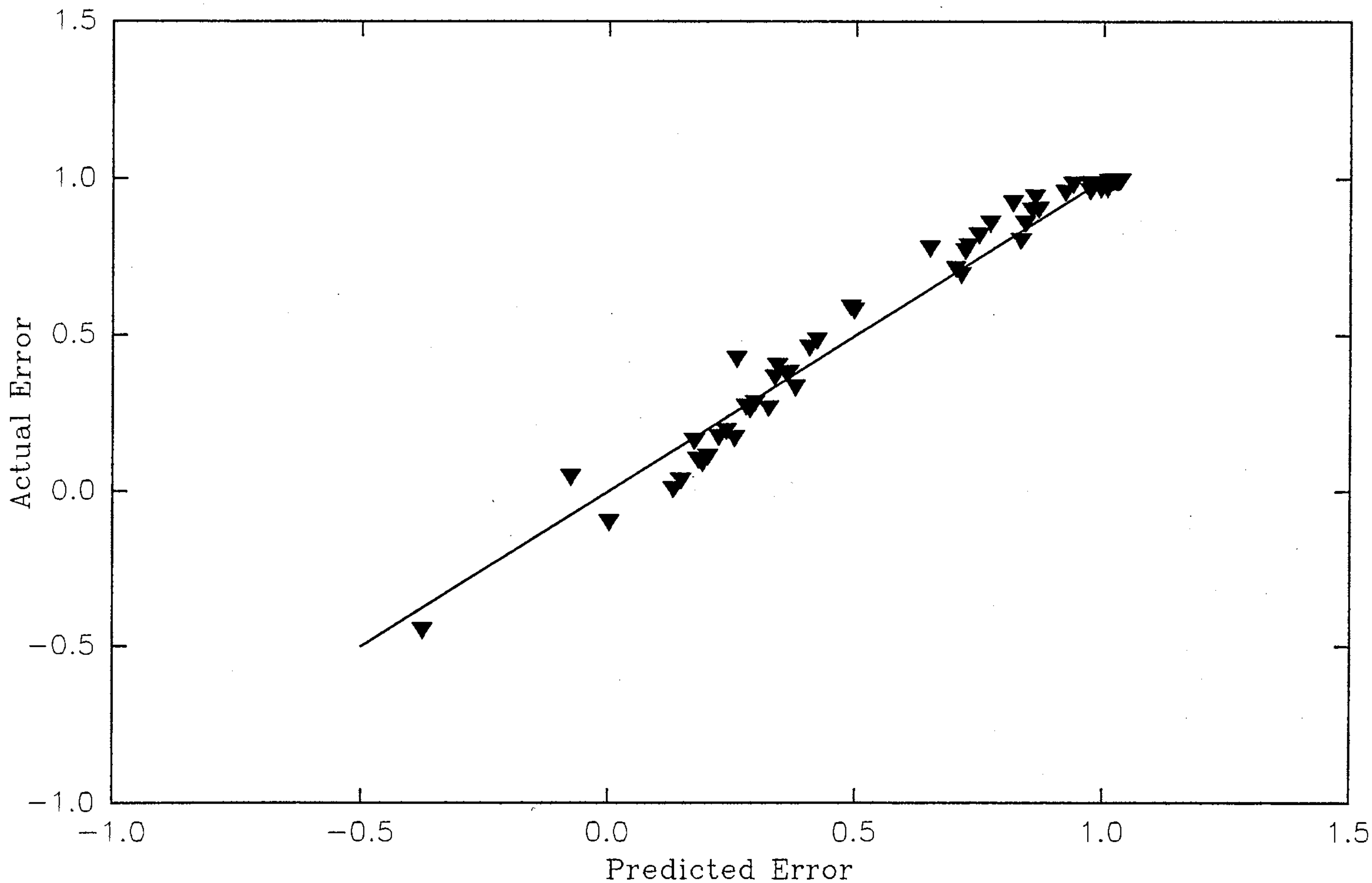

Figure 5−71. Actual vs Predicted Error − Linear Model to Predict Error(−.75) − PMMs

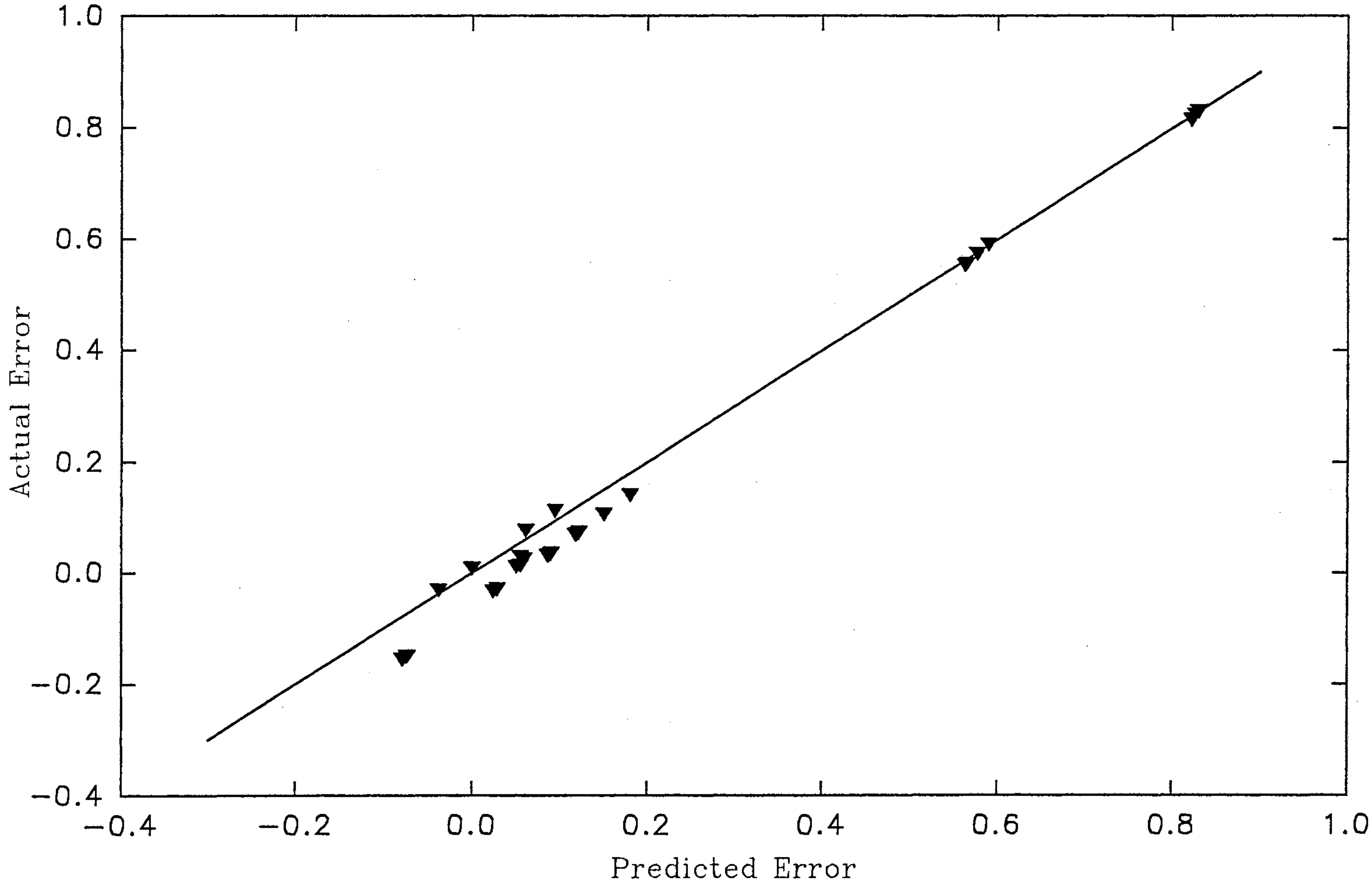

Figure 5−72. Actual vs Predicted Errors − Test Runs with Rho = 0

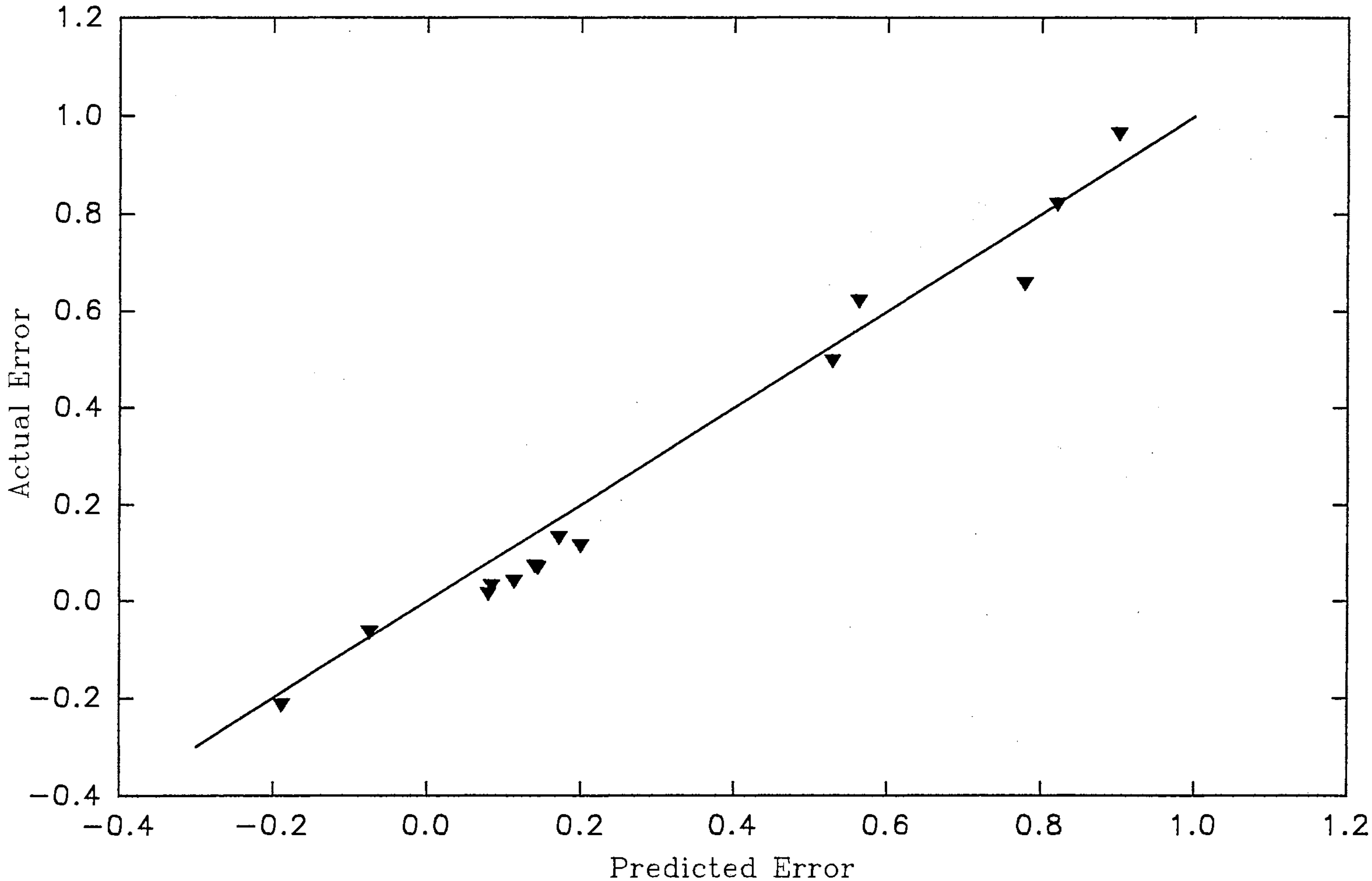

Figure 5−73. Actual vs Predicted Errors − Quadratic Error Model, Rho = 0.25

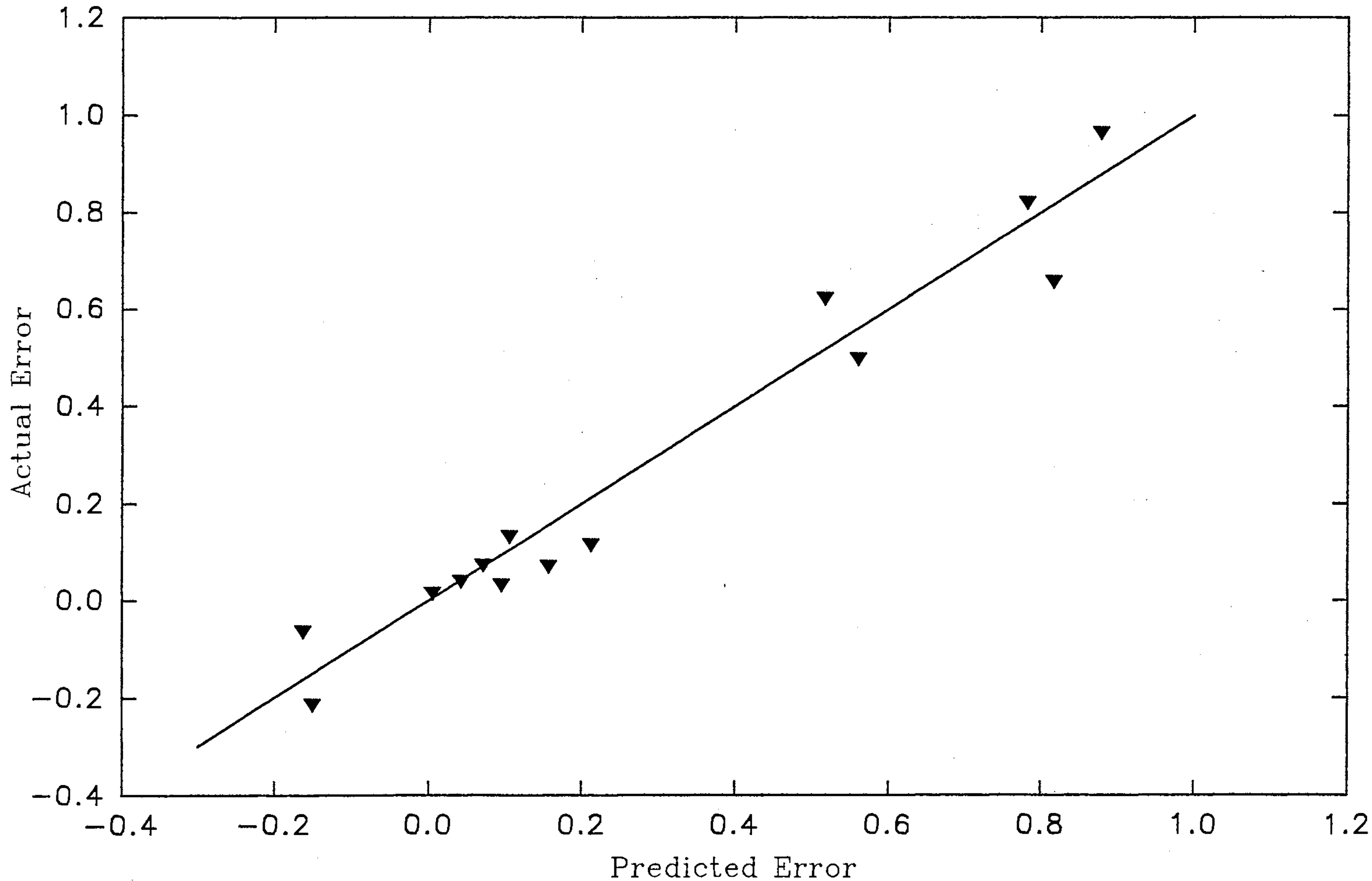

Figure 5−74. Actual vs Predicted Errors − Linear Error Model, Rho = 0.25

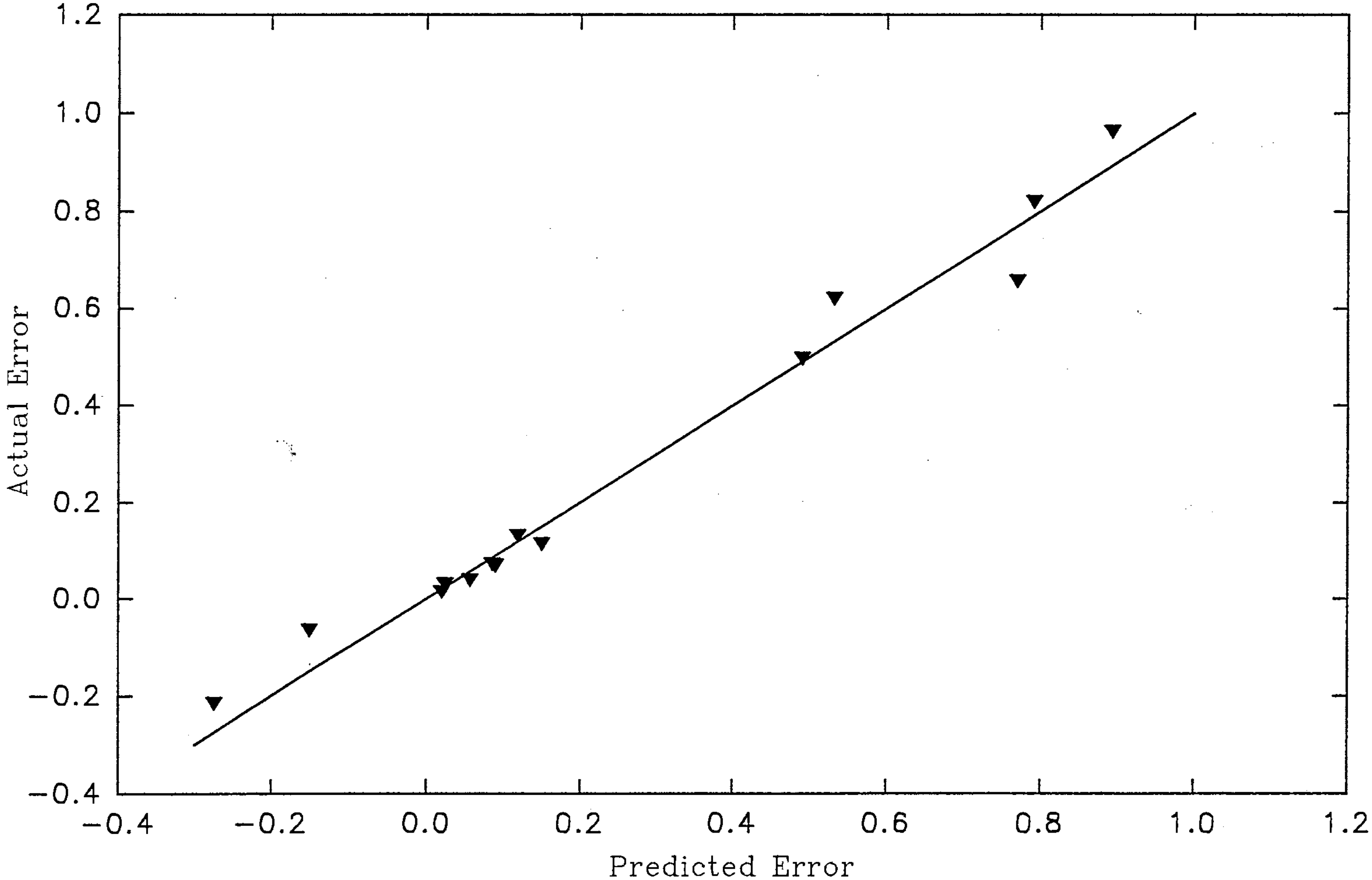

Figure 5−75. Actual vs Predicted Errors − Quadratic Error Model, Rho = −0.25

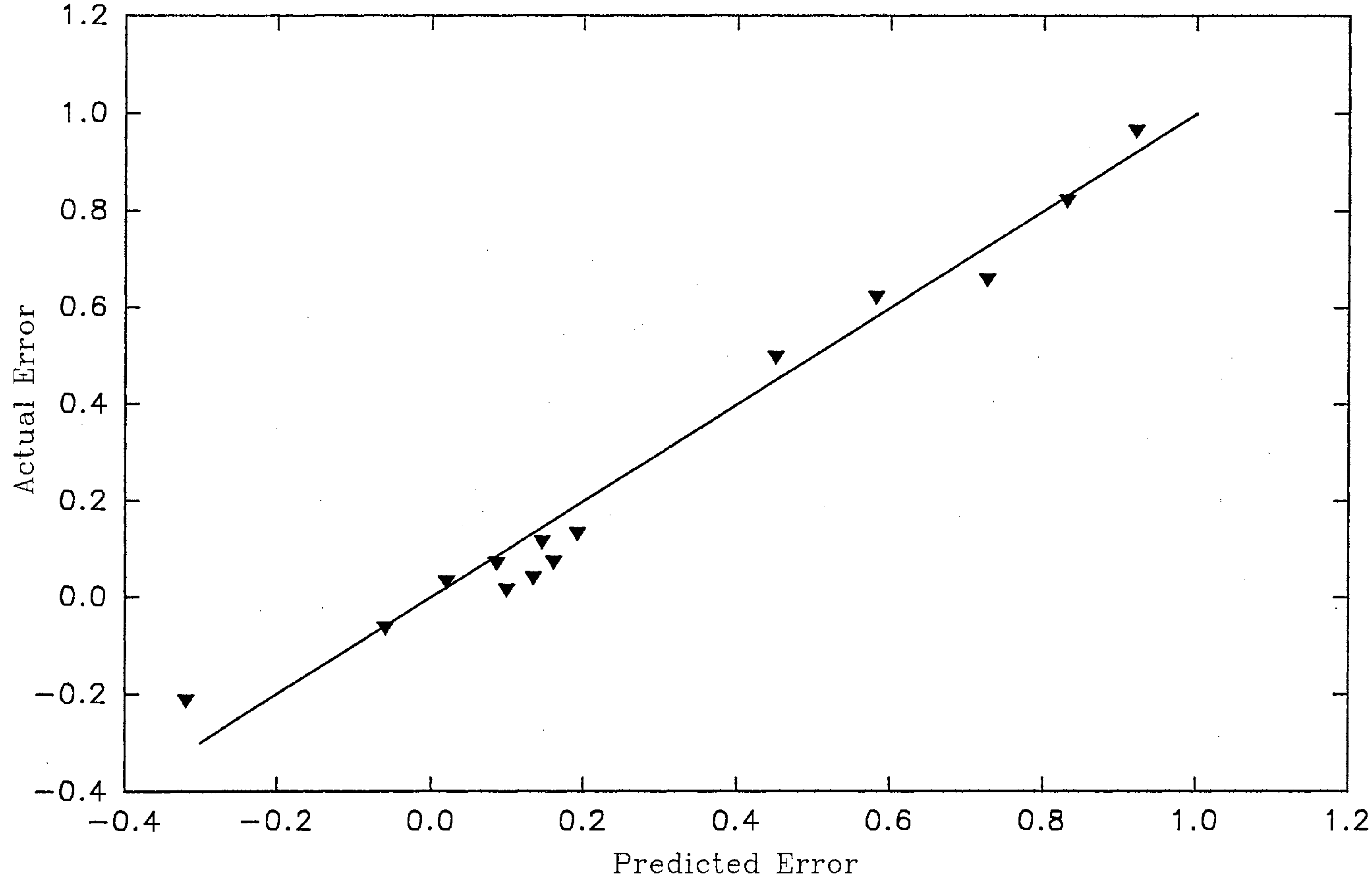

Figure 5−76. Actual vs Predicted Errors − Linear Error Model, Rho = −0.25

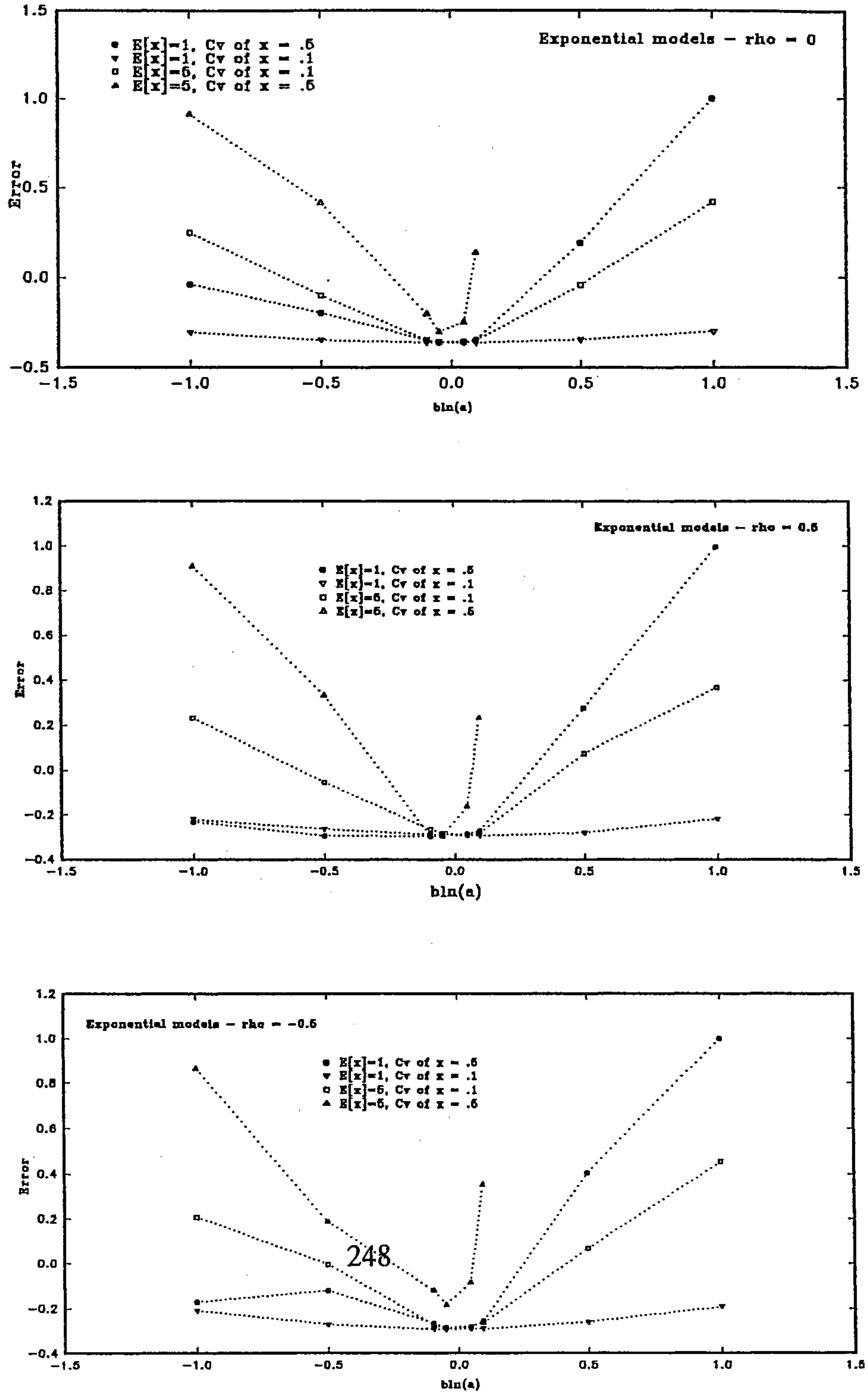

Figure 5–77. Behavior of Error in FOA Variance as a Function of bln(a)

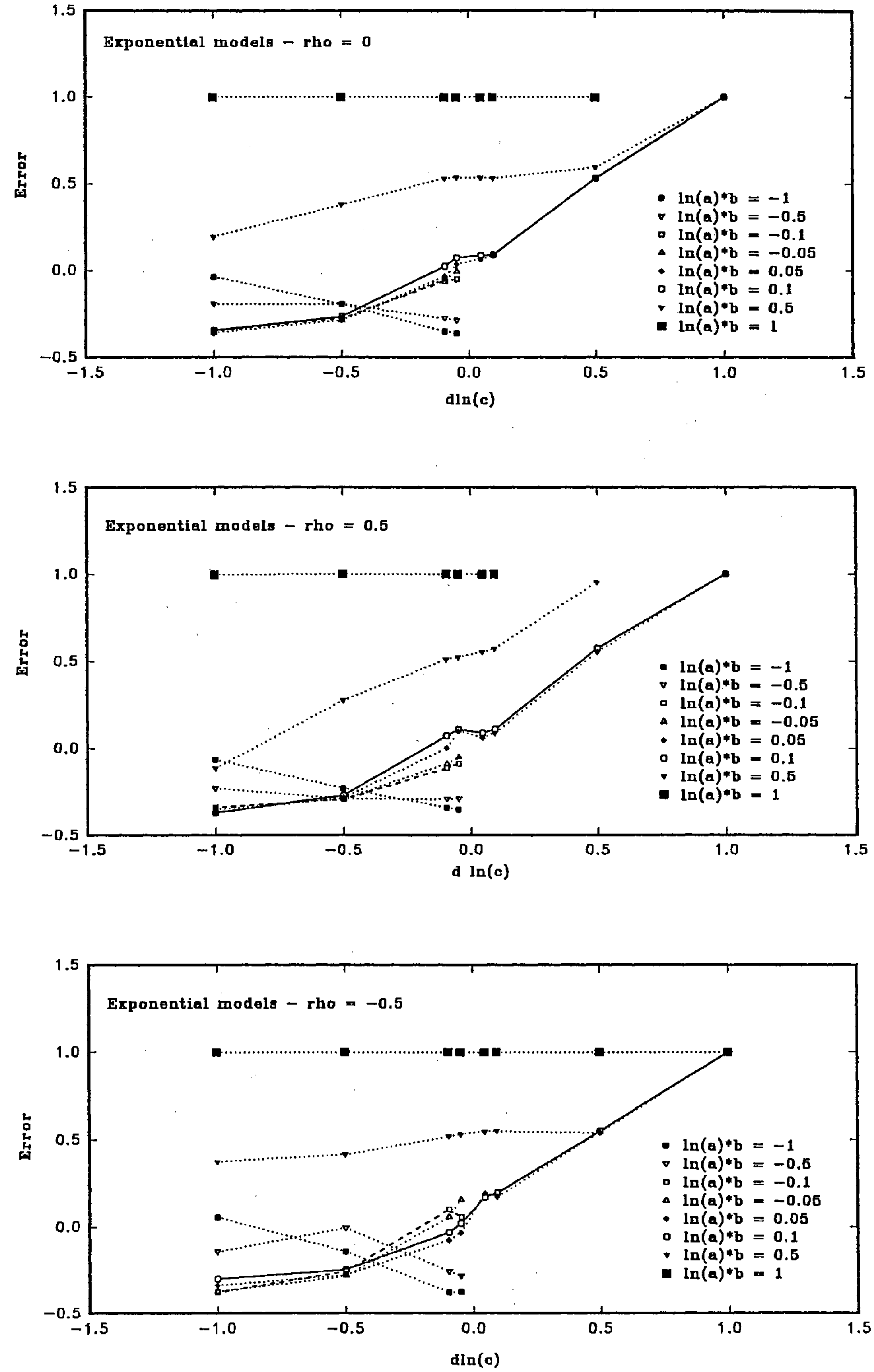

Figure 5–78. Behavior of Error in FOA Variance as a Function of dln(c)

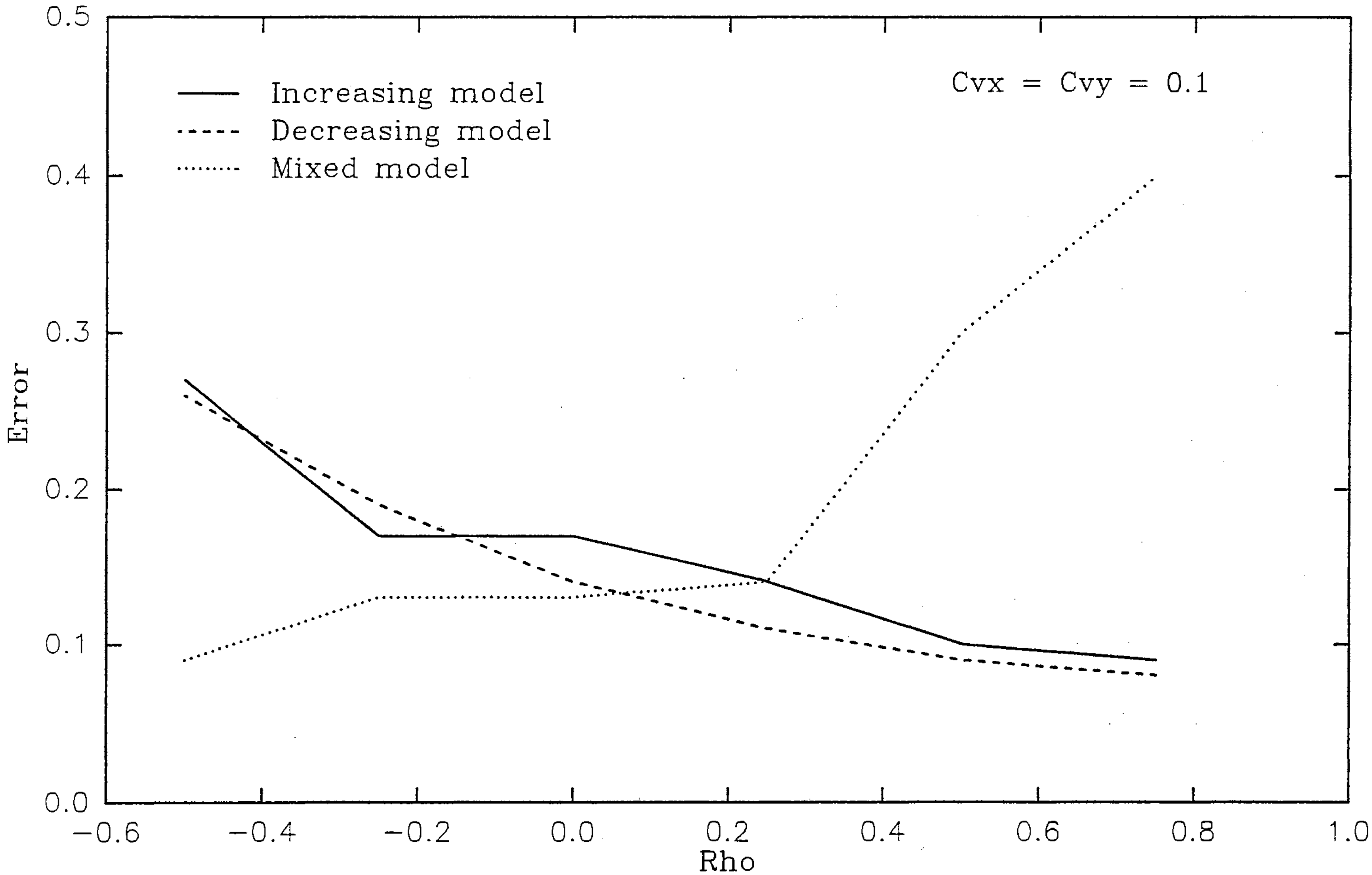

Figure 5−79. Error as a Function of Rho, Cv of x and Cv of y Equal to 0.1

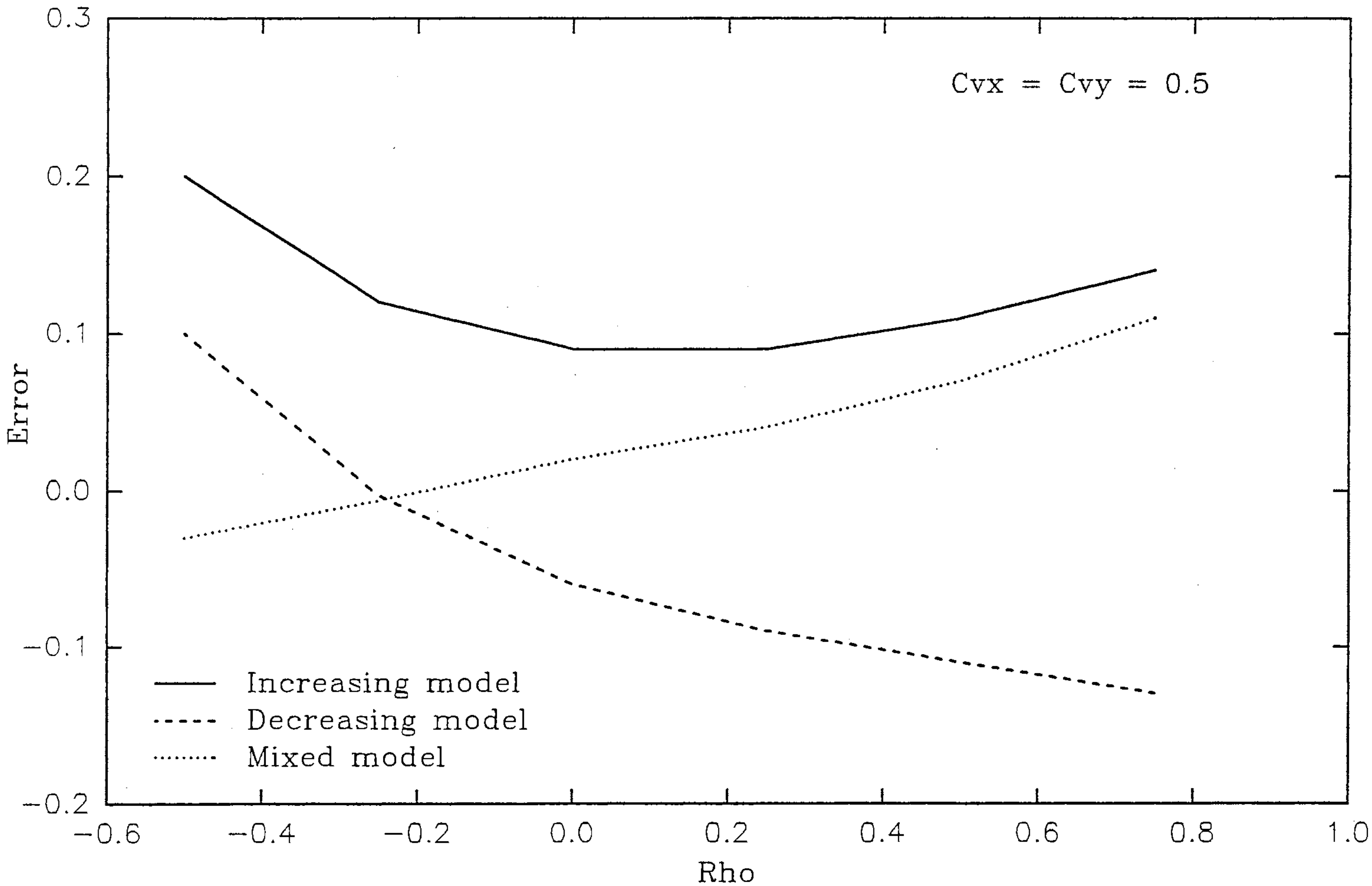

Figure 5−80. Error as a Function of Rho, Cv of x and Cv of y Equal to 0.5

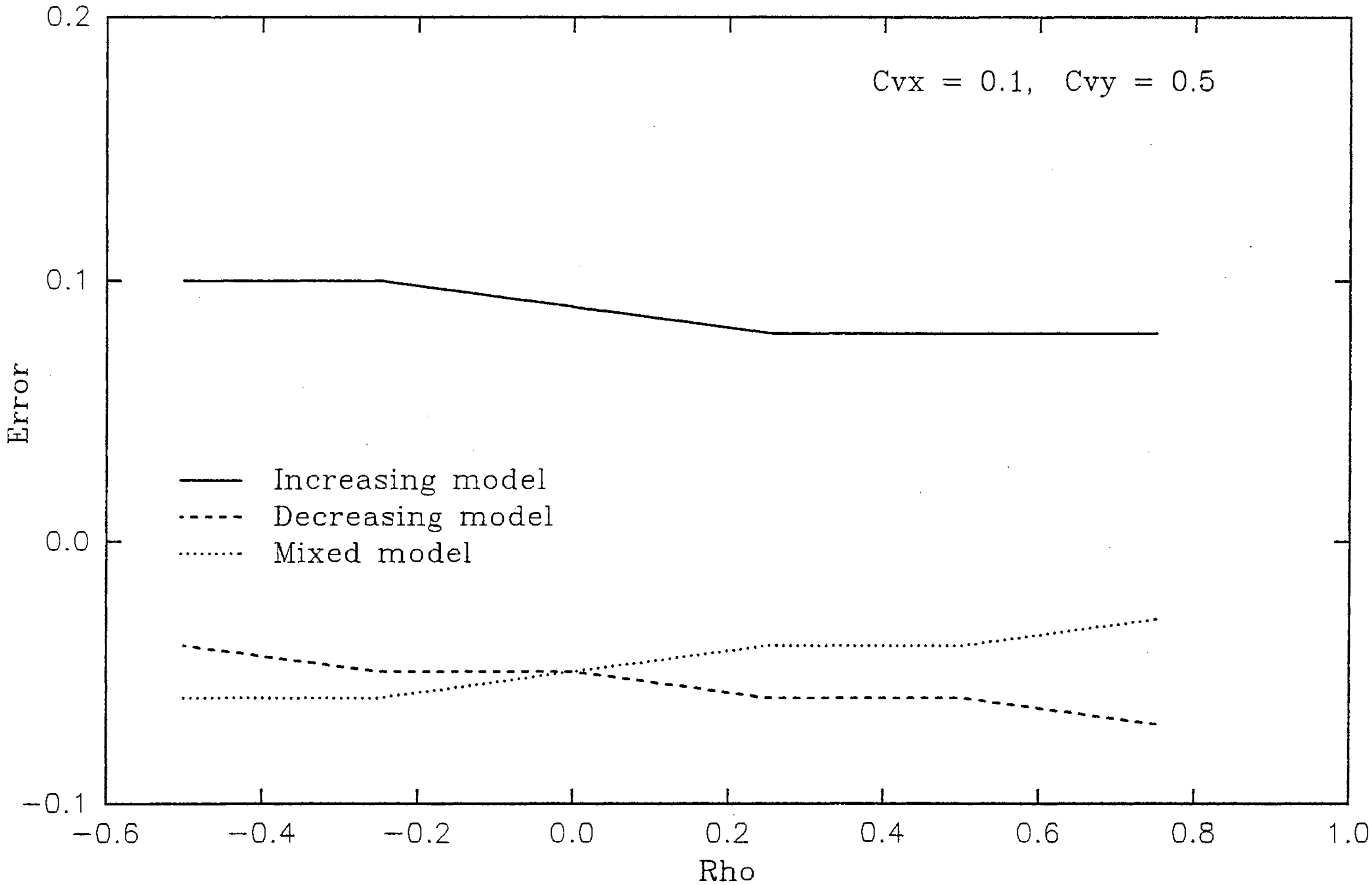

Figure 5−81. Error as a Function of Rho, Cv of x Equal to 0.1
and Cv of y Equal to 0.5

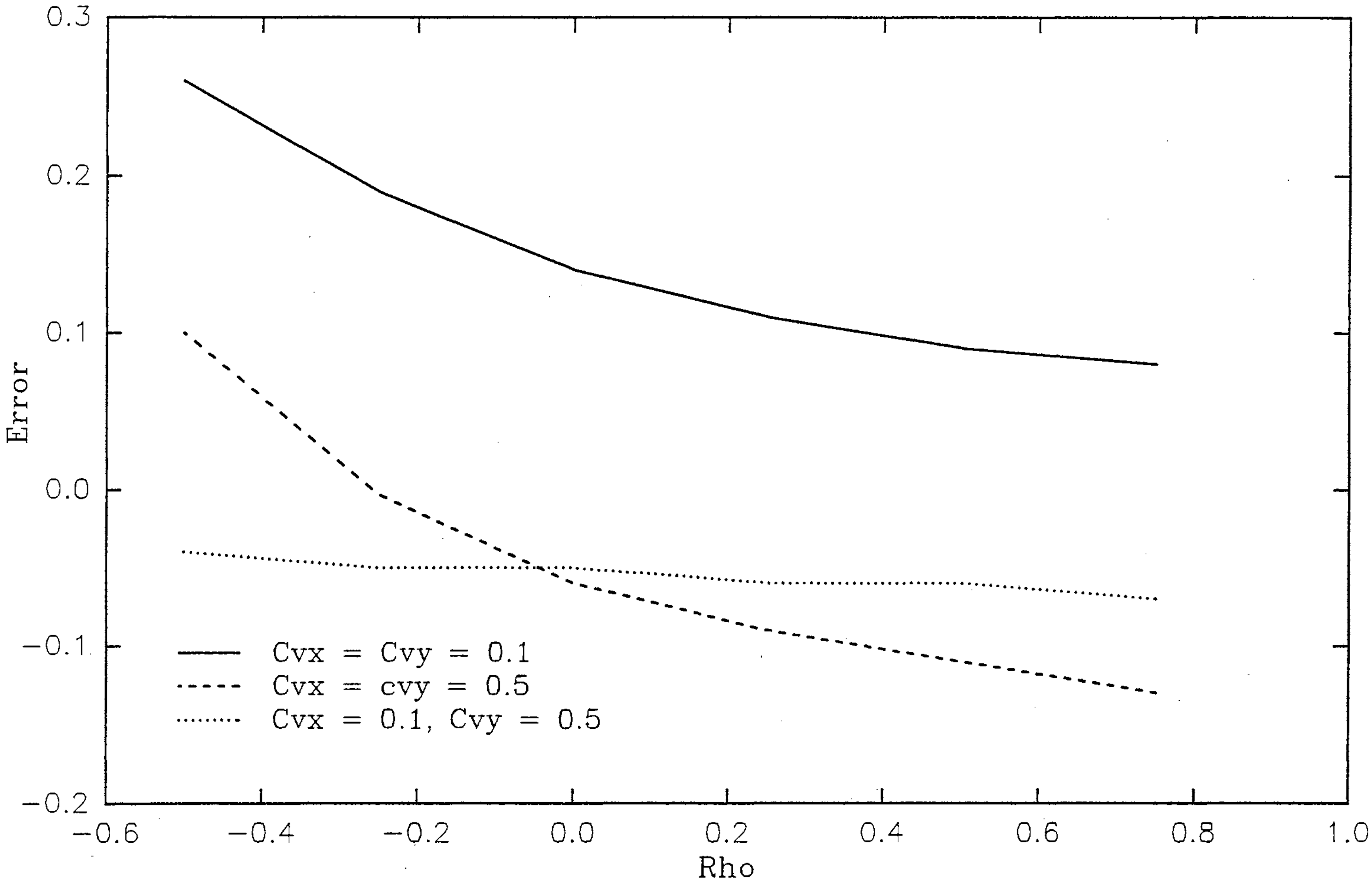

Figure 5−82. Error as a Function of Rho for EDMs

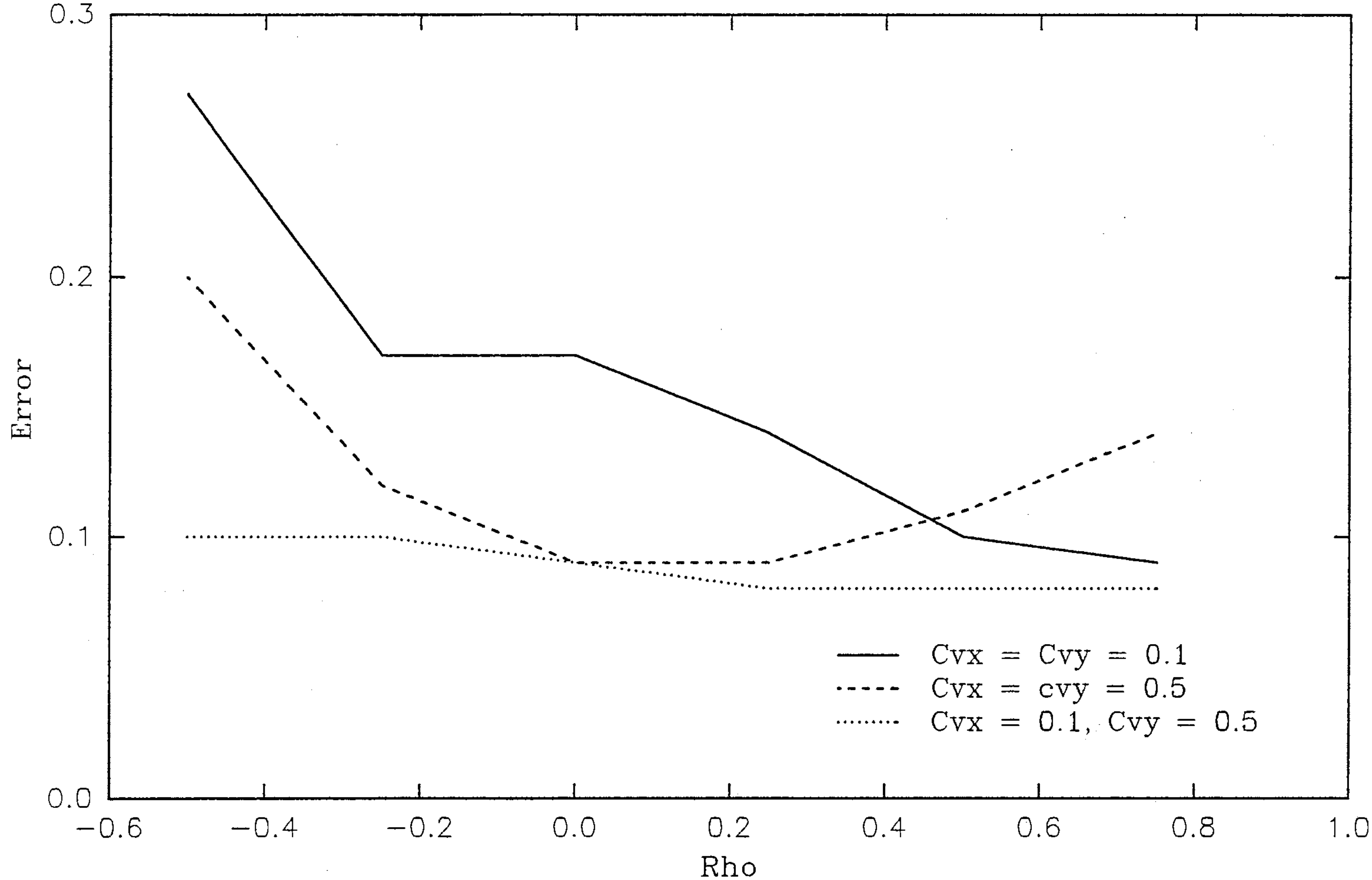

Figure 5−83. Error as a Function of Rho for EIMs

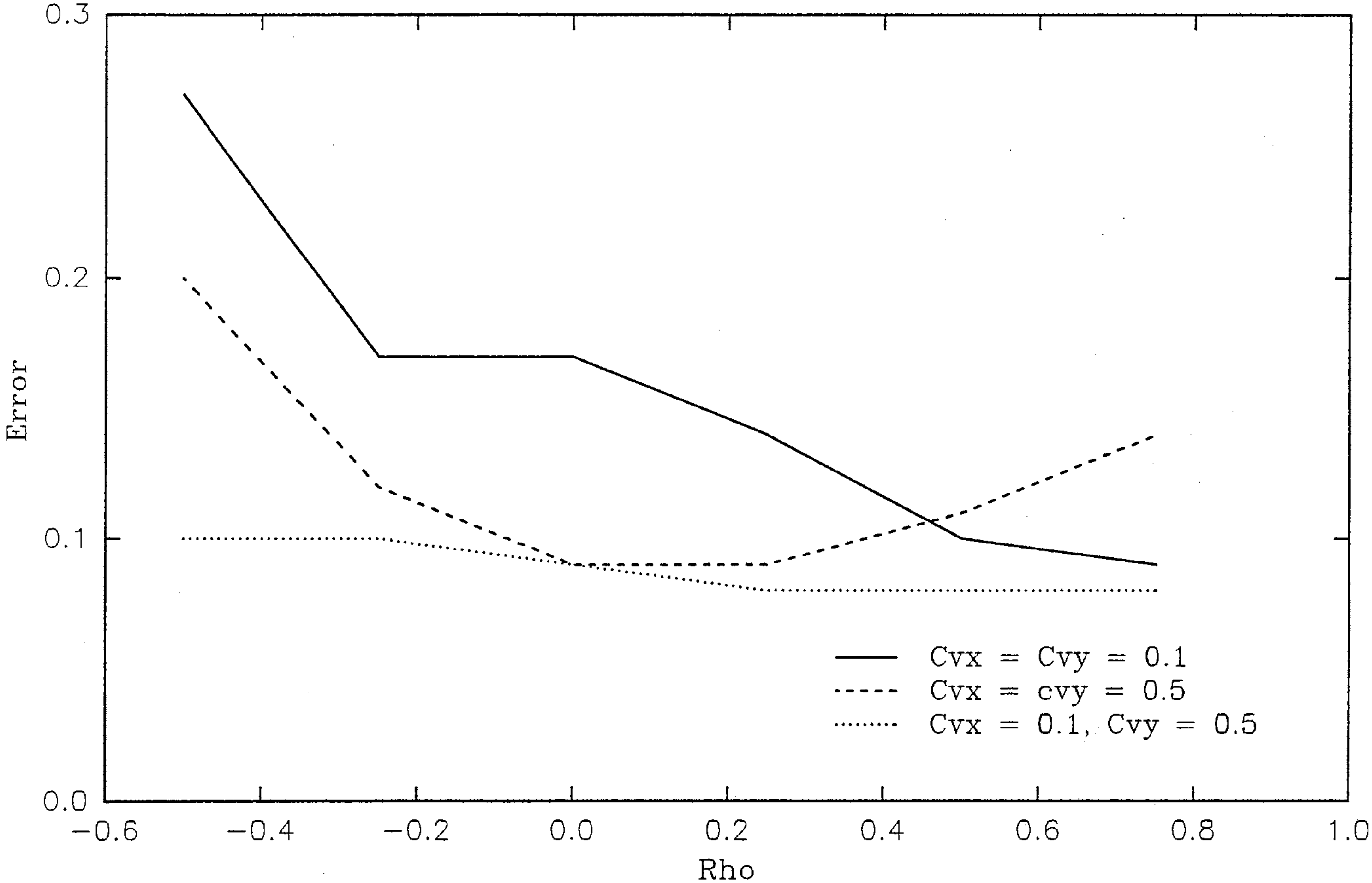

Figure 5−83. Error as a Function of Rho for EIMs

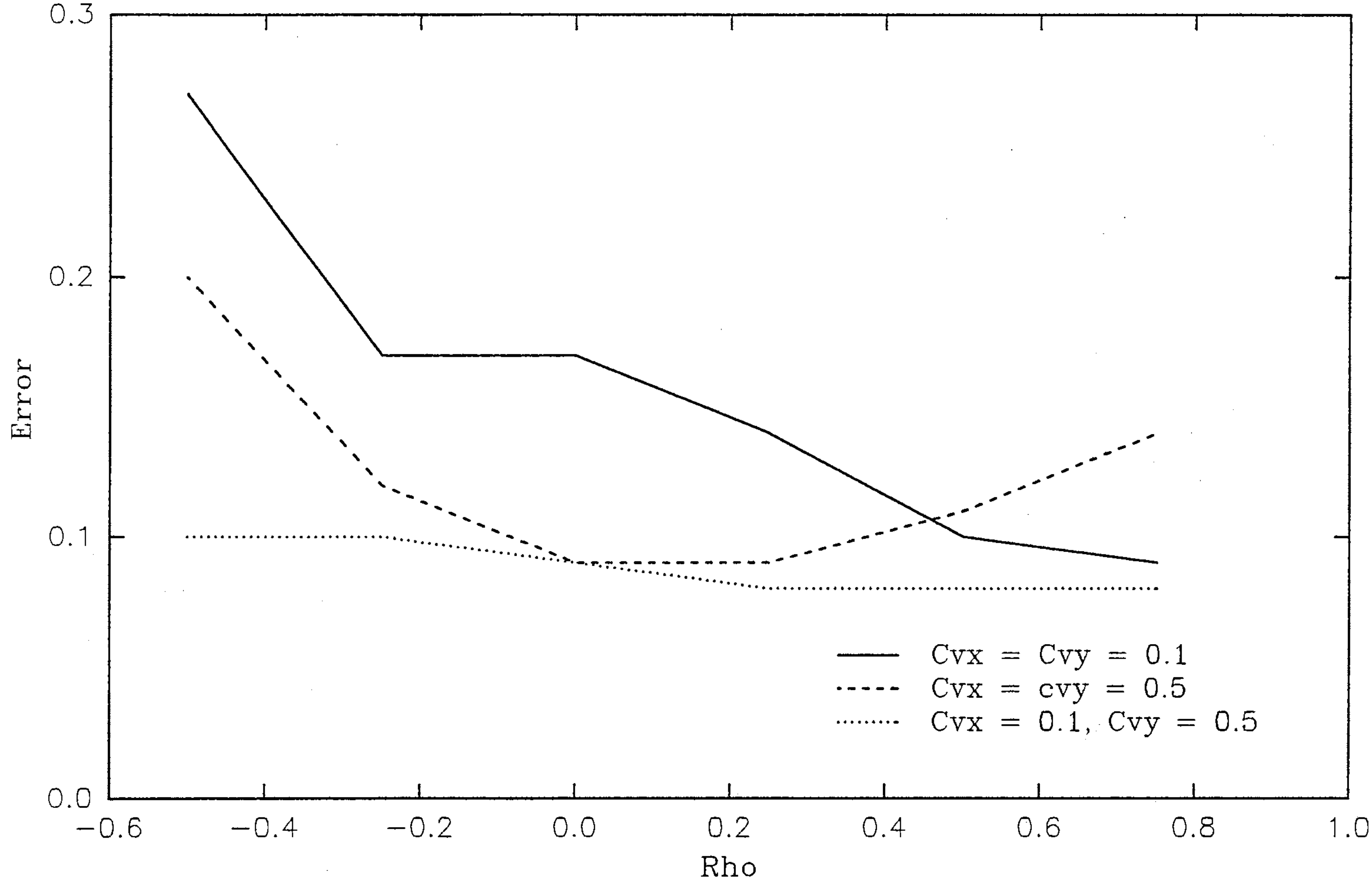

Figure 5−83. Error as a Function of Rho for EIMs

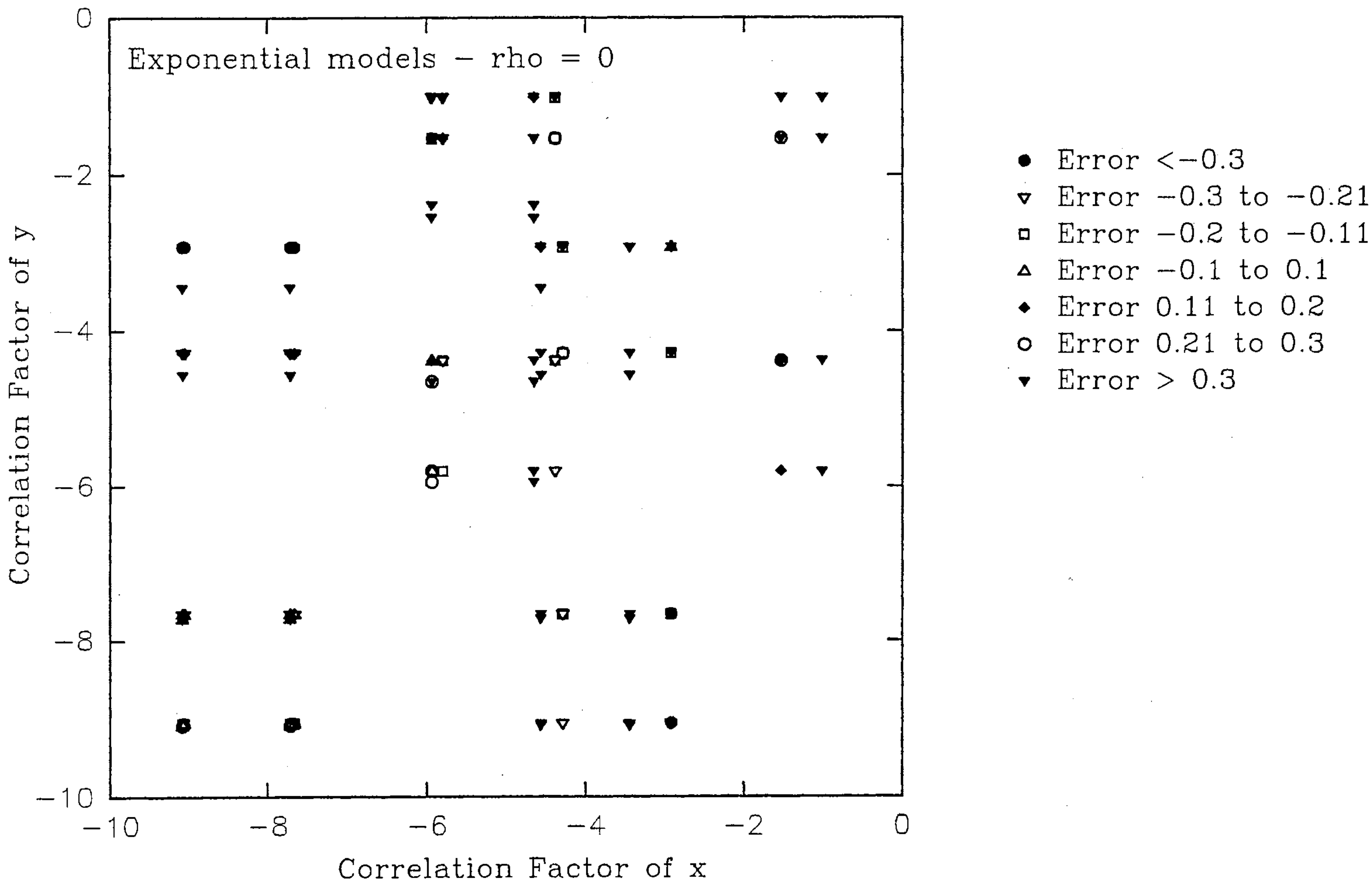

Figure 5-86. Error vs Correlation Factors of x and y

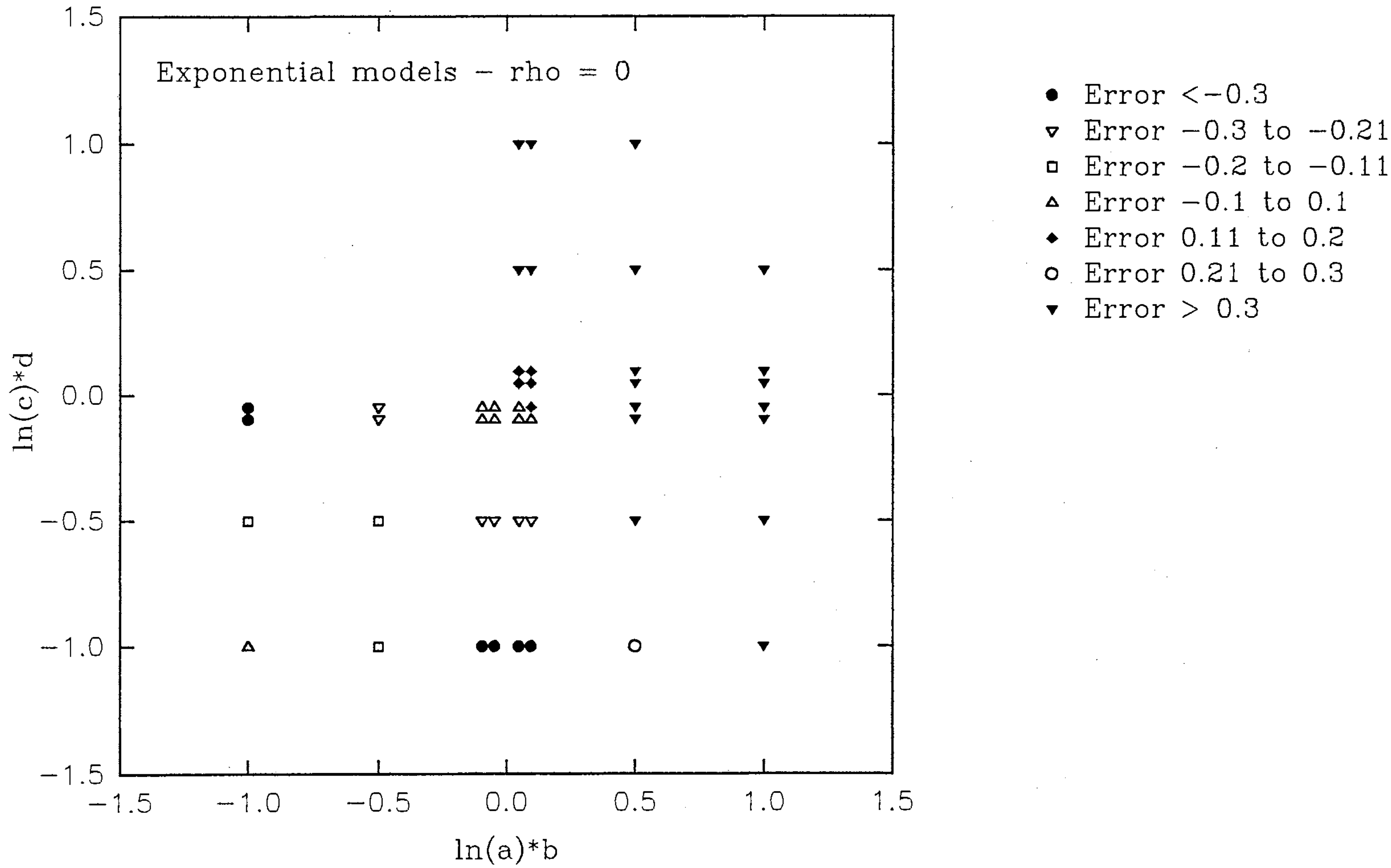

Figure 5−87. Error vs bln(a) and dln(c)

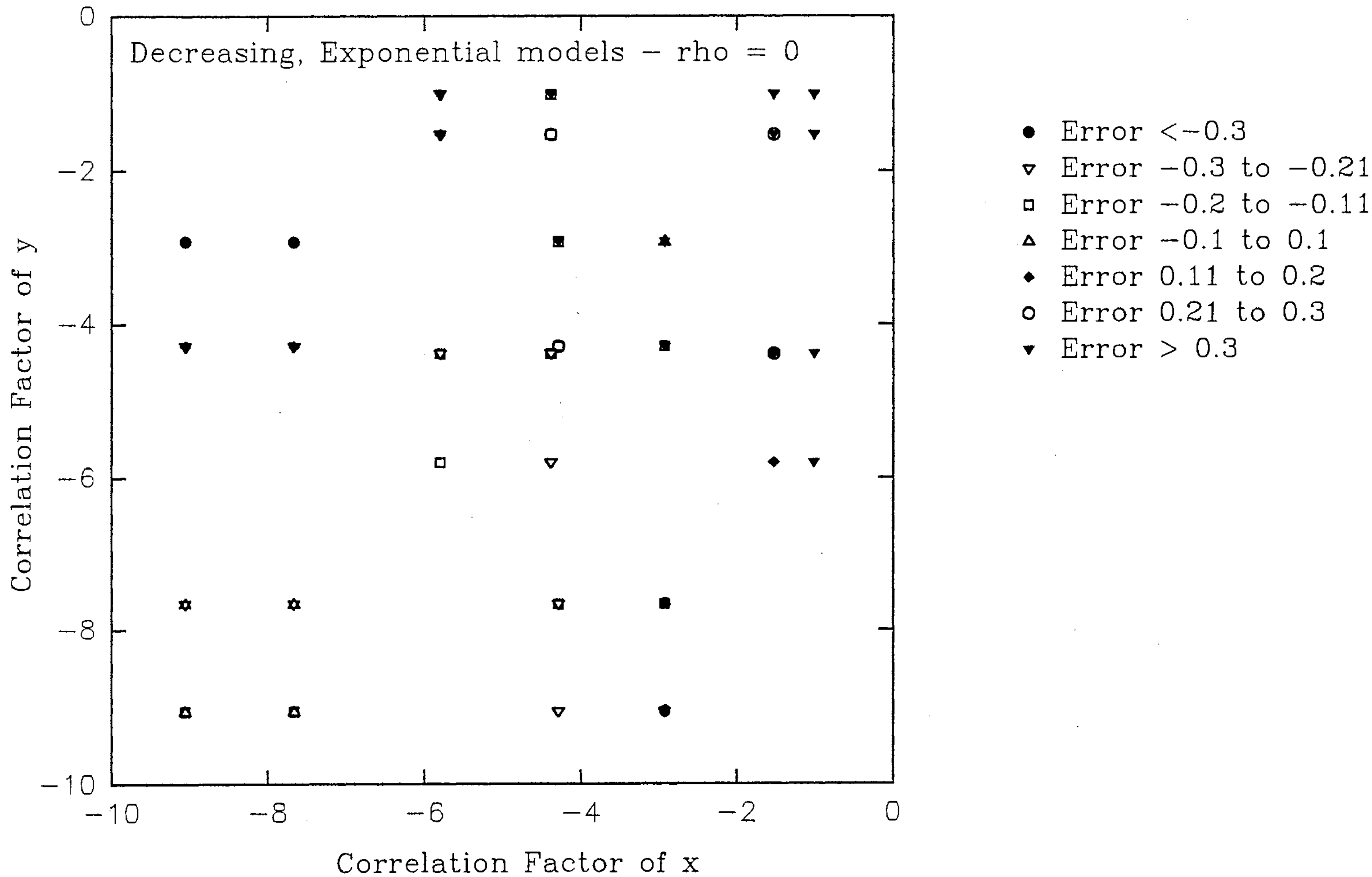

Figure 5-88. Error vs Correlation Factors of x and y - EDMs

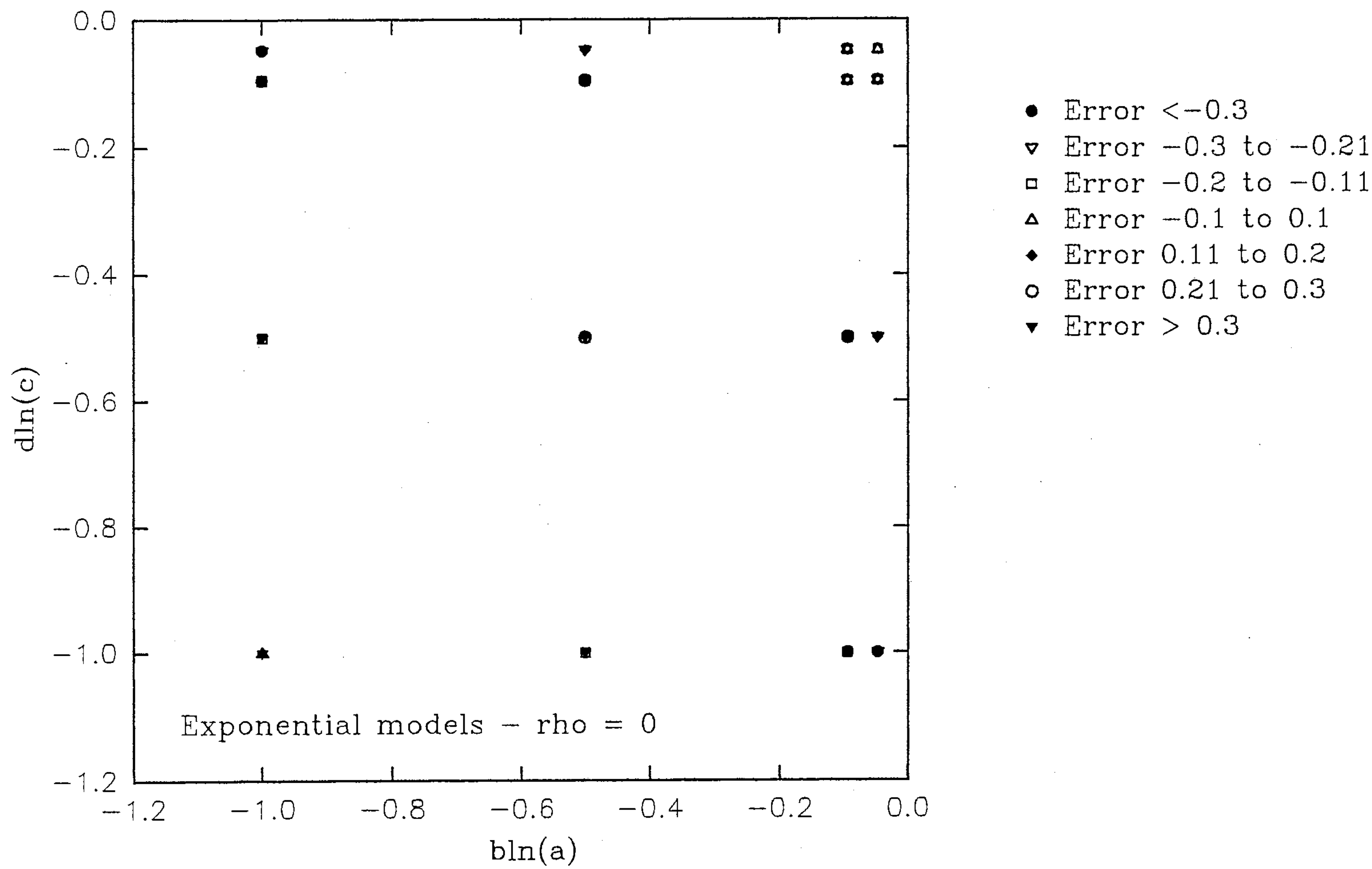

Figure 5−89. Error vs bln(a) and dln(c) − EDMs

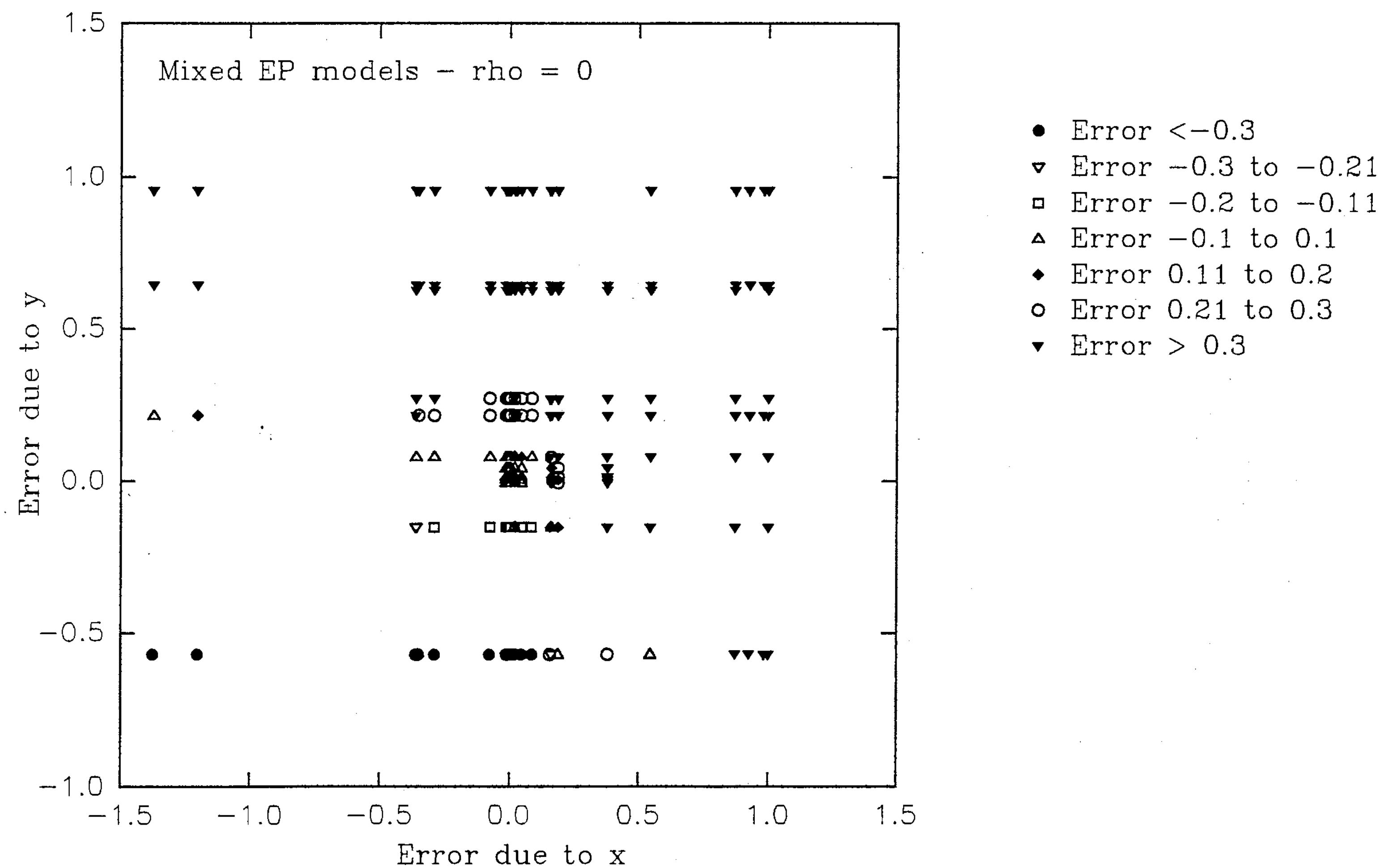

Figure 5−90. Error vs Error Due to x and Error Due to y − EP Models

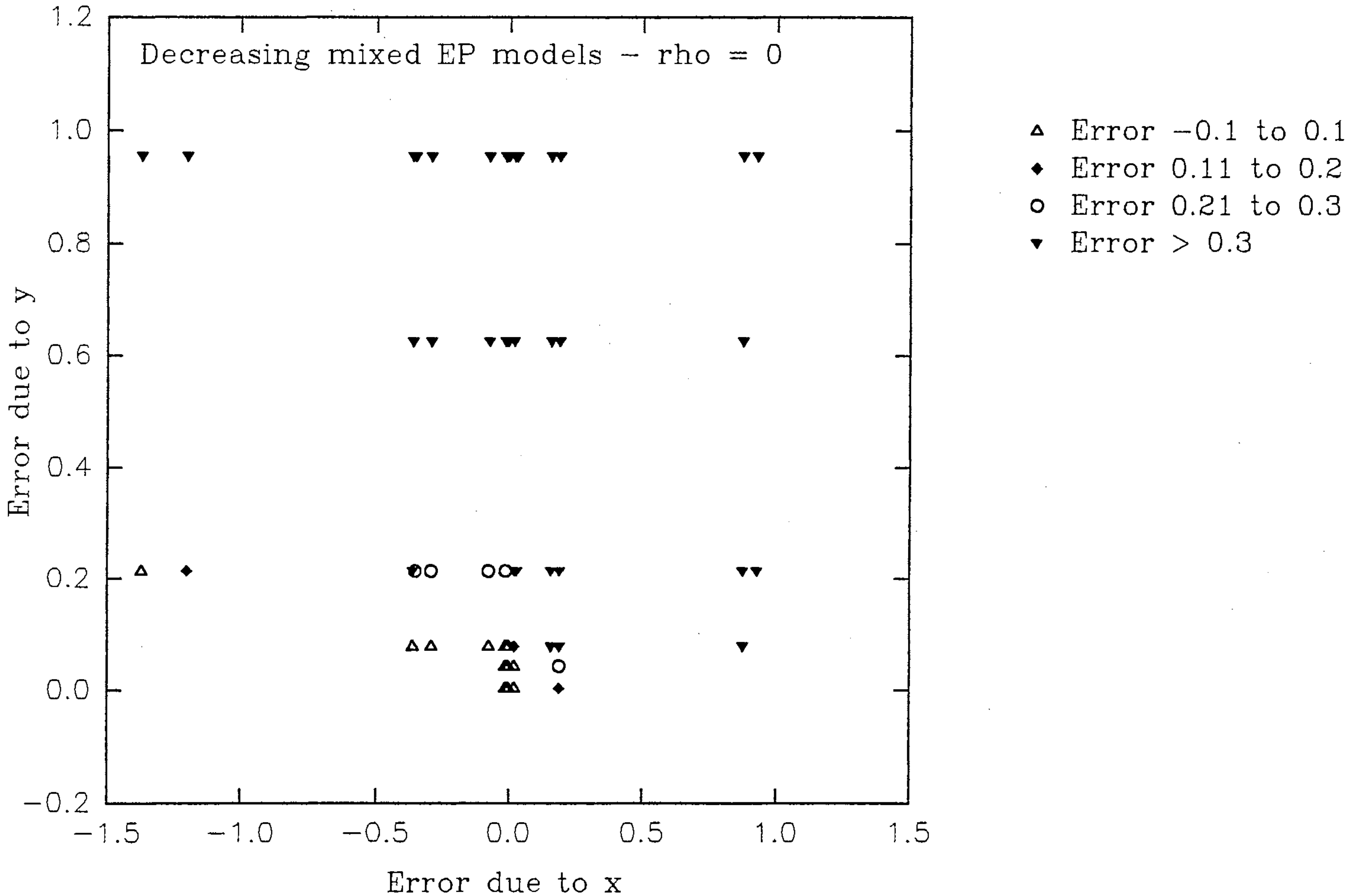

Figure 5−91. Error vs Error Due to x and Error Due to y − EPDMs

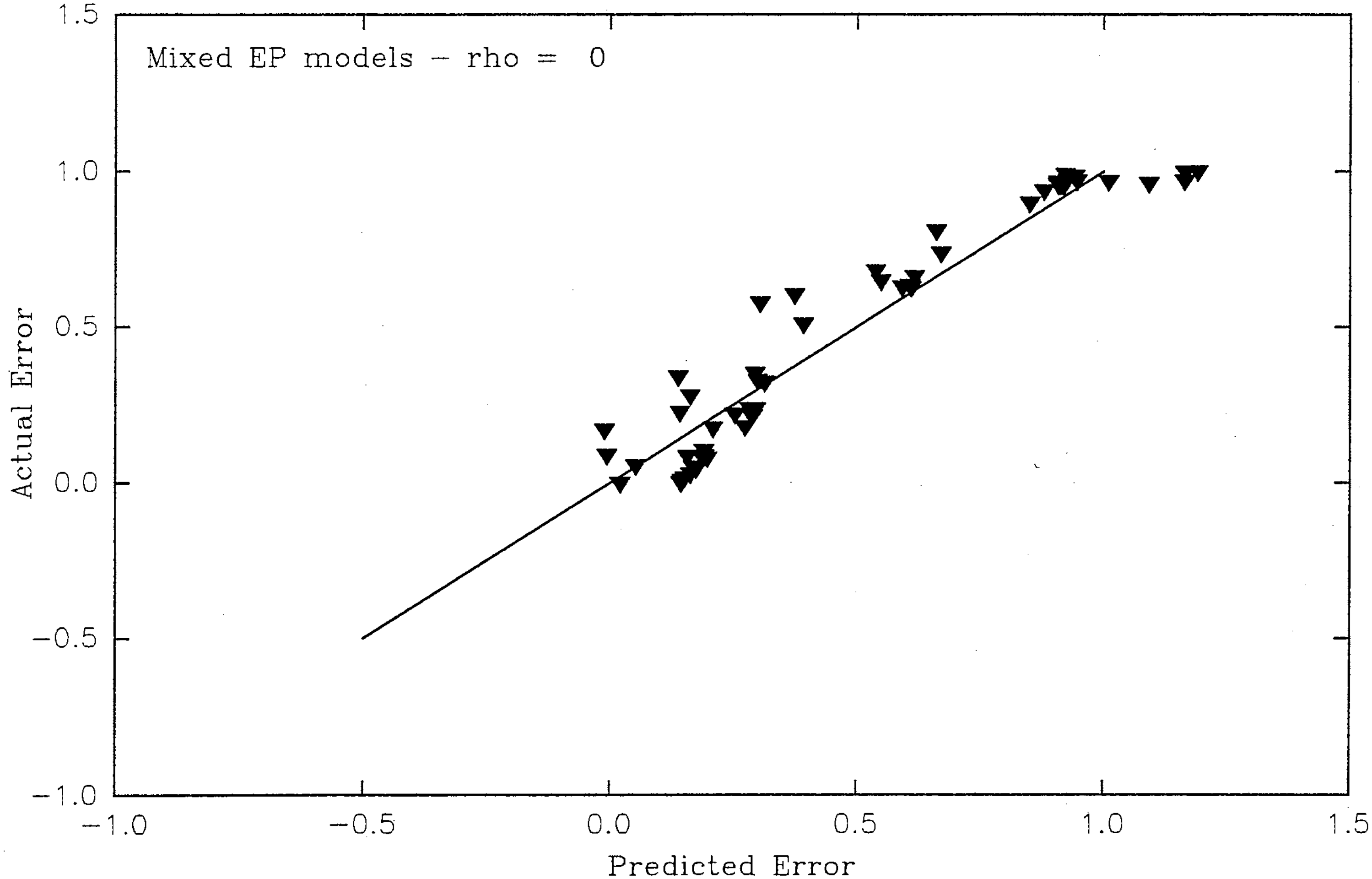

Figure 5-92. Actual vs Predicted Errors - Quadratic Model for EPDMs

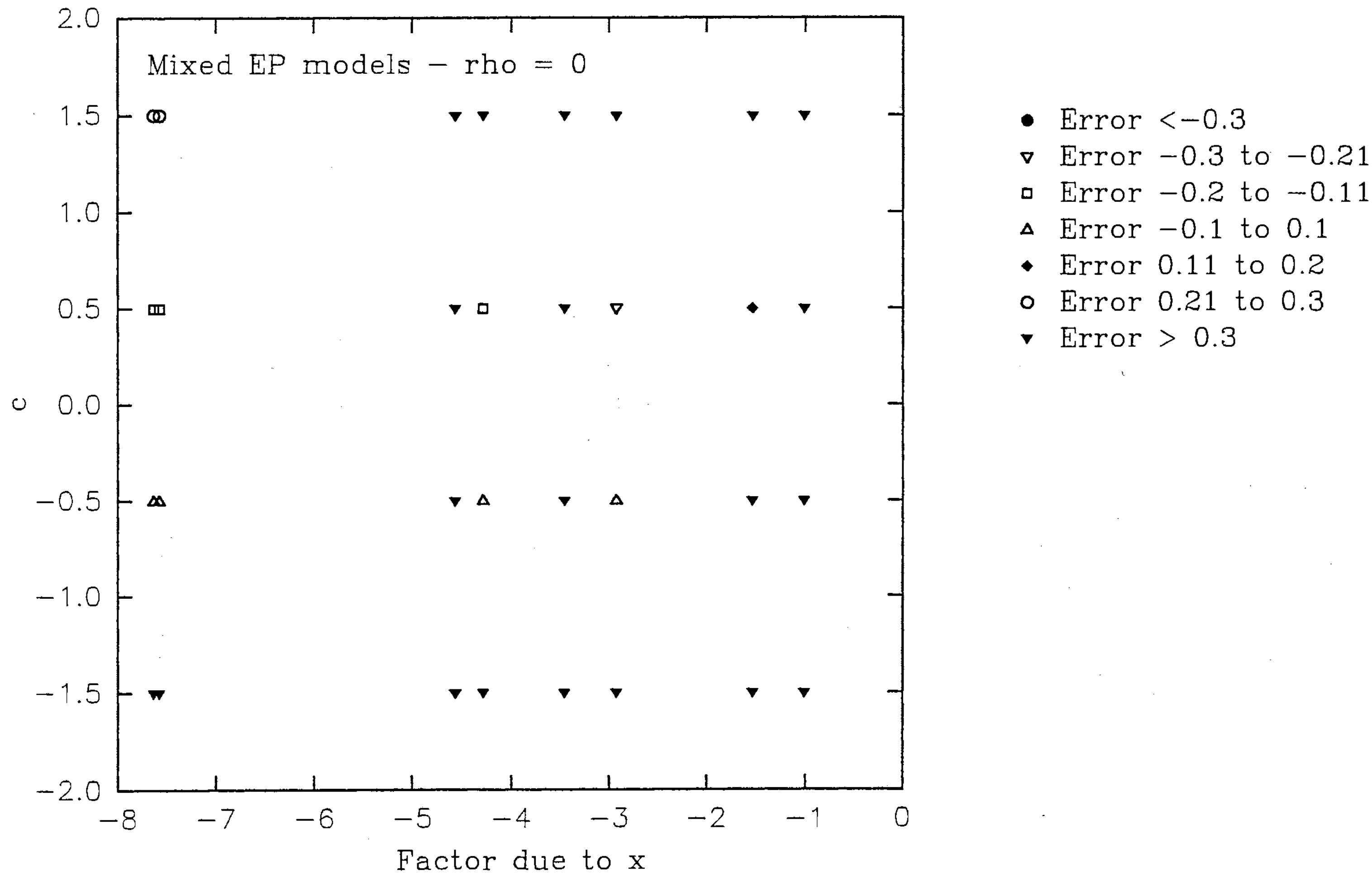

Figure 5–93. Error vs Correlation Factor of x and Power, c

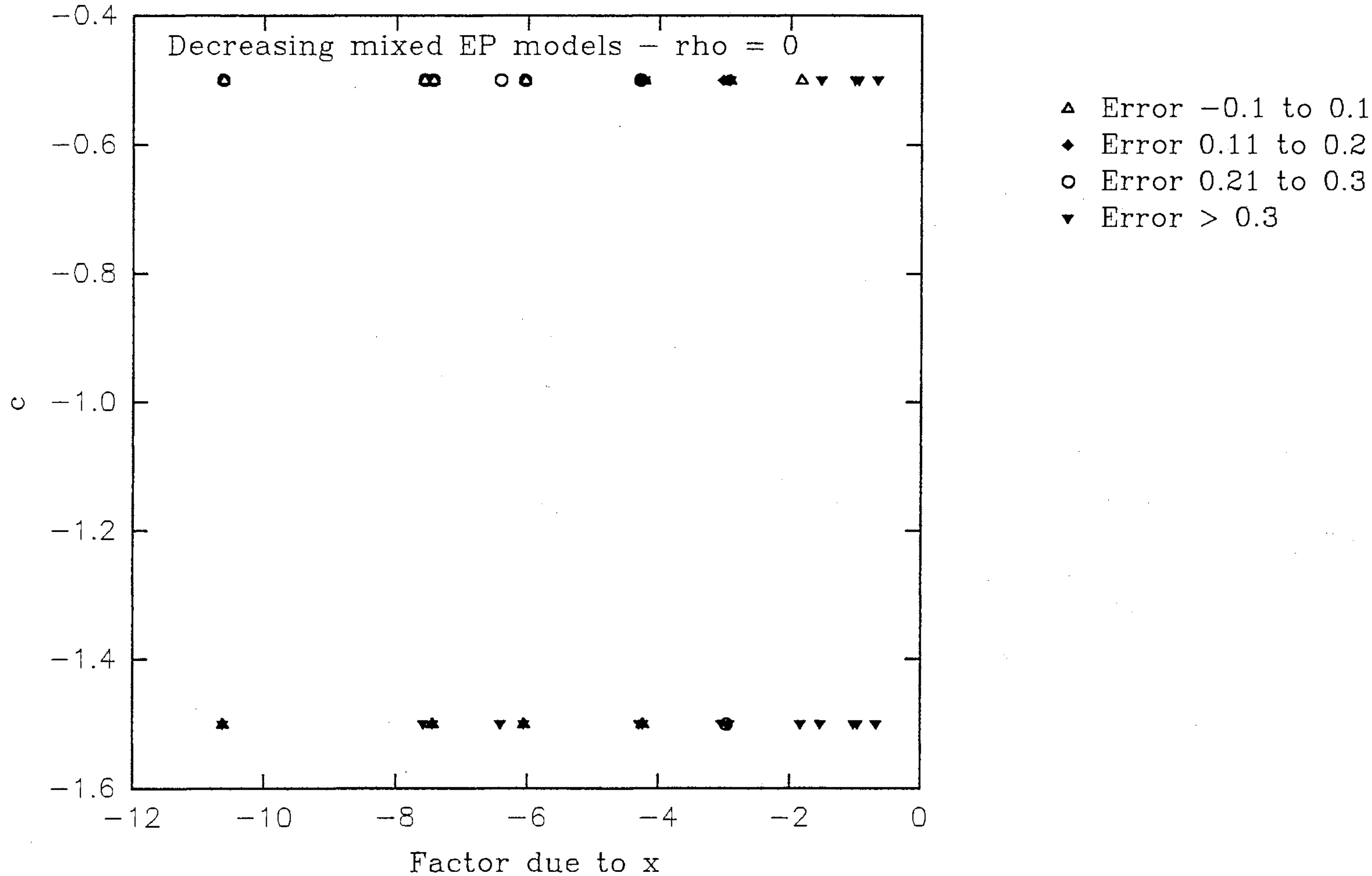

Figure 5–94. Error vs Correlation Factor of x and Power, c – EPDMs

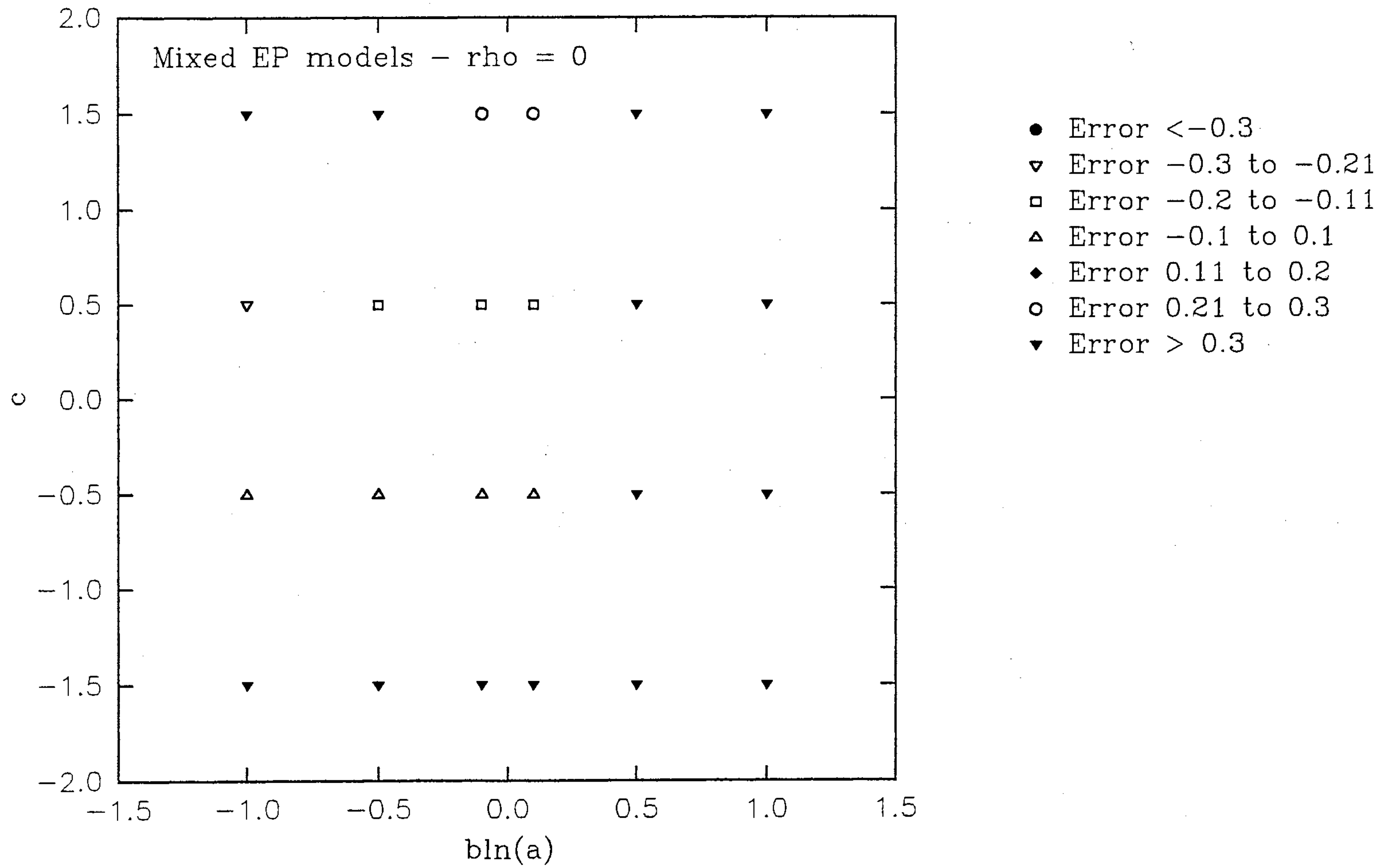

Figure 5–95. Error vs bln(a) and c

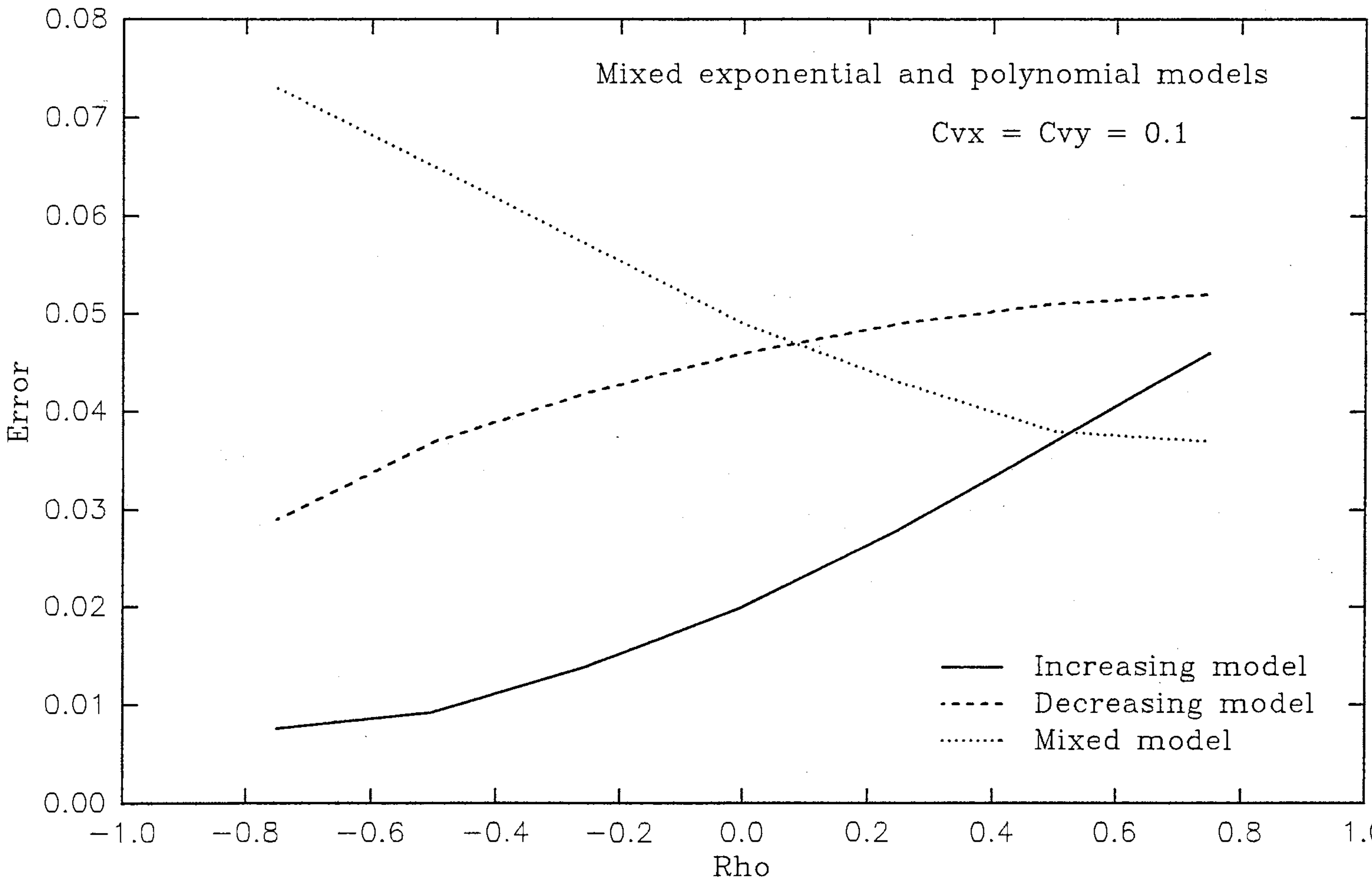

Figure 5−96. Error as a Function of Rho − Cv of x and Cv of y Equal to 0.1

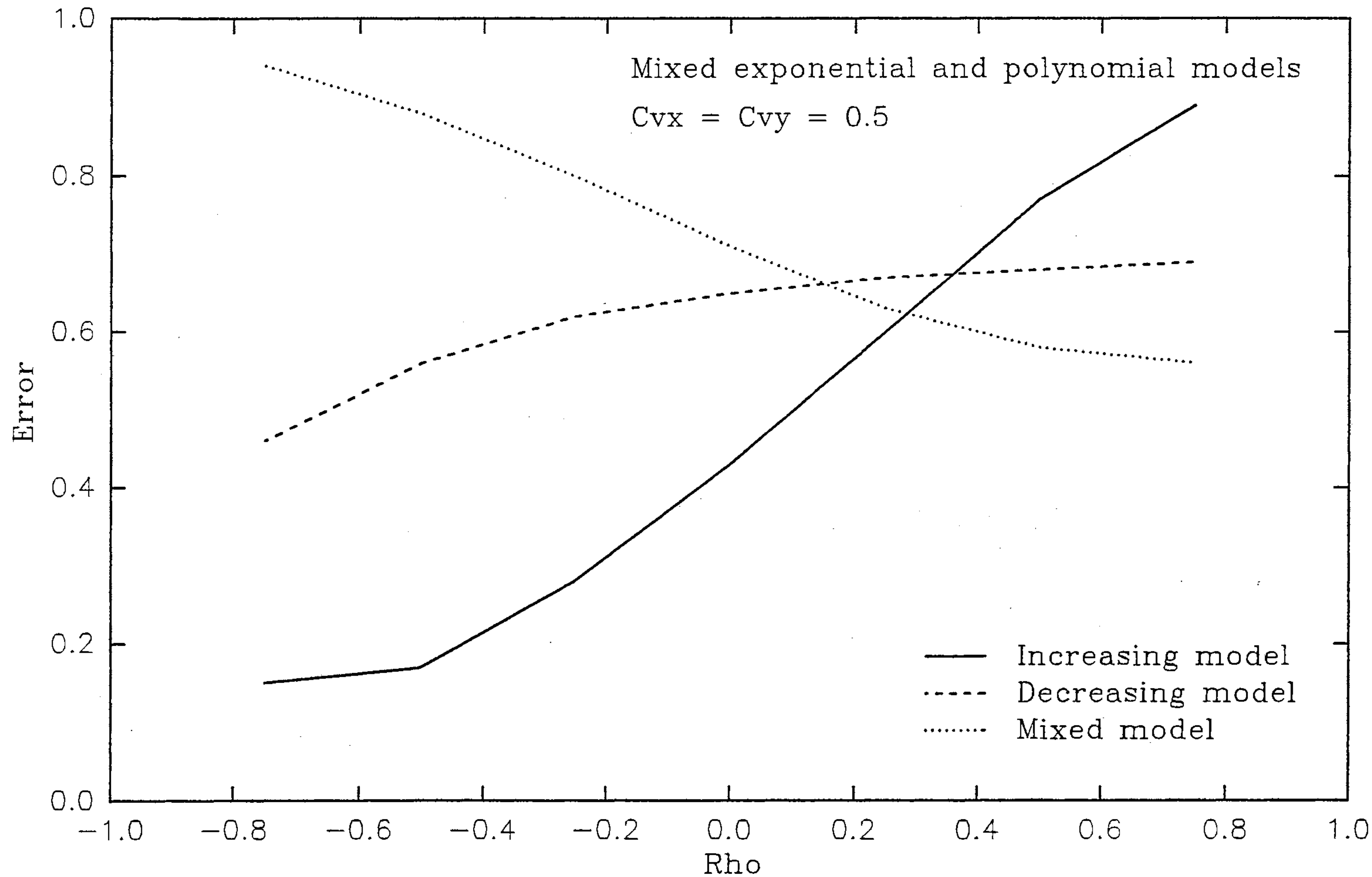

Figure 5−97. Error as a Function of Rho − Cv of x and Cv of y Equal to 0.5

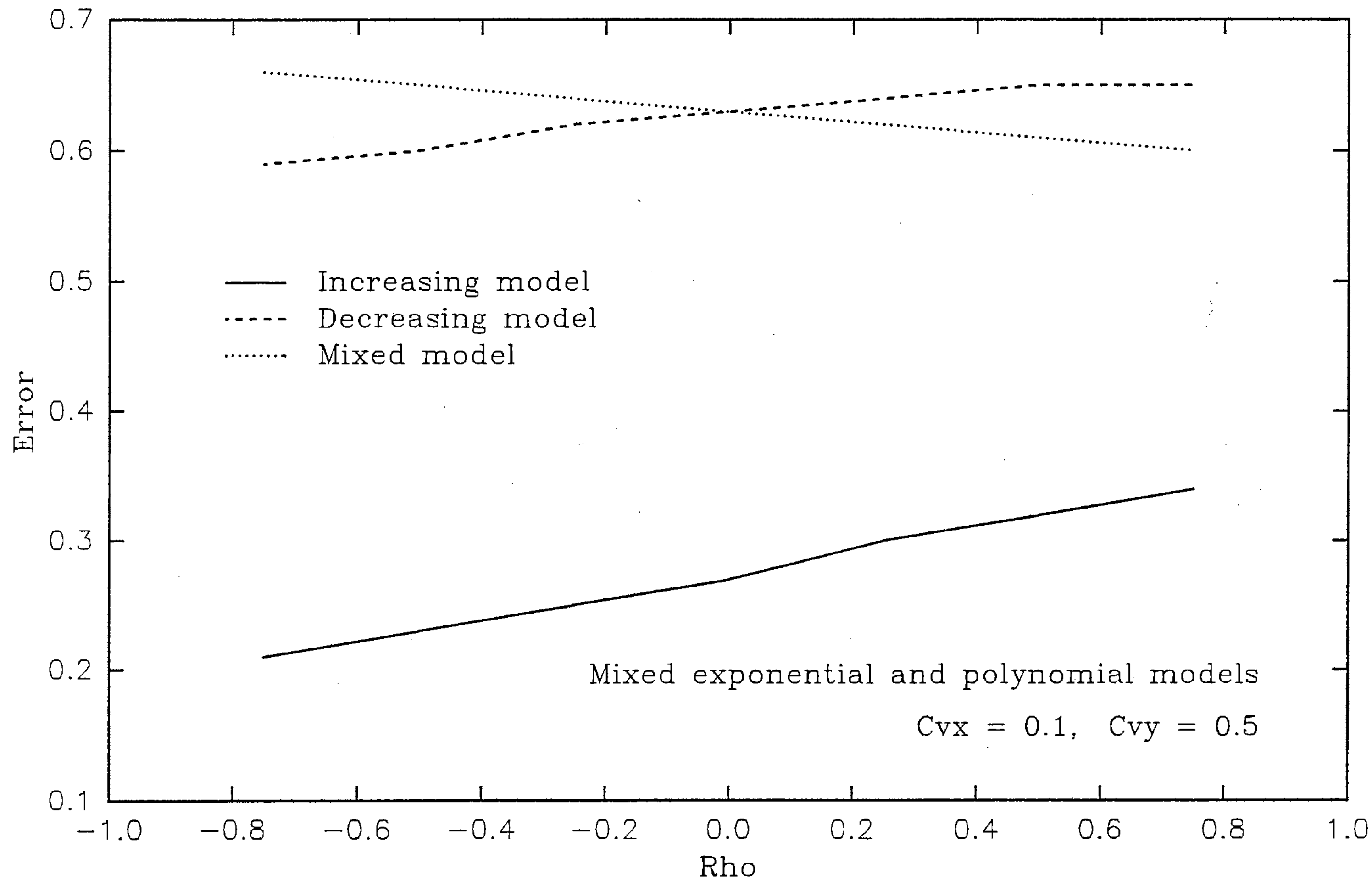

Figure 5−98. Error as a Function of Rho − Cv of x Equal to 0.1 and Cv of y Equal to 0.5

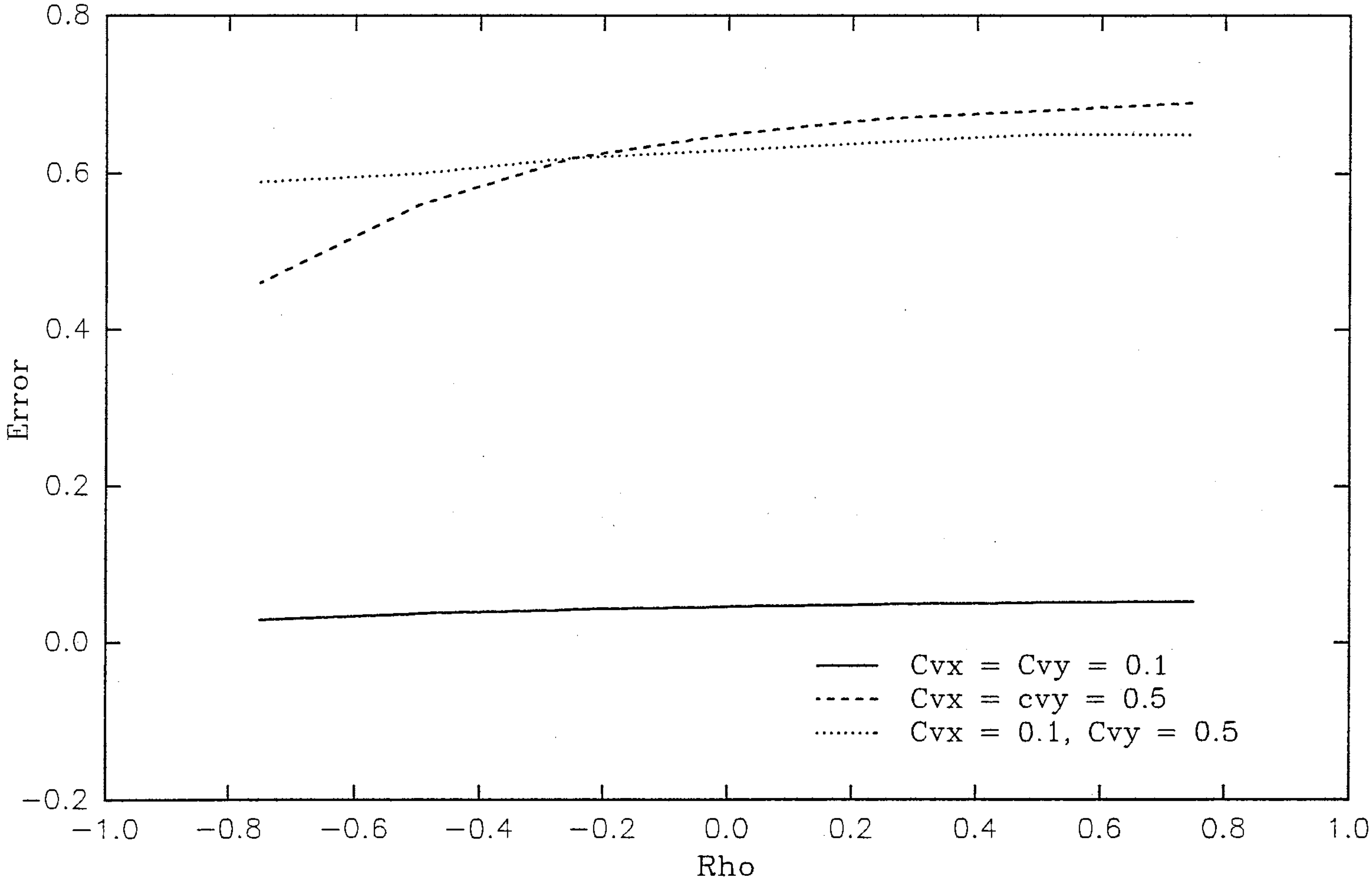

Figure 5−99. Error as a Function of Rho − EPDMs

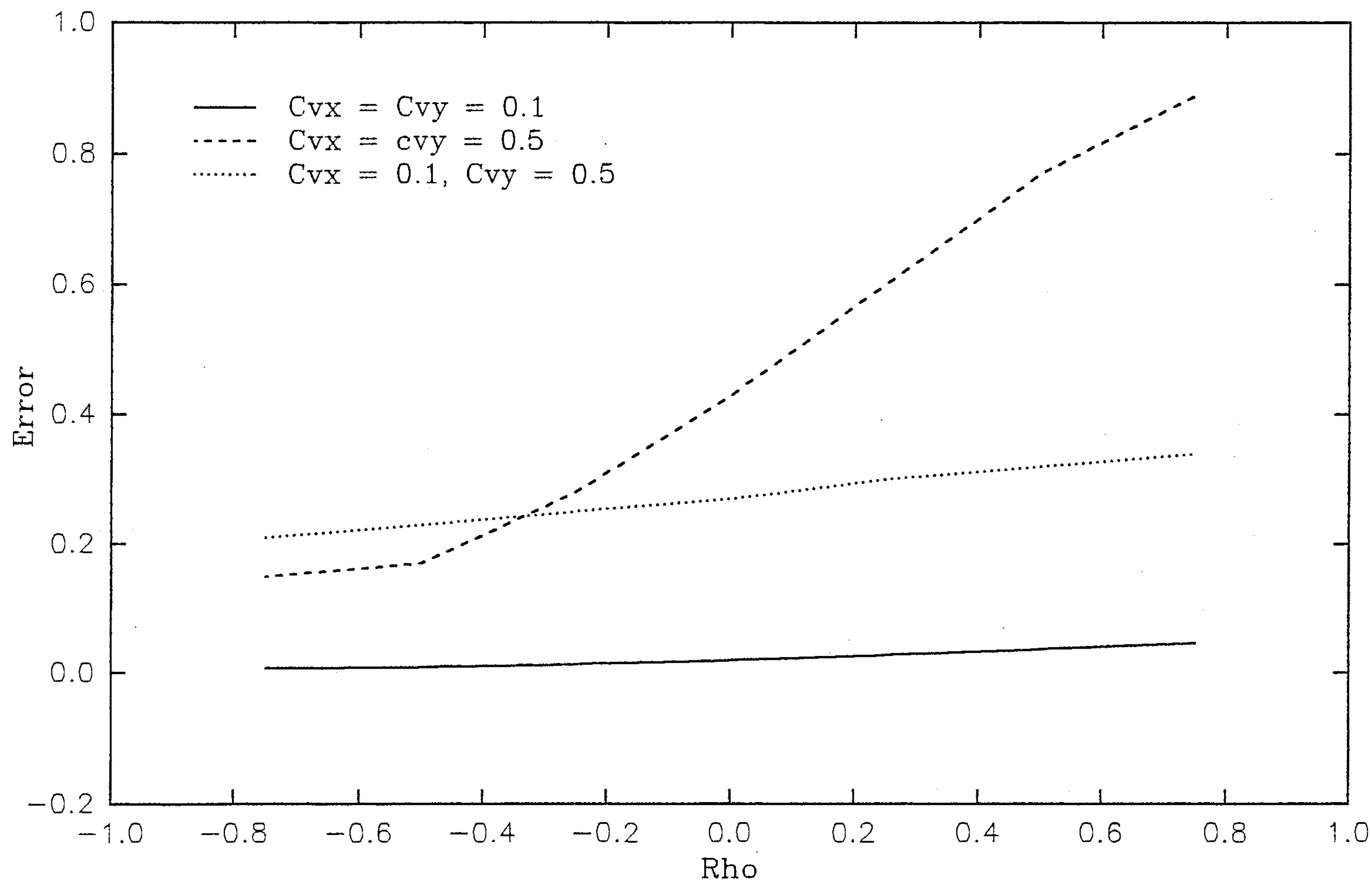

Figure 5−100. Error as a Function of Rho − EPIMs

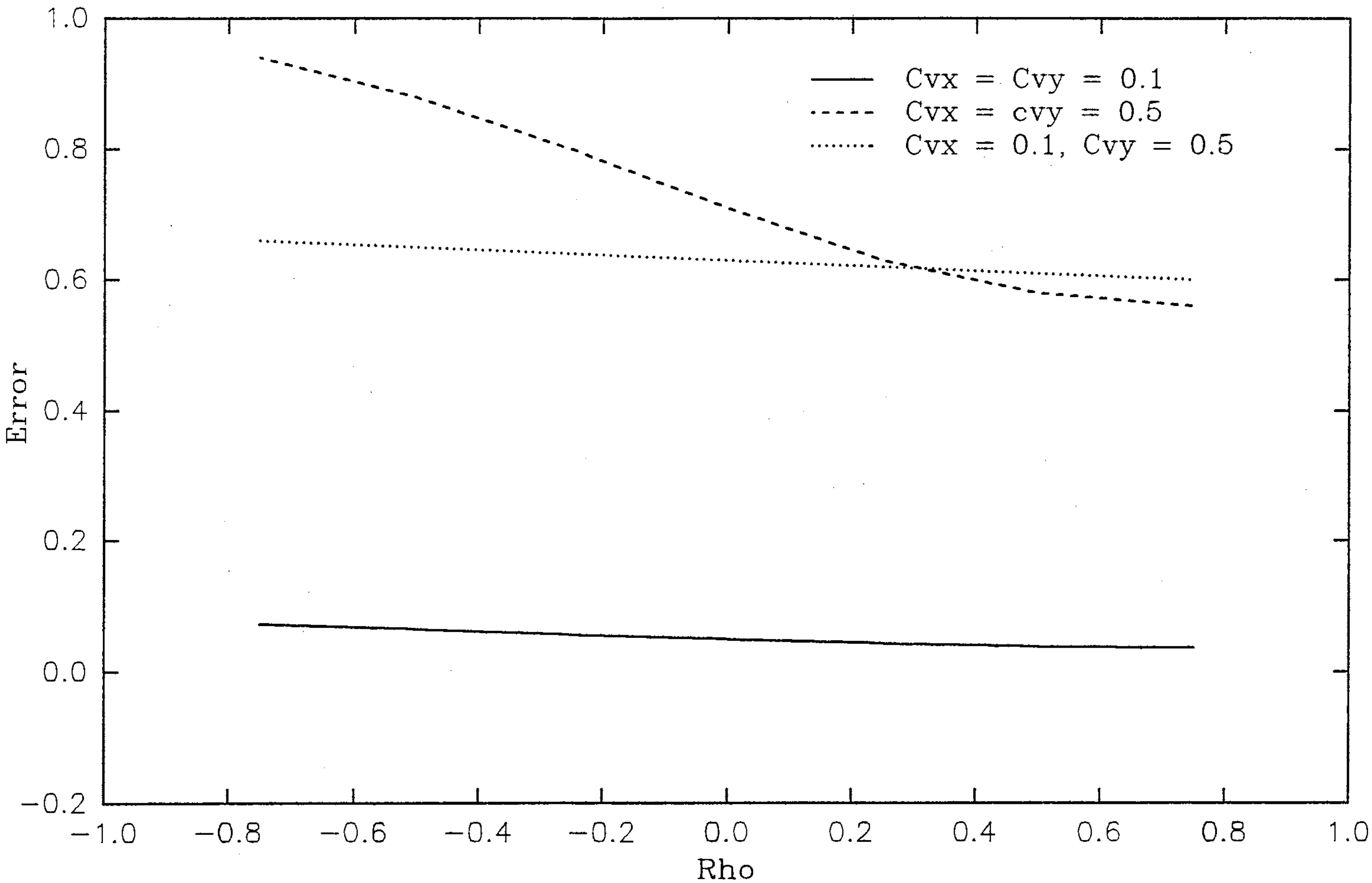

Figure 5−101. Error as a Function of Rho − EPMMs

CHAPTER SIX

SUMMARY, CONCLUSIONS, AND RECOMMENDATIONS

SUMMARY

The objective of this work was to develop a methodology for predicting the error in a FOA variance of a model response. The FOA variance is found by approximating the model response with the first order terms of a TS expansion of the model response about the means of the parameters. The variance of this linear approximation, which can be computed without need for numerical integration, is then computed. Unfortunately, this technique is not particularly useful because the results are not always acceptably accurate, and there is very little published guidance addressing under what circumstances they will be sufficiently accurate.

First, the sources of error in the FOA variance had to be determined. One source of error was the failure of the linear surface to match the nonlinear model response surface. Another source of error was the uncertainty in the parameters. As parameter uncertainty increases, the range of the parameter for which there is significant probability increases. Given a response surface and tangent point, the linear surface at that tangent point will better match the surface if smaller ranges of the parameters are of interest. Thus, as parameter uncertainty increases, the linear surface becomes a poorer approximation of the model response, and the FOA approximate variance increases in error. For exponential models, it was also discovered that the mean of the parameter (point of tangency for the linear approximation) also affected the error in the FOA approximate variance.

To evaluate the error in the FOA variance, a grid of polynomial and exponential models with different nonlinearities and parameter uncertainties was constructed. The "true" variance was found by numerical integration.

It was then discovered that the error in the FOA variance behaved quite differently for models with exponential or polynomial formats. For one parameter exponential models of the form $y = a^{bx}$, the error was a function of the nonlinearity of the model, the uncertainty of the parameter, which is quantified by C_v, and of the mean of the parameter. A factor which takes in the model nonlinearity and the mean is the correlation coefficient between the x's and y's, where five x's are chosen in a specific manner. Curves giving the error vs the correlation factor were then plotted for different values of C_v. Interpolating between curves for C_v's not represented was shown to give satisfactory results.

For one parameter polynomial models, the error was a function of only parameter C_v and model nonlinearity. Given a model of the form $y = ax^b$, the b power was a satisfactory measure of model nonlinearity. Curves giving the error as a function of b for selected C_v's were constructed. If the model was not explicitly in that form, a polynomial model of the form $y = \text{constant} + ax^b$ could be estimated and the b power from the estimation used to enter the curves. Interpolation between curves for C_v's not present gave satisfactory results.

Since different methods were required for polynomial or exponential models, a method to classify models was required. If the ratios of the second to first derivatives at several points were the same, regardless of the points at which they were evaluated, then the model has an exponential form. If that ratio divided by the value of x at which it was evaluated is constant, then the model is polynomial. An alternative method is to estimate exponential and polynomial models and determine which one fits better. There may be some models which are not clearly exponential or polynomial, in which case any error prediction may not be valid.

For two parameter models, there was a much larger grid of models required. For a model $z = f(x,y)$, the form could be polynomial with respect to both x and y, exponential with respect to both x and y, or exponential in one and polynomial in the other. The scope of the model grid increased further to take in various positive and negative correlations of the parameters.

For polynomial models, the error in the FOA variance was a function of the parameter C_v's, the powers to which x and y were raised, and the correlation between parameters. The behavior of the error with respect to any one of these factors was nonlinear and non-monotonic.

For strictly polynomial models with independent parameters, it was possible to formulate an error predicting model. The independent variables in the model were the error found by setting y equal to its mean and predicting an error based on five x - model response pairs, or error due to x, and the equivalent error due to y. It was also possible to formulate a model for ρ equal to ± 0.25. For some higher ρ's, it was possible to formulate models to predict the error with the correlated parameters as a function of the error which would have been present had the parameters been independent. Verification trials of the procedures gave acceptable results when parameter C_v's were the same as those used to estimate the models.

For exponential models, the error in the FOA variance was a function of the parameter means and C_v's, the model nonlinearity, and the parameter correlation. The behavior of the error with respect to any of these factors was extremely nonlinear and was also non-monotonic. All the techniques which had worked for one parameter models or for two parameter polynomial models were tried, and no attempts to formulate any type of predictive methodology were successful. In some cases, it is possible to predict if the error would be greater than or less than a certain value.

The mixed polynomial models had results similar to the strictly exponential models. Here, the error was a function of parameter C_v's, the nonlinearity of the exponential component, the power of the polynomial component, the mean of the parameter in the exponential component, and the correlation between the parameters. Again, this behavior was highly nonlinear and was non-monotonic. Efforts to formulate an error predicting model were unsuccessful. It was possible to identify some conditions under which the error was either greater than or less than a certain amount.

The two parameter models can be classified in either parameter by setting the other parameter equal to its mean and using the procedures for one parameter models. An example application in which the response was not an explicit function of the parameters was demonstrated. The model was classified as polynomial in both its parameters. The error prediction techniques were applied. They were sufficiently accurate that a correct accept or reject decision could be made.

Step-by-Step Procedure for One Parameter Models

To facilitate use of the technique, a step-by-step procedure with accompanying flow chart (Figure 6-1) is presented.

Step 1. Determine parameter C_v. If parameter C_v is greater than 1.5, the procedure is not applicable. (Stop)

Step 2. Compute the model responses, first derivatives, and second derivatives at the five recommended points.

Step 3. Find the ratios of the second to the first derivatives at each of the five points. If the ratios are the same at all five points, the model is clearly exponential and the exponential error predicting procedure may be used. Go to Step 9.

Step 4. Divide each derivative ratio by the value of x at which it was evaluated. If these five quotients are equal, the model is clearly polynomial and the polynomial procedure can be used. Go to Step 10.

Step 5. Estimate polynomial and exponential using the five parameter - response pairs. If the estimated exponential model clearly fits better, the exponential procedure can be used. Go to Step 9.

Step 6. If the estimated polynomial model clearly fits better, the polynomial procedure applies. Go to Step 10.

Step 7. If both models appear to fit well, use both the polynomial and exponential procedures and accept the larger error. Complete Steps 9 and 10 and compare results. (Stop)

Step 8. If neither model appears to fit, the procedure is are not applicable. (Stop)

Step 9. Apply exponential procedure. Compute the correlation factor and find the error using curve(s) for the appropriate C_v(s). (Stop)

Step 10. Apply polynomial procedure. Estimate b power and find the error using the curve(s) for the appropriate C_v(s). (Stop)

Step-by-Step Procedure for Two Parameter Models

To facilitate use of this procedure, a step-by-step listing with accompanying flow chart (Figure 6-2) is presented.

Step 1. Determine parameter C_v's. If either is greater than 1.0, then the procedures are not applicable. (Stop)

Step 2. Set x equal to its mean and evaluate the model at y equal to the five recommended points. Set y equal to its mean and evaluate the model at x equal to the five recommended points. Determine if the model is polynomial, exponential, or unable to classify in both x and y.

Step 3. If it is not possible to classify the model in either x or y, the procedure is not applicable. (Stop)

Step 4. If the model is exponential in both x and y, it may be possible to place limits on the error. Compute error due to x and error due to y and determine if limits may be applied. (Stop)

Step 5. If the model is exponential in one parameter and polynomial in the other, it may be possible to place limits on the error. Compute error due to x and error due y and determine if limits may be applied. (Stop)

Step 6. Find the error due to x and error due to y. If ρ is equal to 0, use the quadratic error predicting model and predict the error. (Stop)

Step 7. If the model is a PDM, PIM, or PMM and if $-0.25 \leq \rho \leq 0.25$, go to Step 13.

Step 8. If the model is a PDM and -0.75 $\leq \rho \leq$ 0.75, go to Step 14.

Step 9. If the model is a PDM and $|\rho| >$ 0.75, the procedure is not applicable. (Stop)

Step 9. If the model is a PIM and -0.25 $\leq \rho \leq$ 0.75, go to Step 14.

Step 10. If the model is a PIM and $\rho <$ -0.25 or $\rho >$ 0.75, the procedure is not applicable. (Stop)

Step 11. If the model is a PMM and -0.75 $\leq \rho \leq$ 0.5, go to Step 14.

Step 12. If the model is a PMM and $\rho <$ -0.75 or $\rho >$ 0.5, the procedure is not applicable. (Stop)

Step 13. Use quadratic error predicting models or use quadratic error predicting model assuming ρ is 0 and then apply linear error model to predict error. (Stop)

Step 14. Use quadratic error predicting model and find error assuming ρ is 0. Use linear error predicting model. (Stop)

CONCLUSIONS

Much of the discussion in the literature about the accuracy of a FOA variance is concerned with limiting the parameter C_v to ensure acceptable results. The example problems (washoff, flood routing, and outflow hydrograph) demonstrated that this concept is valid for models which are not highly nonlinear. In water resources problems, however, parameter C_v is frequently much higher than 0.25. Thus, an FOA variance is rejected as being inaccurate. Given the computational demands of MCS, the output variance is often neglected altogether. The procedures developed herein should enable users to identify situations in which the model is not highly nonlinear and a FOA variance will perform acceptably even in the presence of high parameter C_v.

For highly nonlinear models this work showed that restricting the parameter C_v

to small values is not sufficient to guarantee small errors. The factor vs error and b vs error curves both asymptotically approach a relative error of 1 (100 percent error), even for C_v's as low as 0.1. For two parameter polynomial models, there were models with both parameter C_v's equal to 0.1 with relative errors in FOA variance as high as 0.5 (50 percent).

For two parameter models, it is not possible to predict the error in the FOA variance unless the model is polynomial in both parameters. Even then, the error predicting technique had limited applications, i.e. parameter correlations and C_v's were limited.

With models for which the response is not an explicit function of the parameters, the derivatives required to compute the FOA variance had to be computed numerically. In some cases, changing the step size for the numerical approximation affected the results significantly. It was concluded that an optimal step size should be selected based on agreement between two- and four-point central difference approximations and on agreement between the numerical derivative and the slope of a linear model estimated using five parameter - response combinations.

RECOMMENDATIONS

The error predicting techniques proposed here should primarily be used to make accept - reject decisions concerning FOA approximate variance. They should not in general be used to find errors and then correct an FOA variance to achieve a better estimate. If use of one of the error predicting techniques proposed here does not clearly show that a FOA variance is acceptable, then another method, such as MCS, should be used to estimate the variance.

With one parameter exponential models, the error initially decreases as factor increases, reaches a minimum, and starts rising again. The rising portion of the curve is quite steep, with the steepness increasing as C_v increases. If the computed factor is larger than the factor corresponding to the minimum point, use of the curve to predict the error should be done with extreme caution. This would only be recommended if the model response was known to have exactly the correct form, as confirmed by derivative ratios.

For polynomial models, the error vs b curve has a spike at b equal to zero. If the b power to be used to enter the curve is less than -0.001 or greater than 0.001, then ignoring the presence of the spike should give acceptable results. For b's within that range, predicted errors should be interpreted with caution.

If the R^2 is to be used to classify a model, the estimation should show clearly that the model is one type or the other. If the R^2's differ by less than approximately 0.05 or so, this is not clear evidence that the model is one type or the other. If both models fit well, i.e., both R^2's close to unity, then it is generally safe to assume both forms, estimate errors, and accept the larger error.

Several ideas for future research have emerged throughout the course of this work. A similar analysis could be done with uncertain parameters having normal, uniform, triangular, or other distributions of interest. The search for a factor which can be used to predict error in FOA variance for two parameter exponential and mixed EP models can be continued.

It is probably not worthwhile to try and extend the analysis to models with three uncertain parameters. This would be a massive undertaking given that there are ten combinations of model types, i.e. all polynomial, two polynomial and one exponential, two EP mixed and one polynomial, one of each, etc. For each model type an enormous grid of models would be required to cover the combinations of model nonlinearity and parameter uncertainty. Given that no predictors or models could be identified for most two parameter models, it is even less likely that one can be developed for three parameter models. Attempting to develop this data would not be recommended until prediction methods can be derived for two parameter models.

The issue of step size in numerical derivatives also needs to be resolved. Criteria for determining the optimum step size and for identifying the best numerical estimate of the derivatives are needed.

More work could also be done in the area of classifying the model as to exponential or polynomial. It may be possible to use the R^2 or some other attribute of the curve fitting process to predict if the model is sufficiently close to the correct form for the error predicting method to be applicable.

For the one parameter exponential example (the washoff model), the predicted errors were extremely accurate. They could have been used successfully to find the exact variance as

$$variance = \frac{FOA\ variance}{1 - error} \tag{6-1}$$

This example differed from the other examples in that the exponential classification was confirmed by derivative ratios. Further research could be conducted to determine if, for all cases in which the derivative ratios can be used to classify the model, the predicted error is sufficiently accurate that equation 6-1 can be applied.

Finally, the use of the slope derived by fitting a linear model through a set of parameter - model response pairs as an alternative to the slope of the tangent at the mean in the FOA variance computation should be investigated. Some of the preliminary data developed as part of this study indicated that the approximate variances can be more accurate when the slope from a regression is used. This work would have to address for what sorts of models an improvement is found. An optimum number of points for the regression and how to choose them would also have to be identified.

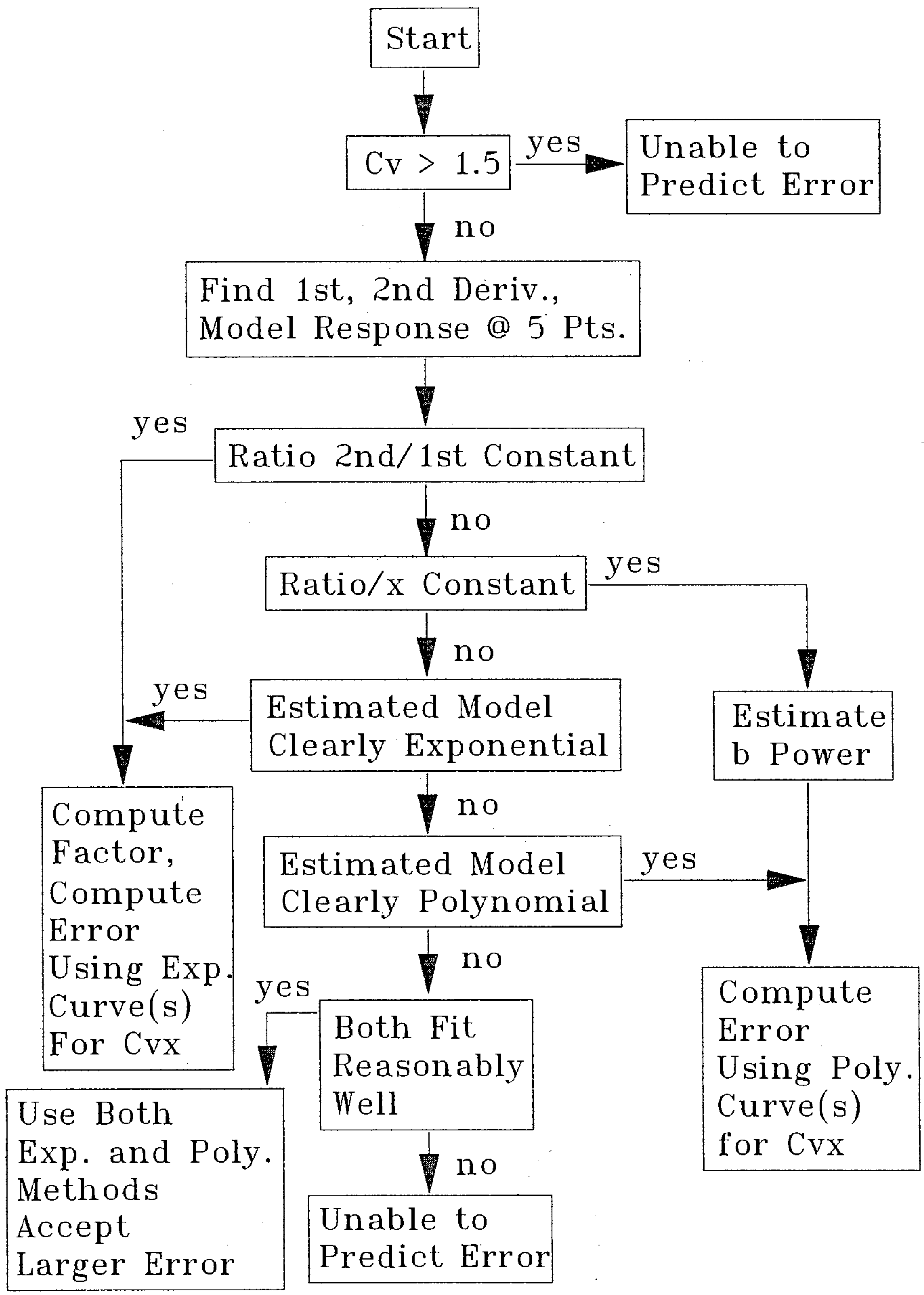

Figure 6-1. Flow Chart for One Parameter Models

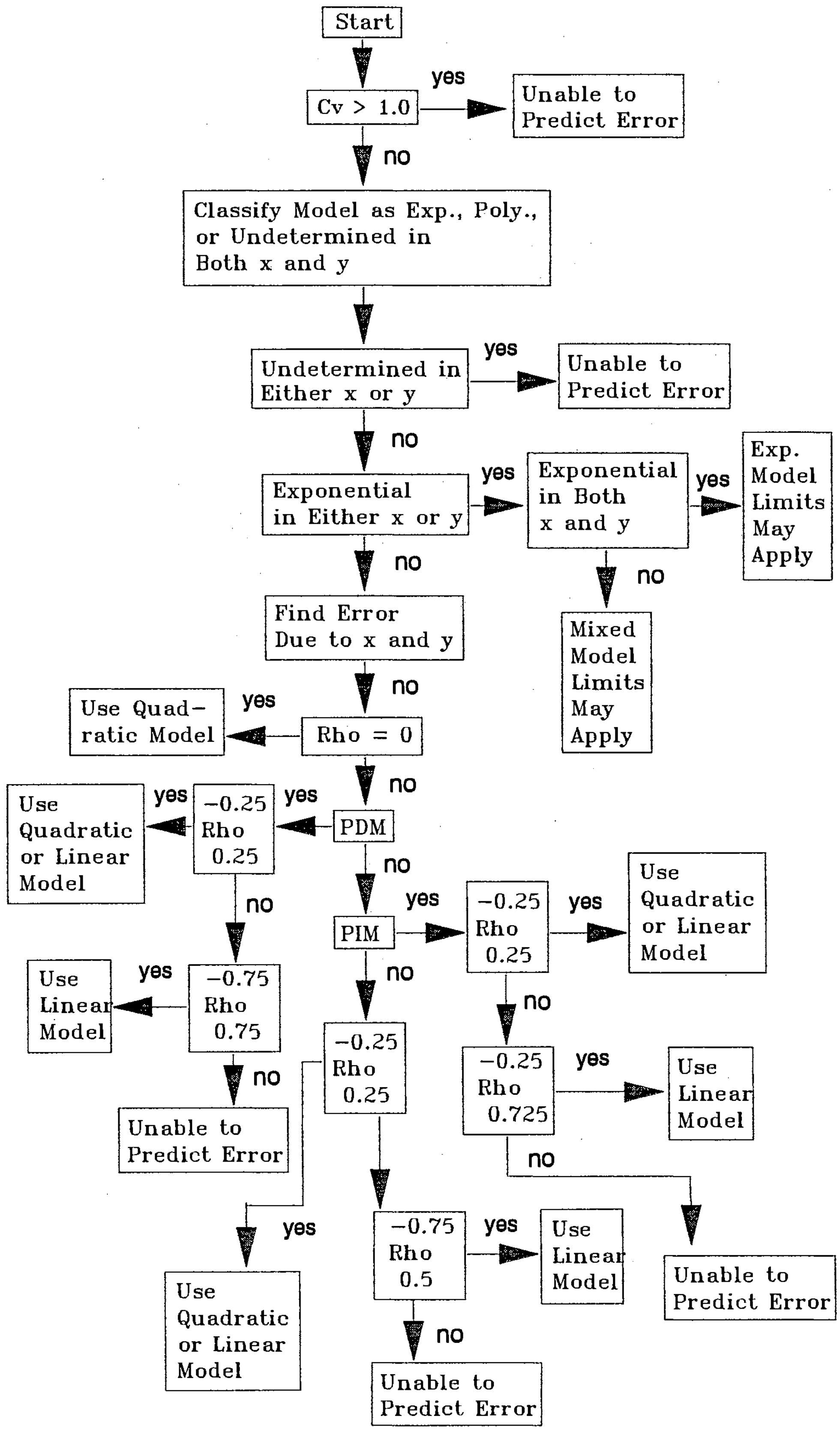

Figure 6−2. Flow Chart for Two Parameter Models

REFERENCES

Alley, W.M. and Smith, P.E. 1982. Multi-Event Urban Runoff Quality Model. USGS Open File Report 82-764.

Asbjornsen, O.A. 1986. Error in the Propagation of Error Formula. AIChE Journal, 32(2):332-334.

Bain, L.J. and Englehardt, M. 1987. Introduction to Probability and Mathematical Statistics. Duxbury Press, Boston, MA, 565 pp.

Barfield, B.J., et al. 1981. Applied Hydrology and Sedimentology for Disturbed Areas. Oklahoma Technical Press, Stillwater, OK, 603 pp.

Bates, B.C. 1988. Nonlinear, Discrete, Flood Event Models, 2. Assessment of Statistical Nonlinearity. Journal of Hydrology, 99:77-89.

Bates, B.C. and Townley, L.R. 1988. Nonlinear, Discrete Flood Event Models, 3. Analysis of Prediction Uncertainty. Journal of Hydrology, 99:91-101.

Bates, D.M. and Watts, D.G. 1980. Relative Measures of Nonlinearity. Journal of the Royal Statistical Society, Series B, 42(1):1-25.

Beale, E.M.L. 1960. Confidence Regions in Nonlinear Estimation. Journal of the Royal Statistical Society, Series B, 22(1):41-76.

Benjamin, J.R. and Cornell, C.A. 1970. Probability, Statistics, and Decision for Civil Engineers. McGraw-Hill, New York, NY, 684 pp.

Borland International, Inc. 1991. Turbo C++ Second Edition User's Guide. 414 pp.

Burges, S.J. 1979. Analysis of Uncertainty in Flood Plain Mapping. Water Resources Bulletin, 15(1):227-243.

Cheng, S-T, et.al. 1986. Sensitivity of Risk Evaluation of Coefficient of Variation. Stochastic and Risk Analysis in Hydraulic Engineering. Water Resources Publications, Littleton, Colorado. pp. 1-34.

D'Errico, J.R., Zaino, N.A. 1988. Statistical Tolerancing Using a Modification of Taguchi's Method. Technometrics 30(4):397-405.

Dettinger M.D. and Wilson, John L. 1981. First Order Analysis of Uncertainty in Numerical Models of Groundwater Flow - Part 1. Mathematical Development. Water Resources Research, 17(1):149-161.

Doctor, P.G. 1989. Sensitivity and Uncertainty Analysis for Performance Assessment Modeling. Engineering Geology, 26:411-429.

Downing, D.J., et al. 1985. An Examination of Response Surface Methodologies for Uncertainty Analysis in Assessment Models. Technometrics, 27(2):151-163.

Garen, D.C. and Burges, S.J. 1981. Approximate Error Bounds for Simulated Hydrographs. Journal of Hydraulic Engineering, 107(11):1519-1534.

Haan, C.T. 1977. Statistical Methods is Hydrology. Iowa State University Press, Ames, IA, 378 pp.

Henderson, F.M. 1966. Open Channel Flow. MacMillan Publishing Company, Inc., New York, NY, 522 pp.

Huang, K. 1986. Reliability Analysis of Hydraulic Design of Open Channel. Stochastic and Risk Analysis in Hydraulic Engineering. Water Resources Publications, Littleton, Colorado, pp. 59-65.

Kuczera, G. 1988. On the Validity of First Order Prediction Limits for Conceptual Hydrologic Models. Journal of Hydrology, 103:229-247.

Kuczera, G. 1990. Assessing Hydrologic Model Nonlinearity Using Response Surface Plots. Journal of Hydrology, 118:143-161.

Logue, K.M. and Green, R.E. 1988. Impact of Data-related Uncertainties in a Pesticide Leaching Assessment. Methods for Groundwater Studies - Proceedings of a National Workshop, Agricultural Research Service, University of Nebraska-Lincoln, Lincoln, NE. pp. 99-119.

Melching, C.S. and Anmangandla, S. 1992. Improved First-Order Uncertainty Method for Water Quality Modeling. Journal of Environmental Engineering, 118(5):791-805.

Mishra, S. and Parker, J.C. 1989. Effects of Parameter Uncertainty on Predictions of Unsaturated Flow. Journal of Hydrology, 108:19-33.

Protopapas, A.L. and Bras, R.L. 1990. Uncertainty Propagation With Numerical Models for Flow and Transport in the Unsaturated Zone. Water Resources Research, 26(10):2463-2474.

Sagar, B. 1984. Stochastic Groundwater Flow Modeling Using the Second Order Method. Rockwell International, Richland, Washington. US Department of Energy Contract DE-AC06-77RL01030.

Sagar, B and Clifton, P.M. 1983. Numerical Modeling of Parametric Uncertainties in Flow Through Porous Media: Development and Initial Testing of PORSTAT. Rockwell International, Richland Washington. US Department of Energy Contract DE-AC06-77RL01030.

Scott, S.H. 1993. Uncertainty Analysis of Dredge Production Measurement and Calculation. Journal of Waterway, Port, and Coastal Engineering, 119(2):193-203.

Smith, V.J. and Charbeneau, R.J. 1990. Probabilistic Soil Contamination Exposure Assessment Procedures. Journal of Environmental Engineering, 116(6):1143-1163.

Soil Conservation Service. 1972. National Engineering Handbook, Section 4, Hydrology.

Song, Q. and Brown, L.C. 1990. DO Model Uncertainty With Correlated Inputs. Journal of Environmental Engineering, 116(6):1164-1180.

Stevens, E. and Haan, C.T. 1993. Effect of Parameter Variation and Model Nonlinearity on First Order Analysis. In J. Marsalek, ed. Proceedings of the Sixth International Conference on Urban Storm Drainage, Niagara Falls, Canada, Setember 12-17 1993.

Taylor, J.R. 1985. Simple Examples of Correlations in Error Propagation. American Journal of Physics, 53(7):663-667.

Thomas, R.E. 1982. Uncertainty Analysis. Battelle Columbus Laboratories, Columbus, Ohio. US Department of Energy, Office of Nuclear Waste Isolation Contract DE-AC606-76-PAO1830-ONWI.

Tung, Y.K. and Hathhorn, W. 1988. Probability Distribution for Critical DO Location in Streams. Ecological Modelling, 42:45-60.

2

VITA

Ellen Weber Stevens

Candidate for the Degree of

Doctor of Philosophy

Thesis: A METHOD TO PREDICT THE ACCURACY OF A FIRST ORDER APPROXIMATION OF MODEL OUTPUT VARIANCE

Major Field: Agricultural Engineering

Biographical:

Education: Graduated from Northern Highlands Regional High School, Allendale, New Jersey in 1970; received Bachelor of Arts degree in Mathematics from Randolph-Macon Woman's College in May 1974; received Bachelor of Science degree in Civil Engineering from West Virginia Institute of Technology in December 1983; received Master of Civil Engineering degree from Mississippi State University in December 1989; completed the requirements for the Doctor of Philosophy degree with a major in Agricultural Engineering at Oklahoma State University in December 1993.

Experience: Employed by West Virginia Division of Vocational Rehabilitation as a disability claims examiner, 1974 to 1984; employed by Dewberry and Davis, Fairfax, Virginia as a civil engineer, 1984 to 1985; employed by US Army Engineer Waterways Experiment Station, Vicksburg, Mississippi as a civil engineer, 1985 to 1988; employed by US Army Corps of Engineers, Vicksburg District as a civil engineer, 1988 to 1990; Employed by Oklahoma State University, Department of Biosystems and Agricultural Engineering as a graduate research assistant, 1990 to present.

Professional Memberships: Oklahoma Society of Professional Engineers, American Society of Civil Engineers, Tau Beta Pi, West Virginia Beta Chapter